

A high-magnification electron micrograph of a biological membrane, showing a complex network of lipid bilayers and various protein structures. A prominent feature is a large, dark, circular protein complex, likely a channel or pore, which is the central focus of the book's title. The overall color palette is a range of browns and oranges, from light tan to deep, dark chocolate and near-black tones.

ADVANCES IN
EXPERIMENTAL
MEDICINE
AND BIOLOGY

Volume 677

Proteins

Membrane Binding and Pore Formation

Edited by
Gregor Anderluh
and Jeremy Lakey

Proteins: Membrane Binding and Pore Formation

ADVANCES IN EXPERIMENTAL MEDICINE AND BIOLOGY

Editorial Board:

NATHAN BACK, *State University of New York at Buffalo*

IRUN R. COHEN, *The Weizmann Institute of Science*

ABEL LAJTHA, *N.S. Kline Institute for Psychiatric Research*

JOHN D. LAMBRIS, *University of Pennsylvania*

RODOLFO PAOLETTI, *University of Milan*

Recent Volumes in this Series

Volume 669

NEW FRONTIERS IN RESPIRATORY CONTROL

Edited by Ikuo Homma and Hiroshi Onimaru

Volume 670

THERAPEUTIC APPLICATIONS OF CELL MICROENCAPSULATION

Edited by José Luis Pedraz and Gorka Orive

Volume 671

FRONTIERS IN BRAIN REPAIR

Edited by Rahul Jandial

Volume 672

BIOSURFACTANTS

Edited by Ramkrishna Sen

Volume 673

MODELLING PARASITE TRANSMISSION AND CONTROL

Edited by Edwin Michael and Robert C. Spear

Volume 674

INTEGRINS AND ION CHANNELS: MOLECULAR COMPLEXES AND SIGNALING

Edited by Andrea Becchetti and Annarosa Arcangeli

Volume 675

RECENT ADVANCES IN PHOTOTROPHIC PROKARYOTES

Edited by Patrick C. Hallenbeck

Volume 676

POLYPLOIDIZATION AND CANCER

Edited by Randy Y.C. Poon

Volume 677

PROTEINS: MEMBRANE BINDING AND PORE FORMATION

Edited by Gregor Anderluh and Jeremy Lakey

A Continuation Order Plan is available for this series. A continuation order will bring delivery of each new volume immediately upon publication. Volumes are billed only upon actual shipment. For further information please contact the publisher.

Proteins

Membrane Binding and Pore Formation

Edited by

Gregor Anderluh, PhD

*Department of Biology, University of Ljubljana
Ljubljana, Slovenia*

Jeremy Lakey, PhD

*Institute for Cell and Molecular Biosciences, The Medical School
University of Newcastle upon Tyne
Newcastle upon Tyne, UK*

Springer Science+Business Media, LLC

Landes Bioscience

Springer Science+Business Media, LLC
Landes Bioscience

Copyright ©2010 Landes Bioscience and Springer Science+Business Media, LLC

All rights reserved.

No part of this book may be reproduced or transmitted in any form or by any means, electronic or mechanical, including photocopy, recording, or any information storage and retrieval system, without permission in writing from the publisher, with the exception of any material supplied specifically for the purpose of being entered and executed on a computer system; for exclusive use by the Purchaser of the work.

Printed in the USA.

Springer Science+Business Media, LLC, 233 Spring Street, New York, New York 10013, USA
<http://www.springer.com>

Please address all inquiries to the publishers:
Landes Bioscience, 1002 West Avenue, Austin, Texas 78701, USA
Phone: 512/ 637 6050; FAX: 512/ 637 6079
<http://www.landesbioscience.com>

The chapters in this book are available in the Madame Curie Bioscience Database.
<http://www.landesbioscience.com/curie>

Proteins: Membrane Binding and Pore Formation, edited by Gregor Anderluh and Jeremy Lakey.
Landes Bioscience / Springer Science+Business Media, LLC dual imprint / Springer series: Advances in Experimental Medicine and Biology.

ISBN: 978-1-4419-6326-0

While the authors, editors and publisher believe that drug selection and dosage and the specifications and usage of equipment and devices, as set forth in this book, are in accord with current recommendations and practice at the time of publication, they make no warranty, expressed or implied, with respect to material described in this book. In view of the ongoing research, equipment development, changes in governmental regulations and the rapid accumulation of information relating to the biomedical sciences, the reader is urged to carefully review and evaluate the information provided herein.

Library of Congress Cataloging-in-Publication Data

Proteins : membrane binding and pore formation / edited by Gregor Anderluh, Jeremy Lakey.

p. ; cm. -- (Advances in experimental medicine and biology ; v. 677)

Includes bibliographical references and index.

ISBN 978-1-4419-6326-0

1. Membrane proteins. 2. Membrane lipids. I. Anderluh, Gregor, 1969- II. Lakey, Jeremy, 1958- III. Series: Advances in experimental medicine and biology ; v. 677.

[DNLM: 1. Membrane Proteins--physiology. 2. Cell Membrane Permeability. 3. Membrane Lipids--physiology. 4. Peptides--physiology. 5. Pore Forming Cytotoxic Proteins--physiology. 6. Protein Binding. W1 AD559 v.677 2010 / QU 55.7 P967 2010]

QP552.M44P757 2010

572'.69--dc22

2010014176

PREFACE

Formation of transmembrane pores is a very effective way of killing cells. It is thus not surprising that many bacterial and eukaryotic toxic agents are pore-forming proteins. Pore formation in a target membrane is a complex process composed of several steps; proteins need to attach to the lipid membrane, possibly aggregate in the plane of the membrane and finally form a pore by inserting part of the polypeptide chain across the lipid bilayer. Structural information about toxins at each stage is indispensable for the biochemical and molecular biological studies that aim to understand how pores are formed at the molecular level. There are currently only two structures of pores available, of α -toxin from *Staphylococcus aureus* and hemolysin E from *Escherichia coli*. Therefore, what we know about these proteins was obtained over many years of intense experimentation. We have nevertheless, in the last couple of years, witnessed a significant rise in structural information on the soluble forms of pore-forming proteins. Surprisingly, many unexpected similarities with other proteins were noted, despite extremely low or insignificant sequence similarity. It appears that lipid membrane binding and formation of transmembrane channels is achieved in many cases by a limited repertoire of structures. This book describes how several of the important pore forming toxin families achieve membrane binding and which structural elements are used for formation of transmembrane pores. Our contributors have thus provided the means for a comparative analysis of several unrelated families.

The introductory chapter by Mike Parker and colleagues gives a comprehensive overview of what we know about these proteins and highlights their general structural properties. The succeeding chapter by William Wimley sets up the stage upon which pore forming toxins act by describing the properties of the lipid membrane and the thermodynamics of membrane binding and insertion. Pore formation may be effectively achieved by simple structures, and the succeeding chapter by Burkhard Bechinger describes the structural requirements for efficient membrane binding and insertion of single alpha helices. The role of lipids was undervalued for a long time, especially in the process of protein insertion and the structural role they may play in the final pore. In recent years it became clear that their role is significant, and the next chapter from Jesús Salgado's group discusses the role of the bilayer

lipids in the pore forming process. After these general chapters all of the important protein toxins families are discussed, specifically cholesterol dependant cytolysins from Gram positive bacteria (Robert Gilbert), the aerolysin protein family (José Miguel Mancheño et al), colicins from *Escherichia coli* and related proteins that act as apoptotic regulators (Ana J. García-Sáez et al), actinoporins from sea anemones, Hemolysin E and related toxins (Peter Artymuik and colleagues), Cry toxins from *Bacillus thuringiensis* (Alejandra Bravo and colleagues) and cardiotoxins from cobra venom (Wen-guey Wu and colleagues). The final chapter by Bruce Kagan and Jyothi Thundimadathil provides a comparison of the properties of membrane channels formed by amyloid proteins and pore forming toxins and discusses the role that amyloid channels may have in disease.

Although in recent years the focus of some studies on pore forming toxins may have changed from structure-function relationships to measuring their effects on cell biology, comparative structural biology still has a lot to teach us. As highlighted in this book, novel structures and biophysical studies upon these proteins define the common threads of how proteins interact with lipid membranes and thus inform us of the rules of the game. We hope that by assembling this book we have helped to define where we currently are and where the science may go in the future. Our work as editors was made fun and interesting by the excellent contributors who have made this volume an engaging and fresh insight to the subject, we thank them for their hard work and our families for their patience.

Gregor Anderluh, PhD

*Department of Biology, University of Ljubljana
Ljubljana, Slovenia*

Jeremy Lakey, PhD

*Institute for Cell and Molecular Biosciences, The Medical School
University of Newcastle upon Tyne
Newcastle upon Tyne, UK*

ABOUT THE EDITORS...



GREGOR ANDERLUH is an Associate Professor of Biochemistry at the Department of Biology, Biotechnical Faculty, University of Ljubljana, Ljubljana, Slovenia. He and his coworkers are studying protein-membrane interactions and how cellular membranes are damaged by proteins. He is the director of the Infrastructural Centre for Surface Plasmon Resonance at the University of Ljubljana, where they study molecular interactions and are developing novel approaches on how to study protein binding to membranes. He received his PhD in Biology from University of Ljubljana and completed his Postdoctoral training at University of Newcastle, UK.

ABOUT THE EDITORS...



JEREMY LAKEY is a Professor of Structural Biochemistry at the Institute for Cell and Molecular Biosciences, University of Newcastle, UK and runs an academic research group based loosely on the theme of protein biophysical chemistry with interests in protein toxins, membranes and bionanotechnology. Following a first degree in Zoology, Jeremy completed a PhD in Membrane Biophysics at the University of East Anglia UK, followed by periods at the Centre de Biophysique Moléculaire, Orléans, France; EMBL, Heidelberg, Germany and the EPFL, Lausanne Switzerland. He is currently an editor of the *Biochemical Journal* and member of the facility access panel for the ISIS pulsed neutron source, UK.

PARTICIPANTS

Gregor Anderluh
Department of Biology
University of Ljubljana
Ljubljana
Slovenia

Peter J. Artymiuk
The Krebs Institute
Department of Molecular Biology
and Biotechnology
University of Sheffield
Sheffield
UK

Biserka Bakrač
Department of Biology
University of Ljubljana
Ljubljana
Slovenia

Burkhard Bechinger
Institut de chimie
CNRS
Université de Strasbourg
Strasbourg
France

Alejandra Bravo
Departamento de Microbiología
Molecular
Instituto de Biotecnología
Universidad Nacional Autónoma
de México
Mexico City
Mexico

Santi Esteban-Martín
Instituto de Ciencia Molecular
University of Valencia
Pol. La Coma
Paterna, Valencia
Spain

Susanne C. Feil
St. Vincent's Institute of Medical
Research
Fitzroy, Victoria
Australia

Gustavo Fuertes
Instituto de Ciencia Molecular
University of Valencia
Paterna, Valencia
Spain

Ana J. García-Sáez
Biotechnologisches Zentrum
der TU Dresden
Tatzberg, Dresden
Germany

Robert J.C. Gilbert
Division of Structural Biology
Wellcome Trust Centre for Human
Genetics
University of Oxford
Oxford
UK

Diana Giménez
Instituto de Ciencia Molecular
University of Valencia
Pol. La Coma
Paterna, Valencia
Spain

Irwin J. Goldstein
Grupo de Cristalografía Macromolecular
y Biología Estructural
Instituto de Química Física Rocasolano
CSIC
Madrid
Spain

Michael A. Gorman
St. Vincent's Institute of Medical
Research
Fitzroy, Victoria
Australia

Isabel Gómez
Departamento de Microbiología
Molecular
Instituto de Biotecnología
Universidad Nacional Autónoma
de México

Jeffrey Green
The Krebs Institute
Department of Molecular Biology
and Biotechnology
University of Sheffield
Sheffield
UK

Stuart Hunt
The Krebs Institute
Department of Molecular Biology
and Biotechnology
University of Sheffield
Sheffield
UK

Christopher L. Johnson
Institute for Cell and Molecular
Biosciences
University of Newcastle upon Tyne
Newcastle upon Tyne
UK

Bruce L. Kagan
Department of Psychiatry
and Biobehavioral Sciences
Semel Institute for Neuroscience
and Human Behavior
David Geffen School of Medicine
at UCLA
University of California
Los Angeles, California
USA

Je-hung Kuo
National Synchrotron Radiation
Research Center
Department of Life Science
National Tsing Hua University
Hsinchu
Taiwan

Jeremy H. Lakey
Institute for Cell and Molecular
Biosciences
The Medical School
University of Newcastle upon Tyne
Newcastle upon Tyne
UK

José Miguel Mancheño
Grupo de Cristalografía Macromolecular
y Biología Estructural
Instituto de Química Física Rocasolano
CSIC
Madrid
Spain

Carlos Muñoz-Garay
Departamento de Microbiología
Molecular
Instituto de Biotecnología
Universidad Nacional Autónoma
de México
Mexico City
Mexico

Liliana Pardo
Departamento de Microbiología
Molecular
Instituto de Biotecnología
Universidad Nacional Autónoma
de México
Mexico City
Mexico

Participants

xiii

Michael W. Parker
St. Vincent's Institute of Medical
Research
Fitzroy, Victoria
Australia

Galina Polekhina
St. Vincent's Institute of Medical
Research
Fitzroy, Victoria
Australia

Helena Porta
Departamento de Microbiología
Molecular
Instituto de Biotecnología
Universidad Nacional Autónoma
de México
Mexico City
Mexico

Helen Ridley
Institute for Cell and Molecular
Biosciences
University of Newcastle upon Tyne
Newcastle upon Tyne
UK

Jesús Salgado
Instituto de Ciencia Molecular
University of Valencia
Pol. La Coma
Paterna, Valencia
Spain

Jorge Sánchez
Departamento de Microbiología
Molecular
Instituto de Biotecnología
Universidad Nacional Autónoma
de México
Mexico City
Mexico

Orlando Sánchez
Instituto de Ciencia Molecular
University of Valencia
Pol. La Coma
Paterna, Valencia
Spain

Daniel Sher
Grupo de Cristalografía Macromolecular
y Biología Estructural
Instituto de Química Física Rocasolano
CSIC
Madrid
Spain

Mario Soberón
Departamento de Microbiología
Molecular
Instituto de Biotecnología
Universidad Nacional Autónoma
de México
Mexico City
Mexico

Jacob Suckale
Medizinisch Theoretisches Zentrum
der TU Dresden
Dresden
Germany

Hiroaki Tateno
Grupo de Cristalografía Macromolecular
y Biología Estructural
Instituto de Química Física Rocasolano
CSIC
Madrid
Spain

Jyothi Thundimadathil
Research and Development Group
Leader
Peptisyntha, Inc.
Torrance, California
USA

Siu-Cin Tjong
National Synchrotron Radiation
Research Center
Department of Life Science
National Tsing Hua University
Hsinchu
Taiwan

William C. Wimley
Department of Biochemistry
Tulane University Health Sciences
Center
New Orleans Louisiana
USA

Karen Wu
National Synchrotron Radiation
Research Center
Department of Life Science
National Tsing Hua University
Hsinchu
Taiwan

Po-long Wu
National Synchrotron Radiation
Research Center
Department of Life Science
National Tsing Hua University
Hsinchu
Taiwan

Wen-guey Wu
National Synchrotron Radiation
Research Center
Department of Life Science
National Tsing Hua University
Hsinchu
Taiwan

CONTENTS

1. INTRODUCTION..... 1

Susanne C. Feil, Galina Polekhina, Michael A. Gorman and Michael W. Parker

Abstract.....	1
Introduction.....	1
Nomenclature	2
Three-Dimensional Structures of Pore-Forming Proteins	2
Membrane Binding.....	7
Oligomerization.....	7
Common Features of Membrane Insertion	8
Conclusion	9

2. ENERGETICS OF PEPTIDE AND PROTEIN BINDING TO LIPID MEMBRANES 14

William C. Wimley

Abstract.....	14
The Lipid Bilayer Phase	14
Hydrophobic Interactions	15
Electrostatic Interactions	17
Additivity between Electrostatic and Hydrophobic Interactions.....	18
The Influence of Peptide and Protein Structure	18
Specific Interactions.....	19
Specificity: The Formation of Ordered Pores	19
Promiscuity: Membrane-Permeabilization by Interfacial Activity.....	21
Conclusion	21

3. MEMBRANE ASSOCIATION AND PORE FORMATION BY ALPHA-HELICAL PEPTIDES 24

Burkhard Bechinger

Abstract.....	24
Introduction.....	24
Alamethicin and Other Peptaibols	24

Cationic Amphipathic Antimicrobial Peptides.....	26
Membrane Proteins.....	27
Conclusion	27

4. ROLE OF MEMBRANE LIPIDS FOR THE ACTIVITY OF PORE FORMING PEPTIDES AND PROTEINS 31

Gustavo Fuertes, Diana Giménez, Santi Esteban-Martín, Ana J. García-Sáez,
Orlando Sánchez and Jesús Salgado

Abstract.....	31
Introduction.....	31
Membrane Interfaces Are Ideal Binding Sites for Pore-Forming Peptides and Proteins.....	32
A Membrane Foldase Activity Configures Peptide and Protein Active Structures	37
Role of Lipids in the Formation and Stabilization of Pores.....	39
Physical Properties of Polypeptide-Induced Pores Related to the Role of Lipids	44
Conclusion	47

5. CHOLESTEROL-DEPENDENT CYTOLYSINS 56

Robert J.C. Gilbert

Abstract.....	56
Functional Studies on CDCs	58
Membrane binding by CDCs	58
Pore Formation by CDCs.....	60
Proteolipid Pores	60
Oligomerisation—A Mechanism for Membrane Insertion	61
Complex Effects of CDCs and Related Proteins	62
Conclusion	62

6. LAETIPORUS SULPHUREUS LECTIN AND AEROLYSIN PROTEIN FAMILY 67

José Miguel Mancheño, Hiroaki Tateno, Daniel Sher and Irwin J. Goldstein

Abstract.....	67
Introduction.....	67
Pore-Forming Hemolytic Lectins	68
A New Member within the Aerolysin Family: The Crystal Structure of LSLa.....	69
Oligomeric State of Water-Soluble LSLa	72
A Common Aerolysin-Like Pore-Forming Module Structure?	73
Other New Members in the Aerolysin Family: Basic Aerolysin Pore-Forming Motifs?	76
Conclusion	78

7. INTERFACIAL INTERACTIONS OF PORE-FORMING COLICINS..... 81

Helen Ridley, Christopher L. Johnson and Jeremy H. Lakey

Abstract.....	81
Introduction.....	81
Structures.....	82
Receptor Binding.....	82
Translocation	82
Crossing the Periplasm.....	85
Inner Membrane Inserted Forms.....	86
Conclusion	87

8. PERMEABILIZATION OF THE OUTER MITOCHONDRIAL MEMBRANE BY Bcl-2 PROTEINS..... 91

Ana J. García-Sáez, Gustavo Fuertes, Jacob Suckale and Jesús Salgado

Abstract	91
Introduction.....	91
The Structure of the Bcl-2 Proteins.....	92
Pore-Forming Properties of Bcl-2 Proteins	95
Regulation of MOM Permeabilization by Bcl-2 Proteins.....	98
Conclusion	100

9. MOLECULAR MECHANISM OF SPHINGOMYELIN-SPECIFIC MEMBRANE BINDING AND PORE FORMATION BY ACTINOPORINS 106

Biserka Bakrač and Gregor Anderluh

Abstract	106
Introduction.....	106
Structural Properties of Actinoporins.....	107
Actinoporins Specifically Bind Sphingomyelin as the First Step in Pore Formation	107
Flexibility of the N-Terminal Region Is Required for Pore Formation	111
Pore Formation Involves Nonlamellar Lipid Structures.....	111
Similarity to Other Proteins.....	112
Conclusion	113

10. HEMOLYSIN E (HlyE, ClyA, SheA) AND RELATED TOXINS 116

Stuart Hunt, Jeffrey Green and Peter J. Artymiuk

Abstract	116
Introduction.....	116
Regulation of <i>hlyE</i> Expression.....	116
Structural Studies on HlyE	117
Process of Membrane Insertion.....	122
HlyE Secretion and Exploitation in Vaccine Development and Tumour	
Targeting.....	123
HlyE-Like Toxins from <i>Bacillus cereus</i>.....	123
Conclusion	124

11. PORE FORMATION BY Cry TOXINS 127Mario Soberón, Liliana Pardo, Carlos Muñoz-Garay, Jorge Sánchez,
Isabel Gómez, Helena Porta and Alejandra Bravo

Abstract.....	127
Introduction.....	127
Mechanism of Action of Cry Toxins	131
Solubilization and Proteolytic Activation of Cry Toxins	132
Binding Interaction with Receptors	132
Role of Cry Toxin-Receptor Interaction in Toxicity	135
Oligomerization of Cry Toxins.....	135
Pore Formation	136
Synergism between Cry and Cyt Toxins	137
Conclusion	138

**12. ROLE OF HEPARAN SULFATES AND GLYCOSPHINGOLIPIDS
IN THE PORE FORMATION OF BASIC POLYPEPTIDES
OF COBRA CARDIOTOXIN..... 143**

Wen-guey Wu, Siu-Cin Tjong, Po-long Wu, Je-hung Kuo and Karen Wu

Abstract.....	143
Introduction.....	143
Amphiphilic Properties of Three-Fingered CTXs.....	144
Diverse Targets of CTX Homologues	145
CTX A3 Pores in Sulfatide Containing Membranes.....	145
Pore Formations also Trigger Endocytosis.....	145
HS Facilitate Cell Surface Retention of CTXs	146
HS Stabilizes Membrane Bound Form of CTX	146
From HS to Membrane Sulfatides.....	146
Peripheral Binding Modes	146
Lipid Headgroup Conformational Change to Facilitate CTX Insertion	146
Pore Dynamics.....	148
Conclusion	148

13. AMYLOID PEPTIDE PORES AND THE BETA SHEET CONFORMATION..... 150

Bruce L. Kagan and Jyothi Thundimadathil

Abstract..... 150
Introduction..... 151
Aggregation and Fibril Formation: Hallmark of Amyloid Peptides..... 152
Interaction of Amyloid Peptides and Membranes during Ion Channel Formation 154
Similarities between Pore-Forming Toxins and Amyloid Pores 159
B-Sheet Peptide Pores..... 160
Mechanism of Ion Channel Formation by Beta Sheet Peptides 162
Conclusion 164

INDEX..... 169

CHAPTER 1

Introduction

Susanne C. Feil, Galina Polekhina, Michael A. Gorman
and Michael W. Parker*

Abstract

Pore-forming proteins (PFPs) possess the intriguing property that they can exist either in a stable water-soluble state or as an integral membrane pore. These molecules can undergo large conformational changes in converting between these two states. Much of what we know about how these proteins change their shape comes from work on bacterial toxins and increasingly, in more recent years, on toxins from other organisms. Surprisingly, a number of pore-forming proteins have recently been characterised that appear to have adopted similar strategies to toxins for binding and inserting into biological membranes.

Introduction

Pore-forming peptides and proteins (PFPs) are produced by many, if not all, organisms. They are secreted as water-soluble proteins but once their target is reached can be transformed into membrane proteins for the purpose of inserting into or translocating across biological membranes. Many of these proteins are toxins where they can aid the digestion of prey or can protect the producing organism by killing invaders. At least a third of the more than 300 protein toxins characterized to date act by disrupting membranes.¹ Many pore-forming toxins (PFTs) appear to function simply by forming pores in cell membranes, disrupting the permeability barrier leading eventually to cell death. In recent years a number of proteins have been characterised that do not function as toxins but nevertheless bind and insert into biological membranes using similar strategies as seen for toxins.

The major steps involved in the generation of pores by PFPs are summarized in Figure 1. In the first step the PFP must be secreted from the host. Organisms have developed a number of ways of secreting PFPs from the less subtle (e.g., colicins are secreted with the help of lysis proteins that punch a hole in the outer membrane of the producing cell)² to the more complex (e.g., proaerolysin appears to be secreted through a complex protein secretion system)³. In order to avoid premature conversion to its membrane-active state, some PFPs protect themselves by being produced as a proprotein and/or as oligomers (generally dimers). The PFPs are then targeted to the correct cells by means of parasitizing a host cell surface feature such as a protein or other substance (e.g., lipids, sugars) and using them as a receptor. Most often the result of concentration is the formation of oligomers on the cell surface although some PFPs may oligomerize in the membrane. Membrane insertion follows leading to formation of the pore that varies in size from less than 10 Å to more than 150 Å in diameter. They tend to form nonspecific pores, not surprisingly since the role for many is to destroy target cells. The pores sometimes are voltage-gated with the channels opened under normal physiological conditions. In some cases the *in vitro* pore-forming activity observed is almost certainly not a biological activity but rather a reflection of their *in vivo* translocating capacity.

*Corresponding Author: Michael W. Parker—St. Vincent's Institute of Medical Research,
9 Princes Street, Fitzroy, Victoria 3065, Australia. Email: mparker@svi.edu.au

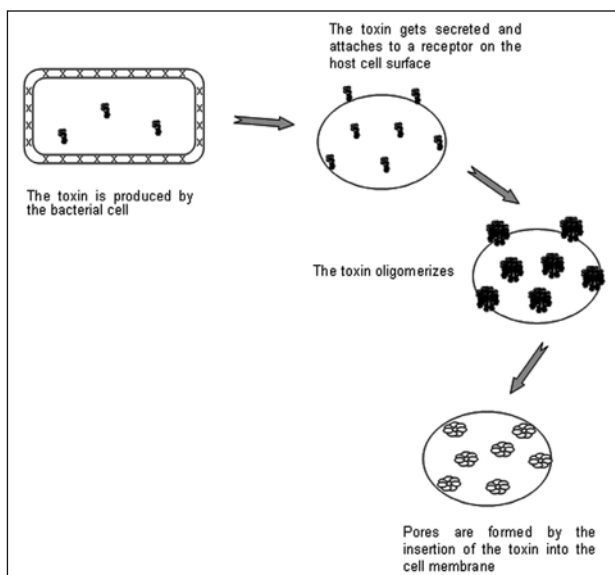


Figure 1. Stages in membrane pore formation. The figure shows the typical stages followed by bacterial toxins in forming pores. With variations, analogous stages are followed by other PFTs and more generally PFPs.

In this introductory chapter an overview is presented of the common features of pore-forming activity of PFPs that are emerging from numerous structural and functional studies.

Nomenclature

PFPs can be classified in a number of ways: for example, according to the organism that produces them, or their size or to a particular function. A particularly useful classification is one used for PFTs which is based on certain structural features because there is often a link between structure and function.⁴ Indeed, the classification can be extended to all PFPs since they share many common features with PFTs as explained below.

The α -PFTs are predicted to form pores using helices. The pore-forming colicins⁵ are the archetypal member of the class that also includes *Pseudomonas aeruginosa* exotoxin A,⁶ some insecticidal δ -endotoxins (Cry)⁷ and diphtheria toxin⁸ (Fig. 2). Members of the Bcl-2 family of apoptotic proteins have been shown to be structurally similar to α -PFTs and also form ion channels in similar fashion to these toxins.⁹

Another major class of pore-forming toxins, termed the β -PFTs, are predicted to insert into membranes to form a β -barrel. The class includes aerolysin,¹⁰ *Clostridium septicum* α -toxin,¹¹ *Staphylococcus aureus* α -hemolysin,¹² anthrax protective antigen,^{13,14} some insecticidal δ -endotoxins¹⁵ and cholesterol-dependent cytolysins.¹⁶ The MACPF superfamily, which includes proteins in the complement cascade of higher organisms, has recently been shown to possess structural similarities to β -PFTs.^{17,18}

Three-Dimensional Structures of Pore-Forming Proteins

Pore-Forming Peptides

Many peptides have been shown to possess pore-forming activities in the presence of biological membranes (see Chapter 3). Such peptides have received considerable interest because of their potential as antibiotics and as carriers of various molecules into cells. Although they

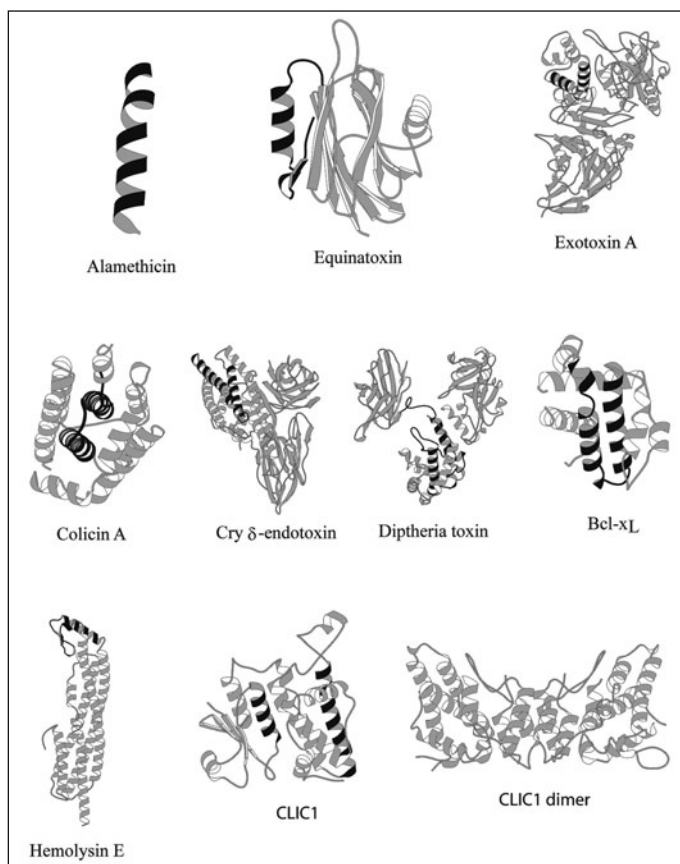


Figure 2. Cartoon pictures of α -PFPs. The regions thought to form the transmembrane stretches that take part in the initial step membrane insertion are highlighted in dark shade. The PFPs with colicin-like folds are shown in the second row. For some of the PFPs shown (equinatoxin, exotoxin, hemolysin E, CLIC1) their categorisation as α -PFPs is only tentative. The coordinates of the models were extracted from the Protein Data Bank (www.rcsb.org/pdb) and are referenced in the text. This picture was generated using MOLSCRIPT.⁹⁴

are structurally diverse they tend to possess amphipathic structures, a property which seems important for membrane interaction. Despite much work on these deceptively simple systems their mechanism of pore formation remains an area of controversy. One of the classical examples of a pore-forming peptide is alamethicin, an alpha-helical peptide that forms clusters of helices upon membrane pore formation (Fig. 2).¹⁹ An example of a peptide thought to form beta-sheet structures in membranes is the defensin family, peptides of ~50 amino acids that are produced and stored in the granules of neutrophils (Fig. 3).²⁰ Thus small pore-forming peptides can be readily classified as either α -PFPs or β -PFPs.

α -PFTs

The α -PFTs are predicted to form pores using helices. The archetype PFT of this class are the colicins which are produced by *E. coli* and closely related bacteria. The organisation of the primary structure of colicins is typical of many α -PFTs where domains can be readily identified, each associated with a distinct step in the toxin's killing activity: receptor binding, translocation

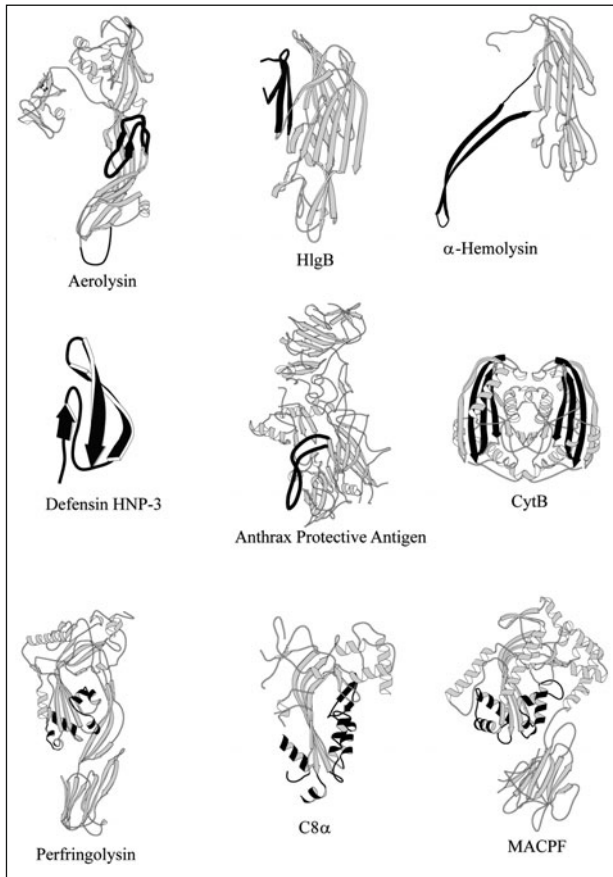


Figure 3. Cartoon pictures of β -PFPs. The regions thought to form the transmembrane stretches are highlighted in dark shade. The archetypical toxins of the family are shown in the first row. Members of the CDC/MACPF superfamily are shown in the bottom row. The coordinates of the models were extracted from the Protein Data Bank (www.rcsb.or/pdb) and are referenced in the text. This picture was generated using MOLSCRIPT.⁹⁴

across the outer membrane and cell death. The first reported crystal structure of a colicin was the pore-forming domain of colicin A (see Chapter 7).^{5,21} The polypeptide chain of 204 amino acids was found to fold into ten α -helices arranged in a three-layer structure with a central hydrophobic helical hairpin (Fig. 2). Subsequently a number of colicin structures have been elucidated and the pore-forming domains shown to be very similar to that of colicin A.²²⁻²⁴

A few years after the determination of the colicin A structure, a couple of other toxin structures were published that bore remarkable resemblance to it despite bearing no obvious sequence similarities. The crystal structure of diphtheria toxin (DT) was found to consist of three domains with the central or translocation domain being entirely α -helical like the colicin fold (Fig. 2).⁸ The crystal structures of Cry δ -endotoxins, produced from *Bacillus thuringiensis*, also revealed colicin-like domains at their N-terminus: a seven helix bundle in which a central helix, helix $\alpha 5$, is surrounded by six outer helices forming a left-handed supercoil (see Fig. 2 and Chapter 11).^{7,25-27} The long, amphipathic helices were suggestive that this domain might play a major role in membrane insertion and pore formation based on analogies with colicins.

Some α -PFTs have considerably less number of helices in their putative pore-forming domains. The crystal structure of *Pseudomonas aeruginosa* exotoxin A (PE) revealed it consists of three domains with the membrane translocation domain adopting an alpha-helical structure of six helices of which two are 30 Å in length and hence long enough to span a membrane (Fig. 2).^{6,28} The crystal and NMR structures of the soluble form of *Actinia equina* (sea anemone) equinatoxin II and the related sticholysin II, from *Stichodactyla helianthus*, reveal that these toxins adopt a 12 stranded β sandwich fold with an α -helix packing against the face of each sheet (Fig. 2 and see Chapter 9).²⁹⁻³¹ The N-terminal α -helical region is thought to form the transmembrane region for this toxin when it forms a pore.

In some cases the classification of a toxin being in the α -PFT class is only tentative as is the case for *Escherichia coli* hemolysin E (see Chapter 10). The crystal structure of this toxin in its water-soluble state reveals an elongated, predominantly helical molecule with the core of the molecule consisting of a four helix bundle, each helix being 80 to 90 Å long, with an additional 35 Å long helix (α_G) at one end to form a five helix bundle (the “tail”) and a β -hairpin (the “ β tongue”) flanked by two short helices laying against the four helix bundle at the opposite end of the molecule (the “head”) (Fig. 2).³² The overall structure does not resemble any other protein although the very long helices are reminiscent of the 200 Å helices found in colicin Ia.²⁴ The β tongue has been implicated in membrane insertion but it is not clear how it could form a continuous transmembrane β -barrel that appears typical of β -PFTs (see below). Furthermore, there are no alternating stretches of hydrophobic/hydrophilic sequences along the length of the protein that could form the amphipathic transmembrane (TM) β strands seen in β -PFTs. The five helix bundle of the tail subdomain has not been completely discounted as the membrane inserting region of toxin since the C-terminal helix, α_G , appears critical for function.³³ If this region does form the pore then there are clear analogies to be made with the pore-forming helical bundles of some of the other α -PFTs.

β -PFTs

β -PFTs are predicted to insert into membranes to form β -barrels. Although these toxins do have domain structures, the domains do not appear to carry distinct biological activities like α -PFTs. The β -PFTs display much more diverse structures than α -PFTs and their pore-forming regions tend to be more cryptic (Fig. 3). The first crystal structure from a member of this class was *Aeromonas hydrophila* proaerolysin (see Chapter 6). The crystal structure revealed that the toxin was composed mainly of β -sheets unlike the previously determined α -PFTs that were mainly α -helical (Fig. 3).¹⁰ The monomer has a distinct bilobal shape with one large, elongated lobe about 100 Å long consisting of three discontinuous domains and a much smaller lobe attached to it by a long linking region.

Staphylococcus aureus α -hemolysin is a 33 kDa water-soluble monomer that, upon binding to a target cell, oligomerizes cooperatively into hexamers or heptamers on the membrane surface. The crystal structure represented the first atomic resolution view of a toxin pore revealing a remarkable mushroom-shaped object consisting of cap, rim and stem domains.¹² The stem or transmembrane (TM) domain is constructed of a 14-stranded β -barrel formed from 7 β -hairpins with each hairpin contributed from a single monomer (Fig. 3). The hairpin consisted of alternating hydrophobic and hydrophilic residues so that when assembled in the membrane the hydrophilic residues formed the lumen of the pore whereas the hydrophobic residues interacted with the membrane core. The crystal structures of the water-soluble forms of various α -hemolysin homologues have also been determined including LukF,³⁴ LukF-PV³⁵ and HlgB (Fig. 3). These structures, all very similar to each other, are considered to represent views of the water-soluble state of α -hemolysin. A comparison to the structure of the α -hemolysin protomer shows that one of the most significant differences is in the stem region: in the homologues this region adopts a 3-stranded amphipathic β -sheet packing against a β -sandwich whereas the β -hairpin that extends away from the β -sandwich in the crystal structure of the membrane pore state of α -hemolysin (Fig. 3). The stacking of the hydrophobic residues of the stem region against the β -sandwich in the α -hemolysin homologues likely promotes their water solubility.

The crystal structure of *Bacillus anthracis* anthrax protective antigen (PA), in both water-soluble and prepore forms, revealed the molecule consisted of four domains, mainly organised into anti-parallel β -sheets with a few short helices (Fig. 3).^{13,14} The N-terminal domain 1 contains PA₂₀, a fragment that is removed by a cell surface protease resulting in exposure of several hydrophobic residues suggesting some conformational changes must take place after proteolysis.¹³ Domain 4 is quite separated from the rest of the molecule and it has been implicated in receptor-binding.¹³ The prepore structure revealed a ring-shaped heptamer with domain 2 lining the lumen and domains 3 and 4 located on the outside of the ring.^{13,14}

The cholesterol-dependent cytolysins (CDCs) exhibit a number of unique features amongst PFTs including an absolute dependence on the presence of cholesterol-rich membranes for their activity and the formation of very large oligomeric transmembrane pores greater than 150 Å in diameter (see Chapter 5). The crystal structures of two CDCs, perfringolysin O (PFO) from *Clostridium perfringens* and intermedilysin (ILY) from *Streptococcus intermedius*, revealed that CDCs are elongated rod-shaped molecules, over 100 Å long, rich in β -sheet and composed of four domains (Fig. 3).^{16,36}

Bacillus thuringiensis produces two major multigenic families of δ -endotoxins, *cry* and *cyt*, the former belonging to the α -PFT class (discussed above) and the latter to the β -PFT class. The Cyt δ -endotoxins are highly specific for dipteran (mosquitoes and black flies) larvae although broadly cytolytic in vitro.³⁷ The crystal structure of CytB in its protoxin form revealed it consisted of a single domain of α/β architecture with two outer layers of α -helix wrapped around a five stranded mixed β -sheet (Fig. 3). The protoxin assembles as a dimer linked by inter-twined β -strands that generate a continuous 12-stranded β -sheet across the dimer interface.¹⁵

Bcl-2 Proteins

The Bcl-2 family of proteins includes key regulators of apoptosis, some of which promote cell death while others prevent it. The first crystal structure of a Bcl-2 family member, Bcl-x_L, surprisingly revealed that its fold resembled the pore-forming/translocation domains of colicins (Fig. 2) (See Chapter 8).³⁸ Based on this observation the authors went on to show that Bcl-x_L could form pores in membranes and hence that certain Bcl family members could be classified as α -PFPs.⁹ The relevance of Bcl pore activity to its function in apoptosis remains controversial³⁹ but the observation nevertheless demonstrates the potential of proteins with colicin-like folds to partition into membranes.

MACPF Superfamily

The MACPF (Membrane Attack Complex/Perforin) domain was originally identified in the sequence of a number of complement proteins (C6, C7, C8 α , C8 β and C9) and perforin.⁴⁰ Despite limited sequence similarity, both perforin and C9 can oligomerize to form pores in membranes. The crystal structures of C8 α ¹⁷ and a bacterial MACPF¹⁸ were recently solved and revealed a surprising structural similarity to CDCs despite no detectable sequence relationship. This led the authors of both studies to suggest that these proteins insert into membranes using a similar mechanism to that established for CDCs (see below) and thus the superfamily can be classified as β -PFPs.

CLICs

The CLIC (Chloride Intracellular Channel) proteins are a family of highly homologous proteins that display both broad tissue and cellular distribution and have been identified in many vertebrates such as amphibians, birds, fish and mammals and in invertebrates such as sea squirts, nematodes and insects.⁴¹ Six CLICs have been identified in humans (CLICs 1 to 6), each consisting of a highly conserved core (40-80% sequence identity) of ~230 amino acids. The first CLIC to be characterised, p64 (now called CLIC5B), was shown to form chloride channels in planar lipid bilayers and lipid vesicles.⁴² Evidence for other CLIC proteins forming channels has been presented.⁴³⁻⁴⁸ CLICs can localise to distinct cellular membranes including the nuclear membrane, lysosomal membranes, mitochondria, Golgi membranes, cell-cell junctions and the plasma membrane.⁴⁹⁻⁵² However, to date most of the evidence that CLIC proteins form

channels is based on in vitro experimental systems and thus their physiological roles remain to be established.

The structure of a number of CLICs have been determined over the last few years and have been shown to adopt similar 3D folds which resemble the fold of the glutathione transferase superfamily (Fig. 2).⁵³⁻⁵⁸ The N-terminal domain adopts a thioredoxin-like fold consisting of a four stranded mixed β -sheet with two α -helices running parallel to the sheet on one face ($\alpha 1$ and $\alpha 3$) and one helix ($\alpha 2$) running perpendicular to the sheet on the other face. There is an intramolecular disulfide bridge between two cysteines in the N-terminal domain of CLIC. The C-terminal domain is all helical and contains a long loop between helices 5 and 6, a feature characteristic of the CLIC family and referred to as the foot loop. The loop is highly charged with acidic residues (between 3 and 7 acidic residues depending on which CLIC). How CLICs form pores remain unresolved although they can be tentatively classified as α -PFPs (see below).

Membrane Binding

PFTs recognise the correct target cells by parasitizing a host cell receptor which is often required for toxic activity although some of the toxins can form pores in artificial systems. Receptors may play a number of roles beyond target cell recognition such as promotion of toxin oligomerization and even toxin-induced cell signalling. Anthrax toxin is an interesting example of how toxins can use receptors to bind to membranes. Anthrax consists of three protein exotoxins: edema factor (EF), lethal factor (LF) and protective antigen (PA). The exotoxins lack toxic activity when administered separately but binary combinations that include PA are toxic.⁵⁹ PA mediates the translocation of the two other moieties, LF or EF, into the cytosol by first binding to a cell surface receptor.^{60,61} The crystal structures of the water-soluble monomer and prepore heptamer forms of PA bound to the receptor CMG2 have been determined and suggest that the receptor acts as a pH-sensitive brace that regulates membrane insertion of PA.^{62,63} PA subsequently forms a heptameric prepore which then binds to LF and/or EF and subsequently allows their translocation into the cytosol.

In a number of cases PFTs can recognise the nonprotein components of protein receptors. For example, δ -endotoxins can bind the N-acetyl galactosamine groups of glycosylphosphatidyl (GPI)-anchored aminopeptidases and in some cases directly to glycolipids (see Chapter 11).⁶⁴⁻⁶⁶ Aerolysin also recognises certain GPI-anchored proteins via domains 1 and 2.⁶⁷⁻⁶⁹ Domain 1 shares a strong structural similarity and possible evolutionary relationship with the S2 and S3 subunits of *Bordetella pertussis* pertussis toxin, which adopt C-type lectin folds and are thought to bind carbohydrate.⁷⁰

There are some instances where lipid components act as receptors. For example, CDCs have an absolute dependence on cholesterol for activity. Early studies suggested that a highly conserved tryptophan-rich undecapeptide near the C-terminus of CDCs is involved in membrane binding^{71,72} and the subsequent crystal structure of PFO suggested a mechanism by which this region might interact with cholesterol. However, recent studies have questioned whether cholesterol acts as a receptor: at least for some CDCs cholesterol appears essential for membrane insertion but not for membrane binding⁷³ and in one case, for ILY, CD59 acts as a receptor.⁷⁴ In another example, equinatoxins have been shown to work almost exclusively on membranes containing sphingomyelin although there are reports that cholesterol can replace sphingomyelin in some instances.⁷⁵ The crystal structure of *Stichodactyla helianthus* sticholysin II complexed to phosphocholine revealed a lipid binding site.³¹

Oligomerization

Oligomerization is an obligatory step in pore formation for many PFTs although the molecular mechanism of this step is poorly understood for most of them. For some α -PFTs (e.g., colicins, DT) most of the evidence suggests they do not oligomerize although it is hard to envisage how pores do form because there doesn't appear to be enough protein contributed from the monomer (see below). For many PFTs the oligomer forms on the membrane surface and this state is referred to as the prepore. A good example are CDCs which form a prepore complex on the membrane

surface by lateral diffusion of membrane-bound monomers (see Chapter 5).⁷⁶⁻⁷⁸ Electron microscopy studies of the CDC, pneumolysin, show that the prepore complex is bound to the membrane via the base of domain 4 where the Trp-rich loop resides.⁷⁹ The smaller β -PFTs oligomers (e.g., aerolysin, *C. septicum* alpha toxin and anthrax PA) regulate their tendency to oligomerize through the requirement of proteolytic cleavage of a propeptide whereas CDC oligomerization is controlled by a short loop in domain 3 that must move for the neighbouring monomer to form interactions with the first monomer.⁸⁰ Regulation of oligomerization of PFTs is a critical property as it is vital that oligomers do not form prematurely before they reach their intended target.

Common Features of Membrane Insertion

α -PFPs

At first sight α -PFPs appear to have little in common beyond possessing a highly helical domain (Fig. 2). Nevertheless, they do exhibit a number of similarities in their pore-forming activities. The receptor binding, membrane insertion/translocation and toxic activities tend to be associated with distinct protein domains. Charged residues have been implicated in the action of some of the toxins suggesting electrostatic interactions with receptors or membranes play an important role in the initial recognition process. Acidic residues have been postulated to play particular roles with many of the α -PFTs work optimally at low pH, conditions they are likely to encounter close to membranes containing negatively charged lipids or in acidic endosomes. Under these conditions acidic residues are likely to be neutralised and hence rendered relatively hydrophobic to aid membrane insertion. The pore-forming domains consist from one or two helices (e.g., alamethicin, equinatoxin) to a large bundle of helices. In the latter case the bundles are assembled in a three layer structure of 6 to 10 helices where each layer is formed by two or more anti-parallel helices, some of which are completely buried (Fig. 2). Thus the bundle represents a soluble form of packaging for the hydrophobic and amphipathic helices that are used to insert (or translocate) the toxin across the membrane. This common fold has sometimes been referred to as an “inside-out” membrane protein. Despite these similarities there is no detectable sequence similarity between the pore-forming domains.

The conversion from a water-soluble form necessitates a large change in conformation. How this is achieved is not totally resolved for any of the toxins. Nevertheless, it does appear that initial interactions of the toxins with the membrane involve a spreading out of helices on the membrane surface with their hydrophobic faces embedded into the bilayer and charged residues interacting with the polar head groups of the bilayer. The available data suggests there are no major changes in secondary structure that accompany the conformational changes. The archetypical example of how the large α -PFPs might insert into membranes is exemplified by the colicins. The crystal structure of colicin A revealed the presence of a completely buried, hydrophobic helical hairpin (Fig. 2) which gave rise to the “umbrella” model of membrane insertion whereby the hydrophobic loop of the helical hairpin initiates insertion into the lipid bilayer followed by spontaneous insertion of the entire hairpin.⁸¹ Because the passage of charged residues into the membrane is not energetically favourable, it was suggested that the insertion of the hairpin causes the colicin structure to open up like an umbrella so that the two outer helical layers stay outside the membrane with their hydrophobic faces embedded into the surface of bilayer. The recent finding that equinatoxins may form pores consisting of both lipid and protein might help explain how some of the other toxins such as the colicins can form pores with what appears to be too little protein to form a fully proteinaceous pore.

β -PFTs

The β -PFTs bear little resemblance since they differ greatly in their primary, tertiary and quaternary structures (Fig. 3). The three unifying features of β -PFTs are rich β -sheet content, lack of a long stretch of hydrophobic residues in their primary structure and a tendency to assemble into higher order oligomeric states when they form a pore. However, it is not easy to identify a common feature amongst β -PFTs that might explain how they insert into membranes. There are

features shared by some members that could lead to the exposure of hydrophobic surfaces such as proteolytic activation (e.g., aerolysin, anthrax PA, CytB δ -endotoxin), domain rearrangements (e.g., aerolysin, anthrax PA, CDCs) and dimer dissociation (e.g., aerolysin, CytB δ -endotoxin).

The crystal structure of the Staphylococcal α -hemolysin pore and subsequent structures of its water-soluble homologues provide a clue to a possible unifying feature of β -PFTs that might be responsible for their competency to penetrate membranes. The TM region of the toxin was shown to be comprised of a β -hairpin that exists as a 3 stranded β -sheet in the structures of the water-soluble homologues. Crystallographic and mutagenesis studies of anthrax PA have suggested that a disordered loop to membrane-spanning β -hairpin transition likely occurs in this toxin.¹³ A series of elegant mutagenesis and spectroscopic studies have revealed that CDCs undergo a similar transition where the initial state consists of a series of small α -helices rather than a disordered loop.⁸² The membrane-spanning region of aerolysin and its homologues is thought to be contributed from a long flexible loop.⁸³⁻⁸⁵ A sequence alignment of the putative TM regions from each toxin highlights the alternating pattern of hydrophobic and hydrophilic residues required for these regions to form transmembrane β -barrels with a hydrophobic face interacting with the hydrophobic core of the bilayer.⁸⁶ It appears likely that there is a concerted insertion of the β -hairpins from all monomers based on energetic arguments with recent supporting evidence in the case of the CDCs.^{87,88}

The apparent need of β -PFTs to adopt higher order oligomeric states can be explained by the need to generate sufficiently large hydrophobic surfaces via accumulation of amphipathic β -hairpins and the need to mask the polar edges of the hairpins from energetically unfavourable interactions with the hydrophobic core of the membrane by forming an enclosed β -barrel.

CLICs

It is not yet clear which PFP classification best describes the CLICs as existing models of membrane insertion are highly speculative. Initial sequencing of CLIC genes indicated that there were two potential TM domains^{89,90} that approximately correspond to helices $\alpha 1$ and $\alpha 6$ in the GST-like structure of the soluble form (Fig. 2).⁴³ Immunological, electrophysiological and proteolysis studies indicate that in the membrane form CLIC proteins cross the lipid bilayer an odd number of times and favour the region around helix $\alpha 1$ as the sole transmembrane region.^{91,92} The N-terminal region has been shown to be necessary for both membrane localisation and biological function.^{55,93} However, it is still possible that helix $\alpha 6$ forms the transmembrane domain as it resides in the all helical C-terminal domain that is similar to α -PFTs such as colicins. Large-scale structural changes in either the N- or C-terminal domain of the soluble form of CLIC would be necessary before either of these helices could insert into a lipid bilayer. CLIC proteins form chloride channels with maximal activity at low pH, reminiscent of α -PFTs that often require low pH for pore formation. A radical structural change has been observed in the N-terminal domain of CLIC1 after oxidation which results in the formation of a noncovalent dimer that is stabilised by an intramolecular disulfide bond between a conserved cysteine and another cysteine (Fig. 2).⁵⁴ This altered conformation has been postulated to represent the membrane docking form of CLIC1. Intriguingly, the N-terminal domain loses all its beta structure in the transition and in doing so adopts a layered α -helical structure not unlike some of the α -PFTs (Fig. 2).

Conclusion

PFTs have developed fascinating strategies to overcome the problem of having to exist in two mutually incompatible states: a water-soluble state so that the toxin can be transported from host to target cell and a membrane state in which the toxin expresses its killing activity. α -PFTs generally hide their TM regions within the fold of the water-soluble state. The TM regions tend to be very hydrophobic and adopt helical conformations in both water-soluble and membrane pore states. In contrast, the β -PFTs possess TM regions that adopt quite different folds in the water-soluble state of the toxin in order to make cryptic potential hydrophobic surfaces that are only revealed by the appropriate trigger/s that convert these regions into β -hairpins upon membrane insertion. The hairpins pair up with neighbouring hairpins of other protomers of the membrane-bound

oligomer in order to generate a large hydrophobic surface in the form of a β -barrel that spans the membrane. There are a number of features present in members of both families that have the potential to promote interaction with membranes. For example, low pH triggers are used to make some toxins more hydrophobic (e.g., DT) and/or to promote unfolding and conformational change (e.g., colicin A, DT, equinatoxin, PE, PA). The presence of cavities within the three-dimensional folds might aid conformational change (e.g., colicins, PFO). Location of aromatic residues on molecular surfaces is another feature that might promote interaction and anchoring to membranes (e.g., equinatoxins, Staphylococcal α -hemolysin, PFO). In many cases the toxins can form pores in artificial bilayers suggesting receptors play little role in the membrane insertion event itself. One of the most surprising discoveries in recent years has been the revelation that Nature has used the same strategies that it has developed for pore-forming toxins in mammalian proteins of diverse biological functions from immune protection to chloride channels.

Acknowledgements

MWP thanks all present and past members of his laboratory and his collaborators who have made major contributions to some of the structural studies of the toxins discussed in this chapter. We thank Julie Malyon for help in preparing this manuscript. This work was supported by project grants from the Australian Research Council (ARC) and the National Health and Medical Research Council of Australia (NHMRC) and NHMRC Fellowships to SCF, GP and MWP. MWP is an ARC Federation Fellow.

References

1. Alouf JE. Pore-forming bacterial protein toxins. In: van der Goot FG, ed. Pore-forming toxins. Heidelberg, Springer Verlag 2001:1-14.
2. Lakey JH, Slatin SL. Pore-forming colicins and their relatives. In: van der Goot FG, ed. Pore-forming toxins. Heidelberg, Springer-Verlag 2001:131-162.
3. Howard SP, Meiklejohn HG, Shivak D et al. A TonB-like protein and a novel membrane protein containing an ATP-binding cassette function together in exotoxin secretion. *Mol Microbiol* 1996; 22:595-604.
4. Gouaux E. Channel-forming toxins: tales of transformation. *Curr Opin Struct Biol* 1997; 7:566-573.
5. Parker MW, Pattus F, Tucker AD et al. Structure of the membrane-pore-forming fragment of colicin A. *Nature* 1989; 337:93-96.
6. Allured VS, Collier RJ, Carroll SF et al. Structure of exotoxin A of *Pseudomonas aeruginosa* at 3.0-Ångstrom resolution. *Proc Natl Acad Sci USA* 1986; 83:1320-1324.
7. Li J, Carrol J, Ellar DJ. Crystal structure of insecticidal delta-endotoxin from *Bacillus thuringiensis* at 2.5 Å resolution. *Nature* 1991; 353:815-821.
8. Choe S, Bennett MJ, Fujii G et al. The crystal structure of diphtheria toxin. *Nature* 1992; 357:216-222.
9. Minn, AJ, Velez P, Schendel SL et al. Bcl-x(L) forms an ion channel in synthetic lipid membranes. *Nature* 1997; 385:353-357.
10. Parker MW, Buckley JT, Postma JP et al. Structure of the *Aeromonas* toxin proaerolysin in its water-soluble and membrane-channel states. *Nature* 1994; 367:292-295.
11. Ballard J, Crabtree J, Roe BA et al. The primary structure of *Clostridium septicum* alpha-toxin exhibits similarity with that of *Aeromonas hydrophila* aerolysin. *Infect Immun* 1995; 63:340-344.
12. Song L, Hobaugh MR, Shustak C et al. Structure of staphylococcal alpha-hemolysin, a heptameric transmembrane pore. *Science* 1996; 274:1859-1866.
13. Petosa C, Collier RJ, Klimpel KR et al. Crystal structure of the anthrax toxin protective antigen. *Nature* 1997; 385:833-838.
14. Lacy DB, Wigelsworth DJ, Melnyk RA et al. Structure of heptameric protective antigen bound to an anthrax toxin receptor: a role for receptor in pH-dependent pore formation. *Proc Natl Acad Sci USA* 2004; 101:13147-13151.
15. Li J, Koni PA, Ellar DJ. Structure of the mosquitocidal delta-endotoxin CytB from *Bacillus thuringiensis* sp. *kyushuensis* and implications for membrane pore formation. *J Mol Biol* 1996; 257:129-152.
16. Rossjohn J, Feil SC, McKinstry WJ et al. Structure of a cholesterol-binding, thiol-activated cytolysin and a model of its membrane form. *Cell* 1997; 89:685-692.
17. Hadders MA, Beringer DX, Gros P. Structure of C8a-MACPF reveals mechanism of membrane attack in complement immune defense. *Science* 2007; 317:1552-1554.

18. Rosado CJ, Buckle AM, Law RHP et al. A common fold mediates vertebrate defense and bacterial attack. *Science* 2007; 317:1548-1551.
19. Fox RO Jr, Richards FM. A voltage-gated ion channel inferred from the crystal structure of alamethicin at 1.5-Å resolution. *Nature* 1982; 300:325-330.
20. Hill CP, Yee J, Selsted ME et al. Crystal structure of defensin HNP-3, an amphiphilic dimer: mechanisms of membrane permeabilization. *Science* 1991; 251:1481-1485.
21. Parker MW, Postma JP, Pattus F et al. Refined structure of the pore-forming domain of colicin A at 2.4 Å resolution. *J Mol Biol* 1992; 224:639-657.
22. Vetter IR, Parker MW, Tucker AD et al. Crystal structure of a colicin N fragment suggests a model for toxicity. *Structure* 1998; 6:863-874.
23. Elkins P, Bunker A, Cramer WA et al. A mechanism for toxin insertion into membranes is suggested by the crystal structure of the channel-forming domain of colicin E1. *Structure* 1997; 5:443-458.
24. Wiener M, Freymann D, Ghosh P et al. Crystal structure of colicin Ia. *Nature* 1997; 385:461-464.
25. Grochulski P, Masson L, Borisova S et al. Bacillus thuringiensis CryIA(a) insecticidal toxin: crystal structure and channel formation. *J Mol Biol* 1995; 254:447-464.
26. Galitsky N, Cody V, Wojtczak A et al. Structure of the insecticidal bacterial delta-endotoxin Cry3Bb1 of *Bacillus thuringiensis*. *Acta Crystallogr D* 2001; 57:1101-1109.
27. Morse RJ, Yamamoto T, Stroud RM. Structure of Cry2Aa suggests an unexpected receptor binding epitope. *Structure* 2001; 9:409-417.
28. Wedekind JE, Trame CB, Dorywalska M et al. Refined crystallographic structure of *Pseudomonas aeruginosa* exotoxin A and its implications for the molecular mechanism of toxicity. *J Mol Biol* 2001; 314:823-837.
29. Anthanasiadis A, Anderlüh G, Maček P et al. Crystal structure of the soluble form of equinatoxin II, a pore-forming toxin from the sea anemone *Actinia equina*. *Structure* 2001; 9:341-346.
30. Hinds MG, Zhang W, Anderlüh G et al. Solution structure of the eukaryotic pore-forming cytolysin equinatoxin II: implications for pore formation. *J Mol Biol* 2002; 315:1219-1229.
31. Mancheño JM, Martín-Benito J, Martínez-Ripoll M et al. Crystal and electron microscopy structures of sticholysin II actinoporin reveal insights into the mechanism of membrane pore formation. *Structure* 2003; 11:1319-1328.
32. Wallace AJ, Stillman TJ, Atkins A et al. *E. coli* hemolysin E (HlyE, ClyA, SheA): X-ray crystal structure of the toxin and observation of membrane pores by electron microscopy. *Cell* 2000; 100:265-276.
33. Atkins A, Wyborn NR, Wallace AJ et al. Structure-function relationships of a novel bacterial toxin, hemolysin E. The role of alpha G. *J Biol Chem* 2000; 275:41150-41155.
34. Olson R, Nariya H, Yokota K et al. Crystal structure of staphylococcal LukF delineates conformational changes accompanying formation of a transmembrane channel. *Nature Struct Biol* 1999; 6:134-140.
35. Pédelacq J-D, Maveyraud L, Prévost G et al. The structure of a *Staphylococcus aureus* leucocidin component (LukF-PV) reveals the fold of the water-soluble species of a family of transmembrane pore-forming toxins. *Structure* 1999; 7:277-287.
36. Polekhina G, Giddings KS, Tweten RK et al. Insights into the action of the superfamily of cholesterol-dependent cytolysins from studies of intermedilysin. *Proc Natl Acad Sci USA* 2005; 102:600-605.
37. Koni PA, Ellar DJ. Biochemical characterization of *Bacillus thuringiensis* cytolytic delta-endotoxins. *Microbiol* 1994; 140:1869-1880.
38. Muchmore SW, Sattler M, Liang H et al. X-ray and NMR structure of human Bcl-xL, an inhibitor of programmed cell death. *Nature* 1996; 381:335-341.
39. Antignani A, Youle RJ. How do Bax and Bak lead to permeabilization of the outer mitochondrial membrane? *Curr Opin Cell Biol* 2006; 18:685-689.
40. Tschopp J, Masson D, Stanley KK. Structural/functional similarity between proteins involved in complement- and cytotoxic T-lymphocyte-mediated cytolysis. *Nature* 1986; 322:831-834.
41. Littler DR. Structural studies of CLIC proteins. PhD thesis, University of New South Wales, Australia 2005.
42. Edwards JC. A novel p64-related Cl⁻ channel: subcellular distribution and nephron segment-specific expression. *Am J Physiol* 1999; 276:F398-F408.
43. Harrop SJ, DeMaere MZ, Fairlie WD et al. Crystal structure of the soluble form of the intracellular chloride ion channel CLIC1 (NCC27) at 1.4Å resolution. *J Biol Chem* 2001; 276:44993-45000.
44. Tulk BM, Schlesinger PH, Kapadia SA et al. CLIC-1 functions as a chloride channel when expressed and purified from bacteria. *J Biol Chem* 2000; 275, 26986-26993.
45. Tulk BM, Kapadia S, Edwards JC. CLIC1 inserts from the aqueous phase into phospholipids membranes where it functions as an anion channel. *Am J Physiol* 2002; 282:C1103-C1112.
46. Littler DR, Harrop SJ, Fairlie WD et al. The intracellular chloride ion channel protein CLIC1 undergoes a redox-controlled structural transition. *J Biol Chem* 2004; 279:9298-9305.

47. Qian Z, Okuhara D, Abe MK et al. Molecular cloning and characterization of a mitogen-activated protein kinase-associated intracellular chloride channel. *J Biol Chem* 1999; 274:1621-1627.
48. Proutski I, Karoulias N, Ashley RH. Overexpressed chloride intracellular channel protein CLIC4 (p64H1) is an essential component of novel plasma membrane anion channels. *Biochem Biophys Res Commun* 2002; 297:317-322.
49. Valenzuela SM, Martin DK, Por SB et al. Molecular cloning and expression of a chloride ion channel of cell nuclei. *J Biol Chem* 1997; 272:12575-12582.
50. Fernandez-Salas E, Sagar M, Cheng C et al. p53 and tumor necrosis factor α regulate the expression of a mitochondrial chloride channel protein. *J Biol Chem* 1999; 274:36488-36497.
51. Tonini R, Ferroni A, Valenzuela SM et al. Functional characterization of the NCC27 nuclear protein in stable transfected CHO-K1 cells. *FASEB J* 2000; 14:1171-1178.
52. Berryman MA, Goldenring JR. CLIC4 is enriched at cell-cell junctions and colocalizes with AKAP350 at the centrosome and midbody of cultured mammalian cells. *Cell Motil Cytoskeleton* 2003; 56:159-172.
53. Harrop SJ, DeMaere MZ, Fairlie WD et al. Crystal structure of the soluble form of the intracellular chloride ion channel CLIC1 (NCC27) at 1.4Å resolution. *J Biol Chem* 2001; 276:44993-45000.
54. Littler DR, Harrop SJ, Fairlie WD et al. The intracellular chloride ion channel protein CLIC1 undergoes a redox-controlled structural transition. *J Biol Chem* 2004; 279:9298-9305.
55. Littler DR, Assaad NN, Harrop SJ et al. Crystal structure of the soluble form of the redox-regulated chloride ion channel protein CLIC4. *FEBS J* 2005; 272:4996-5007.
56. Li Y-F, Li D-F, Zeng Z-H et al. Trimeric structure of the wild soluble chloride intracellular ion channel CLIC4 observed in crystals. *Biochem Biophys Res Commun* 2006; 343:1272-1278.
57. Littler DR, Harrop SJ, Brown LJ et al. Comparison of vertebrate and invertebrate CLIC proteins: the crystal structure of *Caenorhabditis elegans* EXC-4 and *Drosophila melanogaster* DmCLIC. *Proteins* 2008; 71:364-378.
58. Cromer BA, Gorman MA, Hansen G et al. Structure of the Janus protein human CLIC2. *J Mol Biol* 2008; 374:719-731.
59. Pezard C, Berche P, Mock M. Contribution of individual toxin components to virulence of *Bacillus anthracis*. *Infect Immun* 1991; 59:3472-3477.
60. Bradley KA, Mogridge J, Mourez M et al. Identification of the cellular receptor for anthrax toxin. *Nature* 2001; 414:225-229.
61. Scobie HM, Rainey GJ, Bradley KA et al. Human capillary morphogenesis protein 2 functions as an anthrax toxin receptor. *Proc Natl Acad Sci USA* 2003; 100:5170-5174.
62. Lacy DB, Wigelsworth DJ, Melnyk RA et al. Structure of heptameric protective antigen bound to an anthrax toxin receptor: a role for receptor in pH-dependent pore formation. *Proc Natl Acad Sci USA* 2004; 101:13147-13151.
63. Santelli E, Bankston LA, Leppla SH et al. Crystal structure of a complex between anthrax toxin and its host cell receptor. *Nature* 2004; 430:905-908.
64. Knowles BH. Mechanisms of action of *Bacillus thuringiensis* insecticidal δ -endotoxins. *Adv Insect Physiol* 1994; 24:275-308.
65. Knight PJK, Knowles BH, Ellar DJ. Molecular cloning of an insect aminopeptidase N that serves as a receptor for *Bacillus thuringiensis* CryIA(c) toxin. *J Biol Chem* 1995; 270:17765-17770.
66. Griffiths JS, Haslam SM, Yang T et al. Glycolipids as receptors for *Bacillus thuringiensis* crystal toxin. *Science* 2005; 307:922-925.
67. Nelson KL, Raja SM, Buckley JT. The glycosylphosphatidylinositol-anchored surface glycoprotein Thy-1 is a receptor for the channel-forming toxin aerolysin. *J Biol Chem* 1997; 272:12170-12174.
68. Abrami L, Fivaz M, Glauser P-E et al. A pore-forming toxin interacts with a GPI-anchored protein and causes vacuolation of the endoplasmic reticulum. *J Cell Biol* 1998; 140:525-540.
69. MacKenzie CR, Hiram T, Buckley JT. Analysis of receptor binding by the channel-forming toxin aerolysin using surface plasmon resonance. *J Biol Chem* 1999; 274:22604-22609.
70. Rossjohn J, Buckley JT, Hazes B et al. Aerolysin and pertussis toxin share a common receptor-binding domain. *EMBO J* 1997; 16:3426-3434.
71. Sekino-Suzuki N, Nakamura M, Mitsui KI et al. Contribution of individual tryptophan residues to the structure and activity of theta-toxin (perfringolysin O), a cholesterol-binding cytolysin. *Eur J Biochem* 1996; 241:941-947.
72. Jacobs T, Darji A, Frahm N et al. Listeriolysin O: cholesterol inhibits cytolysis but not binding to cellular membranes. *Mol Microbiol* 1998; 28:1081-1089.
73. Giddings KS, Johnson AE, Tweten RK. Redefining cholesterol's role in the mechanism of the cholesterol-dependent cytolysins. *Proc Natl Acad Sci USA* 2003; 100:11315-11320.
74. Giddings KS, Zhao J, Sims PJ et al. Human CD59 is a receptor for the cholesterol-dependent cytolysin intermedilysin. *Nat Struct Mol Biol* 2004; 11:1173-1178.

75. Anderluh G, Maček P. Cytolytic peptide and protein toxins from sea anemones (Anthozoa: Actiniaria). *Toxicon* 2002; 40:111-124.
76. Shepard LA, Shatursky O, Johnson AE et al. The mechanism of pore assembly for a cholesterol-dependent cytolysin: formation of a large prepore complex precedes the insertion of the transmembrane beta-hairpins. *Biochemistry* 2000; 39:10284-10293.
77. Hotze EM, Wilson-Kubalek EM, Rossjohn J et al. Arresting pore formation of a cholesterol-dependent cytolysin by disulfide trapping synchronizes the insertion of the transmembrane beta-sheet from a prepore intermediate. *J Biol Chem* 2001; 276:8261-8268.
78. Hotze EM, Heuck AP, Czajkowsky DM et al. Monomer-monomer interactions drive the prepore to pore conversion of a beta-barrel-forming cholesterol-dependent cytolysin. *J Biol Chem* 2002; 277:11597-11605.
79. Gilbert RJC, Jimenez JL, Chen S et al. Two structural transitions in membrane pore formation by pneumolysin, the pore-forming toxin of *Streptococcus pneumoniae*. *Cell* 1999; 97:647-655.
80. Ramachandran R, Tweten RK, Johnson AE. Membrane-dependent conformational changes initiate cholesterol-dependent cytolysin oligomerization and intersubunit beta-strand alignment. *Nature Struct Mol Biol* 2004; 11:697-705.
81. Parker MW, Tucker AD, Tsernoglou D et al. Insights into membrane insertion based on studies of colicins. *Trends Biochem Sci* 1990; 15:126-129.
82. Shatursky O, Heuck AP, Shepard LA et al. The mechanism of membrane insertion for a cholesterol-dependent cytolysin: a novel paradigm for pore-forming toxins. *Cell* 1999; 99:293-299.
83. Rossjohn J, Raja SM, Nelson KL et al. Movement of a loop in domain 3 of aerolysin is required for channel formation. *Biochemistry* 1998; 37:741-746.
84. Melton J, Parker MW, Rossjohn J et al. The identification and structure of the membrane-spanning domain of the *Clostridium septicum* alpha toxin. *J Biol Chem* 2004; 279:14315-14322.
85. Iacovache I, Paumard P, Scheib H et al. A rivet model for channel formation by aerolysin-like pore-forming toxins. *EMBO J* 2006; 25:457-466.
86. Parker MW. Cryptic clues as to how water-soluble protein toxins form pores in membranes. *Toxicon* 2003; 42:1-6.
87. Heuck AP, Tweten RK, Johnson AE. Beta-barrel pore-forming toxins: intriguing dimorphic proteins. *Biochemistry* 2001; 40:9065-9073.
88. Bonev B, Gilbert RJC, Andrew PW et al. Structural analysis of the protein/lipid complexes associated with pore formation by the bacterial toxin pneumolysin. *J Biol Chem* 2001; 276:5714-5719.
89. Landry D, Sullivan S, Nicolaides M et al. Molecular cloning and characterization of p64, a chloride channel from kidney microsomes. *J Biol Chem* 1993; 268:14948-14955.
90. Valenzuela SM, Martin DK, Por SB et al. Molecular cloning and expression of a chloride ion channel of cell nuclei. *J Biol Chem* 1997; 272:12575-12582.
91. Tonini R, Ferroni A, Valenzuela SM et al. Functional characterization of the NCC27 nuclear protein in stable transfected CHO-K1 cells. *FASEB J* 2000; 14:1171-1178.
92. Duncan RR, Westwood PK, Boyd A et al. Rat brain p64H1: expression of a new member of the p64 chloride channel protein family in endoplasmic reticulum. *J Biol Chem* 1997; 272:23880-23886.
93. Berry KL, Bulow HE, Hall DH et al. A *C. elegans* CLIC-like protein required for intracellular tube formation and maintenance. *Science* 2003; 302:2134-2137.
94. Kraulis P. MOLSCRIPT: a program to produce both detailed and schematic plots of proteins. *J Appl Crystallogr* 1991; 24:946-950.

CHAPTER 2

Energetics of Peptide and Protein Binding to Lipid Membranes

William C. Wimley*

Abstract

In every living cell, the lipid bilayer membrane is the ultimate boundary between the contents of the cell and the rest of universe. A single breach in this critical barrier is lethal. For this reason, the bilayer's permeability barrier is the point of attack of many offensive and defensive molecules, including peptides and proteins. Depending on one's perspective, these pore-forming molecules might be called toxins, venoms, antibiotics or host defense molecules and they can function by many different mechanisms, but they share one feature in common: they must bind to membranes to exert their effects. The thermodynamic and structural principles of polypeptide-membrane interactions are described in this chapter.

The Lipid Bilayer Phase

The hydrocarbon core of an unperturbed lipid bilayer membrane is one of the most hydrophobic microenvironments found in nature, with water concentration, dielectric constant and charge density that are very similar to an alkane phase in equilibrium with water. The hydrophobicity of the bilayer core dominates the membrane interactions of many classes of molecules; from ions and drugs to peptides and proteins.¹ Yet, as little as one nanometer away from the truly nonpolar core, the bilayer membrane contains an interfacial zone rich in polar groups, including water, as well as lipid hydrophobic moieties.¹⁻³ This broad interfacial region contains a sharp gradient of polarity, forming an anisotropic transition zone between the polar aqueous phase and headgroup region and the nonpolar bilayer core. As shown in Figure 1 the lipid bilayer membrane can be represented by three distinct zones of equal total thickness/volume: the hydrocarbon core, bounded on either side by a broad interfacial zone.

The hydrocarbon core of the membrane imparts a strict barrier to the permeation of most polar or charged solutes through the bilayer. Operationally, a "pore-forming" molecule can be defined as one that increases the permeability of a bilayer to polar solutes. There are at least two fundamentally different mechanisms by which a peptide or protein can alter membrane permeability: (1) A molecule can *work with* the hydrocarbon core by utilizing its constraints to drive self-assembly or folding of a polypeptide into a specific three dimensional structure, such as a protein pore, that provides a mostly protein polar channel or pathway through the membrane. This mechanism requires a membrane protein-like match between the hydrophobicity profile of the bilayer and the hydrophobicity profile of the inserted molecule. (2) Alternately, a molecule can *work against* the hydrocarbon core by altering the lipid packing and organization such that a mostly-lipid pathway through the lipids is created that eliminates the requirement for a polar solute to pass through a nonpolar layer. Molecules with this type of activity are amphipathic, but not perfectly amphipathic,

*William C. Wimley—Department of Biochemistry SL43, Tulane University Health Sciences Center, New Orleans, Louisiana, 70112-2699. Email: wwimley@tulane.edu

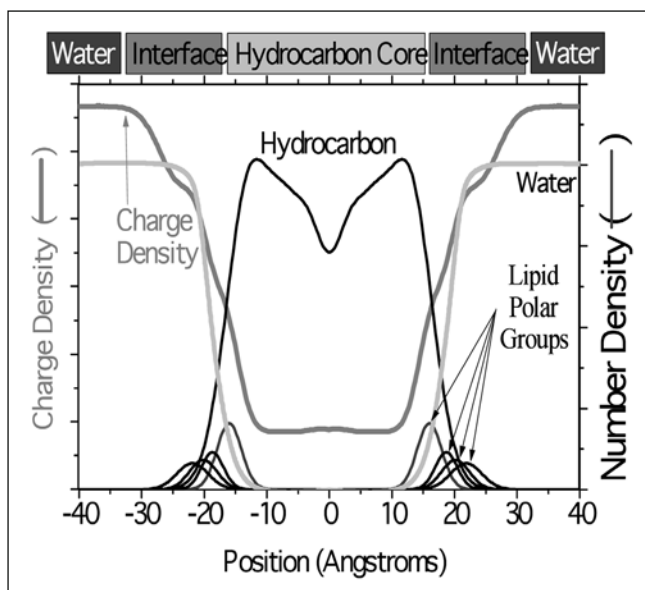


Figure 1. The lipid bilayer membrane. Depth profiles across an unperturbed lipid bilayer membrane. These are experimentally measured distributions of hydrocarbon and polar groups, including water, across a lipid bilayer membrane.¹ The center of the hydrocarbon core is assigned a position of 0 Å. Note that the nonpolar core of the membrane is less than 30 Å wide and is bounded on both sides with a broad anisotropic interfacial zone that contains hydrocarbon, polar groups and water. The charge density profile denotes the polarity gradient across the bilayer. Given the complexities of the bilayer physical chemistry, many types of interactions can take place.

such that the bilayer must be deformed and the hydrocarbon core disrupted (i.e., intermingled with lipid polar groups) to simultaneously accommodate the polar and charged moieties of the polypeptide. Independent of the mechanism, pore-forming peptides and proteins must interact strongly with membranes and that is the subject of this chapter.

Hydrophobic Interactions

Any pore-forming peptide and/or protein must interact more favorably with membranes than with either water or themselves in water. Binding is driven by hydrophobic and electrostatic interactions. Conceptually, it has been useful to consider membrane binding, self-assembly and folding as separate steps linked by thermodynamic cycles. For example Popot and Engelman described a two-state model for insertion and folding of membrane proteins⁴ which was augmented by Wimley and White^{1,5} into a four step cycle comprising interfacial partitioning, folding, insertion and assembly. This four step model is especially appropriate as a foundation to describe the interactions of pore-forming peptides and proteins with membranes because many of them actually follow such a pathway.

Partitioning of polypeptides from water to membranes is often dominated by hydrophobic interactions. To understand or predict interactions with the complex and anisotropic bilayer one must begin with quantitative measure of the propensity of a polypeptide to physically associate with a membrane. The Wimley-White interfacial hydrophobicity scale and octanol partitioning scale are hydrophobicity scales which have been shown to be useful to understand binding, insertion and folding of polypeptides in membranes.^{1,6-9} These are experimentally-determined, whole residue scales that include the cost of partitioning the peptide backbone and thus give absolute free

energies that can be used for predictions and experimental design. These scales also give information on the energetics of folding and how it is coupled to partitioning. The free energy values for the interfacial scale, shown in Figure 2, represent the free energy of partitioning of unstructured peptides into the fluid phase phosphatidylcholine bilayer interface. Only six amino acids are significantly favorable for partitioning into bilayers in the context of a random coil peptide: the aromatic residues: tryptophan, tyrosine and phenylalanine; and the aliphatic residues: methionine, leucine and isoleucine. The aromatic residues make especially large contributions and essentially dominate the interactions of peptides with membrane interfaces. In fact, it is unusual to find a membrane-partitioning polypeptide that does not have at least several aromatic amino acids. The charged amino acids are the only ones that strongly oppose partitioning into the interfacial region of the bilayer, although the energies of only 1-2 kcal/mol are not nearly as large as they were once thought to be. These residues remain fully ionized in bilayers.⁶

The octanol hydrophobicity scale is based on measurements of peptide partitioning into the more nonpolar environment of a hydrated octanol phase. This scale has been shown to be relevant to proteins inserted into the bilayer hydrocarbon core. In fact it allows for very accurate prediction of membranes-spanning segments of membrane proteins.¹⁰ Although hydrated octanol is more polar than the core of an unperturbed bilayer, it must be similar to the local environment experienced by a polypeptide and its associated polar groups in the hydrocarbon core. In the octanol hydrophobicity scale free energy values are roughly double the values for the interfacial scale, except for the aromatics which have a special interaction with bilayer interfaces.¹¹

Based on these hydrophobicity scale data, shown in Figure 2, one can calculate the contribution of hydrophobicity to membrane partitioning and predict polypeptide segments likely to interact with and insert into membranes. If we use the original mole fraction units defined as

Mole-Fraction Partition Coefficient

$$K_x = x_{\text{bilayer}}/x_{\text{water}}$$

$$X_{\text{bilayer}} = [\text{peptide}] \text{ in bilayer} / [\text{lipid}] \text{ in bilayer}$$

$$X_{\text{water}} = [\text{Peptide}] \text{ in water} / [\text{water}] \text{ in water (55.3 M at R.T.)}$$

$$\Delta G_x^0 = -RT \ln K_x$$

then the total free energy of hydrophobic partitioning of a polypeptide can be written as the sum of the whole residue contributions, shown in Figure 2, plus the sum of the contributions from the termini.⁹

$$\Delta G_x^{\text{Interface}} = \left(\sum \Delta G_x^{\text{residue}} \right) + \Delta G_x^{\text{N terminus}} + \Delta G_x^{\text{C terminus}}$$

Mole fraction free energies of binding in the range of -5 to -12 kcal/mol are typical for pore-forming peptides and proteins. In practical terms, mole fraction partition coefficients can be used to calculate the fraction of peptide that is membrane bound as a function of lipid concentration,

$$\text{Fraction of peptide bound} = K_x[L] / (K_x[L] + 55.3 \text{ M})$$

where K_x is the mole fraction partition coefficient, $[L]$ is the molar concentration of lipid and 55.3 is the molar concentration of water. A water-to-bilayer ΔG_x of -4 kcal/mol (favorable) is equal to $K_x = 860$, a partition coefficient that describes a peptide which is less than 2% bound at 1 mM lipid concentration. This level of binding is near the lower limit of detectability and in most experimental systems would not be able to drive membrane permeabilization. A ΔG_x of -10 kcal/mol provides for a very strong interaction in which greater than 99% of peptide is bound at 1 mM lipid. It is difficult to design a hydrophobic peptide with ΔG_x more favorable than about -12 kcal/mol, because loss of peptide solubility makes such extremely hydrophobic peptides very difficult to use. These limits set the range of useful hydrophobic partition coefficients that are consistent with the function of pore-forming polypeptides.

Amino Acid	Interface Scale	Octanol Scale	Terminal group	Interfacial Scale
	(kcal/mol)	(kcal/mol)		(kcal/mol)
Ala	0.17	0.50	+H ₃ N-	0.48
Arg ⁺	0.81	1.81	H ₂ N-	-0.02
Asn	0.42	0.85	Acetyl-	0.10
Asp ⁻	1.23	3.64	-COO-	-0.75
Asp ⁰	-0.07	0.43	-COOH	-3.43
Cys	-0.24	-0.02	-CONH ₂	-2.65
Gln	0.58	0.77	Residues with structure	-0.4/residue
Glu ⁻	2.02	3.63		
Glu ⁰	-0.01	0.11		
Gly	0.01	1.15		
His ⁺	0.96	2.33		
His ⁰	0.17	0.11		
Ile	-0.31	-1.12		
Leu	-0.56	-1.25		
Lys ⁺	0.99	2.80		
Met	-0.23	-0.67		
Phe	-1.13	-1.71		
Pro	0.45	0.14		
Ser	0.13	0.46		
Thr	0.14	0.25		
Trp	-1.85	-2.09		
Tyr	-0.94	-0.71		
Val	0.07	-0.46		

Figure 2. Hydrophobicity scales. Whole-residue, mole-fraction free energy values for peptide partitioning into bilayer interfaces or into hydrated octanol from water. These experimentally determined hydrophobicity scales are described in detail elsewhere.^{1,6,22} The signs have been reversed relative to the original publications to reflect free energies of transfer *from* the water phase, thus a negative ΔG is an interaction that favors partitioning. Determination of the free energy of the termini are described in.⁹ The carboxyl terminal value contains an additional entropic term possibly related to the reduction in dimensionality upon binding. The per residue decrease in ΔG for folding is also experimentally determined. This is an average value that could vary between peptides. Because these are experimentally determined, whole residue values, a prediction of the free energy of hydrophobic partitioning of any peptide can be made from a simple summation of the values, as described in the text.

Electrostatic Interactions

The other major driving force for polypeptide-membrane partitioning is electrostatic interaction. The charged moieties of lipid bilayers are found in the outer-most part of the interfacial zone, comprising the lipid headgroup moieties along with a high concentration of water and other polar groups (Fig. 1). This double-layer of concentrated surface charge can drive strong electrostatic interactions between bilayers and polypeptides. Biological membranes are composed of mixtures of neutral lipids, zwitterionic lipids and anionic lipids. Cationic lipids are extremely rare in nature. Thus biological membranes are often anionic; and membrane-interacting polypeptides are almost always cationic. This is especially true for the small membrane-active peptides such as the lytic toxins or antimicrobial peptides in which net charges can be as high as +10 can be found.

Electrostatic interactions are long-range and can guide polypeptides to a membrane surface where very high interaction free energies can result. Using Figure 1 as a guide, one can consider a polypeptide that has favorable electrostatic and favorable hydrophobic contributions to membrane binding. As a peptide approaches the bilayer surface electrostatic interactions increase rapidly and reach a maximum in the vicinity of the phosphate groups, which reside on the outermost portion of the interfacial zone. In terms of mole fraction partitioning, energies as high as -10 kcal/mol can result from electrostatic interactions under physiological ionic strength and modest surface charge on the bilayers and charge on the peptide. Calculation of electrostatic interactions has been described by Murray.¹²

A universal feature of systems with charged polypeptides binding to bilayers is anti-cooperative binding.⁵ This occurs because the net charge on the bilayer surface is reduced by polypeptide binding and also because the bilayer-accumulated charged peptides disfavor additional binding due to repulsive interactions. Seelig and others have developed methods to deconvolute such contributions to bilayer interactions.¹³ A consequence of anti-cooperative binding is that partitioning experiments will appear to give a saturable binding curve, which one can fit with a classical binding site model. However, such models are inappropriate to describe peptides partitioning into membranes.⁵

Additivity between Electrostatic and Hydrophobic Interactions

At the depth in the bilayer interface where electrostatic interactions are strongest, hydrophobic interactions are weak because the polarity and water content near the charged headgroup moieties are close to the bulk water values. Hydrophobic interactions will become significant only as a polypeptide partitions deeper into the membrane, away from bulk water phase. However this occurs *at the expense* of electrostatic interactions, which decrease as a peptide moves away from the headgroup region of the interface. The equilibrium depth of insertion will depend on the balance of the two interactions and on the ability of the lipids and peptide chain to deform to accommodate them. Strong electrostatic binding, without a hydrophobic component is generally not sufficient to perturb the hydrocarbon core because electrostatically bound polypeptides are bound only to the surface. Importantly, the dissimilar depth profiles for electrostatic and hydrophobic interactions means that free energies will not be additive, which has been shown experimentally.¹⁴

The dissimilar depth profiles of the hydrophobic and polar/charged moieties of the lipid bilayer lends itself to disruption of the hydrophobic core by imperfectly amphipathic polypeptides such as the antimicrobial peptides, because these molecules drive the mixing of polar and charged residues with the hydrophobic core, leading to a situation where the interactions can only be satisfied simultaneously by a highly perturbed bilayer.

The Influence of Peptide and Protein Structure

An open peptide bond is one of the most polar moieties in a polypeptide chain, costing as much to partition into a bilayer as some of the charged side chains. The cost is about 1.2 kcal/mol per residue in the interface and about 2 kcal/mol in the hydrocarbon core. Because the cost of partitioning a hydrogen-bonded peptide bond is lower, there will always be a strong driving force for folding that is coupled to partitioning into a bilayer. Based on various experiments with β -sheet and α -helical peptides, the net free energy change for folding in a bilayer has an average value of about -0.4 kcal/mol/residue (range: -0.2 to -0.5 kcal/mol). The consequence of this effect is that partitioning and folding are tightly coupled and peptides that have partitioned into bilayers will have a dramatically greater propensity for structure in the membrane than in solution. For example, the 22 residue pore-forming peptide melittin is calculated to have a mole fraction partitioning free energy as a random coil of -1 kcal/mol, a value that denotes such weak binding that it is not measurable. In reality, melittin binds very strongly with a ΔG_x of -8 kcal/mol. Strong binding comes about because the weak random coil binding is coupled to a contribution of about -0.4 kcal/mol/residue of folding for each the 15-18 residues that change from random coil to α -helix upon membrane partitioning.¹⁵

Specific Interactions

Pore-forming peptides and proteins that partition into membranes because of hydrophobic interactions will interact with almost any bilayer type. Classical examples of this nonspecific behavior are the α -helical pore-forming peptides melittin and alamethicin and the beta-helix gramicidin A. These pore formers will permeabilize almost any fluid phase bilayer membrane, in a living cell or in a test tube. Some cationic pore-forming peptides, especially the antimicrobial peptides, target anionic membranes specifically by partitioning into them preferentially due to a strong electrostatic component. Nonetheless, peptide-membrane interactions that occur by partitioning are, by definition, relatively nonspecific and will require more than the minimum number of residues to drive the interaction. For example, a minimum of several aromatics or aromatics mixed with aliphatic residues are required for moderately good hydrophobic partitioning.

There are many pore-forming proteins and peptides that interact with membranes by highly specific interactions. For example, diphtheria toxin as well as the pore-forming colicins are targeted to membranes by a highly specific receptor-protein like interaction. Similarly, the antibiotic peptides vancomycin and the type A lantibiotics, such as nisin, have highly specific interactions with particular lipid components of bacterial membranes, which they subsequently permeabilize. The cholesterol-dependent cytolysins are pore-forming proteins with a very strict requirement for cholesterol in the target membranes. All these examples of pore-forming polypeptides coupled to strong and highly specific interactions with individual components of the membrane should probably be treated like a ligand-binding-pocket type of interaction rather than an interaction that is dependent on partitioning. In any case, once a pore-forming peptide or protein has interacted with a target membrane, the membrane is subsequently permeabilized by one of the mechanisms described next.

Specificity: The Formation of Ordered Pores

The three dimensional structure of the *Staphylococcus aureus* α -hemolysin (Fig. 4) is a stunning example of a classical pore-forming protein. However the literature suggests that a stable,

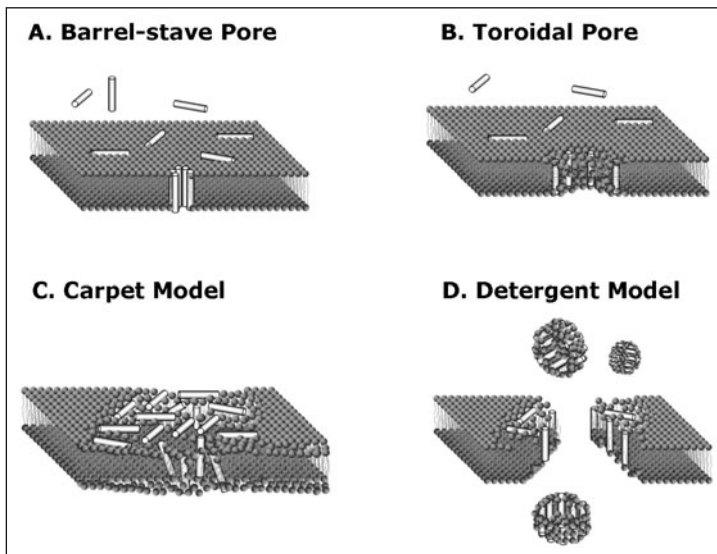


Figure 3. Some models of polypeptide membrane permeabilization. Some mechanistic models of membrane permeabilization by polypeptides. There are many different mechanisms by which membrane permeabilizing peptides and proteins can function. Some of the more commonly described mechanisms are shown in these schematic images. The driving forces and implications for these various models are described in the text.

well structured protein pore with a fixed stoichiometry like α -hemolysin is actually a very rare counter-example to the majority of known pore-forming polypeptides, which number well over 1000. Most do not form such fixed structures but rather bind to membrane surfaces through specific or nonspecific interactions and then self-assemble into flexible, transient or flickering structures which allow permeation of solutes through the membrane. The simplest models of membrane permeation by polypeptides involve the formation of transbilayer pores or channels through the membrane as shown by the models in Figure 3. In a barrel stave pore, peptides interact laterally with one another to form a specific folded structure that is reminiscent of a membrane protein ion channel. In the toroidal pore model, specific peptide-peptide interactions are not present. Instead peptides affect the local curvature of the bilayer in a cooperative manner such that a toroid of high curvature forms through the bilayer. In either case, one can imagine pores that are stable and long lived or pores that are transient in equilibrium with surface bound or monomeric peptide. In fact only a very small fraction of the total peptide need be in a pore state at any moment in time to drive observed rates of leakage through membranes.

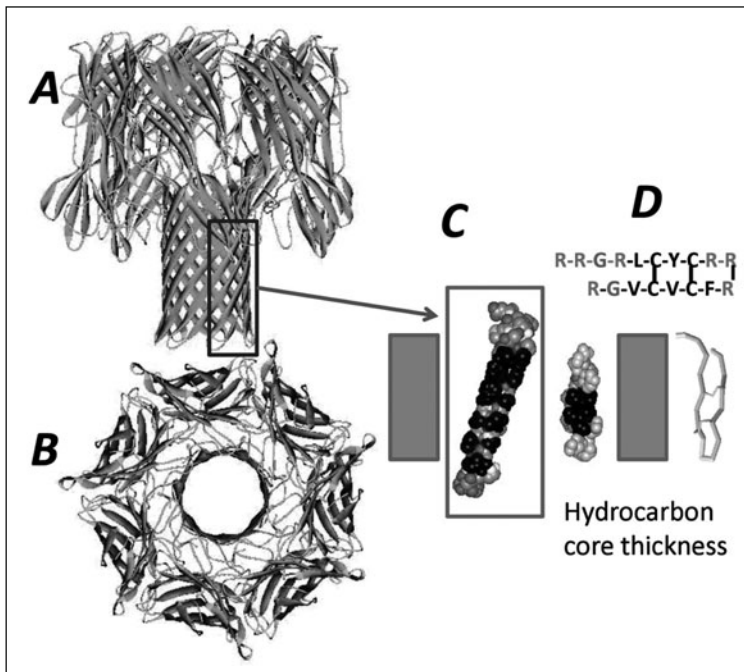


Figure 4. Transbilayer profiles of some pore-forming polypeptides. The structure of the protein α -hemolysin from *Staphylococcus aureus*.²³ A) This classical protein pore assembles into a heptameric ring on susceptible membranes which inserts a β -sheet, barrel stave pore across the membrane. B) The top view shows a distinct open pore through the protein (and through the membrane) which allows unrestricted leakage through the membrane and cell lysis. C) The lipid-facing surface of one of the β -hairpins from α -hemolysin. The thickness of the hydrophobic face (nonpolar residues in black) matches the profile of the hydrocarbon core of the membrane. This is why the barrel stave pore can assemble into an ordered pore in membranes. D) In sharp contrast, protegrin 1, a porcine antimicrobial peptide with a similar β -hairpin secondary structure has a hydrophobic face (in black) that is far smaller than the bilayer hydrocarbon core and is bounded by basic arginine residues. Protegrin binds strongly to bilayer through a combination of hydrophobic and electrostatic interactions. However, instead of forming a transbilayer pore, protegrin disturbs the lipid packing through its interfacial activity and imperfect amphiphaticity.

Barrel stave and toroidal pores are functionally similar, but are fundamentally different in structure and membrane interactions. For example barrel stave pores work with the bilayer hydrocarbon core, using it as a template for amphipathic peptide-self assembly. Specific interactions between amino acids also contribute to self-assembly of the pore. Toroidal pores, on the other hand, work against the hydrocarbon core, disrupting the natural segregation of polar and nonpolar parts of the membrane by providing alternative surfaces for lipid to interact favorably with. Toroidal pores are formed by imperfectly amphipathic peptides.

Protein pore formers can form stable long-lived pores or flickering transient pores. Diphtheria toxin and the pore-forming colicins, for example, can form transient pores across membranes by inserting interfacially-bound amphipathic helices across the membrane subsequent to the initial binding events. Peptides as well can form barrel stave or toroidal pores,¹⁶ although distinguishing them from each other is not straightforward. A classical example of peptide that forms transmembrane pores is alamethicin, which forms an amphipathic alpha helix that can exist, depending on hydration and concentration, either mostly parallel or mostly perpendicular to the lipid bilayer normal.¹⁶ The perpendicular structure is consistent with the image of a transmembrane pore and other evidence suggests a barrel stave pore for alamethicin.

Promiscuity: Membrane-Permeabilization by Interfacial Activity

In addition to the long held models of transmembrane barrel-stave or toroidal pores, a number of nonpore models have been proposed to explain or categorize the mechanism of pore-forming polypeptides in lipid membranes. The mechanism of action of the antimicrobial peptides has been especially difficult to explain with specific pore models. The so called “carpet model” is the most commonly cited phenomenological model and was proposed in 1996 by Shai¹⁷ to explain the mechanism of action of mammalian cecropin P1 on model membranes. Cecropin P1 is a helical peptide that is oriented parallel to the membrane surface and does not form explicit pores. The peptide is active only at high P:L ratios, conditions under which the peptide forms a carpet on the bilayer surface. The “detergent model” is also often cited to explain the catastrophic collapse of membrane integrity observed with some anti microbial peptides at high peptide concentration leading to size-independent, partial leakage of entrapped contents.^{18,19}

The majority of known membrane permeabilizing peptides are antimicrobial peptides and most of these function by a mechanism that is consistent with a nonspecific mechanism of membrane permeabilization.²⁰ This nonspecific activity has been described as “interfacial activity”²⁰ and is dependent on the ability of a peptide to bind to the membrane interface with hydrophobic and electrostatic interactions, followed by perturbation of the bilayer lipid packing driven by the broken, or imperfect amphipathic nature of the peptide (and bilayer). Marrink and colleagues have simulated such systems resulting in a very compelling image of a “pore-forming” antimicrobial peptide (magainin) that permeabilizes membranes by perturbing the bilayer’s lipid packing and organization enough to break down the segregation between interface and core.²¹ This breakdown allows permeation of polar molecules and does so without the formation of a transmembrane “pore” or channel. A realistic image of a peptide “pore” based on the studies of Marrink is shown in Figure 5.

Conclusion

Decades of experiments and modeling of pore-forming proteins and have shown that there are many different ways for a membrane to be permeabilized. These mechanisms range from highly specific, stable pore formation to nonspecific detergent-like membrane disruption. All of these mechanisms occur in nature and have biological relevance. However different the mechanisms, all pore-forming proteins and peptides must interact with membranes through binding, partitioning or a combination of the two followed by the formation of a polypeptide-induced polar pathway through the hydrocarbon core of the membrane. In this

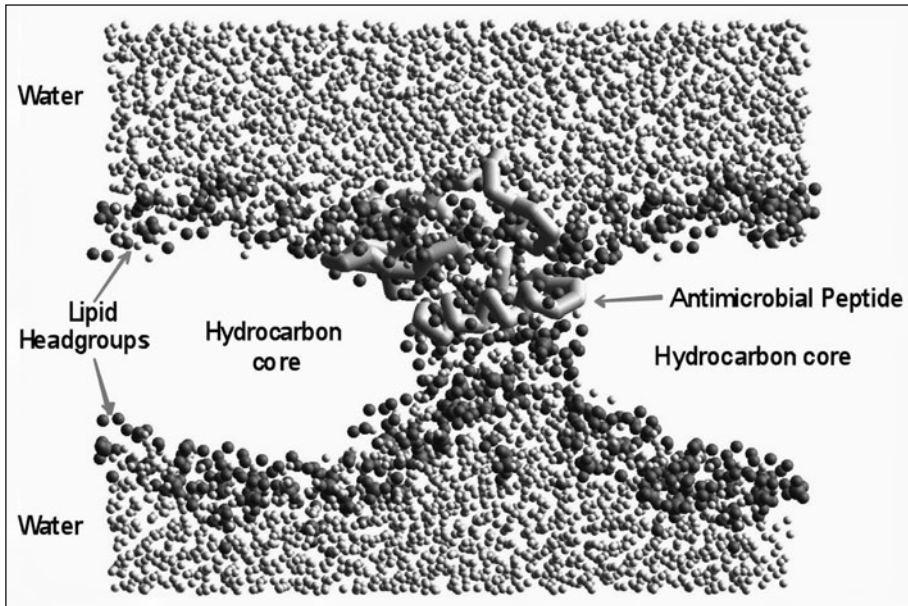


Figure 5. A simulated antimicrobial peptide in membranes. A realistic image of a peptide-induced pore in a bilayer. This image was adopted from the work of Marrink and colleagues²¹ who simulated the interaction of an antimicrobial peptide, magainin, with phospholipid bilayers. Instead of forming a regular, ordered channel, this “pore-forming” peptide acts by using its imperfect amphipathicity to disrupt the segregation of polar and nonpolar parts of the membrane. Notice the high concentration of polar groups infiltrating the nonpolar core in the vicinity of the peptides, shown as tubes. Waters are shown as light gray spheres while lipid polar groups (phosphate, choline and the ester bonds) are shown as darker spheres. Data file used was kindly provided by Das Sengupta and Siewert-Jan Marrink.

chapter, the basic principles of polypeptide binding, partitioning, folding and self assembly in membranes have been discussed.

References

1. White SH, Wimley WC. Membrane protein folding and stability: physical principles. *Annu Rev Biophys Biomol Struct* 1999; 28:319-365.
2. Wiener MC, White SH. Structure of a fluid dioleoylphosphatidylcholine bilayer determined by joint refinement of x-ray and neutron diffraction data. III. Complete structure. *Biophys J* 1992; 61:434-447.
3. White SH, Wimley WC. Hydrophobic interactions of peptides with membrane interfaces. *Biochim Biophys Acta* 1998; 1376:339-352.
4. Popot J-L, Engelman DM. Membrane Protein Folding and Oligomerization—The 2-Stage Model. *Biochemistry* 1990; 29:4031-4037.
5. White SH, Wimley WC, Ladokhin AS et al. Protein folding in membranes: Determining the energetics of peptide-bilayer interactions. *Methods Enzymol* 1998; 295:62-87.
6. Wimley WC, White SH. Experimentally determined hydrophobicity scale for proteins at membrane interfaces. *Nature Struct Biol* 1996; 3:842-848.
7. Jayasinghe S, Hristova K, White SH. Energetics, stability and prediction of transmembrane helices. *J Mol Biol* 2001; 312:927-934.
8. White SH, Ladokhin AS, Jayasinghe S et al. How membranes shape protein structure. *J Biol Chem* 2001; 276:32395-32398.
9. Hristova K, White SH. An experiment-based algorithm for predicting the partitioning of unfolded peptides into phosphatidylcholine bilayer interfaces. *Biochemistry* 2005; 44:12614-12619.

10. Jayasinghe S, Hristova K, White SH. Energetics, stability and prediction of transmembrane helices. *J Mol Biol* 2001; 312:927-934.
11. Yau WM, Wimley WC, Gawrisch K et al. The preference of tryptophan for membrane interfaces. *Biochemistry* 1998; 37:14713-14718.
12. Mulgrew-Nesbitt A, Diraviyam K, Wang J et al. The role of electrostatics in protein-membrane interactions. *Biochim Biophys Acta* 2006; 1761:812-826.
13. Seelig J, Nebel S, Ganz P et al. Electrostatic and nonpolar peptide-membrane interactions. Lipid binding and functional properties of somatostatin analogues of charge $z = +1$ to $z = +3$. *Biochemistry* 1993; 32:9714-9721.
14. Ladokhin AS, White SH. Protein chemistry at membrane interfaces: non-additivity of electrostatic and hydrophobic interactions. *J Mol Biol* 2001; 309:543-552.
15. Ladokhin AS, White SH. Folding of Amphipathic α -Helices on Membranes: Energetics of Helix Formation by Melittin. *J Mol Biol* 1999; 285:1363-1369.
16. Qian S, Wang W, Yang L et al. Structure of the Alamethicin Pore Reconstructed by X-ray Diffraction Analysis. *Biophys J* 2008; 94:3512-3522.
17. Gazit E, Miller IR, Biggin PC et al. Structure and orientation of the mammalian antibacterial peptide cecropin P1 within phospholipid membranes. *J Mol Biol* 1996; 258:860-870.
18. Hristova K, Selsted ME, White SH. Critical role of lipid composition in membrane permeabilization by rabbit neutrophil defensins. *J Biol Chem* 1997; 272:24224-24233.
19. Soloaga A, Ramírez JM, Goñi FM. Reversible denaturation, self-aggregation and membrane activity of *Escherichia coli* α -hemolysin, a protein stable in 6 M urea. *Biochemistry* 1998; 37:6387-6393.
20. Rathinakumar R, Wimley WC. Biomolecular engineering by combinatorial design and high-throughput screening: small, soluble peptides that permeabilize membranes. *J Am Chem Soc* 2008; 130:9849-9858.
21. Sengupta D, Leontiadou H, Mark A et al. Toroidal pores formed by antimicrobial peptides show significant disorder. *Biochim Biophys Acta* 2008; 1778:2308-2317.
22. Wimley WC, White SH. Membrane partitioning: Distinguishing bilayer effects from the hydrophobic effect. *Biochemistry* 1993; 32:6307-6312.
23. Song L, Hobaugh MR, Shustak C et al. Structure of staphylococcal α -hemolysin, a heptameric transmembrane pore. *Science* 1996; 274:1859-1866.

CHAPTER 3

Membrane Association and Pore Formation by Alpha-Helical Peptides

Burkhard Bechinger*

Abstract

Membrane-active peptides exhibit antimicrobial, channel-forming and transport activities and have therefore early on been interesting targets for biophysical investigations. When the peptide-lipid interactions are studied a dynamic view emerges in which the peptides change conformation upon membrane insertion, can adopt a variety of topologies and change the macroscopic phase properties of the membrane locally or globally. Interestingly several proteins have been identified that also interact with the membrane in a dynamic fashion and where the lessons learned from peptides may add to our understanding of the ways these proteins function.

Introduction

Despite the importance and abundance of membrane proteins their structural investigation lags behind that of soluble proteins due to the problems associated with their biochemical preparation in a functional state and the subsequent difficulties associated with their structural investigation using x-ray crystallography or solution NMR spectroscopy. As a consequence, the existing membrane protein structural data bases encompass only a few dozen structures of membrane proteins and these show the formation of helical bundles or beta barrels within the lipid bilayer.^{1,2}

However, early on a number of membrane-active peptides were available from natural sources, such as alamethicin and melittin,³ or by design⁴⁻⁶ and their study by biophysical approaches has provided valuable insight into polypeptide lipid interactions as well as their mechanisms of membrane permeabilization and pore formation. Up to this day their investigation allows us to discover unexpected structural and dynamic features of membrane-associated polypeptides^{7,8} and from such studies a picture emerges with multiple equilibria govern their membrane interactions and conformations (Fig. 1).

Alamethicin and Other Peptaibols

Peptaibols are peptides of fungal origin rich in α -aminobutyric acid (Aib) and the best-known member of this family is the dodecameric peptide alamethicin. When added to planar lipid bilayers voltage-dependent conductance changes are observed and these peptides have therefore early on served as a paradigm for large voltage- or ligand-gated channel proteins (reviewed e.g., in ref. 9). The open alamethicin pore is thought to consist of a 'transmembrane helical bundle' in which the individual helices are grouped with their more hydrophilic side facing the water-filled pore.¹⁰ Notably, recent molecular dynamics calculations of membrane-bound alamethicin suggest that the macromolecular arrangement of the helix bundle is less regular and more asymmetric than the first models suggested.¹¹ Similar transmembrane helical bundle arrangements have been observed

*Burkhard Bechinger—Institut de chimie, CNRS—Université de Strasbourg, UMR 7177, 4, rue Blaise Pascal, 67070 Strasbourg, France. Email: bechinger@chimie.u-strasbg.fr

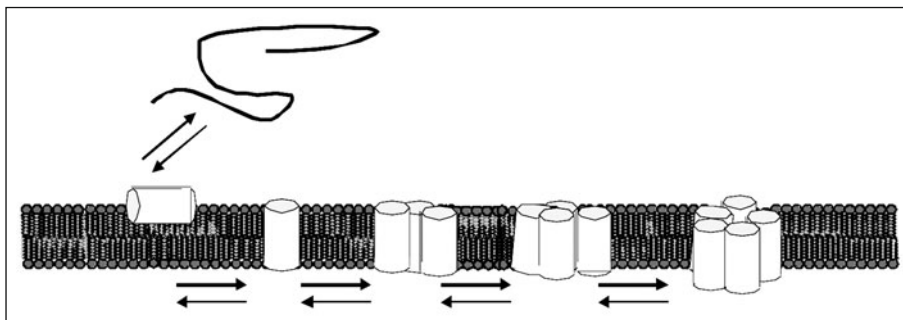


Figure 1. Membrane-associated peptides can adopt a number of different topologies and aggregation states depending on peptide sequence, lipid composition, peptide-to-lipid ratio and other environmental factors.

for a variety of membrane proteins including potassium channels, the acetylcholine receptor, the influenza proton channel or the phospholamban pentamer.¹²⁻¹⁷

The transmembrane helical bundle model is consolidated by structural investigations which indicate that alamethicin exhibits indeed a preference for helical conformations with a flexible hinge region around proline-14.¹⁸⁻²⁰ Furthermore a strong propensity for transmembrane alignments of alamethicin is observed by oriented solid-state NMR spectroscopy.²¹⁻²³ Nevertheless it should be mentioned that biophysical investigations indicate a high degree of conformational flexibility where the degree of helix formation is dependent on the physical state of the lipid, the lipid-peptide ratio, the presence of transmembrane potentials and other environmental parameters (reviewed e.g., in refs. 3,24).

When alamethicin is added to planar lipid bilayers a step-wise reduction of the membrane ohmic resistance is observed resulting in a well-defined pattern of successive conductance levels. Each of them is a few milliseconds in duration and the size of the ionic currents together with molecular modelling suggest that the smallest conducting structures consist of trimers, tetramers or pentamers (reviewed in ref. 3). The activation energies for the initial formation and decay of the lowest conductance state are 50 and 120 kJ/mole, respectively and with this first peptide aggregate formed the addition and subtraction of units occurs quickly on a millisecond time scale (Fig. 1).

Using a variety of biophysical approaches including oriented solid-state NMR and CD spectroscopies it has been observed that alamethicin and related peptaibols can adopt in-planar as well as transmembrane (TM) alignments, with the latter being favoured at high peptide-to-lipid ratios.²⁵ This led to the idea that the in-planar state of alamethicin is an intermediate during membrane association and channel gating¹⁰ and that a series of subsequent equilibria govern the polypeptide interactions within the membrane (in-plane \leftrightarrow transmembrane \leftrightarrow TM oligomers, Fig. 1). Various models for the molecular mechanism of alamethicin pore-formation are based on interactions of its helix dipole with the TM electric field (reviewed in ref. 3), where reorientation of the dipole, enhanced partitioning of alamethicin into the bilayer and/or membrane insertion of the N-terminus result in the voltage-gating of the channel structure.²⁶

With the transmembrane helical bundle model in mind amphipathic model sequences composed of leucine and serine residues have been designed.⁴ However, these sequences reside predominantly at the membrane surface²⁷ although it cannot be excluded that a smaller fraction inserts in a transmembrane fashion and is responsible for the channel forming properties.²⁷ Indeed, depending on the peptide-to-lipid ratio, the length of the peptide sequence and/or the lipid composition peptaibols, including zervamicin IIa (15 residues), ampullosporin A (15 residues) and alamethicin (20 residues), can also adopt alignments parallel to the membrane surface in particular under hydrophobic mismatch conditions.^{8,22,28} This observation is suggestive

that also these peptides can cause membrane permeability increases by mechanisms other than transmembrane helical bundle formation.

Cationic Amphipathic Antimicrobial Peptides

Amphipathic peptides are found in many species where they protect the host against a wide range of antimicrobial infections^{29,30} and from a number of observations it was concluded that these peptides directly interact with the phospholipid membranes rather than with specific receptors (reviewed e.g., in refs. 31, 32). By interacting with the membranes of sensitive organisms these peptides disturb their bilayer integrity, either by disruption or pore formation and thereby develop antimicrobial and toxic activities as well as perform entry to the cell interior.³³

Discrete multi-level conductances have also been observed when cecropins, magainins, melittin or other amphipathic sequences are added to preformed bilayers (reviewed e.g., in ref. 31). Whereas the former two belong to the family of linear cationic peptide antimicrobials, melittin is a 26-residue peptide found in the toxin of the honey bee *Apis mellifera*. However, the channel properties of magainins and cecropins are less well defined and contrast those observed from alamethicin.

In contrast to peptaibols, which adopt amphipathic but mostly uncharged structures in membranes, linear cationic peptide antibiotics are highly charged and soluble in aqueous environments where they exhibit random coil conformations.³¹ By using oriented solid-state NMR spectroscopy it has been possible to show early on that these amphipathic peptides intercalate into the membrane with the helix axis oriented parallel to the membrane surface.³¹ In this configuration the hydrophobic region is localized about 10 Å above the bilayer center in agreement with the amphipathic distribution of polar-charged and hydrophobic residues.³⁴ In this configuration the peptides cause pronounced disordering of the fatty acyl chain packing,³⁵ membrane thinning,³⁶ pore formation³⁷ and macroscopic phase transitions of the peptide-lipid assembly.³⁸

When added to preformed bilayers magainins and melittin partition into the membranes within 10-100 seconds.^{39,40} The association of magainin 2 is characterized by a partitioning coefficient of about 10^3 M^{-1} in the presence of zwitterionic membranes,⁴¹ a value that increases by 2-3 orders of magnitude for negatively charged membranes.⁴² This is easily explained by electrostatic attraction which causes an increase in the local concentration of positively charged peptide next to the anionic membrane surface. However, it seems that association with anionic lipids is different as their membrane permeabilizing activities of negatively charged membranes is reduced when the number of peptides associated with the membrane is taken into explicit consideration.⁴³⁻⁴⁵ Furthermore, it has been shown that in mixed model membranes the cationic peptides preferentially interact with negatively charged membrane surfaces and a segregation of the acidic phospholipids occurs.⁴⁶ Therefore, electrostatic interactions not only control the membrane association of cationic amphiphiles, but they also have a pronounced effect on the lateral distribution of the lipids within mixed bilayers.

When added to lipid bilayers amphipathic peptides have been shown to undergo structural transitions upon membrane insertion as well as membrane alignments that are a function of peptide-to-lipid ratio and other environmental factors (reviewed e.g., in ref. 3). Furthermore, the peptides induce alterations in the lipid macroscopic phase properties an effect which has been described in considerable detail for melittin. Even at very low concentrations (0.1 mole %) this peptide exhibits pronounced effects on the phase properties of membranes made of dipalmitoylphosphatidylcholine indicating that the peptide modifies the membrane beyond its immediate neighbourhood.³ For other sequences it was shown that the bilayer packing is disturbed within an estimated radius of approximately 50 Å due to their insertion into the membrane interface.^{47,48}

When amphipathic helices partition into the bilayer they act as a spacer at the level of the lipid headgroup which would create voids in the hydrophobic region of the bilayer, but the hydrocarbon moieties compensate for such effects by chain bends, increased *trans-gauche* isomerization or chain interdigitation.⁴⁹ Indeed, deuterium and ¹³C solid-state NMR measurements indicate a decrease in the order parameter at the lipid bilayer interior in the presence of magainins and other amphipathic peptides.^{35,50,51} These effects depend on the peptide molecular properties but also the size and shape

of the lipid head groups and as a consequence the membrane lipid composition as well as the peptide structure have a pronounced influence on the membrane-peptide interactions. When added at high concentrations disk-shaped particles form and membrane disruptions occur⁵²⁻⁵⁴ an effect that can be partially compensated for by the presence of inverted wedge shaped lipids.^{38,53,55}

The full plasticity of phospholipid membranes when interacting with peptides is adequately described by phase diagrams representing the wide range of structures, configurations and morphologies as a function of peptide-to-lipid ratio, the detailed membrane composition, temperature, hydration and buffer composition.^{31,49} Depending on the exact conditions regions can be identified where bilayers, slightly perturbed or even stabilized in the presence of polypeptide, exist, lysis and membrane disintegration occur, but also conditions where membrane openings form in a more regular manner. The peptide-induced phase transitions and lipid—dependent interactions have been rationalized by the geometries of the molecules involved in membrane assembly and, therefore, the characteristics of the molecules such as their charge and hydrophobic volume influences how strongly they interact, how deeply they insert and how much curvature strain they exert on the membrane.³⁸ The resulting phase alterations can be transient and local, or they can affect the full supramolecular assembly as a whole.

Membrane Proteins

It is intriguing to note that proteins have been described where the partitioning between the membrane and the water phase constitutes an essential part of their biological regulatory mechanisms. It has even been suggested that in their membrane-associated form some of them resemble an array of loosely linked helices⁵⁶ and the peptides may therefore mirror the behaviour of defined regions of such proteins. For example, the pore-forming domains of several colicins have been shown to form voltage-gated channels in black lipid membranes, a process involving significant structural transitions.⁵⁷⁻⁵⁹ The solution structure of these proteins is characterized by 8-10 α -helices arranged in a three layered sandwich, where the central layer is composed of a hydrophobic helical hairpin,⁶⁰ a structural fold shared with other bacterial toxins as well as with the Bcl-2 family of proteins, the latter being key regulators of apoptosis.^{60,61}

During membrane insertion the colicin pore-domains undergo pronounced conformational changes^{56,62} and a structure is observed in membrane environments where the helices all orient approximately parallel to the surface and form tightly packed structures (pen-knife model).⁵⁸ Additional structural transitions can cause the alignment of the two hydrophobic helices in a transmembrane configuration when at the same time the amphipathic helices form a dynamic array of loosely connected helices.^{56,61} In contrast, the structure of the anti-apoptotic Bcl-x_L protein in the presence of lipid bilayers resembles a type I membrane protein where the C-terminus anchors the protein in the membrane but where the global fold remains largely functional.⁶³ An array structure of Bcl-x_L is however observed in the presence of detergents.⁶⁴ More recent experimental data indeed indicate that various membrane conformations of the colicin E1 and Ia channel domains co-exist and are in exchange with each other.^{65,66} Related structural transitions have also been observed for the diphtheria toxin T domain^{67,68} and such membrane protein structural arrangements agree with pore models where the lipids are part of the channel lining⁵⁹ analogous to the propositions made for amphipathic antimicrobial peptides.³¹

Conclusion

In conclusion, biophysical investigations have altered our view on peptide-lipid interactions and point to a highly dynamic situation and where the peptides as well as the membranes respond by adopting different conformations and morphologies. Whereas the membrane lipid composition has a pronounced effect on the amount of peptides associated, their penetration depth and their topology, the insertion of the peptides has been shown to modify the macroscopic phase properties of the membrane itself.

Acknowledgements

I am most thankful to a great team of coworkers and colleagues that over the years has contributed to our work. The ongoing financial support by *Vaincre la Mucoviscidose* (TG 501), the *Association pour la Recherche sur le Cancer* (no. 3100), the *Agence Nationale de Recherche* (MEMBAX, PolyQ and TRANSPEP) and the Marie-Curie Research and Training Network 33439 of the European Commission, 6th framework programme BIOCONTROL is gratefully acknowledged. The Institute of Supramolecular Chemistry of the University of Strasbourg gratefully hosts the laboratory.

References

1. Tusnady GE, Dosztanyi Z, Simon I. Transmembrane proteins in the protein data bank: identification and classification. *Bioinformatics* 2004; 20:2964-2972.
2. Raman P, Cherezov V, Caffrey M. The membrane protein data bank. *Cell Mol Life Sci* 2006; 63:36-51.
3. Bechinger B. Structure and functions of channel-forming polypeptides: magainins, cecropins, melittin and alamethicin. *J Membrane Biol* 1997; 156:197-211.
4. Lear JD, Wasserman ZR, DeGrado WF. Synthetic amphiphilic peptide models for protein ion channels. *Science* 1988; 240:1177-1181.
5. Bechinger B. Towards membrane protein design: pH dependent topology of histidine-containing polypeptides. *J Mol Biol* 1996; 263:768-775.
6. Killian JA, Salemink I, de Planque MRR et al. Induction of nonbilayer structures in diacylphosphatidylcholine model membranes by transmembrane α -helical peptides: Importance of hydrophobic mismatch and propose role of tryptophans. *Biochemistry* 1996; 35:1037-1045.
7. Hong M. Oligomeric structure, dynamics and orientation of membrane proteins from solid-state NMR. *Structure* 2006; 14:1731-1740.
8. Salnikow ES, Friedrich H, Li X et al. Structure and alignment of the membrane-associated peptaibols ampulsporin A and alamethicin by oriented ^{15}N and ^{31}P solid-state NMR spectroscopy. *Biophys J* 2009; 96:86-100.
9. Leitgeb B, Szekeres A, Manczinger L et al. The history of alamethicin: a review of the most extensively studied peptaibol. *Chem Biodivers* 2007; 4:1027-1051.
10. Sansom MS. Alamethicin and related peptaibols—model ion channels. *Eur Biophys J* 1993; 22:105-124.
11. Thogersen L, Schiott B, Vosegaard T et al. Peptide aggregation and pore formation in a lipid bilayer: a combined coarse-grained and all atom molecular dynamics study. *Biophys J* 2008; 95:4337-4347.
12. Unwin N. Refined structure of the nicotinic acetylcholine receptor at 4Å resolution. *J Mol Biol* 2005; 346:967-989.
13. Oxenoid K, Rice AJ, Chou JJ. Comparing the structure and dynamics of phospholamban pentamer in its unphosphorylated and pseudo-phosphorylated states. *Protein Sci* 2007; 16:1977-1983.
14. Traaseth NJ, Verardi R, Torgersen KD et al. Spectroscopic validation of the pentameric structure of phospholamban. *Proc Natl Acad Sci USA* 2007; 104:14676-14681.
15. Long SB, Tao X, Campbell EB et al. Atomic structure of a voltage-dependent K⁺ channel in a lipid membrane-like environment. *Nature* 2007; 450:376-382.
16. Schnell JR, Chou JJ. Structure and mechanism of the M2 proton channel of influenza A virus. *Nature* 2008; 451:591-595.
17. Stouffer AL, Acharya R, Salom D et al. Structural basis for the function and inhibition of an influenza virus proton channel. *Nature* 2008; 451:596-599.
18. Yee A, Szymczyna B, O'Neil JD. Backbone dynamics of detergent-solubilized alamethicin from amide hydrogen exchange measurements. *Biochemistry* 1999; 38:6489-6498.
19. Jacob J, Duclouhier H, Cafiso DS. The role of proline and glycine in determining the backbone flexibility of a channel-forming peptide. *Biophys J* 1999; 76:1367-1376.
20. Franklin JC, Ellena JF, Jayasinghe S et al. Structure of micelle-associated alamethicin from ^1H NMR. Evidence for conformational heterogeneity in a voltage-gated peptide. *Biochemistry* 1994; 33:4036-4045.
21. North CL, Barranger-Mathys M, Cafiso DS. Membrane orientation of the N-terminal segment of alamethicin determined by solid-state ^{15}N NMR. *Biophys J* 1995; 69:2392-2397.
22. Bechinger B, Skladnev DA, Ogrel A et al ^{15}N and ^{31}P solid-state NMR investigations on the orientation of zervamicin II and alamethicin in phosphatidylcholine membranes. *Biochemistry* 2001; 40:9428-9437.
23. Bak M, Bywater RP, Hohwy M et al. Conformation of alamethicin in oriented phospholipid bilayers determined by N-15 solid-state nuclear magnetic resonance. *Biophys J* 2001; 81:1684-1698.
24. Sansom MSP. The biophysics of peptide models of ion channels. *Prog Biophys Molec Biol* 1991; 55:139-235.
25. Huang HW. Action of antimicrobial peptides: Two-state model. *Biochemistry* 2000; 39:8347-8352.

26. Okazaki T, Sakoh M, Nagaoka Y et al. Ion channels of alamethicin dimer N-terminally linked by disulfide bond. *Biophys J* 2003; 85:267-273.
27. Sudheendra US, Bechinger B. Topological equilibria of ion channel peptides in oriented lipid bilayers revealed by ¹⁵N solid-state NMR spectroscopy. *Biochemistry* 2005; 44:12120-12127.
28. Salnikov ES, De Zotti M, Formaggio F et al. Alamethicin topology in phospholipid membranes by oriented solid-state NMR and EPR spectroscopies: A comparison. *J Phys Chem B* 2009; 113:3034-3042.
29. Zasloff M. Antimicrobial peptides of multicellular organisms. *Nature* 2002; 415:389-395.
30. Boman HG. Antibacterial peptides: basic facts and emerging concepts. *J Intern Med* 2003; 254:197-215.
31. Bechinger B. The structure, dynamics and orientation of antimicrobial peptides in membranes by solid-state NMR spectroscopy. *Biochim Biophys Acta* 1999; 1462:157-183.
32. Shai Y. Mode of action of membrane active antimicrobial peptides. *Biopolymers* 2002; 66:236-248.
33. Brogden KA. Antimicrobial peptides: pore formers or metabolic inhibitors in bacteria? *Nat Rev Microbiol* 2005; 3:238-250.
34. Matsuzaki K, Murase O, Tokuda H et al. Orientational and Aggregational States of Magainin 2 in Phospholipid Bilayers. *Biochemistry* 1994; 33:3342-3349.
35. Salnikov ES, Mason AJ, Bechinger B. Membrane order perturbation in the presence of antimicrobial peptides by ²H solid-state NMR spectroscopy. *Biochimie* 2009; 91:734-743.
36. Ludtke S, He K, Huang H. Membrane thinning caused by magainin 2. *Biochemistry* 1995; 34:16764-1679.
37. Gregory SM, Cavanaugh A, Journigan V et al. A quantitative model for the all-or-none permeabilization of phospholipid vesicles by the antimicrobial peptide cecropin A. *Biophys J* 2008; 94:1667-1680.
38. Bechinger B. Rationalizing the membrane interactions of cationic amphipathic antimicrobial peptides by their molecular shape. *Current Opinion in Colloid and Interface Science, Surfactants* (in press) 2009.
39. Mozsolits H, Wirth HJ, Werkmeister J et al. Analysis of antimicrobial peptide interactions with hybrid bilayer membrane systems using surface plasmon resonance. *Biochim Biophys Acta* 2001; 1512:64-76.
40. Papo N, Shai Y. Exploring peptide membrane interaction using surface plasmon resonance: differentiation between pore formation versus membrane disruption by lytic peptides. *Biochemistry* 2003; 42:458-466.
41. Wieprecht T, Beyermann M, Seelig J. Binding of antibacterial magainin peptides to electrically neutral membranes: Thermodynamics and structure. *Biochemistry* 1999; 38:10377-10378.
42. Wenk M, Seelig J. Magainin 2 amide interaction with lipid membranes: Calorimetric detection of peptide binding and pore formation. *Biochemistry* 1998; 37:3909-3916.
43. Vogt TCB, Bechinger B. The interactions of histidine-containing amphipathic helical peptide antibiotics with lipid bilayers: The effects of charges and pH. *J Biol Chem* 1999; 274:29115-29121.
44. Wieprecht T, Apostolov O, Beyermann M et al. Membrane binding and pore formation of the antibacterial peptide PGLa: thermodynamic and mechanistic aspects. *Biochemistry* 2000; 39:442-452.
45. Dathe M, Nikolenko H, Meyer J et al. Optimization of the antimicrobial activity of magainin peptides by modification of charge. *FEBS Lett* 2001; 501:146-150.
46. Mason AJ, Martinez A, Glaubitz C et al. The antibiotic and DNA-transfecting peptide LAH4 selectively associates with and disorders, anionic lipids in mixed membranes. *FASEB J* 2006; 20:320-322.
47. Chen FY, Lee MT, Huang HW. Evidence for membrane thinning effect as the mechanism for Peptide-induced pore formation. *Biophys J* 2003; 84:3751-3758.
48. Mecke A, Lee DK, Ramamoorthy A et al. Membrane thinning due to antimicrobial peptide binding: an atomic force microscopy study of MSI-78 in lipid bilayers. *Biophys J* 2005; 89:4043-4050.
49. Bechinger B, Lohner K. Detergent-like action of linear cationic membrane-active antibiotic peptides. *Biochim Biophys Acta* 2006; 1758:1529-1539.
50. Dvinskikh S, Durr U, Yamamoto K et al. A high-resolution solid-state NMR approach for the structural studies of bicelles. *J Am Chem Soc* 2006; 128:6326-6327.
51. Mason AJ, Bechinger B. Zwitterionic lipids and sterols modulate antimicrobial peptide-membrane interactions. *Biophys J* 2007; 93:4289-4299.
52. Dufourc EJ, Smith IC, Dufourcq J. Molecular details of melittin-induced lysis of phospholipid membranes as revealed by deuterium and phosphorus NMR. *Biochemistry* 1986; 25:6448-6455.
53. Hallock KJ, Lee DK, Omnaas J et al. Membrane composition determines pardaxin's mechanism of lipid bilayer disruption. *Biophys J* 2002; 83:1004-1013.
54. Bechinger B. Detergent-like properties of magainin antibiotic peptides: A ³¹P solid-state NMR study. *Biochim Biophys Acta* 2005; 1712:101-108.
55. Batenburg AM, van Esch JH, de Kruijff B. Melittin-induced changes of the macroscopic structure of phosphatidylethanolamines. *Biochemistry* 1988; 27:2324-2331.
56. Zakharov SD, Lindeberg M, Griko Y et al. Membrane-bound state of the colicin E1 channel domain as an extended two-dimensional helical array. *Proc Natl Acad Sci USA* 1998; 95:4282-4287.

57. Stroud RM, Reiling K, Wiener M et al. Ion-channel-forming colicins. *Curr Opin Struct Biol* 1998; 8:525-533.
58. Lakey JH, Slatin SL. Pore-forming colicins and their relatives. *Curr Top Microbiol Immunol* 2001; 257:131-161.
59. Zakharov SD, Cramer WA. Colicin crystal structures: pathways and mechanisms for colicin insertion into membranes. *Biochim Biophys Acta* 2002; 1565:333-346.
60. Petros AM, Olejniczak ET, Fesik SW. Structural biology of the Bcl-2 family of proteins. *Biochim Biophys Acta* 2004; 1644:83-94.
61. Pattus F, Massotte D, Wilmsen HU et al. Colicins: prokaryotic killer-pores. *Experientia* 1990; 46:180-192.
62. Sathish HA, Cusan M, Aisenbrey C et al. Guanidine hydrochloride induced equilibrium unfolding studies of colicin B and its channel-forming fragment. *Biochemistry* 2002; 41:5340-5347.
63. Aisenbrey C, Sudheendra US, Ridley H et al. Helix orientations in membrane-associated Bcl-X_L determined by ¹⁵N solid-state NMR spectroscopy. *Eur Biophys J* 2007; 36:451-460.
64. Losonczi JA, Olejniczak ET, Betz SF et al. NMR studies of the anti-apoptotic protein Bcl-x(L) in micelles. *Biochemistry* 2000; 39:11024-11033.
65. Kienker PK, Qiu X, Slatin SL et al. Transmembrane insertion of the colicin Ia hydrophobic hairpin. *J Membrane Biol* 1997; 157:27-37.
66. Aisenbrey C, Cusan M, Lambotte S et al. Specific isotope labeling of colicin E1 and B channel domains for membrane topological analysis by oriented solid-state NMR spectroscopy. *Chem Bio Chem* 2008; 9:944-951.
67. Malenbaum SE, Collier RJ, London E. Membrane topography of the T domain of diphtheria toxin probed with single tryptophan mutants. *Biochemistry* 1998; 37:17915-17922.
68. Chenal A, Prongidi-Fix L, Perier A et al. Deciphering membrane insertion of the diphtheria toxin T domain by specular neutron reflectometry and solid-state NMR spectroscopy. *J Mol Biol* 2009; 391:872-883

CHAPTER 4

Role of Membrane Lipids for the Activity of Pore Forming Peptides and Proteins

Gustavo Fuertes, Diana Giménez, Santi Esteban-Martín, Ana J. García-Sáez, Orlando Sánchez and Jesús Salgado*

Abstract

Bilayer lipids, far from being passive elements, have multiple roles in polypeptide-dependent pore formation. Lipids participate at all stages of the formation of pores by providing the binding site for proteins and peptides, conditioning their active structure and modulating the molecular reorganization of the membrane complex. Such general functions of lipids superimpose to other particular roles, from electrostatic and curvature effects to more specific actions in cases like cholesterol, sphingolipids or cardiolipin.

Pores are natural phenomena in lipid membranes. Driven by membrane fluctuations and packing defects, transient water pores are related to spontaneous lipid flip-flop and non-assisted ion permeation. In the absence of proteins or peptides, these are rare short living events, with properties dependent on the lipid composition of the membrane. Their frequency increases under conditions of internal membrane disturbance of the lipid packing, like in the presence of membrane-bound proteins or peptides. These latter molecules, in fact, form dynamic supramolecular assemblies together with the lipids and transmembrane pores are one of the possible structures of the complex. Active peptides and proteins can thus be considered inducers or enhancers of pores which increase their probability and lifetime by modifying the thermodynamic membrane balance. This includes destabilizing the membrane lamellar structure, lowering the activation energy for pore formation and stabilizing the open pore structure.

Introduction

Biomembranes can be regarded as supramolecular complexes where the structure, dynamics and mechanical properties are dominated by the background physical chemistry of lipids. The lipids impose liquid-crystal order within the membrane complex, including embedded proteins or peptides¹ and may affect their structure, orientation, dynamics and aggregation state.^{2,4} The bound polypeptides, in turn, change the composition and the physicochemical context of the membrane where they are hosted and can end up affecting its molecular organization.^{5,6} Such bilayer perturbations or deformations, which can also be related to the membrane material properties, are important to define the stability and functional structure of the polypeptide-bilayer complex.^{7,8} Thus, many dynamic processes occurring in biological membranes result from the mutual adaptation between lipids and polypeptides. Pore formation is an example of such processes.

*Corresponding Author: Jesús Salgado—Instituto de Ciencia Molecular, University of Valencia Pol. La Coma, 46980 Paterna (Valencia) Spain. Email: jesus.salgado@uv.es

Although with a very low probability, or associated with stress conditions, pores can exist in lipid membranes in the absence of peptides or proteins.⁹⁻¹² It is thus natural to relate polypeptide induced pores and tension-induced lipidic pores as closely connected phenomena.¹³ Even for the cases where polypeptides are clear protagonists, lipids are more than just a passive barrier traversed by the pore.^{5,14-16} However, in analogy with intrinsic membrane-protein channels and transporters, the mechanisms and structures associated to pore formation have most often been studied using proteocentric views. In this chapter we discuss the possible roles of lipids for the activity of pore-forming peptides and proteins, here named generically pore-forming polypeptides, or PFPP(s). With the exception of some specific cases, which will be clearly identified, we will use a general, integrated view for these two types of molecules, supported among other things by the fact that the essentials of the membrane activity of pore forming proteins can be reproduced by individual peptide fragments.¹⁷⁻¹⁹ Additionally, the large number and diversity of polypeptide molecules exhibiting similar pore activities over multiple types of membranes shows that this is a weakly specific phenomenon, loosely codified by the polypeptide sequence. In fact, structure-function relationships in these cases appear to follow special rules, based on interfacial activity and modulated by physicochemical balances of properties like hydrophobicity and amphipathicity.²⁰ Thus, we will favor a generic discussion of the role of lipids, instead of detailed descriptions for particular systems and well known cases of specific roles, like those of sphingolipids (SL), cholesterol (Cho) or cardiolipin (CL), will be just briefly summarized for some examples. The integrated view extends up to the model of the pore formation (see below). For this, we will extract the main consensus ideas of previous models by Matsuzaki, Huang and Shai,²¹ complemented with recent interpretations from molecular dynamics (MD) simulations,^{22,23} kinetics and single-vesicle studies.²⁴⁻²⁷

With this in mind, the role of lipids in pore formation can be envisioned at three different levels. First, lipids can be regarded as receptors or dynamic docking-surfaces for the binding of PFPPs to membranes from the external water milieu. Second, the lipids may condition the structure adopted by PFPPs upon membrane binding. And third, lipids can participate in the molecular reorganization of the polypeptide-membrane complex, to end up with the formation of a pore. Depending on the particular mechanism and the type of pore structure which is finally formed, the lipids can be more or less directly involved. For example, participation is clear when lipids act as specific receptors, like in the cases of Cho for Cho-dependent cytolysins (CDC)²⁸ and sphingomyelin (SM) for actinoporins.²⁹ Lipids play also a very direct role for the so called toroidal pores,^{30,31} where they form part of the pore wall, a model which appears appropriate for most antimicrobial peptides^{21,30-32} and many α -pore forming proteins.^{14,18,33-36} Once pores are formed, the lipids may exert a further active role cooperating with polypeptides in the stabilization of the pore.¹³ We should bear in mind that the first two levels of lipid participation (docking and refolding) apply in general to any spontaneous membrane protein binding, insertion and folding. The third level applies to any case where pores are formed at some stage, even if they are not stable, functional or final structures. For example, it is known that fusion peptides may induce vesicle perturbations defined as pore-like structures³⁷⁻³⁹; as it is also known that cargo peptides work through transient transmembrane pores.^{40,41}

Membrane Interfaces Are Ideal Binding Sites for Pore-Forming Peptides and Proteins

Most natural and synthetic pore-forming peptides as well as membrane active parts of pore-forming proteins are composed of hydrophobic, hydrophilic and cationic residues which arrange into amphipathic structures.^{21,42,43} The lipid bilayer interface provides an optimal region where physicochemical properties complement the amphipathicity of PFPPs for an effective binding (Fig. 1A-D).⁴⁴⁻⁴⁸ The charged and polar residues will prefer to reside in the hydrated headgroup region, where they may participate in a variety of stabilizing electrostatic forces.^{45,49} With most PFPPs being cationic, the positively charged groups (of Lys and Arg residues) interact closely with the phosphate groups of phospholipids.^{5,50-53} This binding mode allows simultaneous immersion of the hydrophobic side-chains into the membrane hydrophobic core, facilitated by the fact that

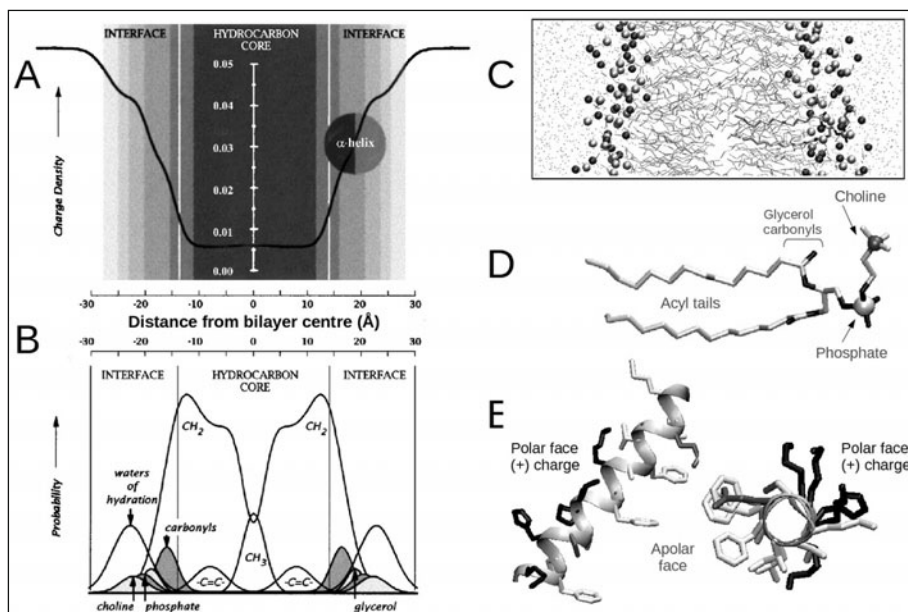


Figure 1. The membrane as a docking surface. Structure of a phospholipid bilayer with emphasis on the physicochemical complexity of the interfaces and its complementarity with amphipathic polypeptides. (A) and (B) show representations of the polarity gradient and structure, respectively of a fluid liquid-crystalline dioleoylphosphatidylcholine (DOPC) bilayer from X-ray and neutron diffraction data.^{44,46,205} The structure in (B) is represented as the time-averaged Gaussian distributions of the main chemical groups of the lipid projected onto the bilayer normal. The interfaces are the regions defined by the distribution of headgroup's water of hydration and the hydrocarbon core is the center slab where the presence of water drops to zero. From these distributions of quasimolecular groups, average charge densities and a polarity profile have been derived.⁴⁴ The profile is represented in (A) by a heavy line and the corresponding polarity gradient is schematized by a gray scale, which in the interface goes from more polar (pale gray) to more hydrophobic (dark gray) and in the hydrocarbon core is a constant black slab. For comparison, a circle representing the cross section of an amphipathic α -helix is drawn to scale and placed at the steepest point of the polarity gradient, corresponding to the position determined by X-ray diffraction.²⁰⁶ The experimental membrane structure can be appropriately modelled at atomic detail by MD simulations, as is shown in (C) for a simulated self-assembled dimyristoylphosphatidylcholine (DMPC) bilayer taken from work reported in reference 1. Acyl-chains are drawn with light-gray lines, phosphate groups as light-grey balls, nitrogens of choline as dark-grey balls and water oxygens as black dots (the oxygens of lipids are not represented). A DMPC lipid highlighted in (C) with thick lines is shown enlarged with more detail in (D) (same colors as in (C) and glycerol oxygens as black lines). In (E) we represent lateral and top views (left and right, respectively) of the amphipathic α -helix structure of magainin 2, solved in detergent micelles²⁰⁷ (pdb ID: 2mag). Only residues 4 to 20 are represented; positively charged residues (Lys and His) are colored black, the negatively charged Glu is colored dark gray and hydrophobic residues are pale gray. Panels (A) and (B) are reprinted with permission from the *Annual Review of Biophysics*, Volume 28 (ref. 46), © 1999 by Annual Reviews, www.annualreviews.org

the charges in Lys and Arg are at the end of long and flexible aliphatic chains and can thus snorkel toward the interface from relatively deep positions.^{50,51} For amphipathic α -helices (Fig. 1E), the binding depth is expected to depend on the helix polar angle, which determines the size of the hydrophobic sector of the helix relative to the polar sector.^{42,54,55} Such an adaptation of amphipathic polypeptides for binding at membrane interfaces has been termed partition-folding coupling⁴⁴

and is explained with more detail in the next section (see Fig. 2A). It implies that the stability of the membrane-polypeptide complex increases as the secondary structure is formed, as it is indeed observed for a number of different systems.^{44,45,56-62} Thus, phospholipid membrane interfaces can be envisioned as ideal binding sites for docking amphipathic, PFPPs (see Fig. 1).^{45,46} Supporting a direct targeting role of phospholipid membranes, with no intervention of receptor proteins, are the facts that PFPPs are active against pure lipid vesicles and at least in the case of peptides, independent on chirality (all D-aminoacid peptides are as active as natural L-aminoacid versions).⁶³

One consequence of the direct lipid-based membrane targeting is a relatively low specificity. For example, scrambled sequences of pore forming peptides tend to have similar activity^{20,64} and in general hundreds of different peptides and proteins, differing in size, secondary, tertiary and quaternary structure, share a similar mode of binding.^{21,32,65,66} Moreover, the similarity extends outside the family of PFPPs to cell penetrating peptides,^{67,68} fusion peptides³⁷ and with striking relationships to membrane active proteins of different types and across disparate organisms.⁶⁵ Nevertheless, lipid-based targeting can be also the source of complex binding schemes, including high affinity, cooperativity and lipid-dependent protein assembly.^{69,70} The general non specific interfacial binding can in some cases superimpose to additional interactions with a different degree of specificity, from strong electrostatic effects, like in the case of negatively charged membranes, to sophisticated and efficient control mechanisms through specific interactions with receptor lipids or lipid-anchored proteins. Some examples of these, more specific, roles are summarized below.

General Effects of Negatively Charged Lipids

Because most PFPPs are cationic, a way to increase their binding from solution is by presence of negatively charged lipids. In neutral membranes, binding of PFPPs depends mainly on their hydrophobicity, which accentuates the importance of structural parameters like hydrophobic moment and helicity.⁴² Partitioning cationic peptides into zwitterionic lipids is generally weak, corresponding to dissociation constants of up to 1 mM. However, the presence of negatively charged lipids, like those with phosphatidylglycerol (PG), phosphatidylserine (PS) and phosphatidylinositol (PI) head groups, pose an electrostatic attraction over the peptides which increases the strength of their binding up to dissociation constants in the μM range. A careful kinetic analysis shows that the stronger binding of cecropin and magainin to acidic lipids is due mainly to a reduced desorption rate.^{24,71} It is also seen that the main contribution of electrostatic interactions is increasing the concentration of the interfacially adsorbed peptide. Thus, discounting this effect on the basis of Gouy-Chapman theory⁷² (i.e., replacing bulk concentrations by surface concentrations) yields similar binding constants and pore activities regardless of the membrane surface-charge density.^{27,56,73,74}

The electrostatic contribution is the main basis for the selective binding of peptide antimicrobials to bacteria,²¹ since the outer membrane of these microorganisms is abundant in negatively charged lipids, in contrast to the plasma membranes of eukaryotic cells, abundant in neutral lipids.⁷⁵ However, this alone cannot explain the selective killing of peptide antibiotics against bacteria, compared to host cells. Such a selectivity can be understood considering the characteristic strong, membrane-mediated cooperativity of these systems, observed as a nonlinear concentration dependence with a rapid rise of activity passed a threshold concentration value.⁶⁹ Thus, the different affinity for neutral compared to acidic membranes places normal extracellular peptide concentrations well above the threshold for bacteria, but below the threshold for eukaryotic cells. The cooperativity originates from the effect of peptide binding on the bilayer material properties^{69,76} and is discussed below with more detail in connexion to the mechanism of pore formation. An additional factor explaining cell-type selectivity of antimicrobial peptides is the presence of Cho in eukaryotic cells, which in general reduces peptide and protein binding to the membrane and affects as well their oligomeric assembly, membrane insertion pattern and pore activity⁷⁷⁻⁷⁹ (see below).

A preferential binding to negatively charged membranes is also observed for some pore forming colicins⁸⁰ and for active fragments of the Bcl-2 family.¹⁸ However, in these cases the

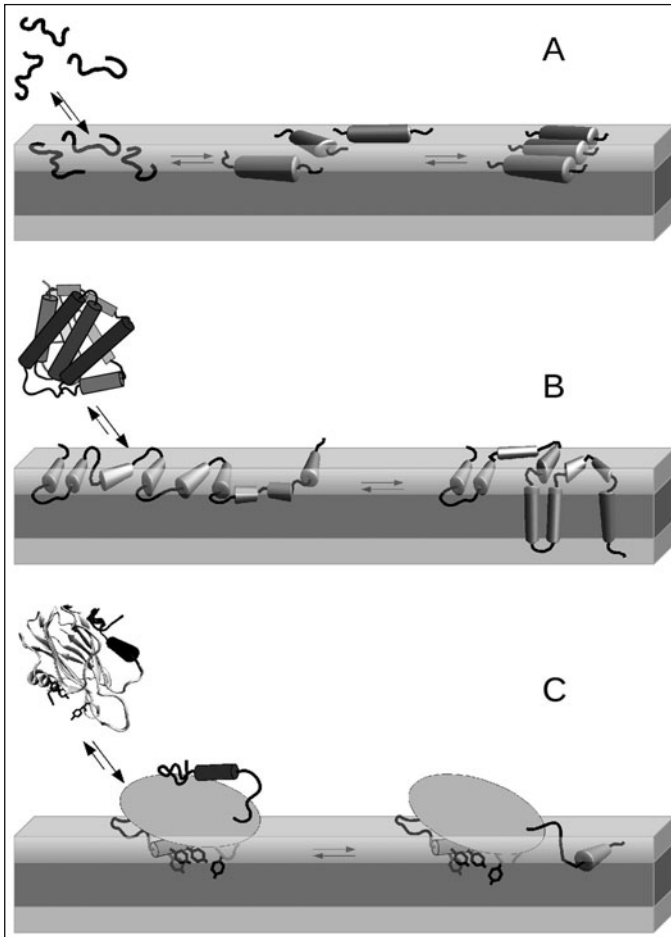


Figure 2. Chaperon-like foldase activity of membranes. Lipid membranes control refolding of polypeptides partitioning into them. A) Partitioning-folding coupling of amphipathic peptides at the bilayer interface. The membrane is represented by three slabs colored light-grey (interfaces) and dark-gray (hydrocarbon core). Curled lines are coil structure and cylinders represent α -helices. The peptides are mostly unstructured in water. Immediately after binding to the membrane surface, the interface promotes the appearance of secondary structure, most often through a coil-to-helix transition, which accentuates amphipathicity and strengthens binding following the interface polarity gradient (see Fig. 1). In some cases the helices might interact with each other forming oligomers. B,C) Partitioning-refolding of globular water-soluble pore-forming proteins as they bind to the membrane. The structure change can be dramatic (B) upon adsorbing into the interface (may also include a molten-globule intermediate¹¹³), like in the case of α -helix bundle proteins (for example channel domains of colicins or Bcl-2 proteins). These form a dynamic two-dimensional array of helices, which may evolve further through intermediates to insert the most hydrophobic helices across the membrane. In (C), sticholysin II (initial structure from ref. 87) suffers a partial refolding upon specific interfacial binding to SM through a cluster or Tyr residues (highlighted with thick black lines). The change of structure affects mainly an N-terminal amphipathic helix, which detaches from an almost unchanged β -sandwich core and lays flat in the membrane. In all cases successive molecular reorganizations give rise to transmembrane pores (not shown), which depending on the case may also involve protein oligomerization.

electrostatic interactions may have also an inhibitory effect on activity, since the strong interfacial binding appears to hinder pore formation. It has been also suggested that some effects of negatively charged lipids are connected to their intrinsic curvature properties, as it seems to be the case for the enhanced activity of Sticholysins I and II in presence of PS, PI, phosphatidic acid (PA) and CL.³³

Some Specific Roles of Lipids for Membrane Binding

In a number of cases, binding of PFPPs can be influenced specifically by the presence of particular lipids. Among them, Cho and SL, which are main constituents of liquid-ordered (L_O) microdomains, also called lipid rafts, are interesting examples. Cho is characteristic of the plasma membrane of mammalian cells, where it represents up to 40 mol %⁷⁵ and is known to be important for the modulation of membrane fluidity through a general condensing effect that stiffens the bilayer and promotes the formation of L_O phases.^{81,82} Due to its effect on the membrane mechanical properties, Cho-rich membranes are generally resistant to leakage induced by polypeptides, by way of reducing their binding to the membrane⁷⁹ and hindering pore formation.⁷⁷ In membranes containing SM and Cho, pore-forming peptides of different families,⁶⁸ as well as the active fragment α -helix 5 from Bax,⁸³ bind preferentially to the liquid-disordered (L_D) domains and induce coalescence of the L_O domains by reducing the line tension at domain boundaries. Cho has been also reported to hinder the membrane insertion of the β -hairpin antimicrobial peptide PG1 and its oligomerization into a β -barrel.⁷⁸

On the other hand Cho is necessary for the effective binding and activity of β -pore forming toxins from the large CDC family, which are highly toxic for mammalian cells.²⁸ The selective binding of CDC to Cho-rich regions, presumably lipid rafts, serves as a mechanism for cell discrimination, as these toxins do not affect the Cho-free bacterial membranes of the source organisms. With the notable exception of intermedilysin, which binds to a specific glycosyl phosphatidylinositol (GPI)-anchored protein receptor,⁸⁴ membrane targeting of CDCs occurs through a direct recognition of Cho via a Trp-rich conserved undecapeptide sequence.^{85,86} This is found as a protruding loop at the tip of a β -sandwich domain (domain 4),⁸⁶ commonly used for the shallow interfacial binding of many peripheral membrane proteins.⁶⁵ Actinoporins, a type of α -pore forming proteins,⁶⁶ share with CDCs the use of a β -sandwich domain to attach to membranes. However in this case the specificity is toward SM,^{29,87,88} where it binds via lipid rafts⁸⁹ and lipid phase coexistence.^{33,90-92} SM in lipid rafts is also responsible for binding of α -hemolysin to erythrocyte membranes.⁷⁰ In this case the site of binding is thought to be configured by phosphocholine (PC) head groups clustered in SM-Cho microdomains, which provide a two-dimensional spatial arrangement able to promote protein oligomerization and simultaneously increase the affinity to the membrane. A similar role of L_O domains as concentration platforms may be common to other toxins exhibiting raft-related activity (see below).⁹³

The mitochondrial permeability increase caused by proteins of the Bcl-2 family during apoptosis is regulated by specific lipids and membrane properties.^{94,95} CL is a characteristic lipid of the mitochondrial inner membrane and has been related to the apoptotic release of cytochrome *c*.^{94,96-100} This negatively charged lipid provides specific targeting of tBid to mitochondria through a high affinity binding domain.⁹⁶ The protein gets access to CL at the contact sites between inner and outer mitochondrial membranes. This, in turn, causes membrane remodelling and reordering of lipids, specially CL, which is mobilized to the outer membrane.⁹⁷⁻⁹⁹ Experiments with vesicles reconstituted with mitochondrial lipids show that CL is also necessary for Bax action,⁹⁴ participating in the recruitment and activation of the protein.¹⁰¹ However, the definition of a specific role of CL for the pore activity of Bcl-2 is complicated, since this lipid is related to multiple other functions, like mitochondrial metabolism, oxidative stress, anchoring and regulation of mitochondrial proteins.¹⁰⁰ For example, CL anchors cytochrome *c* to the mitochondrial inner membrane and is likely involved in the mobilization and release of this protein from its membrane attachment.¹⁰² Additionally, it appears to be connected to the mitochondrial oxidative metabolism, via CL peroxidation, due to exposure to reactive oxygen species.¹⁰³

A Membrane Foldase Activity Configures Peptide and Protein Active Structures

Pore-forming polypeptides can be found in alternative water soluble and membrane bound species with different corresponding structures (Fig. 2). Because their function is performed in the membrane, the change of structure associated to membrane binding is an important step for their activation. The question of how membrane-mediated activation takes place is connected to the more general question of how solvent influences protein folding.⁴⁶ Pore-forming peptides change from an unfolded state in the high dielectric water medium to an organized structure, in most cases α -helical, in the hydrophobic membrane environment (Fig. 2A). Pore-forming proteins have globular compact structures in water, which largely reorganize in the membrane-bound state (Fig. 2B,C). In both cases the structural readaptation follows a multi-step process which typically involves deeper insertion in the membrane and in some instances oligomerization. This role of the lipid membrane in promoting protein activation through a control of protein folding can be described as a chaperon-like foldase activity. How these conformational changes take place can be very different depending on the case, especially for the pore forming proteins.¹⁰⁴ Here, again, we will distinguish a generic role of the membrane, valid for all cases at least to some extent, from other more specific roles.

Structure Remodelling at the Membrane Interface

As we have discussed above, the membrane interface is the receiving surface for PFPs reaching the lipid bilayer. This chemically heterogeneous region, where physicochemical properties vary dramatically with depth (Fig. 1A-D),^{44,45} is ideal for stabilizing polypeptides in different conformations and thus for facilitating their molecular re-adaptation. Because partitioning of free backbone-peptide groups to this environment is very unfavorable, compared to H-bonded groups, there is a strong tendency to form secondary structures.^{46,47,105} Moreover, folding (typically as α -helix) is accompanied by the accentuation of amphipathicity (Fig. 1E), which then increases the stability of the polypeptide in the interface and, following the hydrophobicity gradient, favors a deeper binding.^{45,56} The membrane-dependent coil-to-helix transition of peptides has been described as partitioning-folding coupling (Fig. 2A).⁴⁴ It has been characterized experimentally^{56-60,73,106} and also studied in detail by MD simulations.^{52,53,107,108} Membrane-induced α -helix formation is exothermic and energetically favorable, with reported free energy changes for folding in the range of -0.14 to -0.4 kcal/mol per amino acid residue.^{47,56,57,74,109} Although with more modest thermodynamic consequences, β -structure is also favored by membranes.^{47,61,105,110,111} Thus, for pore-forming peptides, interfacial binding involves a large increase of their secondary structure with respect to their state in water (where they are largely unfolded).^{42,56,57,59,60,73,74,106,109} Nevertheless, molecular dynamics simulations of pores formed by magainin and melittin suggest that well structured α -helices are not a prerequisite for pore formation.^{22,23} In line with that conclusion a D-amino acid synthetic analog of melittin, having predominant β -structure, has been found to be active,⁵⁶ although membrane binding in this case is indeed largely decreased compared to that of the native α -helix peptide.⁵⁶

Pore-forming proteins also reorganize their structure due to membrane binding, which we can name partitioning-refolding (Fig. 2B,C). For α -pore forming proteins such a structural reorganization is in some cases preceded by a pH-dependent molten-globule intermediate^{112,113} and may include the detachment of a single preformed α -helix from the protein core (case of actinoporins, illustrated in Fig. 2C), a general increase of the proportion and average length of various α -helices (case of colicin E1 channel domain)¹¹⁴ and several pH-dependent refolding states (case of Diphtheria toxin T-domain).^{62,115} On the other hand, β -pore forming proteins must often refold part of their structure so that different subunits can donate β strands to form oligomeric β -barrels.¹⁰⁴ This, in the case of CDCs, occurs through a switch of secondary structure from α -helices to β -hairpins.^{28,116}

Another important characteristic of the membrane interface is anisotropy, which constrains the possible molecular configurations in the membrane complex to a small number. This selects a flat arrangement of amphipathic polypeptides (Fig. 2A), with the main axis of peptide segments

running near parallel to the membrane plane. Such is the configuration most often found experimentally for pore-forming peptides.¹¹⁷ In these cases, changes into a perpendicular alignment have been seen accompanying pore formation over a threshold peptide concentration¹¹⁸ (see below and Fig. 6) or associated to a change of the phase of the lipids.^{119,120} For helix-bundle α -pore forming proteins, this corresponds to extended two-dimensional arrays of helices (Fig. 2B), which have been characterized as membrane-dependent refolding intermediates for some colicins^{114,121,122} and members of the Bcl-2 family.¹²³⁻¹²⁵ Because the hydrophobic length of α -helices in these proteins is relatively short (with the exception of a C-terminal helix in some Bcl-2 members), binding across the membrane should be disfavored, at least in monomeric prepore states. However, a characteristic central hairpin of helices is often found in a transmembrane fashion.^{122,126-130}

The Lipid Membrane Controls Inter-Protein Interactions

As another way to reshape peptides and proteins, membrane interfaces can promote inter-molecular association of these molecules. Oligomerization is in many cases a characteristic step for the activation of PFPPs. However, with a few exceptions,¹³¹ the water soluble states are monomeric and oligomers form as prepore structures which are strictly dependent on membrane binding.¹⁰⁴ In general the membrane controls oligomerization at the level of protein (or peptide) folding, by reconfiguring the structure to shape the binding sites and/or by making such binding sites accessible. In the case of pore forming peptides the presence and possible role of oligomers is not always clear.⁷⁶ In molecular dynamics simulations of pore formation by magainin and melittin the appearance of interfacially adsorbed aggregates is a prerequisite for pore induction.^{22,23} A characteristic endothermic step in the calorimetric titration of melittin has been assigned as a reversible peptide aggregation (coupled to pore formation), occurring after membrane binding and α -helix formation.⁵⁶ In that study peptide aggregation is described with a phase diagram depending on the total peptide and lipid concentrations, with three phases corresponding to monomers, aggregates and coexistence of monomers and aggregates and phase boundaries defined by threshold values of the peptide-to-lipid molar fractions (P/L).⁵⁶ Such boundaries correspond to the threshold peptide-to-lipid mole fraction (P/L*) in the two-state model of Huang and colleagues,¹¹⁸ which has been recently reformulated also as a two-phase model.⁶⁹

In some CDCs the release of the oligomerization site is performed through proteolytic cleavage of a propeptide by a membrane-restricted protease.²⁸ Another powerful mechanism for promoting inter-protein oligomerization is by two-dimensional clustering.⁹³ As mentioned above, some toxins bind selectively to lipid rafts, which may function as protein concentration platforms and enhance oligomeric assembly. Reduction of dimensionality, as corresponding to binding in the membrane two dimensional surface, can lead to an effective increase of concentration of about 1.5×10^3 .¹³² Additionally, recruitment of proteins in membrane microdomains can largely increment the concentration factor. This has been described for aerolysin, whose GPI-anchored receptor associates transiently with lipid rafts⁹³ and can also be the case for other toxins which bind to SM-Cho microdomains, like CDCs,²⁸ actinoporins,²⁹ α -hemolysin,⁷⁰ Cry1A toxin¹³³ and lysenin.¹³⁴

The Complex Membrane-Dependent Regulation of Bcl-2 Proteins

The lipid membrane exerts also a principal role for the intricate mechanism of action of pore inducers and inhibitors of the Bcl-2 family. This uses a complicated allosteric mechanism, explained by the "embedded together" model¹³⁵ where the capacity of the pore receptor (tBid), executor (Bax) and inhibitor (Bcl-xL) proteins to interact with each other changes after binding to the mitochondrial outer membrane, as this causes conformational changes that alter and/or expose new binding surfaces.^{136,137} Docking of tBid to mitochondrial membranes converts this protein into a high affinity receptor for Bax. A subsequent membrane dependent interaction of Bax to tBid is responsible of further activation involving the formation of a Bax oligomer, which can finally form a pore.^{136,137} The inhibition of this process by Bcl-xL can occur at different levels, but it is in any case also membrane dependent. This may consist, on the one hand, on the blockage of membrane-bound tBid, which can no longer receive Bax and on the other hand on a direct binding to Bax, which abolish the formation of the Bax oligomeric pore.^{136,137}

Role of Lipids in the Formation and Stabilization of Pores

The Latent Membrane Pores: Relatives of Pores Induced by Polypeptides?

Although rare, spontaneous pores are inherent to lipid bilayer membranes. They occur independently of the presence of peptides or proteins, although in the absence of tension their frequency is very low. In pure lipid membranes pore formation is kinetically hindered by a large energy barrier, which cannot be easily overcome by thermal energy (Fig. 3).^{10,12,138-143} However, the fluctuation of bilayer lipids gives a chance for stochastic disruptions of the equilibrium bilayer structure, explaining, among other things, the spontaneous formation of pores.^{10,12,138} For example, the transbilayer movement of lipids, known as flip-flop, which in cell membranes is accelerated by a number of specialized catalytic proteins,¹⁴⁴ can occur in pure lipid vesicles in time scales from hours to days, depending on the type of lipids and experimental conditions.¹⁴⁵⁻¹⁴⁸ Such unassisted flip-flop has been proposed to be mediated by lipid-packing defects.^{149,147} MD simulations have shown recently that this process may occur via transient water-pores (Fig. 4A) which allow passage of the hydrated charged groups of the lipids across the membrane hydrophobic slab.¹² The pores are structurally similar to the ones simulated under mechanical and electrical stress (Fig. 4B),^{11,139} a type of bilayer disruption which is well known experimentally.^{9,10,150,151} These flip-flop coupled pores might also be responsible for the passive ion permeation through membranes,^{12,139,152,153} although they represent a negligible contribution to water permeation.¹²

The background spontaneous lipid flip-flop and pore formation can be largely affected by the phase state and composition of the membrane. For example, the passive permeability of lipid bilayers exhibits a maximum at conditions of coexistence of gel domains and fluid domains.^{147,154,155} On the other hand the presence of Cho increases the free energy barrier for

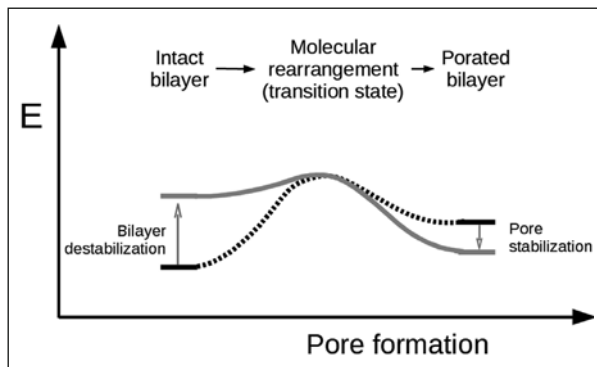


Figure 3. Free energy of pore formation along the reaction coordinate. Relative stability of intact and pored states of a lipid bilayer in the absence and presence of PFPPs. Pore formation in pure lipid bilayers with no tension (black, dotted line) is unfavorable and kinetically hindered by a large activation energy barrier. Membrane-bound PFPPs destabilize the bilayer, increasing its energy via elastic deformations (left, arrow pointing upwards) and pore formation may then become favorable (gray, continuous line). The likelihood of the pore state increases if the PFPP stabilize the pore once it is open (right, arrow pointing downwards). The rate-limiting step is the rearrangement of the lipids and the PFPP through a high energy transition state (middle). Such pore activation energy is, in a first instance, reduced by the changes of the relative stability of intact and pored bilayers, caused by the PFPP and could be decreased even further if the PFPP stabilizes the transition state. Note that the intact and pored bilayer states may correspond to the *S*-state and *I*-state in Huang's model,^{69,118} as well as to the *B_{ex}*-state and *P*-state in Tamba and Yamazaki's model.^{26,27} However, there are fundamental differences between these two models in the definition and properties of the states (see the text). Thus, we think that this open and more general definition of the states would in either case be valid.

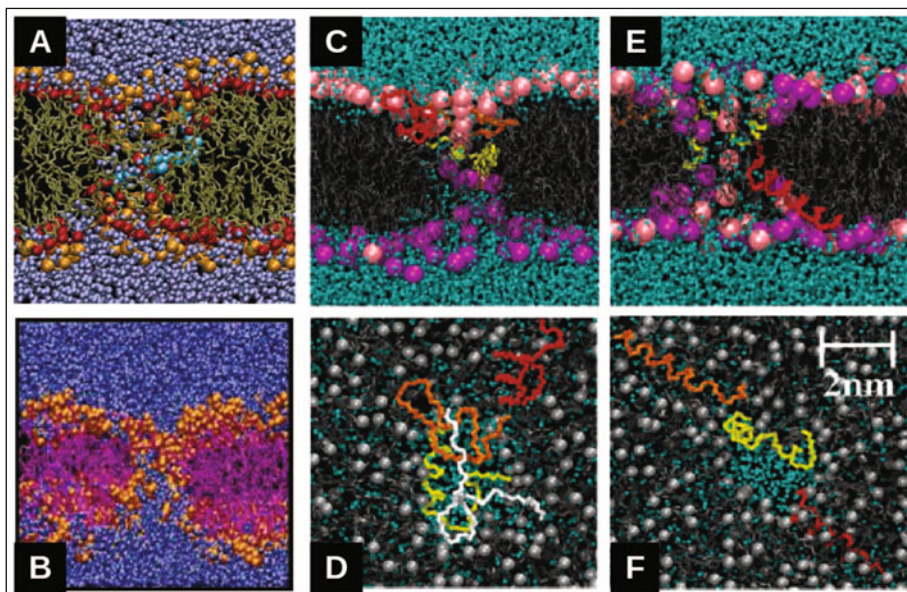


Figure 4. Comparison of flip-flop assisting, stress induced and peptide induced pores. All structure models are from MD simulations of DOPC bilayers. Flip-flop assisting pores (A)¹² are transient defects which form as the charged groups of a phospholipid (constrained in position during the simulation) traverse the low dielectric membrane interior. Neighboring lipids rearrange moving deeper into the membrane and allowing the formation of a water-pore defect, which is highly dynamic. In the graph, small blue spheres are water oxygen atoms, orange spheres are nitrogen and phosphate, red spheres are oxygens in the lipid glycerol linkage, brown bonds are lipid chains and the constrained lipid is represented in space-filling cyan color. Similar structures can be seen in pores induced by electrical stress, shown in panel (B) as a snapshot of the trajectory ~ 3.35 ns after applying an electric field of 0.5 V/nm (water shown in blue, lipid chains in purple and lipid headgroups in orange).¹¹ Lipidic pores are also observed in simulations of 128 DOPC lipids in presence of 4 magainin peptides, when they are placed either initially near the membrane in the bulk water (C, top view in D) or self-assembled with the lipids form initially random configurations (E, top view in F).²² These peptide induced pores are largely disorganized, with variable positions of the peptides with respect to the rim of the pore. The unfolded peptide structure in (C) and (D) is probably due to the system being far from equilibrium. Colors in (C-F) are as follows: The backbones of the peptides are shown in yellow, orange, red and white. Lipid tails are gray. Water oxygens are green. In (C) and (E) the phosphate atoms of the headgroups are pink or purple depending on the monolayer where they initially resided. In (D) and (F) the gray spheres represent the glycerol moieties. Figures reprinted with permission from the *Journal of the American Chemical Society*, Volume 128 (A, ref. 12; C-F, ref. 22), © 2006 by the American Chemical Society and Volume 125 (B, ref. 11), © 2003 by the American Chemical Society.

water pore formation^{82,156} and on the contrary, the presence of ceramide facilitates flip-flop and the formation of large and stable lipidic channels.¹⁵⁷⁻¹⁶¹ Including proteins in the membrane composition has also been observed to affect lipid flip-flop, like in presence of α -helical proteins, in principle not related to pore formation, from the plasma membrane of bacteria.¹⁶² This latter effect appears weakly specific, since it is also found for other polypeptides, like glycophorin¹⁶³ and synthetic model transmembrane peptides.¹⁶⁴ It has been speculated that this type of protein-facilitated flip-flop is due to a much lower barrier for defect (water-pore) formation¹² as a consequence of the protein-membrane interaction. Induction of lipid flip-flop

is also a common phenomenon associated to the activity of many PFPPs.^{30,165-168} The large increase of transbilayer movement observed in these cases is often explained as due to lateral diffusion of lipids at points of monolayer fusion existing in the edge of the pore and it is one of the preferred tests to distinguish different types of pores¹⁶⁶⁻¹⁷⁰ (see below). Additionally, similar to intrinsic lipid flip-flop, pore formation by peptides and proteins is in many cases described as an stochastic process related to membrane disruption and nucleation of defects.^{22,24-26,91}

The basic action of specialized pore-forming peptides and proteins may then overlap with the intrinsic pore-formation capacity of membranes. A number of specific examples support this idea: osmotic tension and class L amphipathic peptides act synergistically as they induce pores in vesicles.¹⁷¹ The general attenuation of membrane permeability exerted by Cho affects also the activity of pore forming peptides.^{77,79} For more sophisticated protein pores, like those formed by the Cho dependent *Vibrio cholerae* cytolysin, the pore inducer ceramide enhances the activity of the toxin.¹⁷² On the other hand, the lipidic pores induced by ceramide can be disassembled by Bcl-2,¹⁷³ the physiological inhibitor of the α -pore forming protein Bax. And in some other cases, pore formation is favored by defect-rich domain boundaries⁹¹ and at the phase transition temperature.¹⁷⁴ The lipopeptide syringomycin E, which forms a characteristic lipidic pore, provides an interesting example linking intrinsic membrane pores and polypeptide induced pores.¹⁷⁵ The charge and dipolar moment of host membrane lipids modifies the effective gating charge of the syringomycin E ionic channel. Additionally the channel is inhibited in the presence of nonlamellar lipids with negative spontaneous curvature. Similarly, effects of lipid charge and intrinsic curvature have been observed for channels formed by peptides¹⁸ or proteins.¹⁶⁸

Can we then establish mechanistic connections between intrinsic membrane pores and pores induced by peptides and proteins? In an attempt to do that, we make now an overview of different proposed models and extract from them a minimum general consensus from the point of view of the role of lipids.

A Consensus View of Pore Formation Stressing the Role of Lipids

There have been a number of different classical (general) models of pore formation by membrane active polypeptides. Previous work has often stressed the differences between particular models, amplified by detailed (not always justified) drawings. Instead, we want to underline here their common points, as many of their apparent contradictions can be regarded as either superficial or arising from the use of different experimental conditions. Although mostly developed for membranolytic peptides, many of these ideas can be extended to pore-forming proteins^{14,29,43,66}; they essentially leave a prominent role for lipids around the postulate of more or less stable and more or less organized, lipid-based pores.

Matsuzaki proposed a supramolecular peptide-lipid dynamic complex in order to explain the simultaneous transbilayer diffusion of magainin and membrane lipids, coupled to leakage of vesicles.³⁰ In this model both, lipids and peptides form the pore wall, where the presence of acidic phospholipids may counteract repulsion between the positively charged peptides and explain the cation selectivity of the channel.¹⁷⁶ This is basically the same as the toroidal wormhole model, proposed almost simultaneously by Huang's group on the basis of neutron in-plane scattering and oriented circular dichroism (OCD) data.³¹ Huang's view is sustained on the membrane thinning that accompanies peptide embedding in the head-group region (*S*-state). Above a certain threshold P/L^* this triggers a molecular reorganization which involves the re-orientation of some peptide molecules (*I*-state) and formation of a pore.^{177,178} Noteworthy, from a similar *S*-state the model postulates different *I*-states for alamethicin-type peptides: barrel stave of interacting transmembrane peptides forming a relatively small pore, than for magainin-type peptides: larger pore where the two monolayers fuse like in a torus and the curvature strain is alleviated by peptides bound across the membrane, in the interface of lipids making the pore wall.¹¹⁸ From the membrane side, these two alternative pore states correspond to the two possible lipid structures at the edge of a pore, which have been experimentally observed by reconstructing the lipid electron density profiles from X-ray diffraction^{179,180} (Fig. 5). This thermodynamic

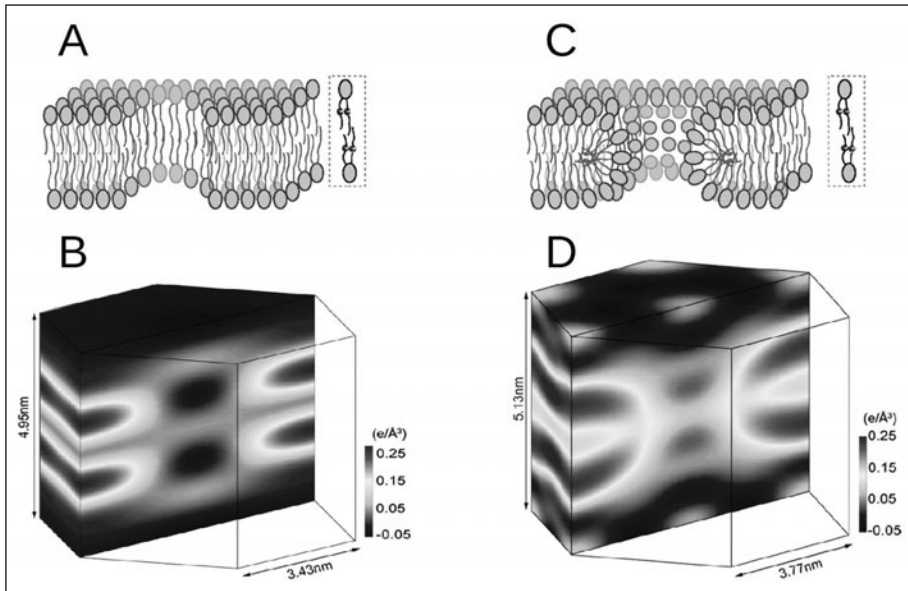


Figure 5. Bilayer structure at the edge of peptide-induced pores. The two paradigmatic types of pore, for long time postulated as alternative models (here illustrated with drawings (A) and (C) are viewed from the electron density of brominated lipids resolved by grazing angle X-ray diffraction^{179,180} (B and D). The bromine labels in the acyl-chains of lipids are represented as small balls in lipids within dashed-line boxes in (A) and (C). Two distinct membrane structures at the pore edge are found. The alamethicin induced pores leave bilayer holes with no contact of electron density between the two monolayers (B). This corresponds to the schematic drawing in (A) and indicates that the pore wall is formed exclusively by peptide molecules, in agreement with a barrel-stave arrangement of alamethicin peptide units (not shown in the drawing). In contrast, the structure induced by the α -5 active fragment of the protein Bax shows continuous electron density between the two monolayers at the pore edge, as expected for the case of toroidal pores with a wall lined (at least partially) by lipids, drawn schematically in (C). Because these experiments do not provide data about the peptide part, this is omitted in drawings (A) and (C) (the reader can see possible models for the peptide arrangement in Figure 6C,D). Figures (B) and (D) are reprinted with permission from PNAS, Volume 105 (ref. 180) ©2008 National Academy of Sciences, USA.

model,^{13,69,181} derived from equilibrium experiments, has been complemented by kinetic experiments performed with single giant unilamellar vesicles (GUVs) in the presence of melittin.²⁵ The kinetic analysis presents pore formation as a probabilistic phenomenon dependent on the nucleation of defects on the lipid bilayer, which occurs after area expansion, due to interfacial binding of the peptides, reaches a limit value. Thus, the pore is the response of the bilayer to a polypeptide-induced internal tension, which in turn helps to maintain a stable pore and with a defined size.^{13,25,31} Direct evidence and a low resolution structure for such a lipid-based arrangement, in this case induced by an active fragment from the protein Bax,^{18,166} have been provided by grazing-angle X-ray diffraction¹⁸⁰ (Fig. 5D).

Disruption of the bilayer is also the main ingredient of the carpet model proposed by Shai et al,³² which is similar to the so called sinking raft,¹⁸² or more generally the detergent-like activity.^{183,184} It essentially consists on an extensive surface coverage at the level of the head group of phospholipids by cationic peptides, up to the point of yielding the disintegration of the

membrane.³² In this case the toroidal pore is adopted as a disordered early transient stage, before membrane rupture occurs through micellisation. Leaving this latter complete disruption aside, as it is observed only at very high peptide concentrations,^{183,185} both Matsuzaki and Shai coincide on proposing pore formation as due to asymmetric membrane disturbance or mass imbalance over the external (accessible) monolayer, where the peptide primarily binds. It follows that pores are necessarily transient, because they will close at equilibrium as soon as mass imbalance dissipates through the pore. This is supported by recent kinetic interpretations of content release experiments from large unilamellar vesicle (LUV) suspensions by Almeida's group,^{24,71} as well as kinetic studies with single GUVs by Tamba and Yamazaki,^{26,27} which also introduce the idea of stochastic pores (or pores opening at random after a threshold stress). The latter authors propose a two state $B_{ex} \rightarrow P$ transition model²⁶ where the B_{ex} state corresponds to the peptide bound only to the external monolayer, the rate-limiting step is the insertion of the peptide across the membrane and the P state is a metastable transient pore.^{26,27} Although these ideas have some resemblance with Huang's two state model,^{25,69,180} there are two main contrasting points: (i) In Huang's S -state the peptides are assumed to reequilibrate fast across the membrane⁷⁶ through small transient pores occurring even at low concentration,¹⁸⁶ meaning that the stress responsible for pore induction is exerted symmetrically in the two monolayers. (ii) The pores in Huang's I -state correspond to minimum energy and are thus stable once they are formed.^{31,69,180,181}

The toroidal "pores in action" reported by MD simulations also form stochastically and after the asymmetric attack to the bilayer.^{22,23} In this case the interesting feature is the low level of molecular organization within the pore, both for lipids and peptides (Fig. 4C-F),²³ which is put in contrast to Huang's view. However, the disagreement may be illusory. Thus, on the lipid side the regular torus reported by Huang is an averaged structure which cannot be directly compared with single pores in non-equilibrium, relatively short MD trajectories.¹⁸⁰ On the peptide side, there is no precise information about the number of peptides involved per pore, or their position and orientation with respect to the pore. For example, in the case of melittin, the estimates of the peptide aggregation number accompanying pore formation vary from 5 to 8 in an analysis of membrane thinning⁶⁹ and up to 20 in analysis of calorimetry data.⁵⁶ It should also be noted that Huang's measurements of peptide reorientation upon pore formation, performed by OCD, do not give accurate orientation values, but rather inform of a change of tilt.^{177,178,187,188} Thus, the OCD results, normally interpreted as a transition between two extreme states, parallel and perpendicular to the membrane, might as well be compatible with other linear combinations of extreme tilts, or even a distribution of peptide orientations at or near the pore rim,¹⁸⁸ perhaps similar to that seen in simulations (Fig. 4E,F).^{22,23} Membrane insertion of pore forming peptides at tilts other than perpendicular to the membrane has been described in the case of PGLa^{119,188} and for an active fragment of Bax.¹⁸

Thus, the three main classical models of pore formation have important elements in common, recognized by Zasloff, who termed them collectively as the Shai-Matsuzaki-Huang (SMH) mechanism.²¹ Considering the new ingredients from MD simulations^{22,23} and kinetic and single vesicle studies,^{24-27,71} the emerging main consensus ideas are as follows: membrane disruption due to interfacial binding is the basic mechanism of polypeptide-induced pore formation. It proceeds through a stochastic cooperative transition, assisted by bilayer defects, in a two-state process modulated by the membrane elastic properties (see below). This, depending on the type of protein or peptide, may form barrel-like pores (stable cylindrical peptide or protein aggregates) or disordered mixed lipidic-proteic (or peptidic) pores. These ideas are valid for most (if not all) membranolytic peptides. Among the pore-forming proteins, the β -type form preferentially barrels of interacting β -strands^{66,104} while the α -type seem to prefer toroidal pores, so far described for colicins,¹⁶⁸ actinoporins^{33,34} and Bcl-2 apoptotic regulators^{35,167,189} as well as their active fragments.^{18,83,166,180} In any case, the importance of membrane disturbance and nucleation of defects to facilitate protein insertion and pore formation, modulated by the membrane elastic properties, should be of general validity.

Physical Properties of Polypeptide-Induced Pores Related to the Role of Lipids

Surface Tension, Line Tension and the Stability of Membrane Pores

As we have discussed above, the lytic pores induced by polypeptides have many ingredients of general lipidic pores, like those formed under tension (mechanical or electrical tension or osmotic swelling). According to proposed mechanisms,^{11,190} pores form after a build up of a critical surface tension (~ 10 pN/nm),¹⁹¹ which increases the probability of appearance of nucleation sites of packing defects. Theoretical models describe these pores as meta-stable arrangements, with free energy of formation being a function of the pore radius (r) as: $E_r^0 = 2\pi r\gamma - \pi r^2\sigma$. The first term is the energy needed to expand the rim of the pore and γ is the line tension, opposing the pore. The second term, proportional to the pore area, represents the work done by the membrane to open the pore, σ being the membrane tension, which favours pore opening and expansion.^{150,192} This model predicts an intrinsically unstable pore which tends to close for $r < \gamma/\sigma$ and expands indefinitely for $r > \gamma/\sigma$. Thus, while external tension effects increase the pore lifetime and can lead to vesicle rupture, different lipids as well as non lipid inclusions, like detergents, may affect the pore stability by changes in the line tension.¹⁵⁰

In a generalization of this model to polypeptide-induced toroidal pores, it has been proposed that pore forming peptides (we may extend it to PFPPs) act by affecting both, the line tension and membrane tension terms and making the open-pore state energetically favourable (see Fig. 3).¹³ This can occur through an effect of the PFPPs on the membrane elastic properties (see also below). The membrane thinning (area expansion) accompanying the interfacial binding of PFPPs is a source of (internal) surface tension which above a threshold value (~ 8 pN/nm in DOPC,¹⁸¹ similar to the rupture tension of vesicles of the same lipid¹⁹¹) overcomes the energy barrier to open the pore. Additionally, the binding of PFPPs at or near the pore rim may act by reducing the line tension.^{35,68,83} Evidence of this latter effect has been obtained as shape changes and coalescence of L_O domains in phase-separated lipid bilayers, observed by fluorescence microscopy of GUVs and in situ atomic force microscopy (AFM) in presence of the Bax- $\alpha 5$ fragment and the reduction of line tension was quantified using AFM-film rupture experiments.⁸³ A extensive AFM study of membrane remodelling for a variety of pore-forming and cell penetrating peptides suggests that line-tension activity may be a common ingredient of the mechanism of these systems.⁶⁸

Lipid-Driven Cooperativity: A Many-Body Effect Triggering Pore Formation

Kinetic,^{24,25,27,71} structural^{31,76} and thermodynamic⁵⁶ studies agree on describing pore formation by active peptides as a cooperative process. It is manifested as a nonlinear concentration dependence of activity and a rapid rise to saturation as the concentration exceeds a threshold value and it consists on a steep transition between two main structural states of the peptide-membrane complex.^{76,177,178,193} This cooperativity phenomenon is not due to direct peptide-peptide binding, but rather to a membrane mediated peptide-peptide interaction which originates on the elastic properties of the membrane, in the form of area expansion^{25,194} and membrane thinning (Fig. 6).^{25,195,196} The interfacial binding of the peptide in the S -state (below a threshold P/L^*) expands the membrane area and causes a local thinning. This corresponds to a positive energy of elastic deformation, proportional to the ratio of peptides bound per lipid. The consequence is an increase of the free energy of the S -state (Fig. 3) which reaching a threshold value (corresponding to a limit tension, see above) triggers a molecular reorganization (I -state) with the opening of lipidic pores and a change of orientation of a few peptides per pore.^{181,193} This has been recently interpreted as similar to a micellisation process (and the two states have been renamed phases).⁶⁹ The new analysis allows an estimation of the number of peptides per pore (a minimum of 4) involved in the transition.⁶⁹

Interestingly, the membrane-mediated cooperativity of pore-forming peptides suggests a model for the activity of α -helical pore-forming proteins, like proapoptotic Bax, pore-forming colicins and diphtheria toxin.⁶⁹ The prepore state of these proteins is thought to consist on an extended two-dimensional array of helices, which has been characterized for some colicins^{114,121,122} and members

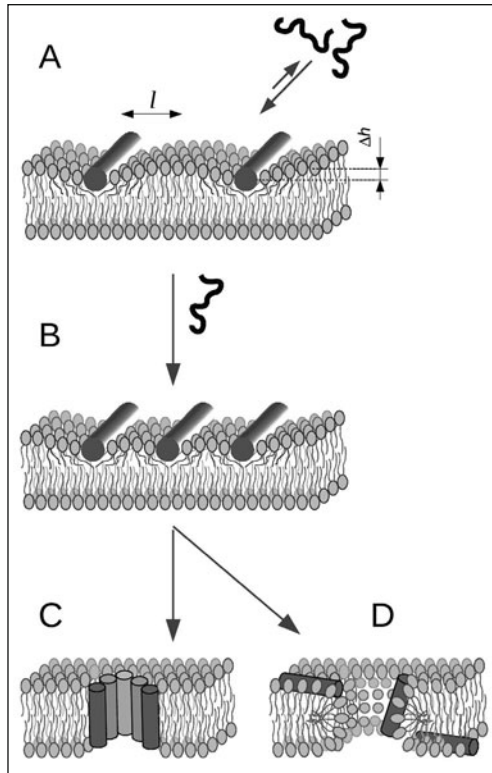


Figure 6. Lipid-dependent cooperativity of pore formation by polypeptides. The general nonlinear concentration dependence of the activity of PFPPs has been described for the case of antimicrobial peptides as a phenomenon arising from the deformation of the bilayer.^{69,76,181} A) Upon the initial interfacial adsorption of the peptide, a non homogeneous monolayer expansion at the level of the headgroups causes disordering of the acyl chains, which occupy the space left below the peptide and thus membrane thinning (Δh).²⁰⁸ The local thinning effect extends up to a persistence length (l) depending on the membrane elastic properties and it is the origin of lipid mediated peptide-peptide interaction (repulsive or slightly attractive depending on the peptide-peptide distance). The corresponding positive elastic energy destabilizes the bilayer proportionally to the amount of adsorbed peptide (B, see also Fig. 3). Close to a threshold peptide density (B) the stressed lamellar state is close in energy to the transition state for pore formation (Fig. 3) and the pore will eventually open (C, D). (A) and (B) correspond to Huang's *S*-state and (C) and (D) to the two alternative *I*-states (barrel-stave and toroidal pore). These, are essentially similar to the Tamba and Yamazaki's B_{ex} -state and *P*-state²⁶ (the main differences between the *S* and B_{ex} and *I* and *P* states, discussed in the text, are not relevant for this model of cooperativity). This model explains the formation of both barrel-stave (C) and toroidal pores (D) and although formulated for peptides can also be extended to proteins.⁶⁹

of the Bcl-2 family.¹²³⁻¹²⁵ Such a configuration would correspond to the *S*-state, where each helical segment of the array contributes to membrane thinning. Moreover, because the different segments are linked within the same polypeptide chain, they keep confined in a small membrane area, which corresponds to a high effective density of amphipathic α -helices. This should facilitate the transition to the pore (*I*-) state which can be expected to occur at a low threshold protein-to-lipid ratio. In fact, these proteins are known to be active at nanomolar concentrations.¹⁶⁷ A similar effect may be valid for the pore formation by protein toxins from other families.

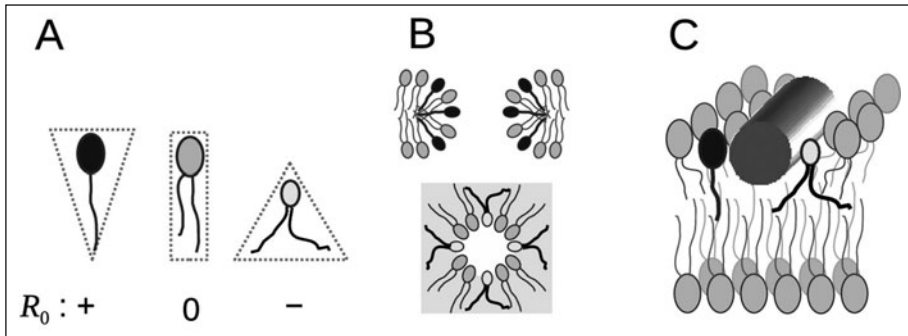


Figure 7. Classical and nonclassical lipid curvature effects in pores formed by polypeptides. The tendency of lipids to bend the monolayer can be measured by the radius of spontaneous curvature, R_0 . This depends on the lipid morphology (A) and can be near zero (cylindrical shape, like PC lipids) positive (inverted-cone shape, like lysolipids) or negative (cone-shape, like diacylglycerols and PE lipids). The classical interpretation of the effect of lipid spontaneous curvature^{34,166,199} arises from the fact that toroidal pores are highly curved structures (B). The curvature strain in the plane perpendicular to the membrane (B, top) is alleviated by lipids with positive curvature, which are said to stabilize the pore. On the contrary, negatively curved lipids would destabilize the pore. The opposite is expected for the lipid arrangement in the bilayer plane (B, bottom), although the effect in this case would be important only for small pores. The spontaneous curvature of lipids can also affect the strain produced by polypeptides adsorbed at the interface (C, nonclassical effect),^{69,193} In this case, the cross-sectional area occupied by the polypeptide inclusion is larger at the level of the head-group region, producing disordering of the acyl tails and membrane thinning (see Fig. 5). The polypeptide inclusion can be viewed as introducing positive curvature strain,²⁰⁴ which can be compensated by negatively curved lipids. Thus, these latter lipids would generally stabilize the adsorbed state and oppose the pore state, while positively curved lipids would destabilize the adsorbed state and promote the pore.

The Elusive Role of Spontaneous Curvature: Classical and Nonclassical Effects

Because the pores imply bilayer deformations, they are also related to bilayer elastic (mechanical) properties, namely the isothermal area compressibility modulus (K_a), the bending modulus (k_c) and the monolayer spontaneous radius of curvature (R_0).^{77,197,198} These three parameters depend on the bilayer composition.¹⁹⁸ The energy of bilayer deformation contains terms accounting for area changes, proportional to K_a and curvature-elastic effects, proportional to k_c/R_0 and both have been observed to correlate linearly with the melittin-induced leakage.⁷⁷ It is proposed that the interfacial adsorption of the peptide induces a bending moment in the bilayer causing deformations which act as a nucleation site for pore opening. The opening probability, stability and size of the pores is then determined by the deformation energy of the lipids and it thus depends on the intrinsic lipid curvature.⁷⁷ This observations are in line with the characteristic high curvature strain of lipidic and proteo-lipidic toroidal pores^{143,150,199,200} (Fig. 7).

Strong positive curvature arises from the bending/fusion of the two monolayers at the pore edge, forming a structure with a radius of approximately half of the membrane width as it can be visualized in a plane perpendicular to the bilayer traversing the pore (Fig. 7B).^{34,166,199} Thus, the pore rim would be stabilized by lipids with wedge or inverted-cone shape, which are said to have positive spontaneous curvature (most generally lysolipids, Fig. 7A). This concept predicts also that cone-shaped negatively curved lipids, which are those that induce the hexagonal H_{II} phase,²⁰¹ should have an opposite effect, i.e., destabilize the pore.^{150,192} For the case of PFPPs the activating/stabilizing effect of positively curved lipids has been shown to be valid in a number of instances.^{77,166,189,200,202} However, the effect of negatively curved lipids seems to be less general and they have been reported to both, inhibit^{77,166,189,200,202} and facilitate^{18,33,166,168} pore formation. This heterodox role of negative curvature has been related to the fact that a toroidal arrangement of

lipids in the pore edge possess also regions of negative curvature strain in a plain parallel to the membrane (Fig. 7B).^{34,166,199} Such an effect is predicted to be strictly dependent on the pore size, being comparable to the positive curvature effect for a pore radius of ~2 nm (approximately half of membrane thickness) and vanishing small as the pores increase in size.¹⁹⁹ Thus, it has been argued that the activating effect of negatively curved phosphatidylethanolamine (PE) lipids in pores formed by a Bax $\alpha 5$ fragment,^{18,166} compared to the classical inhibitory effect observed for complete Bax,^{167,189} may be due to the formation of smaller pores in the former. However, the pores induced by Bax $\alpha 6$ (another active Bax fragment), despite being apparently of a size comparable (or even smaller) to that of Bax $\alpha 5$ pores, are inhibited by the presence of PE.¹⁶⁶ Other conflicting examples have been explained by additional properties of lipids complementing or compensating the curvature effects. Such are the cases of the stimulated opening of large conductance 600 pS ion channels of colicin E1 at increased lipid negative curvature, compared to the case of small conductance 60 pS channels¹⁶⁸ and the increased activity of pores formed by sticholysins I and II in the presence of negatively charged PA, PS PG, PI and CL as well as zwitterionic PE. In the case of the colicin E1 600 pS channels, the increase of opening probability has been related to a simultaneous stimulating effect due to hydrophobic mismatch.¹⁶⁸ With respect to the pores of sticholysins, the observed behavior is attributed to intrinsic negative curvature of the assayed lipids,³³ which due to their negative charge, is enhanced in the presence of positively charged residues of the membrane-bound protein.^{201,203} Additionally, the existence of distorted toroidal pores²³ might also explain the heterogeneity of negative curvature effects, since they are related to the local pore radius which will be variable in a complex manner for noncylindrical pores.

Based on structural measurements (membrane thinning), Huang et al have described a different effect of lipid spontaneous curvature, which we term nonclassical curvature effect (Fig. 7C).¹⁹³ In agreement with leakage experiments, negatively and positively curved lipids increase and reduce, respectively, the threshold P/L value for the *S*-state to *I*-state transition. However, the observed correlations are similar for barrel-stave pores (alamethicin, Fig. 6C) and toroidal pores (melittin, Fig. 6D) and in either case the relative stabilities of the *S* and *I* states appear weakly dependent on lipid curvature.^{76,193} So, it appears that the bending stress of the toroidal pore is efficiently released by the peptides,²⁰⁴ in agreement with a reduction of the line tension (which implies that the peptides stabilize the lipidic pore, see Fig. 3).^{68,83} Instead, the major effect of varying the spontaneous curvature of lipid is a change of the degree of membrane thinning that accompanies the interfacial adsorption of the peptide (Fig. 6).¹⁹³ This can be understood by considering that cone-shaped negatively curved lipids, with a smaller head-group area, compared to the area occupied by the lipid tails, accommodate better the interfacially adsorbed peptides (attenuate membrane thinning and increase the threshold for the *S*→*I* transition) and the opposite occurs for inverted cone-shaped (positively curved) lipids (Fig. 7C).

Conclusion

On the functional scene, pores formed by peptides and proteins have a lot in common, as they all are systems for defense and attack, or in a more general sense related to cell death. In contrast, reports about these functions often put the accent on diversity, helped by an ever increasing number and variety of structures and mechanisms. Membrane lipids and the lipid bilayer properties are a unifying ingredient in this Universe of pore forming peptides and proteins and we can find a minimum of convergent ideas concerning the role of lipids. The compromise of the bilayer integrity is an intrinsic capability of lipid membranes, which can be modulated at a basic level by the lipid composition and phase changes. Polypeptides employed for pore formation use in part this intrinsic capability, while adding different levels of complexity which allow specificity and regulation. These ideas have benefited from recent improvements of structural techniques and the incorporation of new powerful methods, like single vesicle approaches and multiscale molecular simulations. Thus, the lipid part can now be studied as a protagonist of pore-formation, rather than a mere passive medium, which will surely introduce a new focus to help understanding this complex function.

Acknowledgments

This work is supported by the Spanish *Ministerio de Ciencia e Innovación* through the grant BFU2007-67097/BMC, financed in part by the European Regional Development Fund (ERDF). GF DJ and OS are granted by the University of Valencia. We thank Huey W. Huang and Paulo Almeida for stimulating discussions about models and mechanisms of pore formation.

References

1. Esteban-Martín S, Salgado J. Self-assembling of peptide/membrane complexes by atomistic molecular dynamics simulations. *Biophys J* 2007; 92:903-912.
2. Nyholm TKM, Özdirekcan S, Killian JA. How protein transmembrane segments sense the lipid environment. *Biochemistry* 2007; 46:1457-1465.
3. Kandasamy SK, Larson RG. Molecular dynamics simulations of model trans-membrane peptides in lipid bilayers: a systematic investigation of hydrophobic mismatch. *Biophys J* 2006; 90:2326-2343.
4. Esteban-Martín S, Salgado J. The dynamic orientation of membrane-bound peptides: bridging simulations and experiments. *Biophys J* 2007; 93:4278-4288.
5. Khandelia H, Ipsen JH, Mouritsen OG. The impact of peptides on lipid membranes. *Biochim Biophys Acta* 2008; 1778:1528-1536.
6. Hickel A, Danner-Pongratz S, Amenitsch H et al. Influence of antimicrobial peptides on the formation of nonlamellar lipid mesophases. *Biochim Biophys Acta* 2008; 1778:2325-2333.
7. Andersen OS, Koeppe RE. Bilayer thickness and membrane protein function: an energetic perspective. *Annu Rev Biophys Biomol Struct* 2007; 36:107-130.
8. Tribet C, Vial F. Flexible macromolecules attached to lipid bilayers: impact on fluidity, curvature, permeability and stability of the membranes. *Soft Matter* 2008; 4:68-81.
9. Sandre O, Moreaux L, Brochard-Wyart F. Dynamics of transient pores in stretched vesicles. *Proc Natl Acad Sci USA* 1999; 96:10591-10596.
10. Evans E, Heinrich V, Ludwig F et al. Dynamic tension spectroscopy and strength of biomembranes. *Biophys J* 2003; 85:2342-2350.
11. Tieleman DP, Leontiadou H, Mark AE et al. Simulation of pore formation in lipid bilayers by mechanical stress and electric fields. *J Am Chem Soc* 2003; 125:6382-6383.
12. Tieleman DP, Marrink S. Lipids out of equilibrium: energetics of desorption and pore mediated flip-flop. *J Am Chem Soc* 2006; 128:12462-12467.
13. Huang HW, Chen F, Lee M. Molecular mechanism of peptide-induced pores in membranes. *Phys Rev Lett* 2004; 92:198304.
14. Zakharov SD, Kotova EA, Antonenko YN et al. On the role of lipid in colicin pore formation. *Biochim Biophys Acta* 2004; 1666:239-249.
15. Matsuzaki K. Why and how are peptide-lipid interactions utilized for self-defense? Magainin and tachyplesins as archetypes. *Biochim Biophys Acta* 1999; 1462:1-10.
16. Tillman TS, Cascio M. Effects of membrane lipids on ion channel structure and function. *Cell Biochem Biophys* 2003; 38:161-190.
17. Lins L, El Kirat K, Charlotiaux B et al. Lipid-destabilizing properties of the hydrophobic helices H8 and H9 from colicin E1. *Mol Membr Biol* 2007; 24:419-430.
18. García-Sánchez AJ, Coraiola M, Dalla Serra M et al. Peptides derived from apoptotic Bax and Bid reproduce the poration activity of the parent full-length proteins. *Biophys J* 2005; 88:3976-3990.
19. Gerber D, Shai Y. Insertion and organization within membranes of the delta-endotoxin pore-forming domain, helix 4-loop-helix 5 and inhibition of its activity by a mutant helix 4 peptide. *J Biol Chem* 2000; 275:23602-23607.
20. Rathinakumar R, Wimley WC. Biomolecular engineering by combinatorial design and high-throughput screening: small, soluble peptides that permeabilize membranes. *J Am Chem Soc* 2008; 130:9849-9858.
21. Zasloff M. Antimicrobial peptides of multicellular organisms. *Nature* 2002; 415:389-95.
22. Leontiadou H, Mark AE, Marrink SJ. Antimicrobial peptides in action. *J Am Chem Soc* 2006; 128:12156-12161.
23. Sengupta D, Leontiadou H, Mark AE et al. Toroidal pores formed by antimicrobial peptides show significant disorder. *Biochim Biophys Acta* 2008; 1778:2308-2317.
24. Gregory SM, Pokorny A, Almeida PFF. Magainin 2 Revisited: A Test of the Quantitative Model for the All-or-None Permeabilization of Phospholipid Vesicles. *Biophys J* 2009; 96:116-131.
25. Lee M, Hung W, Chen F et al. Mechanism and kinetics of pore formation in membranes by water-soluble amphipathic peptides. *Proc Natl Acad Sci USA* 2008; 105:5087-5092.
26. Tamba Y, Yamazaki M. Single giant unilamellar vesicle method reveals effect of antimicrobial peptide magainin 2 on membrane permeability. *Biochemistry* 2005; 44:15823-15833.

27. Tamba Y, Yamazaki M. Magainin 2-Induced Pore formation in the lipid membranes depends on its concentration in the membrane interface. *J Phys Chem B* 2009; 113:4846-4852.
28. Tweten RK. Cholesterol-dependent cytolysins, a family of versatile pore-forming toxins. *Infect Immun* 2005; 73:6199-6209.
29. Alvarez C, Mancheño JM, Martínez D et al. Sticholysins, two pore-forming toxins produced by the caribbean sea anemone *Stichodactyla helianthus*: their interaction with membranes. *Toxicon* 2009; 54:1135-1147.
30. Matsuzaki K, Murase O, Fujii N et al. An antimicrobial peptide, magainin 2, induced rapid flip-flop of phospholipids coupled with pore formation and peptide translocation. *Biochemistry* 1996; 35:11361-11368.
31. Ludtke SJ, He K, Heller WT et al. Membrane pores induced by magainin. *Biochemistry* 1996; 35:13723-13728.
32. Shai Y. Mechanism of the binding, insertion and destabilization of phospholipid bilayer membranes by alpha-helical antimicrobial and cell nonselective membrane-lytic peptides. *Biochim Biophys Acta* 1999; 1462:55-70.
33. Valcarcel CA, Serra MD, Potrich C et al. Effects of lipid composition on membrane permeabilization by sticholysin I and II, two cytolysins of the sea anemone *stichodactyla helianthus*. *Biophys J* 2001; 80:2761-2774.
34. Anderluh G, Dalla Serra M, Viero G et al. Pore formation by equinatoxin II, a eukaryotic protein toxin, occurs by induction of nonlamellar lipid structures. *J Biol Chem* 2003; 278:45216-45223.
35. Basañez G, Nechushtan A, Drozhinin O et al. Bax, but not Bcl-xL, decreases the lifetime of planar phospholipid bilayer membranes at subnanomolar concentrations. *Proc Natl Acad Sci USA* 1999; 96:5492-5497.
36. Tilley SJ, Orlova EV, Gilbert RJC et al. Structural basis of pore formation by the bacterial toxin pneumolysin. *Cell* 2005; 121:247-256.
37. Nir S, Nieva J. Interactions of peptides with liposomes: pore formation and fusion. *Prog Lipid Res* 2000; 39:181-206.
38. Nieva J, Agirre A. Are fusion peptides a good model to study viral cell fusion? *Biochim Biophys Acta* 2003; 1614:104-115.
39. Longo ML, Waring AJ, Hammer DA. Interaction of the influenza hemagglutinin fusion peptide with lipid bilayers: area expansion and permeation. *Biophys J* 1997; 73:1430-1439.
40. Deshayes S, Plénat T, Charnet P et al. Formation of transmembrane ionic channels of primary amphipathic cell-penetrating peptides. Consequences on the mechanism of cell penetration. *Biochim Biophys Acta* 2006; 1758:1846-1851.
41. Yandek LE, Pokorny A, Florén A et al. Mechanism of the cell-penetrating peptide transportan 10 permeation of lipid bilayers. *Biophys J* 2007; 92:2434-2444.
42. Dathe M, Wieprecht T. Structural features of helical antimicrobial peptides: their potential to modulate activity on model membranes and biological cells. *Biochim Biophys Acta* 1999; 1462:71-87.
43. Menestrina G, Serra MD, Lazarovici P, ed(s). *Pore-forming Peptides and Protein Toxins. Series: Cellular and Molecular Mechanisms of Toxin Action, Vol. 5.* London: CRC Press (Taylor and Francis Group), 2003.
44. White SH, Wimley WC. Hydrophobic interactions of peptides with membrane interfaces. *Biochim Biophys Acta* 1998; 1376:339-352.
45. Fernández-Vidal M, Jayasinghe S, Ladokhin AS et al. Folding amphipathic helices into membranes: amphiphilicity trumps hydrophobicity. *J Mol Biol* 2007; 370:459-470.
46. White SH, Wimley WC. Membrane protein folding and stability: Physical principles. *Annu Rev Biophys Biomol Struct* 1999; 28:319-365.
47. Seelig J. Thermodynamics of lipid-peptide interactions. *Biochim Biophys Acta* 2004; 1666:40-50.
48. Hristova K, Dempsey CE, White SH. Structure, location and lipid perturbations of melittin at the membrane interface. *Biophys J* 2001; 80:801-811.
49. Aliste MP, MacCallum JL, Tieleman DP. Molecular dynamics simulations of pentapeptides at interfaces: salt bridge and cation-pi interactions. *Biochemistry* 2003; 42:8976-8987.
50. Killian JA, von Heijne G. How proteins adapt to a membrane-water interface. *Trends Biochem Sci* 2000; 25:429-434.
51. Planque MRD, Kruijtzter JA, Liskamp RM et al. Different membrane anchoring positions of tryptophan and lysine in synthetic transmembrane alpha-helical peptides. *J Biol Chem* 1999; 274:20839-20846.
52. Kandasamy SK, Larson RG. Binding and insertion of alpha-helical anti-microbial peptides in POPC bilayers studied by molecular dynamics simulations. *Chem Phys Lipids* 2004; 132:113-132.
53. Johnston JM, Cook GA, Tomich JM et al. Conformation and environment of channel-forming peptides: a simulation study. *Biophys J* 2006; 90:1855-1864.

54. Pérez-Méndez O, Vanloo B, Decout A et al. Contribution of the hydrophobicity gradient of an amphipathic peptide to its mode of association with lipids. *Eur J Biochem* 1998; 256:570-579.
55. Uematsu N, Matsuzaki K. Polar angle as a determinant of amphipathic alpha-helix-lipid interactions: a model peptide study. *Biophys J* 2000; 79:2075-2083.
56. Klocek G, Schulthess T, Shai Y et al. Thermodynamics of melittin binding to lipid bilayers. Aggregation and pore formation. *Biochemistry* 2009; 48:2586-2596.
57. Wieprecht T, Apostolov O, Beyermann M et al. Thermodynamics of the alpha-helix-coil transition of amphipathic peptides in a membrane environment: implications for the peptide-membrane binding equilibrium. *J Mol Biol* 1999; 294:785-794.
58. Li Y, Han X, Tamm LK. Thermodynamics of fusion peptide-membrane interactions. *Biochemistry* 2003; 42:7245-7251.
59. Tucker MJ, Tang J, Gai F. Probing the kinetics of membrane-mediated helix folding. *J Phys Chem B* 2006; 110:8105-8109.
60. Tang J, Signarvic RS, DeGrado WF et al. Role of helix nucleation in the kinetics of binding of mas-toparan X to phospholipid bilayers. *Biochemistry* 2007; 46:13856-13863.
61. Meier M, Seelig J. Thermodynamics of the coil \rightleftharpoons beta-sheet transition in a membrane environment. *J Mol Biol* 2007; 369:277-289.
62. Ladokhin AS, Legmann R, Collier RJ et al. Reversible refolding of the diphtheria toxin T-domain on lipid membranes. *Biochemistry* 2004; 43:7451-7458.
63. Wade D, Boman A, Wählin B et al. All-D amino acid-containing channel-forming antibiotic peptides. *Proc Natl Acad Sci USA* 1990; 87:4761-4765.
64. Hilpert K, Elliott MR, Volkmer-Engert R et al. Sequence requirements and an optimization strategy for short antimicrobial peptides. *Chem Biol* 2006; 13:1101-1107.
65. Anderluh G, Lakey JH. Disparate proteins use similar architectures to damage membranes. *Trends Biochem Sci* 2008; 33:482-490.
66. Parker MW, Feil SC. Pore-forming protein toxins: from structure to function. *Prog Biophys Mol Biol* 2005; 88:91-142.
67. Magzoub M, Eriksson LEG, Gräslund A. Comparison of the interaction, positioning, structure induction and membrane perturbation of cell-penetrating peptides and nontranslocating variants with phospholipid vesicles. *Biophys Chem* 2003; 103:271-288.
68. Shaw J, Epanand R, Hsu J et al. Cationic peptide-induced remodelling of model membranes: Direct visualization by in situ atomic force microscopy. *J Struct Biol* 2008; 162:121-138.
69. Huang HW. Free Energies of molecular bound states in lipid bilayers: lethal concentrations of antimicrobial peptides. *Biophys J* 2009; 96:3263-3272.
70. Valeva A, Hellmann N, Walev I et al. Evidence that clustered phosphocholine head groups serve as sites for binding and assembly of an oligomeric protein pore. *J Biol Chem* 2006; 281:26014-26021.
71. Gregory SM, Cavanaugh A, Journigan V et al. A quantitative model for the all-or-none permeabilization of phospholipid vesicles by the antimicrobial peptide cecropin A. *Biophys J* 2008; 94:1667-1680.
72. McLaughlin S. The electrostatic properties of membranes. *Annu Rev Biophys Chem* 1989; 18:113-136.
73. Wieprecht T, Apostolov O, Beyermann M et al. Membrane binding and pore formation of the antibacterial peptide PGLa: thermodynamic and mechanistic aspects. *Biochemistry* 2000; 39:442-452.
74. Wieprecht, Apostolov, Seelig. Binding of the antibacterial peptide magainin 2 amide to small and large unilamellar vesicles. *Biophys Chem* 2000; 85:187-198.
75. van Meer G, Voelker DR, Feigenson GW. Membrane lipids: where they are and how they behave. *Nat Rev Mol Cell Biol* 2008; 9:112-124.
76. Huang HW. Molecular mechanism of antimicrobial peptides: the origin of cooperativity. *Biochim Biophys Acta* 2006; 1758:1292-1302.
77. Allende D, Simon SA, McIntosh TJ. Melittin-induced bilayer leakage depends on lipid material properties: evidence for toroidal pores. *Biophys J* 2005; 88:1828-1837.
78. Mani R, Cady SD, Tang M et al. Membrane-dependent oligomeric structure and pore formation of a beta-hairpin antimicrobial peptide in lipid bilayers from solid-state NMR. *Proc Natl Acad Sci USA* 2006; 103:16242-16247.
79. Wessman P, Strömstedt AA, Malmsten M et al. Melittin-lipid bilayer interactions and the role of cholesterol. *Biophys J* 2008; 95:4324-4336.
80. Zakharov SD, Heymann JB, Zhang YL et al. Membrane binding of the colicin E1 channel: activity requires an electrostatic interaction of intermediate magnitude. *Biophys J* 1996; 70:2774-2783.
81. McMullen T, Lewis R, McElhane R. Cholesterol-phospholipid interactions, the liquid-ordered phase and lipid rafts in model and biological membranes. *Curr Opin Colloid Interface Sci* 2004; 8:459-468.
82. Bennett WFD, MacCallum JL, Tieleman DP. Thermodynamic analysis of the effect of cholesterol on dipalmitoylphosphatidylcholine lipid membranes. *J Am Chem Soc* 2009; 131:1972-1978.

83. García-Sáez AJ, Chiantia S, Salgado J et al. Pore formation by a Bax-derived peptide: effect on the line tension of the membrane probed by AFM. *Biophys J* 2007; 93:103-112.
84. Giddings KS, Zhao J, Sims PJ et al. Human CD59 is a receptor for the cholesterol-dependent cytolysin intermedilysin. *Nat Struct Mol Biol* 2004; 11:1173-1178.
85. Soltani CE, Hotze EM, Johnson AE et al. Structural elements of the cholesterol-dependent cytolysins that are responsible for their cholesterol-sensitive membrane interactions. *Proc Natl Acad Sci USA* 2007; 104:20226-20231.
86. Rossjohn J, Feil SC, McKinstry WJ et al. Structure of a cholesterol-binding, thiol-activated cytolysin and a model of its membrane form. *Cell* 1997; 89:685-692.
87. Mancheño JM, Martín-Benito J, Martínez-Ripoll M et al. Crystal and electron microscopy structures of sticholysin II actinoporin reveal insights into the mechanism of membrane pore formation. *Structure* 2003; 11:1319-1328.
88. Bakrač B, Gutiérrez-Aguirre I, Podlesek Z et al. Molecular determinants of sphingomyelin specificity of a eukaryotic pore-forming toxin. *J Biol Chem* 2008; 283:18665-18677.
89. Alegre-Cebollada J, Rodríguez-Crespo I, Gavilanes JG et al. Detergent-resistant membranes are platforms for actinoporin pore-forming activity on intact cells. *FEBS J* 2006; 273:863-871.
90. Martínez D, Otero A, Alvarez C et al. Effect of sphingomyelin and cholesterol on the interaction of St II with lipidic interfaces. *Toxicol* 2007; 49:68-81.
91. Schön P, García-Sáez AJ, Malovrh P et al. Equinatoxin II permeabilizing activity depends on the presence of sphingomyelin and lipid phase coexistence. *Biophys J* 2008; 95:691-698.
92. Barlič A, Gutiérrez-Aguirre I, Caaveiro JMM et al. Lipid phase coexistence favors membrane insertion of equinatoxin-II, a pore-forming toxin from *Actinia equina*. *J Biol Chem* 2004; 279:34209-34216.
93. Abrami L, van Der Goet FG. Plasma membrane microdomains act as concentration platforms to facilitate intoxication by aerolysin. *J Cell Biol* 1999; 147:175-184.
94. Kuwana T, Mackey MR, Perkins G et al. Bid, Bax and lipids cooperate to form supramolecular openings in the outer mitochondrial membrane. *Cell* 2002; 111:331-342.
95. Lucken-Ardjomande S, Montessuit S, Martinou J. Contributions to Bax insertion and oligomerization of lipids of the mitochondrial outer membrane. *Cell Death Differ* 2008; 15:929-937.
96. Lutter M, Fang M, Luo X et al. Cardiolipin provides specificity for targeting of tBid to mitochondria. *Nat Cell Biol* 2000; 2:754-761.
97. Scorrano L, Ashiya M, Buttke K et al. A distinct pathway remodels mitochondrial cristae and mobilizes cytochrome c during apoptosis. *Dev Cell* 2002; 2:55-67.
98. Gonzalez F, Pariselli F, Dupaigne P et al. tBid interaction with cardiolipin primarily orchestrates mitochondrial dysfunction and subsequently activates Bax and Bak. *Cell Death Differ* 2005; 12:614-626.
99. Tyurin VA, Tyurina YY, Osipov AN et al. Interactions of cardiolipin and lyso-cardiolipins with cytochrome c and tBid: conflict or assistance in apoptosis. *Cell Death Differ* 2006; 14:872-875.
100. Ott M, Zhivotovsky B, Orrenius S. Role of cardiolipin in cytochrome c release from mitochondria. *Cell Death Differ* 2007; 14:1243-1247.
101. Lucken-Ardjomande S, Montessuit S, Martinou J. Contributions to Bax insertion and oligomerization of lipids of the mitochondrial outer membrane. *Cell Death Differ* 2008; 15:929-937.
102. Ott M, Robertson JD, Gogvadze V et al. Cytochrome c release from mitochondria proceeds by a two-step process. *Proc Natl Acad Sci USA* 2002; 99:1259-1263.
103. Orrenius S, Gogvadze V, Zhivotovsky B. Mitochondrial oxidative stress: implications for cell death. *Annu Rev Pharmacol Toxicol* 2007; 47:143-183.
104. Tilley SJ, Saibil HR. The mechanism of pore formation by bacterial toxins. *Curr Opin Struct Bio* 2006; 16:230-236.
105. Wimley WC, White SH. Reversible unfolding of beta-sheets in membranes: a calorimetric study. *J Mol Biol* 2004; 342:703-711.
106. Silvestro L, Axelsen P. Membrane-induced folding of cecropin A. *Biophys J* 2000; 79:1465-1477.
107. Im W, Brooks III CL. Interfacial folding and membrane insertion of designed peptides studied by molecular dynamics simulations. *Proc Natl Acad Sci USA* 2005; 102:6771-6776.
108. Marrink SJ, de Vries AH, Tieleman DP. Lipids on the move: simulations of membrane pores, domains, stalks and curves. *Biochim Biophys Acta* 2009; 1788:149-168.
109. Ladokhin AS, White SH. Folding of amphipathic alpha-helices on membranes: energetics of helix formation by melittin. *J Mol Biol* 1999; 285:1363-1369.
110. Wimley WC, Hristova K, Ladokhin AS et al. Folding of beta-sheet membrane proteins: a hydrophobic hexapeptide model. *J Mol Biol* 1998; 277:1091-1110.
111. Meier M, Seelig J. Length dependence of the coil \longleftrightarrow beta-sheet transition in a membrane environment. *J Am Chem Soc* 2008; 130:1017-1024.
112. Perier A, Chassaing A, Raffestin S et al. Concerted Protonation of Key Histidines Triggers Membrane Interaction of the Diphtheria Toxin T Domain. *J Biol Chem* 2007; 282:24239-24245.

113. van der Goot FG, González-Mañas JM, Lakey JH et al. A 'molten-globule' membrane-insertion intermediate of the pore-forming domain of colicin A. *Nature* 1991; 354:408-410.
114. Zakharov SD, Lindeberg M, Griko Y et al. Membrane-bound state of the colicin E1 channel domain as an extended two-dimensional helical array. *Proc Natl Acad Sci USA* 1998; 95:4282-4287.
115. Oh KJ, Zhan H, Cui C et al. Organization of diphtheria toxin T domain in bilayers: a site-directed spin labeling study. *Science* 1996; 273:810-812.
116. Rossjohn J, Polekhina G, Feil SC et al. Structures of perfringolysin o suggest a pathway for activation of cholesterol-dependent cytolytins. *J Mol Biol* 2007; 367:1227-1236.
117. Bechinger B. The structure, dynamics and orientation of antimicrobial peptides in membranes by multidimensional solid-state NMR spectroscopy. *Biochim Biophys Acta* 1999; 1462:157-183.
118. Huang HW. Action of Antimicrobial Peptides: Two-State Model. *Biochemistry* 2000; 39:8347-8352.
119. Afonin S, Grage SL, Ieronimo M et al. Temperature-dependent transmembrane insertion of the amphiphilic peptide PGLa in lipid bilayers observed by solid state (19)F NMR spectroscopy. *J Am Chem Soc* 2008; 130:16512-16514.
120. Afonin S, Durr U, Wadhvani P et al. Solid state NMR structure analysis of the antimicrobial peptide gramicidin S in lipid membranes: concentration-dependent re-alignment and self-assembly as a beta-barrel. In: Peters T, ed. *Bioactive Conformation II*. Berlin: Springer International, 2008: 139-154.
121. Luo W, Yao X, Hong M. Large structure rearrangement of colicin ia channel domain after membrane binding from 2D 13C spin diffusion NMR. *J Am Chem Soc* 2005; 127:6402-6408.
122. Lindeberg M, Zakharov SD, Cramer WA. Unfolding pathway of the colicin E1 channel protein on a membrane surface. *J Mol Biol* 2000; 295:679-692.
123. Aisenbrey C, Sudheendra US, Ridley H et al. Helix orientations in membrane-associated Bcl-X(L) determined by 15N-solid-state NMR spectroscopy. *Eur Biophys J* 2007; 37:71-80.
124. Gong X, Choi J, Franzin C et al. Conformation of membrane-associated proapoptotic tBid. *J Biol Chem* 2004; 279:28954-28960.
125. Oh KJ, Barbuto S, Meyer N et al. Conformational changes in BID, a pro-apoptotic BCL-2 family member, upon membrane binding. A site-directed spin labeling study. *J Biol Chem* 2005; 280:753-767.
126. Annis MG, Soucie EL, Dlugosz PJ et al. Bax forms multispinning monomers that oligomerize to permeabilize membranes during apoptosis. *EMBO J* 2005; 24:2096-2103.
127. García-Sáez AJ, Mingarro I, Pérez-Payá E et al. Membrane-insertion fragments of Bcl-xL, Bax and Bid. *Biochemistry* 2004; 43:10930-10943.
128. Franzin CM, Choi J, Zhai D et al. Structural studies of apoptosis and ion transport regulatory proteins in membranes. *Magn Reson Chem* 2004; 42:172-179.
129. Rosconi MP, Zhao G, London E. Analyzing topography of membrane-inserted diphtheria toxin T domain using BODIPY-streptavidin: at low pH, helices 8 and 9 form a transmembrane hairpin but helices 5-7 form stable nonclassical inserted segments on the cis side of the bilayer. *Biochemistry* 2004; 43:9127-9139.
130. Zhao G, London E. Behavior of diphtheria toxin T domain containing substitutions that block normal membrane insertion at Pro345 and Leu307: control of deep membrane insertion and coupling between deep insertion of hydrophobic subdomains. *Biochemistry* 2005; 44:4488-4498.
131. Chattopadhyay K, Banerjee KK. Unfolding of *Vibrio cholerae* hemolysin induces oligomerization of the toxin monomer. *J Biol Chem* 2003; 278:38470-38475.
132. McLaughlin S, Aderem A. The myristoyl-electrostatic switch: a modulator of reversible protein-membrane interactions. *Trends Biochem Sci* 1995; 20:272-276.
133. Zhuang M, Oltean DI, Gómez I et al. *Heliothis virescens* and *Manduca sexta* lipid rafts are involved in CryIA toxin binding to the midgut epithelium and subsequent pore formation. *J Biol Chem* 2002; 277:13863-13872.
134. Yamaji-Hasegawa A, Makino A, Baba T et al. Oligomerization and pore formation of a sphingomyelin-specific toxin, lysenin. *J Biol Chem* 2003; 278:22762-22770.
135. Leber B, Lin J, Andrews DW. Embedded together: the life and death consequences of interaction of the Bcl-2 family with membranes. *Apoptosis* 2007; 12:897-911.
136. Billen LP, Kokoski CL, Lovell JF et al. Bcl-XL inhibits membrane permeabilization by competing with Bax. *PLoS Biology* 2008; 6:e147.
137. Lovell JF, Billen LP, Bindner S et al. Membrane binding by tBid initiates an ordered series of events culminating in membrane permeabilization by Bax. *Cell* 2008; 135:1074-1084.
138. Farago O, Santangelo C. Pore formation in fluctuating membranes. *J Chem Phys* 2005; 122:044901.
139. Gurtovenko AA, Vattulainen I. Pore formation coupled to ion transport through lipid membranes as induced by transmembrane ionic charge imbalance: atomistic molecular dynamics study. *J Am Chem Soc* 2005; 127:17570-17571.
140. de Vries AH, Mark AE, Marrink SJ. Molecular dynamics simulation of the spontaneous formation of a small DPPC vesicle in water in atomistic detail. *J Am Chem Soc* 2004; 126:4488-4489.

141. Wang Z, Frenkel D. Pore nucleation in mechanically stretched bilayer membranes. *J Chem Phys* 2005; 123:154701.
142. Tolpekina TV, den Otter WK, Briels WJ. Nucleation free energy of pore formation in an amphiphilic bilayer studied by molecular dynamics simulations. *J Chem Phys* 2004; 121:12060-12066.
143. Marrink SJ, Lindahl E, Edholm O et al. Simulation of the spontaneous aggregation of phospholipids into bilayers. *J Am Chem Soc* 2001; 123:8638-8639.
144. Daleke D. Phospholipid flippases. *J Biol Chem* 2007; 282:821-825.
145. Kornberg RD, McConnell HM. Inside-outside transitions of phospholipids in vesicle membranes. *Biochemistry* 1971; 10:1111-1120.
146. Wimley WC, Thompson TE. Exchange and flip-flop of dimyristoylphosphatidylcholine in liquid-crystalline, gel and two-component, two-phase large unilamellar vesicles. *Biochemistry* 1990; 29:1296-1303.
147. De Kruijff B, Van Zoelen EJ. Effect of the phase transition on the transbilayer movement of dimyristoyl phosphatidylcholine in unilamellar vesicles. *Biochim Biophys Acta* 1978; 511:105-115.
148. Nakano M, Fukuda M, Kudo T et al. Flip-flop of phospholipids in vesicles: kinetic analysis with time-resolved small-angle neutron scattering. *J Phys Chem B* 2009; 113:6745-6748.
149. Wimley WC, Thompson TE. Transbilayer and interbilayer phospholipid exchange in dimyristoylphosphatidylcholine/dimyristoylphosphatidylethanolamine large unilamellar vesicles. *Biochemistry* 1991; 30:1702-1709.
150. Karatekin E, Sandre O, Guitouni H et al. Cascades of transient pores in giant vesicles: line tension and transport. *Biophys J* 2003; 84:1734-1749.
151. Rodríguez N, Cribier S, Pincet F. Transition from long- to short-lived transient pores in giant vesicles in an aqueous medium. *Phys Rev E* 2006; 74.
152. Toyoshima Y, Thompson TE. Chloride flux in bilayer membranes: chloride permeability in aqueous dispersions of single-walled, bilayer vesicles. *Biochemistry* 1975; 14:1525-1531.
153. Gurtovenko AA, Vattulainen I. Ion leakage through transient water pores in protein-free lipid membranes driven by transmembrane ionic charge imbalance. *Biophys J* 2007; 92:1878-1890.
154. Bramhall J, Hofmann J, DeGuzman R et al. Temperature dependence of membrane ion conductance analyzed by using the amphiphilic anion 5/6-carboxyfluorescein. *Biochemistry* 1987; 26:6330-6340.
155. Clerc SG, Thompson TE. Permeability of dimyristoyl phosphatidylcholine/dipalmitoyl phosphatidylcholine bilayer membranes with coexisting gel and liquid-crystalline phases. *Biophys J* 1995; 68:2333-2341.
156. Simons K, Vaz WLC. Model systems, lipid rafts and cell membranes. *Annu Rev Biophys Biomol Struct* 2004; 33:269-295.
157. Ruiz-Argüello M, Basáñez G, Goñi F et al. Different effects of enzyme-generated ceramides and diacylglycerols in phospholipid membrane fusion and leakage. *J Biol Chem* 1996; 271:26616-26621.
158. Siskind LJ, Colombini M. The lipids C2- and C16-ceramide form large stable channels. Implications for apoptosis. *J Biol Chem* 2000; 275:38640-38644.
159. Contreras F, Basanez G, Alonso A et al. Asymmetric addition of ceramides but not dihydroceramides promotes transbilayer (flip-flop) lipid motion in membranes. *Biophys J* 2005; 88:348-359.
160. Goñi FM, Alonso A. Biophysics of sphingolipids I. Membrane properties of sphingosine, ceramides and other simple sphingolipids. *Biochim Biophys Acta* 2006; 1758:1902-1921.
161. Anishkin A, Sukharev S, Colombini M. Searching for the molecular arrangement of transmembrane ceramide channels. *Biophys J* 2006; 90:2414-2426.
162. Kol MA, van Dalen A, de Kroon AIPM et al. Translocation of phospholipids is facilitated by a subset of membrane-spanning proteins of the bacterial cytoplasmic membrane. *J Biol Chem* 2003; 278:24586-24593.
163. de Kruijff B, van Zoelen EJ, van Deenen LL. Glycophorin facilitates the transbilayer movement of phosphatidylcholine in vesicles. *Biochim Biophys Acta* 1978; 509:537-542.
164. Kol MA, de Kroon AI, Rijkers DT et al. Membrane-spanning peptides induce phospholipid flip-flop: a model for phospholipid translocation across the inner membrane of *E. coli*. *Biochemistry* 2001; 40:10500-10506.
165. Fattal E, Nir S, Parente RA et al. Pore-forming peptides induce rapid phospholipid flip-flop in membranes. *Biochemistry* 1994; 33:6721-6731.
166. García-Sáez AJ, Coraiola M, Dalla Serra M et al. Peptides corresponding to helices 5 and 6 of Bax can independently form large lipid pores. *FEBS J* 2006; 273:971-981.
167. Terrones O, Antonsson B, Yamaguchi H et al. Lipidic pore formation by the concerted action of proapoptotic BAX and tBID. *J Biol Chem* 2004; 279:30081-30091.
168. Sobko AA, Kotova EA, Antonenko YN et al. Lipid dependence of the channel properties of the colicin E1-lipid toroidal pore. *J Biol Chem* 2006; 281:14408-14416.

169. Müller P, Schiller S, Wierprecht T et al. Continuous measurement of rapid transbilayer movement of a pyrene-labeled phospholipid analogue. *Chem Phys Lipids* 2000; 106:89-99.
170. Epand R, Martinou J, Montessuit S et al. Transbilayer lipid diffusion promoted by Bax: Implications for apoptosis. *Biochemistry* 2003; 42:14576-14582.
171. Polozov IV, Anantharamaiah GM, Segrest JP et al. Osmotically induced membrane tension modulates membrane permeabilization by class L amphipathic helical peptides: nucleation model of defect formation. *Biophys J* 2001; 81:949-959.
172. Zitzer A, Bittman R, Verbicky CA et al. Coupling of cholesterol and cone-shaped lipids in bilayers augments membrane permeabilization by the cholesterol-specific toxins streptolysin O and *Vibrio cholerae* cytolysin. *J Biol Chem* 2001; 276:14628-14633.
173. Siskind LJ, Feinstein L, Yu T et al. Anti-apoptotic Bcl-2 Family Proteins Disassemble Ceramide Channels. *J Biol Chem* 2008; 283:6622-6630.
174. Weinstein J, Klausner R, Innerarity T et al. Phase-transition release, a new approach to the interaction of proteins with lipid vesicles. Application to lipoproteins. *Biochim Biophys Acta* 1981; 647:270-284.
175. Malev VV, Schagina LV, Gurnev PA et al. Syringomycin E channel: a lipidic pore stabilized by lipopeptide? *Biophys J* 2002; 82:1985-1994.
176. Cruciani RA, Barker JL, Durell SR et al. Magainin 2, a natural antibiotic from frog skin, forms ion channels in lipid bilayer membranes. *Eur J Pharmacol* 1992; 226:287-296.
177. Ludtke SJ, He K, Wu Y et al. Cooperative membrane insertion of magainin correlated with its cytolytic activity. *Biochim Biophys Acta* 1994; 1190:181-184.
178. Chen F, Lee M, Huang HW. Sigmoidal concentration dependence of antimicrobial peptide activities: a case study on alamethicin. *Biophys J* 2002; 82:908-914.
179. Qian S, Wang W, Yang L et al. Structure of the alamethicin pore reconstructed by x-ray diffraction analysis. *Biophys J* 2008; 94:3512-3522.
180. Qian S, Wang W, Yang L et al. Structure of transmembrane pore induced by Bax-derived peptide: evidence for lipidic pores. *Proc Natl Acad Sci USA* 2008; 105:17379-17383.
181. Lee M, Chen F, Huang HW. Energetics of pore formation induced by membrane active peptides. *Biochemistry* 2004; 43:3590-3599.
182. Pokorny A, Birkbeck TH, Almeida PFF. Mechanism and Kinetics of δ -Lysin Interaction with Phospholipid Vesicles. *Biochemistry* 2002; 41:11044-11056.
183. Dufourc EJ, Bonmatin JM, Dufourcq J. Membrane structure and dynamics by 2H- and 31P-NMR. Effects of amphipathic peptidic toxins on phospholipid and biological membranes. *Biochimie* 1989; 71:117-123.
184. Bechinger B, Lohner K. Detergent-like actions of linear amphipathic cationic antimicrobial peptides. *Biochim Biophys Acta* 2006; 1758:1529-1539.
185. Pott T, Dufourc E. Action of melittin on the DPPC-cholesterol liquid-ordered phase: a solid state 2H- and 31P-NMR study. *Biophys J* 1995; 68:965-977.
186. Latorre R, Alvarez O. Voltage-dependent channels in planar lipid bilayer membranes. *Physiol Rev* 1981; 61:77-150.
187. Wu Y, Huang HW, Olah GA. Method of oriented circular dichroism. *Biophys J* 1990; 57:797-806.
188. Bürck J, Roth S, Wadhvani P et al. Conformation and membrane orientation of amphiphilic helical peptides by oriented circular dichroism. *Biophys J* 2008; 95:3872-3881.
189. Basañez G, Sharpe JC, Galanis J et al. Bax-type apoptotic proteins porate pure lipid bilayers through a mechanism sensitive to intrinsic monolayer curvature. *J Biol Chem* 2002; 277:49360-49365.
190. Glaser RW, Leikin SL, Chernomordik LV et al. Reversible electrical breakdown of lipid bilayers: formation and evolution of pores. *Biochim Biophys Acta* 1988; 940:275-287.
191. Olbrich K, Rawicz W, Needham D et al. Water permeability and mechanical strength of polyunsaturated lipid bilayers. *Biophys J* 2000; 79:321-327.
192. Puech P, Borghi N, Karatekin E et al. Line Thermodynamics: Adsorption at a Membrane Edge. *Phys Rev Lett* 2003; 90:128304.
193. Lee M, Hung W, Chen F et al. Many-body effect of antimicrobial peptides: on the correlation between lipid's spontaneous curvature and pore formation. *Biophys J* 2005; 89:4006-4016.
194. Longo M, Waring A, Gordon L et al. Area expansion and permeation of phospholipid membrane bilayers by influenza fusion peptides and melittin. *Langmuir* 1998; 14:2385-2395.
195. Chen F, Lee M, Huang HW. Evidence for membrane thinning effect as the mechanism for peptide-induced pore formation. *Biophys J* 2003; 84:3751-3758.
196. Li C, Salditt T. Structure of magainin and alamethicin in model membranes studied by x-ray reflectivity. *Biophys J* 2006; 91:3285-3300.
197. Huang HW. Deformation free energy of bilayer membrane and its effect on gramicidin channel lifetime. *Biophys J* 1986; 50:1061-1070.

198. Nielsen C, Goulian M, Andersen OS. Energetics of inclusion-induced bilayer deformations. *Biophys J* 1998; 74:1966-1983.
199. Fosnarić M, Kralj-Iglic V, Bohinc K et al. Stabilization of pores in lipid bilayers by anisotropic inclusions. *J Phys Chem B* 2003; 107:12519-12526.
200. Matsuzaki K, Sugishita K, Ishibe N et al. Relationship of membrane curvature to the formation of pores by magainin 2. *Biochemistry* 1998; 37:11856-11863.
201. Cullis PR, Hope MJ, Tilcock CP. Lipid polymorphism and the roles of lipids in membranes. *Chem Phys Lipids* 1986; 40:127-144.
202. Sobko AA, Kotova EA, Antonenko YN et al. Effect of lipids with different spontaneous curvature on the channel activity of colicin E1: evidence in favor of a toroidal pore. *FEBS Lett* 2004; 576:205-210.
203. de Kruijff B, Cullis PR. The influence of poly(L-lysine) on phospholipid polymorphism. Evidence that electrostatic polypeptide-phospholipid interactions can modulate bilayer/nonbilayer transitions. *Biochim Biophys Acta* 1980; 601:235-240.
204. Zemel A, Ben-Shaul A, May S. Modulation of the Spontaneous Curvature and Bending Rigidity of Lipid Membranes by Interfacially Adsorbed Amphipathic Peptides. *J Phys Chem B* 2008; 112:6988-6996.
205. Wiener MC, White SH. Structure of a fluid dioleoylphosphatidylcholine bilayer determined by joint refinement of x-ray and neutron diffraction data. III. Complete structure. *Biophys J* 1992; 61:434-447.
206. Hristova K, Wimley WC, Mishra VK et al. An amphipathic alpha-helix at a membrane interface: a structural study using a novel X-ray diffraction method. *J Mol Biol* 1999; 290:99-117.
207. Gesell J, Zasloff M, Opella SJ. Two-dimensional ¹H NMR experiments show that the 23-residue magainin antibiotic peptide is an alpha-helix in dodecylphosphocholine micelles, sodium dodecylsulfate micelles and trifluoroethanol/water solution. *J Biomol NMR* 1997; 9:127-135.
208. Ludtke S, He K, Huang H. Membrane thinning caused by magainin 2. *Biochemistry* 1995; 34:16764-16769.

CHAPTER 5

Cholesterol-Dependent Cytolysins

Robert J.C. Gilbert*

Abstract

The cholesterol-dependent cytolysins (CDCs) are part of a large family of pore-forming proteins that include the human proteins perforin and the complement membrane attack complex. The activity of all family members is focused on membranes, but the proteins are themselves involved in a diverse range of phenomena. An overview of some of these phenomena is provided here, along with an historical perspective of CDCs themselves and how our understanding of their mechanism of action has developed over the years. The way in which pore formation depends on specific characteristics of the membrane under attack as well as of the protein doing the attacking is emphasised.

The cholesterol-dependent cytolysins (CDCs) have been the focus of a renewed keen research interest for over ten years now.¹⁻⁴ Their importance has been even further enhanced by the homology now identified between them and the membrane attack complex/perforin (MACPF) family of proteins, which includes several components of the complement cascade as well as perforin itself.⁵⁻⁹ In this chapter I aim to provide an overview of our understanding of the interaction between CDCs and other members of what is now called the MACPF/CDC superfamily, with their target membranes.

CDCs (also in the past known as thiol-activated toxins or cholesterol-binding toxins) were originally identified from four Gram-positive bacterial genera (*Clostridium*, *Listeria*, *Bacillus* and *Streptococcus*). Well-known examples include listeriolysin, perfringolysin, streptolysin and pneumolysin. Listeriolysin from *L. monocytogenes* is responsible for the escape of bacteria from the phagosome to colonise the cytoplasm¹⁰ and has been applied as a protein adjuvant in the development of vaccines against cancer and tuberculosis, for example.¹¹⁻¹³ Perfringolysin from *C. perfringens* (Fig. 1A) has become perhaps the most studied CDC⁴ and has an important role in pathology associated with infection (gangrene).¹⁴⁻¹⁶ Streptolysin from *S. pyogenes* is another intensely studied CDC and has been applied widely in experimental permeabilisation of biological membranes.^{17,18} Pneumolysin is a major virulence determinant for *S. pneumoniae*, allowing bacterial invasion of tissues and mediating inflammation and the activation of the complement cascade.^{19,20} However, CDCs have now, for example, been identified in the bacteria *Arcanobacterium pyogenes* and *Gardnerella vaginalis*⁸ and there also appear to be homologues outside prokaryotes such as the sea anemone *Metridium senile* pore-forming toxin metridiolysin.²¹ The homology with the MACPF family was unknown until the first structures of the canonical fold of that family were solved, revealing the now characteristic MACPF/CDC fold of a twisted β -sheet around which helices are clustered (Fig. 1A and D). Without any significant other sequence homology, the fold of this superfamily of pore-forming and membrane-binding proteins has been conserved by compensatory mutation around a handful of key conserved glycines.^{6,8,9} The glycines presumably act as critical hinges during the dramatic refolding that CDCs are known to undergo and which

*Robert J.C. Gilbert—Division of Structural Biology, Wellcome Trust Centre for Human Genetics, University of Oxford, Roosevelt Drive, Oxford OX3 7BN, UK. Email: gilbert@strubi.ox.ac.uk

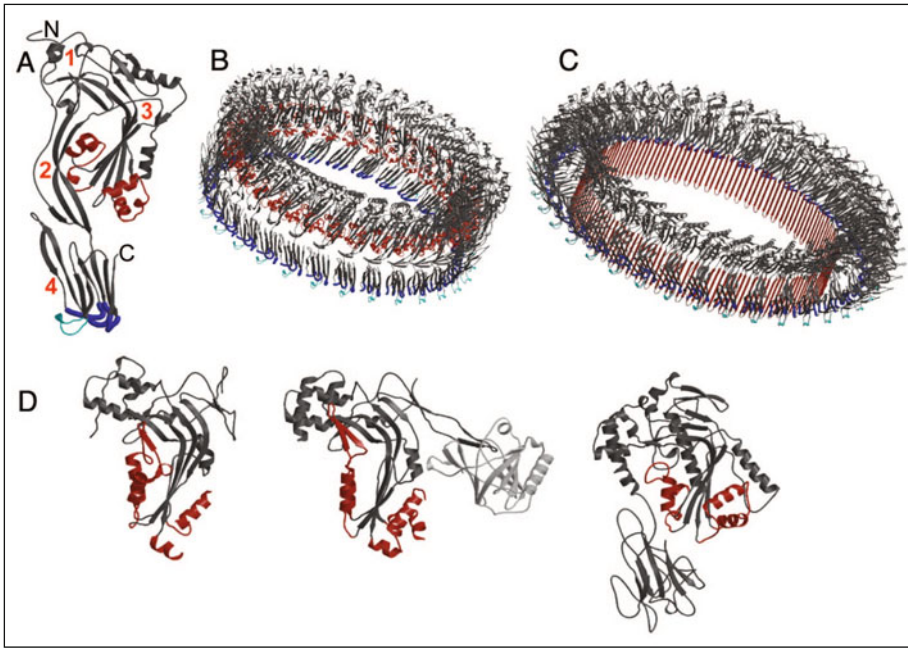


Figure 1. A) Atomic structure of perfringolysin⁷⁸ depicted as a grey ribbon. The two helical regions which refold into the membrane as a β -hairpin are coloured red, the loops at the base of domain 4 implicated in cholesterol binding blue with an expanded coil radius and the tryptophan-rich loop upon which cholesterol impacts in pore formation in cyan. B) Atomic model of the prepore state of CDCs when a full ring oligomer is formed, modeling the perfringolysin crystal structure into a cryo-EM map for the prepore.²⁷ Regions of the structure are coloured as in panel (A). C) Atomic model of the pore state of CDCs as a full ring, as in (B) for the prepore. D) Atomic models of complement protein C8 α (left), a complex of C8 α and C8 γ (center) and the Plu-MACPF domain, a prokaryotic MACPF protein (right). The regions of each structure correlating to the membrane-inserting regions of CDCs are coloured red in each case and in the central panel C8 γ is coloured a lighter shade of grey.

is presumably the selective advantage of this specific structure that has caused it to be conserved over such a vast evolutionary timescale. While not all MACPF domains are involved in pore formation—for example, C6 and C8 β —they are all apparently involved in action on membranes.^{8,22} The dramatic refolding undergone by CDCs is tightly coupled to their oligomerisation and results in the conversion of the helices hemming the core β -sheet of the MACPF/CDC domain into a pair of β -hairpins which in tandem and alongside those from other subunits within the oligomer insert into the membrane to create a pore^{2,4,23-27} (Fig. 1A-C). It is obviously the basic assumption that where nonCDC members of the superfamily—such as complement proteins and perforin—act on membranes they do so by a mechanism involving similar refolding.^{5,8} Even where a member of the MACPF/CDC superfamily is not known to form a pore, or has been shown not to—at least alone—the same conformational change could have other adaptive functions during activity on or at membranes. However, the bicomponent nature of some pore-forming toxins²⁸ alerts us that showing an absence of activity for one pure protein does not mean that they do not contribute to pore formation quite directly, since that may require the presence of another MACPF/CDC family member or members from the same specific system. Complement acts by a combination of the C5b-8 complex of proteins preassembled on a target membrane recruiting C9 to form a lesion, which may be a complete ring of C9 associated with the C5b-8 or an arc—electron microscopy

images show both possibilities.^{29,30} Perforin acts in concert with granzymes, to trigger apoptosis when delivered by cytotoxic cells at their targets (damaged, transformed and infected host cells). Incomplete rings are visible for perforin also³¹⁻³³ and there are many unresolved issues concerning its mechanism and the dependence of granzymes on it for their delivery.³⁴⁻³⁸

Functional Studies on CDCs

CDCs were the subject of kinetic and electron microscopy studies in the 1990s, which sought to define their mechanism and to interpret it in terms of a molecular/mechanical model. Earlier images of ring-shaped and arc-shaped structures on membranes clearly represented oligomers,^{21,39} but the question was how did they assemble and what was the temporal and therefore mechanistic relationship between their assembly and the appearance of pores? Some kinetic studies indicated that the oligomerisation process preceded the appearance of pores, i.e., was complete by the stage at which pore activity appeared⁴⁰ and this key insight has only been strengthened by subsequent data.^{2,4} However, other studies showed that incomplete rings (arcs) may be functional or have some distinctive kinetic role,⁴¹ leading to a model of pore formation in which arcs were inserted into the membrane and formed pores and they could increase in size after a pore had formed.^{41,42} This was in fact a model for CDC activity that had been current for several years,³⁹ alongside the model in which the oligomer formed completely before a pore was generated.⁴⁰ For some time it appeared that these two views of CDC activity were irreconcilable, which left inexplicable either the data showing that arcs had functional significance^{39,41,42} or the data showing that oligomerisation was complete when pores form.^{23,25,26,40,43} However, all the available data are potentially explicable if the two models are combined whereby arcs can form pores, but oligomer growth is halted when they do.² On this view, a distinctive prepore structure does precede the appearance of a pore, but it is not necessarily a full ring as it can also be an arc (Fig. 2), as strikingly seen in an atomic force microscopy study of perfringolysin.^{2,43} Yet this synthesis leaves open a number of key questions, many of them to do with the way in which the CDCs interact with the membranes they target.

Membrane Binding by CDCs

The coining of the name 'thiol-activated toxin' as the first term by which CDCs were known derived from the observation that they became inactivated in impure preparations and could be re-activated by addition of cysteine or hydrogen sulphide.⁴⁴ It was later shown that the single cysteine possessed by most CDCs is not in itself critical for activity,⁴⁵ but clearly reaction with it blocks or hinders in some other way a key step in the process by which they act on membranes. Not only that, but it also appears to prevent self-oligomerisation,⁴⁶ which for some CDCs occurs spontaneously at high concentrations in solution to produce structures that are closely related to those formed during pore formation itself.^{2,27,47} This cysteine is found at the bottom of the C-terminal fourth CDC domain, as part of a tryptophan-rich loop (ECTGLAWEWWR) that has long been implicated in the process by which CDCs adhere to membranes and which is highly conserved. Some mutations within this 11-residue motif have severe effects on CDC activity and a spontaneously-occurring mutant form is found in the human-specific CDC intermedilysin from *S. intermedius*, where it reads GATGLAWEPWR.⁴⁸ Intermedilysin does not use cholesterol as its membrane receptor, but instead the protein CD59—a GPI-anchored molecule responsible for inhibition of complement activity at host cell membranes,⁴⁹ but the altered specificity does not derive from mutations in the conserved undecapeptide. Instead, mutations elsewhere at the base of domain 4 (Fig. 1A) are presumably responsible, since the location of cholesterol recognition in the other CDCs is found there.⁵⁰ And yet, despite the fact that intermedilysin does not bind to cholesterol in order to attach to a target membrane, it requires it for pore formation subsequent to binding.^{49,51} That cholesterol is otherwise the receptor for CDCs remains the general view, though this is accepted more by default than acclamation. Nevertheless, the cholesterol specificity of the CDCs has been tested thoroughly and historically was one of the earliest aspects of them to be well characterized. For some it has been directly observed⁵²⁻⁵⁵ and features of cholesterol that appear necessary include a β conformation of the cholesterol hydroxyl group on carbon-3 and the aliphatic

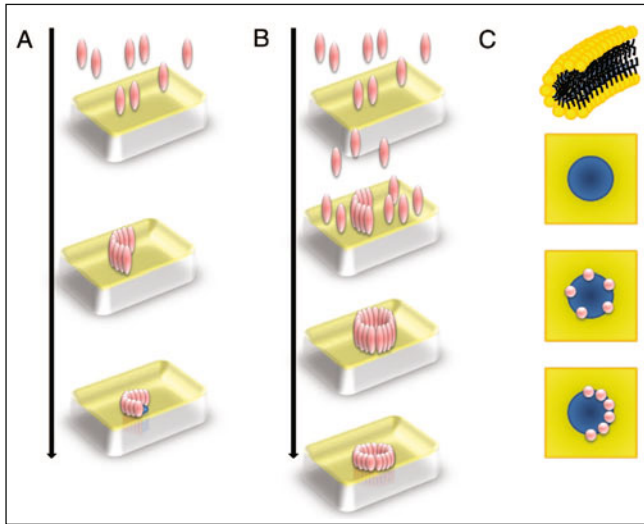


Figure 2. A) Cartoon of pore formation by a CDC oligomeric arc, in which the prepore (middle panel) is an incomplete ring, presumably due to a lack of further monomers for incorporation, and the pore consists of a protein arc abutting a lipid membrane in a toroidal arrangement of lipids (see panel C). The membrane is yellow, the CDC red and the pore blue. B) Cartoon of pore formation by a CDC oligomeric ring, in which the prepore (third image) is a complete ring due to sufficient monomeric toxin being present. Colours as in panel (B). C) *Top* cartoons of the arrangement of lipids expected to form the wall of a lipid-only or proteolipid mosaic pore, in which the upper and lower leaflets of a bilayer are joined through the lumen of the pore. *Second image* how this would look from above in the case of electroporation⁷¹; the whole wall surrounding the blue pore would be formed from this arrangement of lipids. *Third image* how this would look in the case that a mosaic of peptides and lipids form the pore, as with Bax⁷² (red objects represent inserted peptide). *Bottom image* how this would look in the case argued for CDCs in which an arc of protein triggers pore formation.

chain found on carbon-17.⁵⁶ In direct measurements, it was possible to show a 1:1 stoichiometry between cholesterol and pneumolysin, which again supports the idea that it acts as a receptor for such CDCs.⁵⁷ The affinity profile of CDC (perfringolysin) binding to membranes also suggests that a lipid receptor is involved, since there were two different affinity binding sites (of ~ 100 nM and ~ 1 nM Kd) and the balance between them is modulated by the lengths of the lipid aliphatic chains.^{58,59} For example, with just C(18) lipid tails the high affinity sites appeared when the cholesterol was at a mole-percentage of 31, 40% for 0.4:0.6 C(16):C(18) and 43% for just C(16) tails⁵⁸ and high affinity sites did not seem to arise at all with C(14) tails,⁵⁹ while carbon-carbon double bonds promoted binding of CDCs.⁶⁰ This suggests that it is possible a transmembrane dimer of cholesterol is the high affinity site structure.⁵⁵ A more recent study⁶¹ has strikingly recapitulated many of these findings previously made by Ohno-Iwashita and colleagues, underscoring that the lipid composition, besides cholesterol itself, affects the availability of cholesterol for CDCs to bind to. It seems that the cholesterol preferentially bound is free cholesterol (i.e., not in rafts/microdomains) and the high concentrations of sterol required to sustain CDC binding in model liposomal systems is due to the need to have such free cholesterol.⁶¹ This is effected by having saturated lipids otherwise forming close associations with cholesterol which may be achieved in living target cells by the presence of proteins and other lipids which are not recognized by CDCs but which can bind to phospholipids in similar ways to cholesterol.⁶¹

Pore Formation by CDCs

The interaction of the CDCs with the membrane is a two-stage process, firstly involving the C-terminal domain (domain 4; Fig. 1A) binding the bilayer surface and then the insertion of the pendant domain 3 from above its surface through its depth.^{23,25-27,43} Three loops at the base of domain 4 associate with cholesterol in the binding event and a fourth loop containing the conserved 11-residue CDC signature motif is especially critical in cholesterol-dependent prepore-to-pore transition.⁵⁰ This chimes especially neatly with the detailed characteristics of some of the mutant forms of CDCs that have been modified in this region; the pneumolysin mutant in which the first of the three tryptophans was modified to phenylalanine displays only 1% wild type activity but forms larger pores in general.⁶²⁻⁶⁴ This suggests that by affecting the prepore-to-pore transition for which this region of the protein is critical⁵⁰ it allows time for more larger (more complete) pores to form and less arcs are able to form pores, as previously argued.² The fact that pore size is affected by the effects of mutations on the prepore-to-pore transition is a striking piece of evidence that arcs of CDCs can form pores, alongside the fact that mutations which cap oligomerisation tend to reduce the measured pore size.⁴² It has in contrast been argued that only large pores are found, for example by the use of cargo leakage studies on liposomes⁶⁵ but that conclusion rather depends on what 'large' means. Even pores formed by arcs might be 'large' and may not be easily differentiated from those formed by rings by these means, particularly given the likelihood that the lipids completing the pore wall where the arc runs out will display flexibility and fluidity. A finer resolution readout on pore size might be provided by electrical conductance measurements and there is evidence from such readings that pore size varies significantly enough that a role for arcs is indicated in creating pores significantly smaller than CDC oligomeric rings^{62,64,66}—which might still seem 'large' by leakage. In addition, the effects that cations have on pores—for example causing them to close^{62,66}—is very hard to explain if the large CDC oligomeric ring equates always to the pore—a zinc ion, for example, will hardly be capable of sterically blocking such pores. If however zinc ions interacted with the charged headgroups of lipids participating in the pore structure and caused them to be reorganized then this phenomenon would be explained. Another key piece of evidence in favour of pores forming by the action of incomplete rings comes from what happens when prepore-to-pore transition is deliberately halted by locking the prepore state. This was achieved by introduction of a disulphide into perfringolysin that prevents the conformational change leading from the prepore to the pore.²⁵ The resulting structures are far more predominantly rings, both as prepores and when pores are subsequently allowed to form by reduction of the disulphide, than they are when the CDC is allowed to go through from prepore to pore in an uninterrupted fashion.⁴³ This demonstrates a kinetic aspect to pore formation by CDCs, by showing that kinetic interruption affects the end result of oligomerisation.² It also neatly therefore links back to the earlier study that suggested that arcs are 'kinetically significant intermediates'.^{2,41}

Proteolipid Pores

If arcs are capable of forming pores then the interface between the arc and the membrane must somehow define the pore lumen (Fig. 2A,C). How this is achieved is unknown but data from other systems suggests a mechanism, while also highlighting the way in which the interaction of CDCs with the membrane is a two-way phenomenon, similar to the way that the phospholipid composition also affects the number and the nature of binding sites formed by cholesterol.^{58,59} It is not a matter of the protein acting on an inert membrane, which is the model implicitly behind thinking of pore forming proteins as if they were in the end a special kind of facultative integral membrane protein, but of the collision of two active systems—the dynamic membrane environment and the affinity-driven process of coupled oligomerisation and membrane insertion of the CDC. Other systems in which a similar clash occurs include the process by which enveloped viruses fuse with the cell membranes of their hosts and by which SNAREs and other proteins mediate vesicle fusion—for example the fusion brought about by the vacuolar ATPase *c*-ring⁶⁷⁻⁶⁹ (Fig. 2C). With both cellular and viral membrane fusion the focal point is a highly curved toroidal arrangement of lipids in which alongside the fusion proteins a continuous surface of phospholipid headgroups extends over

the surface of the fusion pore. A similar arrangement of lipids is envisaged for the pores formed by equinatoxins,⁷⁰ as part of a proteolipid mosaic and for the pores created in electroporation,⁷¹ but obviously without any proteins being specifically involved. Direct evidence for a mosaic of lipids and a peptide being responsible for the structure of a pore has been obtained by X-ray crystallographic analysis of pores formed by a fragment of the apoptotic regulator Bax, the lipids being explicitly observable due to the presence of bromine atoms in their headgroups.⁷² The kind of structure envisaged for a CDC arc-generated pore would in a sense be a third kind of structure to those already described for viral and vesicle fusion and electroporation; halfway between the two, instead of alternating protein or peptide and lipid (Fig. 2B), or just electrically-perturbed lipid (Fig. 2A), there would be protein on one side and lipid on the other (Fig. 2C). The remaining problems with this interpretation of how arcs form pores concern satisfaction of the hydrogen bonding patterns found in β -sheets and the long term stability of proteolipid pores. Unlike α -helices, β -sheets rely on hydrogen bonds formed between spatially adjacent but sequentially separate portions of the peptide chain, rather than spatially and sequentially contiguous regions. The unclosed edges of a CDC pore-forming arc would therefore have unsatisfied permanent dipoles, except that the presence of the charged lipid headgroups in the surface of the pore could provide countercharges for them. The arc pores, if they exist, do appear relatively stable since they can be observed using atomic force microscopy⁴³ and electron microscopy.^{39,42,73} This might be surprising if they consist in a proteolipid mosaic, but since we know that Bax can induce such structures stably so that they can be studied using X-rays⁷² it may just be a feature of these novel structures. If arcs form pores by inducing a toroidal lipid surface as found in the presence of Bax peptide, during vesicle fusion and during electroporation, then this would explain where the lipid from the centre of the oligomer is removed to, since it would be free to move away from the protein ring and leave behind a pore. It also suggests a mechanism for this movement since the charged nature of the luminal face of the inserted β -sheet could even function, as a localized electrical charge, in a way directly analogous to electroporation.

Oligomerisation—A Mechanism for Membrane Insertion

Complete ring-shaped oligomers formed by CDCs consist of 30-50 subunits. These were first visualized in detail by rotational correlation analysis of perfringolysin⁷⁴ and pneumolysin⁷⁵ oligomers. Later three-dimensional studies of pneumolysin by cryo-EM^{27,47} and of perfringolysin by atomic force microscopy⁴³ confirmed their large size (for the pore up to 44 subunits) and showed in detail how the crystal structure is essentially maintained in the prepore but dramatically altered in the pore. Alongside fluorescence data showing the insertion of the transmembrane hairpins into the membrane^{24-26,65,76,77} these data allowed the overall mechanism to be characterized by which CDCs reorganize themselves from a soluble aqueous monomer or dimer (for example pneumolysin is monomeric but perfringolysin is dimeric^{2,78-80}) into a membrane-inserted oligomer. The first three-dimensional structure determined was of pneumolysin as a helical oligomer⁴⁷ in which it adopts a conformation apparently very similar to that found in the pore.^{2,27} It is hard to believe that the helix exists at any stage in a prepore-like conformation, since no such helical structures were observed and the helices were on occasion very long (300 nm and more) which would require very extensive cooperativity in the prepore-like-to-pore transition within a rather open structure. This means that pneumolysin (at least) has the structural plasticity to convert from the soluble monomer to the aggregated pore-conformation oligomer in a single step. On membranes, however, the prepore is a necessary staging post, because penetration of the membrane represents a significant energetic barrier which the CDCs vault over by their strong affinity for self-association coupled to an energetically favourable and irreversible conversion to a membrane-inserted state. Whether arcs or rings form pores is kinetically governed by the continuing ability to recruit further protomers to a nascent prepore oligomer² (Fig. 2A,B). If the source of new protomers dries up, then prepore-to-pore conversion will occur even if the ring is incomplete, but this can be inhibited either stringently but reversibly, as with the locking of domain 3 against conversion,^{25,43} or incompletely as is the case with the mutant W433F in pneumolysin referred to above.^{62,64} The membrane therefore constitutes a

new challenge to CDC oligomerisation, one which these proteins are adapted to deal with and which again underscores the way in which their action needs to be viewed from both sides—the activity of the protein on the membrane and the effects of the membrane on the protein. The reason why pneumolysin appears to be particularly susceptible to oligomerisation in solution is likely that it is a monomer, whereas those CDCs which are antiparallel dimers (like perfringolysin is) are antoinhibited until their constitutive subunits separate on cholesterol binding.² Therefore the demonstration that anthrolysin from *B. anthracis* is a monomer like pneumolysin⁸¹ would suggest that it too will have enhanced capacity for self-association in solution. Clearly, native CDC activity is on membranes, but if an aspect of that activity, such as oligomerisation, can be induced in solution then that provides insights into how it occurs at all.

Complex Effects of CDCs and Related Proteins

While it is attractive to think of the CDCs as facultative integral membrane proteins, the variety of effects on cells observed with them indicate that they are far more complex a system than that approach alone allows. Even in a simple model liposomal system a range of effects are observed, such as blebbing of membranes and the shedding of oligomeric toxin complexed with lipids into solution.^{2,82,83} To take one specific example, when images of pneumolysin forming pores were being collected by cryo-EM it was frequently observed that liposomes covered with protein structures could be found adjacent to liposomes with none. This suggests that the liposomes with none either had no cholesterol, which seems unlikely, or that they resulted from the action of the toxin; this would agree with solid-state NMR data showing that protein-free liposomes persisted after mixing of liposomes and pneumolysin but that they were smaller than the liposomes before mixing.^{82,83} Furthermore, the same images also contained distended, elongated lipid structures with pneumolysin oligomers peppering their surfaces with the appearance that the lipids were festooned from the CDC oligomers, as if the whole structure had been assembled by them. In any case the variety of forms taken by the liposomes once pneumolysin had been mixed with them was much greater than that pertaining before its addition, as shown by NMR and EM.^{82,83} Add to these observations that pores in membranes can apparently be resealed or shed or endocytosed—even possibly in a way involving the CDC itself (data in a recent paper would support this interpretation, see ref. 84)—and the cellular effects of these proteins must be understood to be possibly a great deal more complex than simply forming a hole. Beyond the individual cell, the fact that CDCs are known to induce inflammatory cytokines and in the case of pneumolysin at least to activate the complement system, adds further complications to our attempts to understand how they really act in health and disease.^{19,85} It also means that with the discovery that the same domain is used by CDCs and MACPFs, the assumption that it is necessarily simply deployed in pore formation per se needs careful examination. As argued already, the MACPF/CDC domain is doubtless adapted for deployment against membranes, but beyond that level of insight a range of different effects could actually be in play, including things like inducing membrane fusion events—or, as already documented for the perforin-like proteins of apicomplexan parasites, facilitating exit of toxoplasma from human host cells⁸⁶ or plasmodium gliding through the human dermis⁸⁷ or into the mosquito gut.⁸⁸ Functions of this kind are much easier to understand if MACPF/CDCs as a superfamily are not facultative integral membrane proteins whose pores possess defined perimeters, but have versatile activity against membranes and act in a way attuned to the pre-existing dynamic lipid mosaic bilayer environment.

Conclusion

CDCs are a family of proteins that act in a well-conserved way to induce diverse effects on membranes, a selective pressure being the biophysics of their target lipid bilayers. The critical role of cholesterol and the possibility that pore structures incorporate lipids as well as protein affirm this, and may underlie the versatility of phenotype conferred by members of the broader MACPF/CDC superfamily.

References

1. Gilbert RJ. Pore-forming toxins. *Cell Mol Life Sci* 2002; 59:832-844.
2. Gilbert RJ. Inactivation and activity of cholesterol-dependent cytolysins: what structural studies tell us. *Structure* 2005; 13:1097-1106.
3. Tilley SJ, Saibil HR. The mechanism of pore formation by bacterial toxins. *Curr Opin Struct Biol* 2006; 16:230-236.
4. Tweten RK. Cholesterol-dependent cytolysins, a family of versatile pore-forming toxins. *Infect Immun* 2005; 73:6199-6209.
5. Anderluh G, Lakey JH. Disparate proteins use similar architectures to damage membranes. *Trends Biochem Sci* 2008; 33:482-490.
6. Hadders MA, Beringer DX, Gros P. Structure of C8 alpha-MACPF reveals mechanism of membrane attack in complement immune defense. *Science* 2007; 317:1552-1554.
7. Rosado CJ, Buckle AM, Law RH et al. A common fold mediates vertebrate defense and bacterial attack. *Science* 2007; 317:1548-1551.
8. Rosado CJ, Kondos S, Bull TE et al. The MACPF/CDC family of pore-forming toxins. *Cell Microbiol* 2008; 10:1765-1774.
9. Slade DJ, Lovelace LL, Chruszcz M et al. Crystal structure of the MACPF domain of human complement protein C8 alpha in complex with the C8 gamma subunit. *J Mol Biol* 2008; 379:331-342.
10. Birmingham CL, Canadien V, Kaniuk NA et al. Listeriolysin O allows *Listeria monocytogenes* replication in macrophage vacuoles. *Nature* 2008; 451:350-354.
11. Grode L, Seiler P, Baumann S et al. Increased vaccine efficacy against tuberculosis of recombinant mycobacterium bovis bacille calmette-guerin mutants that secrete listeriolysin. *J Clin Invest* 2005; 115:2472-2479.
12. Neeson P, Pan ZK, Paterson Y. Listeriolysin O is an improved protein carrier for lymphoma immunoglobulin idiotype and provides systemic protection against 38C13 lymphoma. *Cancer Immunol Immunother* 2008; 57:493-505.
13. Peng X, Treml J, Paterson Y. Adjuvant properties of listeriolysin O protein in a DNA vaccination strategy. *Cancer Immunol Immunother* 2007; 56:797-806.
14. Awad MM, Ellemor DM, Boyd RL et al. Synergistic effects of alpha-toxin and perfringolysin O in *Clostridium perfringens*-mediated gas gangrene. *Infect Immun* 2001; 69:7904-7910.
15. Christianson KK, Tweten RK, Iandolo JJ. Transport and processing of staphylococcal enterotoxin A. *Appl Environ Microbiol* 1985; 50:696-697.
16. Rood JI. Virulence genes of clostridium perfringens. *Annu Rev Microbiol* 1998; 52:333-360.
17. Bhakdi S, Weller U, Walev I et al. A guide to the use of pore-forming toxins for controlled permeabilization of cell membranes. *Med Microbiol Immunol* 1993; 182:167-175.
18. Weimbs T, Low SH, Li X et al. SNAREs and epithelial cells. *Methods* 2003; 30:191-197.
19. Kadioglu A, Weiser JN, Paton JC et al. The role of streptococcus pneumoniae virulence factors in host respiratory colonization and disease. *Nat Rev Microbiol* 2008; 6:288-301.
20. Marriott HM, Mitchell TJ, Dockrell DH. Pneumolysin: a double-edged sword during the host-pathogen interaction. *Curr Mol Med* 2008; 8:497-509.
21. Bernheimer AW, Rudy B. Interactions between membranes and cytolytic peptides. *Biochim Biophys Acta* 1986; 864:123-141.
22. Ponting CP. Chlamydial homologues of the MACPF (MAC/perforin) domain. *Curr Biol* 1999; 9:R911-913.
23. Heuck AP, Hotze EM, Tweten RK et al. Mechanism of membrane insertion of a multimeric beta-barrel protein: perfringolysin O creates a pore using ordered and coupled conformational changes. *Mol Cell* 2000; 6:1233-1242.
24. Hotze EM, Heuck AP, Czajkowsky DM et al. Monomer-monomer interactions drive the prepore to pore conversion of a beta-barrel-forming cholesterol-dependent cytolysin. *J Biol Chem* 2002; 277:11597-11605.
25. Hotze EM, Wilson-Kubalek EM, Rossjohn J et al. Arresting pore formation of a cholesterol-dependent cytolysin by disulfide trapping synchronizes the insertion of the transmembrane beta-sheet from a prepore intermediate. *J Biol Chem* 2001; 276:8261-8268.
26. Shatursky O, Heuck AP, Shepard LA et al. The mechanism of membrane insertion for a cholesterol-dependent cytolysin: a novel paradigm for pore-forming toxins. *Cell* 1999; 99:293-299.
27. Tilley SJ, Orlova EV, Gilbert RJ et al. Structural basis of pore formation by the bacterial toxin pneumolysin. *Cell* 2005; 121:247-256.
28. Menestrina G, Dalla Serra M, Comai M et al. Ion channels and bacterial infection: the case of beta-barrel pore-forming protein toxins of *Staphylococcus aureus*. *FEBS Lett* 2003; 552:54-60.

29. Bhakdi S, Trantum-Jensen J. On the cause and nature of C9-related heterogeneity of terminal complement complexes generated on target erythrocytes through the action of whole serum. *J Immunol* 1984; 133:1453-1463.
30. Bhakdi S, Trantum-Jensen J. C5b-9 assembly: average binding of one C9 molecule to C5b-8 without poly-C9 formation generates a stable transmembrane pore. *J Immunol* 1986; 136:2999-3005.
31. Podack ER, Dennert G. Assembly of two types of tubules with putative cytolytic function by cloned natural killer cells. *Nature* 1983; 302:442-445.
32. Young JD, Hengartner H, Podack ER et al. Purification and characterization of a cytolytic pore-forming protein from granules of cloned lymphocytes with natural killer activity. *Cell* 1986; 44:849-859.
33. Young LH, Joag SV, Zheng LM et al. Perforin-mediated myocardial damage in acute myocarditis. *Lancet* 1990; 336:1019-1021.
34. Froelich CJ, Pardo J, Simon MM. Granule-associated serine proteases: granzymes might not just be killer proteases. *Trends Immunol* 2009; 30:117-123.
35. Metkar SS, Wang B, Aguilar-Santelises M et al. Cytotoxic cell granule-mediated apoptosis: perforin delivers granzyme B-serglycin complexes into target cells without plasma membrane pore formation. *Immunity* 2002; 16:417-428.
36. Trapani JA, Voskoboinik I. The complex issue of regulating perforin expression. *Trends Immunol* 2007; 28:243-245.
37. Voskoboinik I, Smyth MJ, Trapani JA. Perforin-mediated target-cell death and immune homeostasis. *Nat Rev Immunol* 2006; 6:940-952.
38. Keefe D, Shi L, Feske S et al. Perforin triggers a plasma membrane-repair response that facilitates CTL induction of apoptosis. *Immunity* 2005; 23:249-262.
39. Bhakdi S, Trantum-Jensen J, Sziegoleit A. Mechanism of membrane damage by streptolysin-O. *Infect Immun* 1985; 47:52-60.
40. Harris RW, Sims PJ, Tweten RK. Kinetic aspects of the aggregation of Clostridium perfringens theta-toxin on erythrocyte membranes. A fluorescence energy transfer study. *J Biol Chem* 1991; 266:6936-6941.
41. Palmer M, Valeva A, Kehoe M et al. Kinetics of streptolysin O self-assembly. *Eur J Biochem* 1995; 231:388-395.
42. Palmer M, Harris R, Freytag C et al. Assembly mechanism of the oligomeric streptolysin O pore: the early membrane lesion is lined by a free edge of the lipid membrane and is extended gradually during oligomerization. *EMBO J* 1998; 17:1598-1605.
43. Czajkowsky DM, Hotze EM, Shao Z et al. Vertical collapse of a cytolysin prepore moves its transmembrane beta-hairpins to the membrane. *EMBO J* 2004; 23:3206-3215.
44. Cohen B, Schwachman H, Perkins ME. Inactivation of pneumococcal hemolysin by certain sterols. *Proc Soc Exp Biol Med* 1937; 35:586-591.
45. Saunders FK, Mitchell TJ, Walker JA et al. Pneumolysin, the thiol-activated toxin of Streptococcus pneumoniae, does not require a thiol group for in vitro activity. *Infect Immun* 1989; 57:2547-2552.
46. Gilbert RJ, Heenan RK, Timmins PA et al. Studies on the structure and mechanism of a bacterial protein toxin by analytical ultracentrifugation and small-angle neutron scattering. *J Mol Biol* 1999; 293:1145-1160.
47. Gilbert RJ, Jimenez JL, Chen S et al. Two structural transitions in membrane pore formation by pneumolysin, the pore-forming toxin of Streptococcus pneumoniae. *Cell* 1999; 97:647-655.
48. Nagamune H, Whiley RA, Goto T et al. Distribution of the intermedilysin gene among the anginosus group streptococci and correlation between intermedilysin production and deep-seated infection with Streptococcus intermedius. *J Clin Microbiol* 2000; 38:220-226.
49. Giddings KS, Zhao J, Sims PJ et al. Human CD59 is a receptor for the cholesterol-dependent cytolysin intermedilysin. *Nat Struct Mol Biol* 2004; 11:1173-1178.
50. Soltani CE, Hotze EM, Johnson AE et al. Structural elements of the cholesterol-dependent cytolysins that are responsible for their cholesterol-sensitive membrane interactions. *Proc Natl Acad Sci USA* 2007; 104:20226-20231.
51. Giddings KS, Johnson AE, Tweten RK. Redefining cholesterol's role in the mechanism of the cholesterol-dependent cytolysins. *Proc Natl Acad Sci USA* 2003; 100:11315-11320.
52. Geoffroy C, Alouf JE. Interaction of alveolysin A sulfhydryl-activated bacterial cytolytic toxin with thiol group reagents and cholesterol. *Toxicon* 1982; 20:239-241.
53. Ohno-Iwashita Y, Iwamoto M, Mitsui K et al. Protease-nicked theta-toxin of Clostridium perfringens, a new membrane probe with no cytolytic effect, reveals two classes of cholesterol as toxin-binding sites on sheep erythrocytes. *Eur J Biochem* 1988; 176:95-101.
54. Harris JR, Adrian M, Bhakdi S et al. Cholesterol-streptolysin O interaction: an EM study of wild-type and mutant streptolysin O. *J Struct Biol* 1998; 121:343-355.
55. Sonnen AF, Rowe AJ, Andrew PW et al. Oligomerisation of pneumolysin on cholesterol crystals: similarities to the behaviour of polyene antibiotics. *Toxicon* 2008; 51:1554-1559.

56. Howard JG, Wallace KR, Wright GP. The inhibitory effects of cholesterol and related sterols on haemolysis by streptolysin O. *Br J Exp Pathol* 1953; 34:174-180.
57. Nollmann M, Gilbert R, Mitchell T et al. The role of cholesterol in the activity of pneumolysin, a bacterial protein toxin. *Biophys J* 2004; 86:3141-3151.
58. Ohno-Iwashita Y, Iwamoto M, Ando S et al. Effect of lipidic factors on membrane cholesterol topology—mode of binding of theta-toxin to cholesterol in liposomes. *Biochim Biophys Acta* 1992; 1109:81-90.
59. Ohno-Iwashita Y, Iwamoto M, Mitsui K et al. A cytolysin, theta-toxin, preferentially binds to membrane cholesterol surrounded by phospholipids with 18-carbon hydrocarbon chains in cholesterol-rich region. *J Biochem* 1991; 110:369-375.
60. Delattre J, Badin J, Canal J et al. Influence of lecithins on the inhibitory effect of cholesterol towards streptolysin O. *C R Acad Sci Hebd Seances Acad Sci D* 1973; 277:441-443.
61. Flanagan JJ, Tweten RK, Johnson AE et al. Cholesterol exposure at the membrane surface is necessary and sufficient to trigger perfringolysin O binding. *Biochemistry* 2009; 48:3977-3987.
62. El-Rachkidy RG, Davies NW, Andrew PW. Pneumolysin generates multiple conductance pores in the membrane of nucleated cells. *Biochem Biophys Res Commun* 2008; 368:786-792.
63. Hill J, Andrew PW, Mitchell TJ. Amino acids in pneumolysin important for hemolytic activity identified by random mutagenesis. *Infect Immun* 1994; 62:757-758.
64. Korchev YE, Bashford CL, Pederzoli C et al. A conserved tryptophan in pneumolysin is a determinant of the characteristics of channels formed by pneumolysin in cells and planar lipid bilayers. *Biochem J* 1998; 329:571-577.
65. Heuck AP, Tweten RK, Johnson AE. Assembly and topography of the prepore complex in cholesterol-dependent cytolysins. *J Biol Chem* 2003; 278:31218-31225.
66. Menestrina G, Bashford CL, Pasternak CA. Pore-forming toxins: experiments with *S. aureus* alpha-toxin C, perfringens theta-toxin and *E. coli* haemolysin in lipid bilayers, liposomes and intact cells. *Toxicol* 1990; 28:477-491.
67. Almers W. Fusion needs more than SNAREs. *Nature* 2001; 409:567-568.
68. Kielian M, Rey FA. Virus membrane-fusion proteins: more than one way to make a hairpin. *Nat Rev Microbiol* 2006; 4:67-76.
69. Peters C, Bayer MJ, Buhler S et al. Trans-complex formation by proteolipid channels in the terminal phase of membrane fusion. *Nature* 2001; 409:581-288.
70. Anderluh G, Dalla Serra M, Viero G et al. Pore formation by equinatoxin II, a eukaryotic protein toxin, occurs by induction of nonlamellar lipid structures. *J Biol Chem* 2003; 278:45216-45223.
71. Weaver JC. Molecular basis for cell membrane electroporation. *Ann N Y Acad Sci* 1994; 720:141-152.
72. Qian S, Wang W, Yang L et al. Structure of transmembrane pore induced by Bax-derived peptide: evidence for lipidic pores. *Proc Natl Acad Sci USA* 2008; 105:17379-17383.
73. Morgan PJ, Hyman SC, Byron O et al. Modeling the bacterial protein toxin, pneumolysin, in its monomeric and oligomeric form. *J Biol Chem* 1994; 269:25315-25320.
74. Olofsson A, Hebert H, Thelestam M. The projection structure of perfringolysin O (*Clostridium perfringens* theta-toxin). *FEBS Lett* 1993; 319:125-127.
75. Morgan PJ, Hyman SC, Rowe AJ et al. Subunit organisation and symmetry of pore-forming, oligomeric pneumolysin. *FEBS Lett* 1995; 371:77-80.
76. Shepard LA, Heuck AP, Hamman BD et al. Identification of a membrane-spanning domain of the thiol-activated pore-forming toxin *Clostridium perfringens* perfringolysin O: an alpha-helical to beta-sheet transition identified by fluorescence spectroscopy. *Biochemistry* 1998; 37:14563-14574.
77. Shepard LA, Shatursky O, Johnson AE et al. The mechanism of pore assembly for a cholesterol-dependent cytolysin: formation of a large prepore complex precedes the insertion of the transmembrane beta-hairpins. *Biochemistry* 2000; 39:10284-10293.
78. Rossjohn J, Feil SC, McKinstry WJ et al. Structure of a cholesterol-binding, thiol-activated cytolysin and a model of its membrane form. *Cell* 1997; 89:685-692.
79. Solovyova AS, Nollmann M, Mitchell TJ et al. The solution structure and oligomerization behavior of two bacterial toxins: pneumolysin and perfringolysin O. *Biophys J* 2004; 87:540-552.
80. Rossjohn J, Polekhina G, Feil SC et al. Structures of perfringolysin O suggest a pathway for activation of cholesterol-dependent cytolysins. *J Mol Biol* 2007; 367:1227-1236.
81. Bourdeau RW, Malito E, Chenal A et al. Cellular functions and X-ray structure of anthrolysin O, a cholesterol-dependent cytolysin secreted by *Bacillus anthracis*. *J Biol Chem* 2009; 284:14645-14656.
82. Bonev B, Gilbert R, Watts A. Structural investigations of pneumolysin/lipid complexes. *Mol Membr Biol* 2000; 17:229-235.
83. Bonev BB, Gilbert RJ, Andrew PW et al. Structural analysis of the protein/lipid complexes associated with pore formation by the bacterial toxin pneumolysin. *J Biol Chem* 2001; 276:5714-5719.
84. Idone V, Tam C, Goss JW et al. Repair of injured plasma membrane by rapid Ca²⁺-dependent endocytosis. *J Cell Biol* 2008; 180:905-914.

85. Mitchell TJ. Virulence factors and the pathogenesis of disease caused by *Streptococcus pneumoniae*. *Res Microbiol* 2000; 151:413-419.
86. Kafsack BF, Pena JD, Coppens I et al. Rapid membrane disruption by a perforin-like protein facilitates parasite exit from host cells. *Science* 2009; 323:530-533.
87. Amino R, Giovannini D, Thiberge S et al. Host cell traversal is important for progression of the malaria parasite through the dermis to the liver. *Cell Host Microbe* 2008; 3:88-96.
88. Ecker A, Pinto SB, Baker KW et al. *Plasmodium berghei*: plasmodium perforin-like protein 5 is required for mosquito midgut invasion in *Anopheles stephensi*. *Exp Parasitol* 2007; 116:504-508.

CHAPTER 6

Laetiporus sulphureus Lectin and Aerolysin Protein Family

José Miguel Mancheño,* Hiroaki Tateno, Daniel Sher and Irwin J. Goldstein

Abstract

The parasitic mushroom *Laetiporus sulphureus* produces a family of lectins (LSL's) sharing 80-90% sequence identity that possesses a low but significant sequence similarity to the bacterial pore-forming toxins mosquitoicidal toxin Mtx-2 from *Bacillus sphaericus* and α toxin from *Clostridium septicum*. The crystal structure of one member of the *L. sulphureus* lectins family (LSLa) reveals unexpected structural similarities to the β -pore-forming toxins from the aerolysin family, namely, aerolysin from the Gram-negative bacterium *Aeromonas hydrophila*, ϵ -toxin from *Clostridium perfringens* and parasporin from *B. thuringiensis*. This similarity presumably indicates that the hemolytic activity of LSLa proceeds through a molecular mechanism that involves the formation of oligomeric transmembrane β -barrels. Comparison of the crystal structures of the above mentioned proteins reveals common pore-forming modules, which are then distributed both in bacteria and fungi. Currently, it can be stated that the above three dimensional structures have been key in revealing structural similarities that were elusive at the sequence level. A potential corollary from this is that structural studies aimed at determining high resolution structures of aerolysin-like pore-forming toxins, whose biological activity involves large conformational changes, are mandatory to define protein domains or structural motifs with membrane-binding properties.

Introduction

The isolation and partial characterization of a lectin with hemolytic and hemagglutinating properties produced by the mushroom *Laetiporus sulphureus* were first reported by the Kanska group.¹ The isolated lectin was stated to be a heterotetrameric species of 190 kDa composed of two distinct types of subunits (about 36 and 60 kDa, respectively). This analysis also revealed that the lectin was specific for N-acetyllactosamine residues and that both hemagglutinating and hemolysis activities were supported by the same site. More recently, the Goldstein group² undertook a detailed analysis on the sugar binding specificity of the hemolytic lectin and closely related lectins from *L. sulphureus* and also carried out the corresponding cDNA cloning, heterologous expression and characterization of the recombinant lectin proteins. Analysis of the protein sequences revealed that the *L. sulphureus* lectins contain three tandemly repeated subdomains at their N-termini. Each subdomain possesses the highly conserved QXF motif, which resembles the QXW motif present in the ricin B-chain. Therefore, the *L. sulphureus* lectins are members of the R-type lectins, the lectin family found in both prokaryotes (bacteria) and eukaryotes (*C. elegans*, Drosophila, vertebrates, plants). Due to the high degree of conservation in structure and

*Corresponding Author: José Miguel Mancheño—Grupo de Cristalografía Macromolecular y Biología Estructural. Instituto de Química Física Rocasolano, CSIC. Serrano 119, 28006 Madrid. Spain. Email: xjosemi@iqfr.csic.es

in sugar-binding function, a gene encoding an R-type lectin has been thought to have moved laterally between species. Conversely, the sequence analysis of the C-termini of the lectins revealed the lack of close homologues and only a low sequence similarity was identified with sequences from bacterial pore-forming toxins, in particular with mosquitocidal toxin Mtx-2 from *Bacillus sphaericus* and α toxin from *Clostridium septicum*. Recent high resolution structural analysis on the hemolytic lectin finally rendered the novel crystal structure of the protein at 2.6 Å resolution.³ The structure revealed that the lectin is a highly symmetrical hexameric species, with each monomeric subunit being composed of two functionally and structurally distinct domains: an N-terminal β -trefoil lectin domain and an elongated C-terminal domain which unexpectedly revealed clear similarities with domains present in members of the aerolysin family of β -pore-forming toxins. These findings permitted for the first time to delimit a minimum pore-forming domain in this family of toxins and also to reveal structural similarities in spite of very low levels of similarity in the primary amino acid sequences.

Pore-Forming Hemolytic Lectins

Lectins are defined as glycan-binding proteins or glycoproteins of non-immune origin,⁴ which have ability to discriminate extremely diverse glycan structures; stereoisomers and branch numbers and positions. Though recognition of glycans on cell surfaces and glycoconjugates, lectins have ability to agglutinate cells and/or precipitate glycoconjugates. Some lectins are also known to have cytotoxicity as represented by ricin.⁵ Ricin is a type II ribosome-inactivating protein isolated from *Ricinus communis*, consisting of two disulfide-linked polypeptides, A-chain and B-chain. Binding of ricin to β -linked galactose at the cell surface mediated by the two lectin (QXW)₃ domains of B-chain, is a prerequisite for the membrane translocation of the enzymatically active A-chain. Upon reaching the cytosol, active A-chain specifically inactivates the ribosomes. Conversely, other cytotoxic lectins have ability to lyse as well as agglutinate cells. Such lectins are called hemolytic lectins. Hemolytic lectins make pores within the membrane of the target cells, such as the one produced by the marine invertebrate *Cucumaria echinata* (CEL-III),^{6,7} or those produced by the mushroom *L. sulphureus*^{1,2} (LSL's). In both cases, the hemagglutinating and hemolysis activities are mediated by binding of the protein to specific carbohydrate chains of the cells, followed by the formation of discrete ion-permeable pores in the cell membrane of the target cells through oligomerization of the protein. After formation of the pores, erythrocytes are ruptured by colloid osmotic shock. Osmotic protection experiments indicated that LSLa formed pores with a functional diameter smaller than 3.8 nm in the cell membrane of human erythrocytes.²

Analysis of the primary structures of LSLa and CEL-III revealed a negligible level of similarity between them. Nevertheless, in both cases a substructure of tandemly repeated subdomains at their N-termini was identified analogously to those from the B-chains of the toxic lectins ricin⁵ and abrin⁸ from *Abrus precatorius*: three subdomains in LSLa² and six in CEL-III.⁹ The recently described crystal structures of both hemolytic lectins^{3,10} supported this conclusion (Fig. 1). The structure of CEL-III reveals a three-domain architecture with two carbohydrate-binding domains at the N-terminus (domains 1 and 2, respectively) and a C-terminal pore-forming domain (domain 3) which has no structurally similar proteins in the Protein Data Bank. Domains 1 (residues 1-149) and 2 (residues 150-283) share an identical β -trefoil fold (r.m.s. deviation of 0.77 Å for 115 aligned C α atoms), despite sharing a 33.8% sequence identity for 145 residues. The C α backbones of the three basic motifs constituting the β -trefoil fold (see below) are almost identical (average pairwise r.m.s.d. 0.62 Å for 29 aligned C α atoms) and with the exception of motif 1 β , bound one Ca²⁺ ion through coordination by two conserved aspartic acid residues.¹⁰ These complexes may help explaining the dependence of the carbohydrate-binding activity on Ca²⁺ concentration.

The pore-forming modules (PFM's) of LSLa (residues 151-314) and CEL-III (residues 284-432) are dissimilar, probably indicating unlike molecular mechanisms of membrane pore-formation. Whereas PFM from LSLa shows structural similarities to aerolysin-like proteins (see below), that from CEL-III has no related protein domain. This last domain comprises two α -helices and an eight-stranded β -sandwich⁹ whose β -sheets are held together by hydrophobic

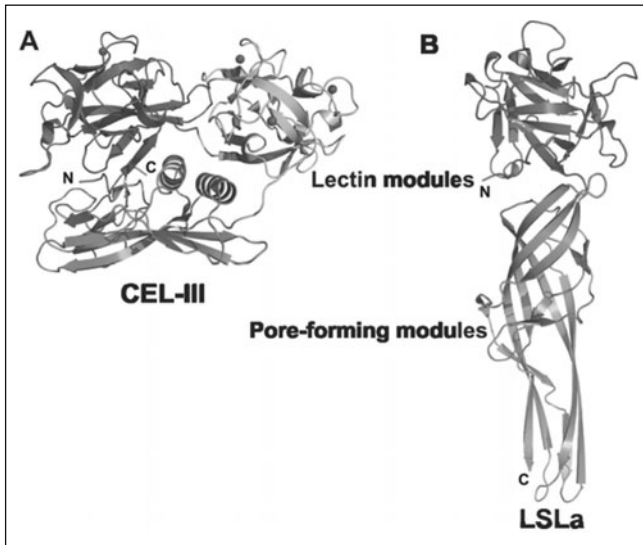


Figure 1. Modular architecture of the hemolytic lectins LSLa and CEL-III. Protein molecules are shown as cartoon representation. A) CEL-III from *C. echinata* possesses two lectin β -trefoil folds and a C-terminal pore-forming domain comprised by two α -helices and an eight-stranded β -sandwich whose β -sheets are held together by hydrophobic interactions. Calcium atoms are shown as spheres. B) LSLa from *L. sulphureus* possesses an N-terminal β -trefoil lectin domain and a C-terminal pore-forming domain which shows structural similarities with bacterial toxins from the aerolysin family.

interactions. The two helices lie on the surface of the β -sandwich in parallel with the β -sandwich surface. A C-terminal helical loop of 25 residues is stabilized by two disulfide bonds what clearly restrains its flexibility.

Two different pore-formation mechanisms have been proposed for CEL-III by the Hatakeyama group.⁹ The first scenario considers that after an initial recognition of the carbohydrate molecular receptor mediated by the lectin domains 1 and 2, CEL-III would behave as a β -pore-forming toxin, with the α -helices from domain 3 making a conformational change to a 42-residue amphipathic β -hairpin. Six such hairpins then associate to make up a β -barrel with 1.7 nm in diameter within the erythrocyte membranes. After formation of the pores, erythrocytes are ruptured by colloid osmotic shock. Conversely, the second mechanism would involve insertion of the complete domain 3 into the erythrocyte membrane after a similar alpha-to-beta conformational transition.

A distinct feature of these two pore-forming hemolytic lectins when considered in the context of aerolysin family of proteins is that they can be defined as linear modular proteins, i.e., the modules that make up the final complex architecture of the protein are independent from each other at the primary level.

A New Member within the Aerolysin Family: The Crystal Structure of LSLa

The aerolysin family of β -pore-forming toxins unexpectedly received a new member as a result of the crystallographic studies on the hemolytic lectin LSLa produced by *L. sulphureus*.^{3,11} The crystal structure revealed that LSLa is a homohexamer endowed with 32 point group symmetry, composed of noncovalently bound subunits of ~35 kDa. Sedimentation equilibrium analyses carried out in a wide range of protein concentrations confirmed this finding as the results indicate

that LSLa behaves in solution as a monomer-hexamer associative system essentially displaced to the oligomeric form, in perfect agreement with the crystallographic results.

The structure of each monomeric subunit consists of two different modules corresponding to the functional modules, lectin and pore-forming (Fig. 1). The lectin module (residues 1-150) has a globular structure ($39 \times 32 \times 32 \text{ \AA}^3$), consisting of a β -trefoil fold. Conversely, the pore-forming module (residues 151-314) has an elongated shape ($72 \times 23 \times 23 \text{ \AA}^3$) and can be effectively divided into two distinct domains: domain 2 is a twisted five-stranded antiparallel β -sheet and a long amphipathic loop and domain 3 consisting of a β -sandwich with one two-stranded and one three-stranded sheet. This last module reveals clear structural similarity between LSLa and the large lobe of aerolysin¹² a β -pore-forming toxin from the Gram-negative bacterium *Aeromonas hydrophila*, despite negligible sequence identity. This structural analogy together with previous results¹² suggests that LSLa is indeed a β -pore-forming toxin (β -PFT).

The N-Terminal Lectin Module

The N-terminal module of LSLa consists of a β -trefoil (Fig. 2), a well known protein fold within the lectin realm.¹³⁻¹⁵ It is formed by a six-stranded antiparallel β -barrel capped on one end by three two-stranded hairpins (strand pairs $\beta 2$ and $\beta 3$, $\beta 6$ and $\beta 7$, $\beta 10$ and $\beta 11$). The global structure of the β -trefoil results from the tandem repetition of an underlying motif (called α , β , γ , respectively) composed of four strands separated by three loops, the third one containing a single-turn 3_{10} helix (Fig. 2). Each basic motif may have evolved from a primordial galactose-binding peptide of ~ 40 residues,¹⁶ with the β -trefoil being the outcome of successive gene duplication cycles. Obviously, the β -trefoil architecture provides the structural basis of the subdomains previously found at the primary level.² Analysis of the primary and tertiary structure of these three motifs reveals that in effect they are homologous with each other, but also reveals the existence of notable divergences. Thus, pairwise sequence comparisons between motifs reveal identities around 20%, with only four residues being conserved in the three motifs. Yet, despite this degeneration, the three dimensional structure of the C_α backbone is essentially conserved. Structural comparison with known folds with DALI¹⁷ reveals high homology with sugar-binding domains of toxins that exert their cytotoxic action by binding glycoproteins, such as *C. botulinum* cytotoxin^{18,19} and the above mentioned ricin,⁵ abrin⁸ or CEL-III.¹⁰ In all these cases, the level of similarity at the primary level is very low, which suggests that the β -trefoil is versatile protein architecture that withstands dramatic sequence departures.

Previous work demonstrated that lactose, N-acetyl-lactosamine and other galactose-related saccharides inhibited the hemagglutination and hemolytic activities of LSLa,² indicating that sugar-binding is involved in both molecular processes. Presumably, a specific recognition of carbohydrates would precede the formation of pores within the erythrocyte membrane.

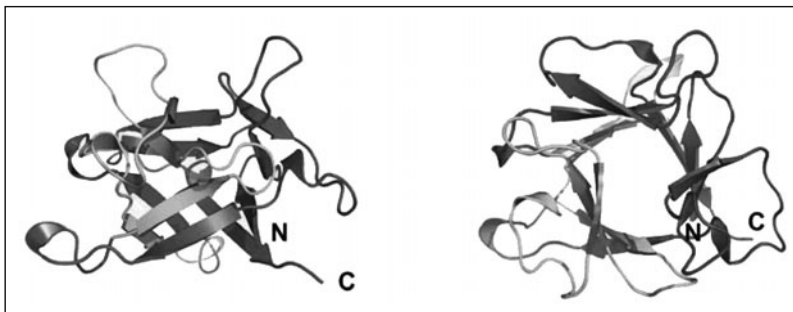


Figure 2. The lectin β -trefoil fold. Two orthogonal views of the N-terminal β -trefoil fold of LSLa are shown in cartoon representation. The structure of the LSLa β -trefoil is based on the tandem repetition of a basic motif composed of four strands separated by three loops. As a result, the structure exhibits a pseudo three-fold symmetry clearly identified when viewed along the molecular symmetry axis (*right panel*).

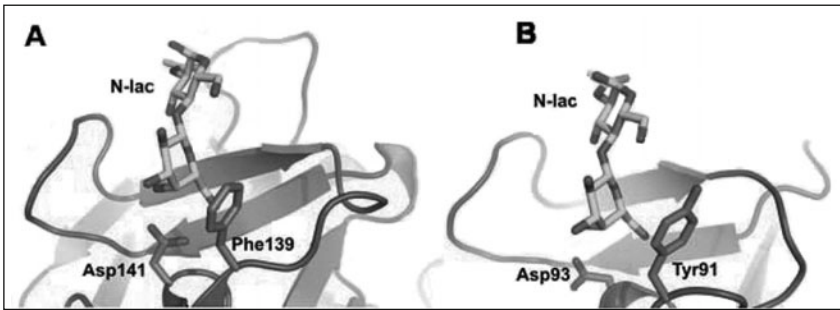


Figure 3. Sugar-binding to the lectin module of LSLa. A) Structure of the N-acetyllactosamine bound (A) to the γ -motif and (B) to the β -motif of LSLa. The two critical amino acid residues for sugar-binding from each motif are shown as *stick* representation. Tyr91 and Phe139 stack against the galactose ring of N-acetyllactosamine and Asp93 and Asp141 hydrogen bonds with the axial C4 hydroxyl group of galactose.

The crystal structures of LSLa complexed with lactose or N-acetyl-lactosamine show sugar binding at two (β and γ) of the three possible sites³ (Fig. 3) and have permitted identifying residues directly participating in sugar-binding and also explaining the lack of sugar binding to the α site. This binding mode presents close structural similarities to others previously reported for lectin-lactose complexes.²⁰⁻²³ Among others, the main common interactions identified are stacking interactions between the galactose ring and an aromatic side chain (Tyr-91 and Phe-139) and hydrogen bonds between the axial C4 hydroxyl group of galactose and an acidic lectin side chain (Asp-93 and Asp-141).

The C-Terminal Pore-Forming Module

The pore-forming module (PFM) of LSLa (residues 151-314) is elongated (70 Å long and 20-40 Å in thickness) and can be split into two domains containing mainly β -sheets (Fig. 4). Domain 2 is a five-stranded antiparallel β -sheet with an amphipathic loop on one side (residues 212-241). Besides, domain 3 is a β -sandwich with a two- and a three-stranded sheet, respectively. Although positive hits (in terms of Z-score) were not detected in structural comparisons carried out with the DALI server, structural similarities can be readily identified between domains 2 and 3 of LSLa with domains 3 and 4 of aerolysin,¹² domains 2 and 3 of ϵ -toxin from *C. prefringens*²⁴ and domains 2 and 3 of parasporin from *B. thuringiensis*²⁵ (Fig. 4). As can be observed in this last figure, all these proteins exhibit a virtually identical arrangement of the secondary structures within the compared domains despite a low sequence identity (<20%). Nonetheless, it is interesting to note that in contrast to the large lobe of aerolysin, ϵ -toxin or parasporin, the PFM of LSLa is composed of a continuous stretch of the protein sequence. We believe that this finding is remarkable as it may indicate the existence of an aerolysin-like pore-forming module structure whose defining characteristics are essentially topological (secondary level) and physico-chemical (primary level) and thus only loosely dependent on specific primary structures. Obviously, this finding raises important questions regarding protein folding and stability as to how essentially unrelated amino acid sequences yield a common protein fold both structurally and functionally. This last issue is especially relevant within the context of membrane pore-forming proteins as these macromolecules experience dramatic conformational changes between a (meta)stable water-soluble state of the toxin and a membrane-embedded functional protein.^{26,27}

Regarding the specific role of the above mentioned structural elements of LSLa in pore formation, analysis carried out on the aerolysin-like *C. septicum* α toxin²⁸ and aerolysin²⁹ shows that the amphipathic loop in domain 2 lines the channel when inserted into the membrane. The loop presents an almost perfectly conserved alternating pattern of hydrophobic residues that is characteristic of amphipathic transmembrane β -hairpins.^{3,29} The crystal structure of LSLa shows that the size

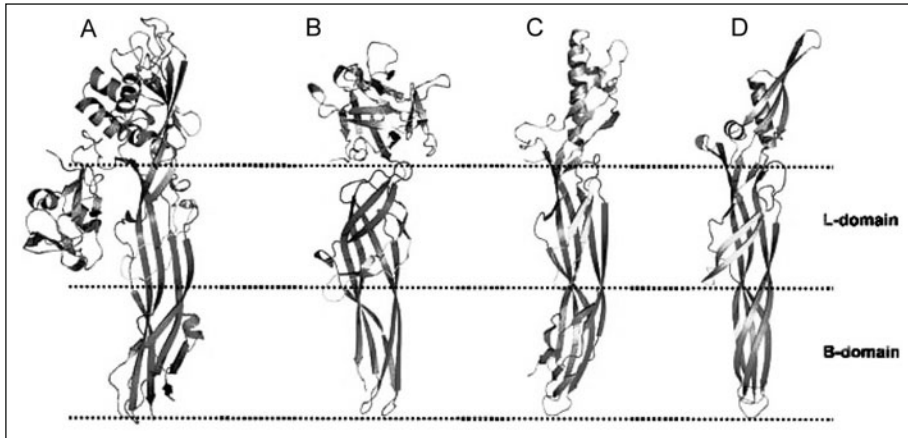


Figure 4. Three dimensional modular architecture of β -pore-forming proteins of the aerolysin family. The protein structures are shown in cartoon representation. A) Proaerolysin¹² from *A. hydrophila*, (B) LSLa³ from the mushroom *L. sulphureus*, (C) ϵ -toxin²⁴ from *C. perfringens* and (D) parasporin from *B. thuringiensis*.²⁵ The structural similarity appears when the corresponding pore-forming modules are compared; in all cases this module can be split into a L-domain (see the text) composed of a five-stranded β -sheet and an amphipathic loop that lies on it and a B-domain based on a β -sandwich fold.

of the amphipathic β -hairpin, ~ 30 residues, is similar to *Staphylococcus aureus* α -hemolysin,³⁰ the anthrax protective antigen³¹ and the two transmembrane hairpins of the cholesterol-dependent cytolysin perfringolysin O.^{32,33}

Oligomeric State of Water-Soluble LSLa

The crystal structure of LSLa shows that it is a homo-hexamer endowed with 32 point group symmetry, i.e., LSLa subunits are first organized around 3-fold symmetry axes forming tripoid-like trimers which in turn associate forming a dimer of trimers which are organized around a 2-fold symmetry axis (Fig. 5). The overall dimensions of the hexameric assembly are $70 \times 80 \times 150 \text{ \AA}^3$ which implies that LSLa has an overall cylindrical shape. Conversely, sedimentation equilibrium analyses in a wide range of protein concentrations indicate that LSLa is a

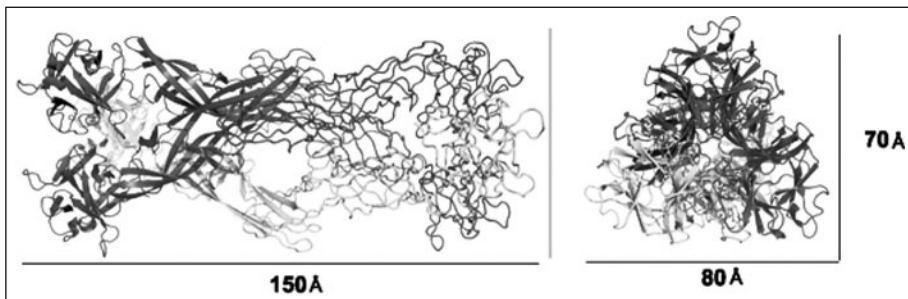


Figure 5. Oligomeric structure of LSLa. Two orthogonal views of the hexameric assembly of LSLa are shown. The three subunits that make up one tripoid-like trimer are shown as cartoon representation and the other three as ribbon models. The dimensions of the oligomer are also shown. The *left panel* shows the hexamer when viewed perpendicular to the molecular two-fold symmetry axis and the right panel when viewed along the three-fold symmetry axis.

monomer-hexamer associative system, essentially displaced to the oligomeric form (equilibrium dissociation constant $10 \mu\text{M}^5$).

Previous biochemical characterization of LSL has shown that both native and recombinant LSL are tetramers in solution with subunits of ~ 35 kDa as determined by gel-filtration combined with SDS-PAGE.^{1,2} The discrepancy between these results and the crystallographic studies may be explained by the clearly nonglobular hydrodynamic behavior of LSLa.

The main contacting interface between subunits ($\sim 680 \text{ \AA}^2$) is contributed by their domains 3, particularly through interactions between strands β -21 and β -23, which acting as “sticky” adapters between the two contacting sandwiches determine the formation of a large intersubunit β -sandwich. The contacting interface is mainly hydrophobic yet polar residues, in particular threonine and serine residues, are also identified. In this regard, it is remarkable the abundance of these small and polar residues in the region flanking the amphipathic loop, constituting the 42% and 46% of the total residues of strands β 16 and β 21. As shown below, this feature is shared by the other members of the aerolysin-like proteins which suggests this physicochemical property may be a requisite for pore-forming activity. It is obvious that the oligomeric state of LSLa in solution raises questions regarding the structural rearrangements required for pore-formation and the nature of the factor(s) that trigger such process. In this sense, the magnitude of the area of the contacting interface between protomers ($\sim 680 \text{ \AA}^2$) and its hydrophobic nature agrees well with strong and non-obligate complexes.^{34,35}

A Common Aerolysin-Like Pore-Forming Module Structure?

As above mentioned, the structural results described so far point to a structural similarity at the secondary level between domains 3 and 4 of aerolysin¹² from *A. hydrophila*, ϵ -toxin²⁴ from *C. prefringens*, domains 2 and 3 of parasporin from *B. thuringiensis*²⁵ and domains 2 and 3 of LSLa.³ For the sake of simplicity, we define as L-domains (from loop-containing domain) those analogous to domain 3 of aerolysin and B-domains (from β -sandwich-containing domain) those analogous to domain 4 of aerolysin.

L-Domains

The L-domains of the members of the aerolysin-like pore-forming toxins are formed by a four or five-stranded β -sheet on one face and a long loop on the other face (Fig. 6). As can be observed in the figure the topology of the sheet is strictly conserved in all the proteins. Two main features are easily identified within this region: first, a cluster of aromatic residues located in the contacting interface between the inner face of the sheet and the amphipathic loop and secondly a predominance of serine and threonine residues mainly distributed in the outer face of the sheet (Table 1). It is noteworthy that with the exception of LSLa where the PFM is continuous in the primary structure, the rest of the PFM's are not delineated on the primary structure³⁶ but results from the three dimensional arrangement of the corresponding secondary regular elements and therefore are necessarily interconnected with other protein modules. This observation points to the working hypothesis that this group of β -pore-forming toxins may represent the evolutionary outcome of structural convergence to a common module notably efficient in membrane-binding and pore-formation. Although the possibility of a common ancestor cannot be discarded the discontinuous nature of the PFM architecture of aerolysin, ϵ -toxin and parasporin does not fit well with recent studies that strongly support the notion that multidomain proteins have evolved mechanisms to minimize the problems of interdomain misfolding.³⁷ On the contrary, the continuous modular nature of LSLa agrees well with the protein having evolved from shuffling of domains with individual functions whose association renders a protein with a new level of functional complexity. The modular structure of LSLa suggests that the PFM may be an autonomous folding unit, a hypothesis that is partially reinforced by the fact that the domain interface is small³ and also because the lectin module of LSLa properly folds when heterologously produced in *E. coli* (unpublished results).

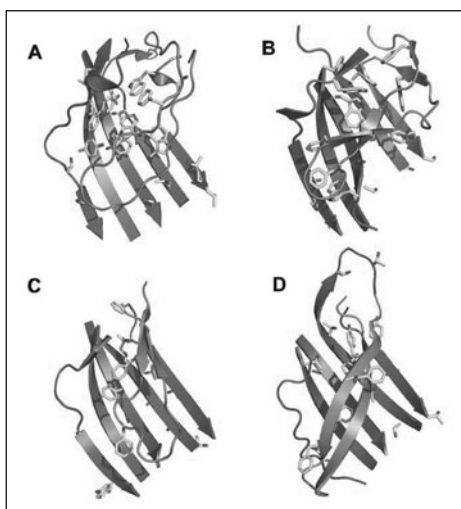


Figure 6. Structure of the L-domains of the areolysin pore-forming module. The C α backbone is shown as cartoon representation. The scaffold of the L-domain is based on an antiparallel five-stranded sheet with a long loop lying on one of its faces. Aromatic and serine/threonine residues present in the domain are shown as stick models. A) L-domain from proaerolysin from *A. hydrophila*, B) from LSLa from *L. sulphureus*, C) from greek epsilon toxin from *C. perfringens* and D) from parasporin from *B. thuringiensis*.

As can be observed in Figure 6, both the length and the three dimensional structure of the long loop that lies on the β -sheet of the L-domains is highly variable. The structural complexity of these regions makes the very definition of its boundaries a difficult and rather arbitrary issue which somehow explains the different alignments reported in the literature.^{3,29,38} Thus, we herein operatively define these boundaries in terms of their three dimensional structure as the sequence stretches comprised between residues: V239-W265 (aerolysin); A215-N239 (LSLa); A127-S147 (ϵ -toxin) and G102-E122 (parasporin). In Table 2 are shown the residues from these loops whose side chains are mostly buried. It is obvious that an imperfect, alternating pattern of buried hydrophobic residues is observed what would parallel only partially the behavior expected for a membrane-spanning β -hairpin.³⁰ As above mentioned, it has been reported for α toxin²⁸ from *C. septicum* and aerolysin²⁹ that this loop becomes the transmembrane β -hairpin when inserted

Table 1. Aromatic and hydroxylated amino acid residues present in L-domain of aerolysin-like proteins

Protein	Aromatic Residues	Serine/Threonine
Aerolysin	F184; W227; W247; W265; Y304; Y306; F404	T190; S228; T230; T232; S264; S267; S272; T274
LSLa	Y158; F202; F216; F223; F228; W238; W240; F246; F279; W290; W304	S167; S168; T169; T197; T199; S200; T205; T245; S247; S302; S303;
ϵ-toxin	Y79; F131; F135; Y146; F-148; Y244	S76; T110; T112; T114; T116; T151; T153; T155; S157; S245
Parasporin	Y104; F105; F109; F110; F121; Y131; F164	T51; T83; S84; T86; S87; S88; T90; T98; T101; S115; T132; T136; T168; T228; S230

Table 2. Buried residues from the loop within the L-domain of aerolysin-like proteins

Protein	Buried Residues
Aerolysin	T241; F245; W247; P248; V250; T253; L255; I257; I259
LSLa	F216; L220; P221; F223; F228; V234; W238
ϵ-toxin	A127; F131; V133; P134; F135; V140; L142; T144; Y146
Parasporin	Y104; A106; L108; F110; I119; F121

into the lipid bilayer what is consistent with a mechanism involving the formation of a β -barrel within the membrane similarly to α -hemolysin from *S. aureus*.³⁰ If this is the case, the mechanism of pore-formation by aerolysin-like proteins would necessarily involve large-scale conformational changes of the loop that should translocate to the lipid bilayer in order for oligomer contacts to be established. In this sense, the need for the loop movement for aerolysin's toxic activity has been demonstrated by mutagenesis studies that incorporated a disulfide-bridge between the loop and the wall of the sheet.³⁸ The reduced form of the double mutant behave as wild-type toxin but the oxidized form could not oligomerize. Furthermore, the movement of the loop would also demand the existence of a hinge region that supposedly should be located around the boundaries of this structural motif. The identity of this hinge region remains nowadays unknown for aerolysin-like proteins and in this regard, it is noteworthy that no region around the loop shows sequence similarity to the putative hinge region of α -hemolysin (around residues 103-111 and 147-152) and temperature factors of the structures do not permit to deduce highly flexible or dynamic regions around the loops.

B-Domains

The basic structural fold of the B-domains is based on a β -sandwich scaffold. The structures of the sandwiches shown in Figure 7 reveal a minimum common β -sandwich core composed of a three-stranded and a two-stranded antiparallel β -sheets, respectively together with additional specific elements present in proaerolysin and ϵ -toxin which are related to the proteolytic step required for their respective activation. In the case of aerolysin, the C-terminal activation peptide adopts a strand-helix-strand, with the proteolytic reaction taking place in the loop between residues 422-440.³⁸ Conversely, in the case of ϵ -toxin the position of the last two strands lie on opposite sides of the sheets.²⁴ Doubtless, one of the most conspicuous characteristics of the B-domains is the abundance of serine and threonine residues (Table 3) which are mainly located in the exposed face of the two-stranded β -sheet (Fig. 7). Precisely, these last two strands are the ones which flank the amphipathic loop from the L-domain. A potential role for these residues in oligomerization may come from the detailed analysis of the crystal structure of LSLa, in particular, from the analysis of the subunit interactions within the hexamer. LSLa subunits essentially interact through their B-domains, specifically through interactions between strands β -21 and β -23

Table 3. Hydroxylated amino acid residues present in B-domain of aerolysin-like proteins

Protein	Serine/Threonine
Aerolysin	T218; T223; T275; S276, S278; S280; T284; S461; S463
LSLa	T175; T177; T181; S182; T185; S189; S193; T195; T196; T249; T251; T253; S255; T263; S268; T269; S270; T309; T311; S312; T314
ϵ-toxin	T91; T94; S102; S104; T106; T161; S166; S287; S289
Parasporin	S65; T67; S69; S71; S77; S79; S142; T144

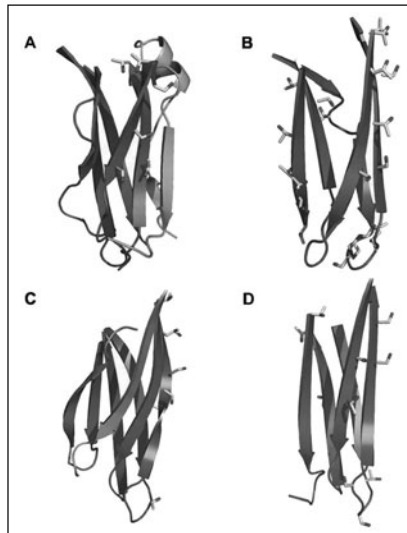


Figure 7. Structure of the B-domains of the areolysin pore-forming module. The C α backbone is shown as cartoon representation. The scaffold of the B-domain is based on a β -sandwich fold. A conspicuous feature of this domain is that they are rich in serine/threonine residues (stick model), mainly located at the two-stranded sheet of the β -sandwich (see the text). A) B-domain from proaerolysin from *A. hydrophila*, B) from LSLa from *L. sulphureus*, C) from ϵ -toxin from *C. perfringens* and D) from parasporin from *B. thuringiensis*.

which are exceptionally rich in serine plus threonine residues (β -21: 249-TYTATFSVRA-258; β -23: 306-LRHHTLSVTA-314). We believe that the overall hydrophobicity of these sequences together with the presence of small and polar residues (potential hydrogen bond acceptors and donors) makes them suitable adapters for intermolecular interactions. In fact, this mechanism is the one proposed for the aggregation of β -barrels into amyloid-like fibrils by the Dobson^{39,40} group. Interestingly and in agreement with this hypothesis, the intermolecular interactions between parasporin molecules identified within the crystal structure are established exclusively through β -strand 5 from the B-domain which is both hydrophobic and contains two serine residues. Additionally, this proposal would agree with the scenario proposed for the proteolytic activation of proaerolysin³⁸ where the loss of the activation peptide would determine the exposure of a large hydrophobic surface which then would promote protein oligomerization. Also, it has been shown that in *C. septicum* α toxin the C-terminal peptide has an inhibitory effect on oligomerization when applied in excess, indicating the importance of removal of the C terminus for successful oligomerization.⁴¹

Other New Members in the Aerolysin Family: Basic Aerolysin Pore-Forming Motifs?

Considering the above results that indicate structural similarity despite very low sequence similarity between the members of the aerolysin family, the search for new homologous β -pore-forming proteins exclusively by sequence analyses is not a straightforward task. In this regard, the work carried out by the Zlotkin⁴²⁻⁴⁴ group on hydralysins (Hln's) from the cnidarian *Chlorohydra viridissima* has been especially valuable. Hydralysins are β -pore-forming proteins which make oligomeric pores within the erythrocyte membrane, with an internal diameter of ~ 1.2 nm.⁴² Unlike other cnidarian toxins which are found in nematocytes, hydralysins are produced by digestive cells surrounding the gastrovascular cavity of *C. viridissima* and have been suggested to be involved in prey digestion.⁴⁴ Once the pore-forming activity of hydralysins had been demonstrated, an exhaustive search of related

proteins within public databases permitted to conclude that Hln's are indeed β -pore-forming proteins, revealing similarities with members of the aerolysin family (Fig. 8). The same search also detected additional proteins sharing what can be defined as a putative "pore-forming motif". This motif can be described as a region with an alternating pattern of hydrophobic residues flanked by two regions exceedingly rich in serine/threonine residues. In addition, the C-terminal flanking Ser/Thr-rich region is followed by another region rich in hydrophobic residues, with a highly conserved diad of proline residues in the center.⁴³ The three dimensional interpretation of these results indicates that the *aerolysin pore-forming motif* identified would be made up of the complete two-stranded sheet from the B-domain together with two strands from the other sheet and also by the loop from the L-domain. It is interesting to note that according to the scenario proposed previously, these regions would provide structural elements directly participating in pore-formation (the loop from the L-domain) and oligomerization (β -strands from the B-domain) which reinforces the suggestions that this alignment reveals key features of pore-forming proteins.

Conclusion

One promising future avenue for research is elucidating the biological roles played by pore-forming proteins, in the context of the producing organism and the ecosystem in which it lives. Pore-forming proteins produced by pathogenic bacteria are often part of the chemical armament used to establish infection.⁴⁵ However, the role of other pore-forming proteins is unclear—proteins suggested to contain the aerolysin pore forming motif⁴² (as described above) are found in the skin and gut of amphibians,^{46,47} as subunits of moth yolk protein⁴⁸ and as components of earthworm innate immunity.⁴⁹ Even the role LSL's play in the biology of the *L. sulphureus* fruiting body is unclear. The ability of pore-forming proteins to create de-novo transmembrane channels in a receptor-mediated, spatially and temporally-restricted manner enables them to perform many different tasks, including the formation of intracellular chloride⁵⁰ and calcium channels^{51,52} and participation in apoptosis, e.g., Bcl-2 family.^{53,54} Having learned how different pore-forming proteins contain similar structural motifs, further research will help elucidate the way the structures of the proteins have evolved to enable them to fulfill what we believe to be diverse biological roles.

Acknowledgements

J.M.M. acknowledges the Spanish Ministry of Science and Innovation for supporting his research on membrane-interacting proteins (BFU2007-67404/BMC) and also the Factoria de Cristalizacion (Consolider-Ingenio-2007). D.S. acknowledges the support of the Israel Science Foundation (grant 476/01 to Eliahu Zlotkin).

References

1. Kanska G, Guillot J, Dusser M et al. Isolation and characterization of an N-acetylglucosamine-binding lectin from the mushroom *Laetiporus sulphureus*. *J Biochem* 1994; 116:519-523.
2. Tateno, H, Goldstein, IJ. Molecular cloning, expression and characterization of novel hemolytic lectins from the mushroom *Laetiporus sulphureus*, which show homology to bacterial toxins. *J Biol Chem* 2003; 278:40455-40463.
3. Mancheño JM, Tateno H, Goldstein IJ et al. Structural analysis of the *Laetiporus sulphureus* hemolytic pore-forming lectin in complex with sugars. *J Biol Chem* 2005; 280:17251-17259.
4. Goldstein IJ, Hughes RC, Monsigny M et al. What should be called a lectin? *Nature* 1980; 285:66.
5. Olsnes S, Kozlov JV. *Ricin*. *Toxicol* 2001; 39:1723-1728.
6. Hatakeyama T, Nagatomo H, Yamasaki N. Interaction of the hemolytic lectin CEL-III from the marine invertebrate *Cucumaria echinata* with the erythrocyte membrane. *J Biol Chem* 1995; 270:3560-3564.
7. Hatakeyama T, Furukawa M, Nagatomo H et al. Oligomerization of the hemolytic lectin CEL-III from the marine invertebrate *Cucumaria echinata* induced by the binding of carbohydrate ligands. *J Biol Chem* 1996; 271:16915-16920.
8. Tahirov TH, Lu TH, Liaw YC et al. Crystal structure of abrin-a at 2.14 Å. *J Mol Biol* 1995; 250:354-367.
9. Nakano M, Tabata S, Sugihara K et al. Primary structure of hemolytic lectin CEL-III from marine invertebrate *Cucumaria echinata* and its cDNA: structural similarity to the B-chain from plant lectin, ricin. *Biochim Biophys Acta* 1999; 1435:167-176.

10. Uchida T, Yamasaki T, Eto S et al. Crystal structure of the hemolytic lectin CEL-III isolated from the marine invertebrate *Cucumaria echinata*. *J Biol Chem* 2004; 279:37133-37141.
11. Mancheño JM, Tateno H, Goldstein IJ et al. Crystallization and preliminary crystallographic analysis of a novel haemolytic lectin from the mushroom *Laetiporus sulphureus*. *Acta Crystallog Sect D Biol Crystallog* 2004; 60:1139-1141.
12. Parker MW, Buckley JT, Postma JPM et al. Structure of the *Aeromonas* toxin proaerolysin in its water-soluble and membrane-channel states. *Nature* 1994; 367:292-295.
13. McLachlan AD. Three-fold structural pattern in the soybean trypsin inhibitor (Kunitz). *J Mol Biol* 1979; 133:557-563.
14. Murzin AG, Lesk AM, Chothia C. beta-Trefoil fold. Patterns of structure and sequence in the Kunitz inhibitors interleukins-1 beta and 1 alpha and fibroblast growth factors. *J Mol Biol* 1992; 223:531-543.
15. Hazes B. The (QxW)₃ domain: a flexible lectin scaffold. *Prot Sci* 1996; 5:1490-1501.
16. Rutenber E, Ready M, Robertus JD. Structure and evolution of ricin B chain. *Nature* 1987; 326: 624-626.
17. Holm L, Sander C. Protein structure comparison by alignment of distance matrices. *J Mol Biol* 1993; 233:123-138.
18. Fujinaga Y, Inoue K, Watanabe S et al. The haemagglutinin of *Clostridium botulinum* type C progenitor toxin plays an essential role in binding of toxin to the epithelial cells of guinea pig small intestine, leading to the efficient absorption of the toxin. *Microbiology* 1997; 143:3841-3847.
19. Fujinaga Y, Inoue K, Nomura T et al. Identification and characterization of functional subunits of *Clostridium botulinum* type A progenitor toxin involved in binding to intestinal microvilli and erythrocytes. *FEBS Lett* 2000; 467:179-183.
20. Rini JM. Lectin structure. *Annu Rev Biophys Biomol Struct* 1995; 24:551-577.
21. Poget SF, Legge GB, Proctor MR et al. The structure of a tunicate C-type lectin from *Polyandrocarpa misakiensis* complexed with D-galactose. *J Mol Biol* 1999; 290:867-879.
22. Cioci G, Mitchell EP, Gautier C et al. Structural basis of calcium and galactose recognition by the lectin PA-IL of *Pseudomonas aeruginosa*. *FEBS Lett* 2003; 555:297-301.
23. Walker JR, Nagar B, Young NM et al. X-ray crystal structure of a galactose-specific C-type lectin possessing a novel decameric quaternary structure. *Biochemistry* 2004; 43:3783-3792.
24. Cole AR, Gibert M, Popoff M et al. *Clostridium perfringens* ϵ -toxin shows structural similarity to the pore-forming toxin aerolysin. *Nat Struct Mol Biol* 2004; 11:797-798.
25. Akiba T, Higuchi K, Mizuki E et al. Nontoxic crystal protein from *Bacillus thuringiensis* demonstrates a remarkable structural similarity to β -pore-forming toxins. *Proteins: Struct Funct Bioinf* 2006; 63:243-248.
26. Heuck AP, Tweten RK, Johnson AE. Beta-barrel pore-forming toxins: intriguing dimorphic proteins. *Biochemistry* 2001; 40:9065-9073.
27. Gouaux E. Channel-forming toxins: tales of transformation. *Curr Opin Struct Biol* 1997; 7:566-573.
28. Melton JA, Parker MW, Rossjohn J et al. The identification and structure of the membrane-spanning domain of the *Clostridium septicum* alpha-toxin. *J Biol Chem* 2004; 279:14315-14322.
29. Iacovache I, Paumard P, Scheib H et al. A rivet model for channel formation by aerolysin-like pore-forming toxins. *EMBO J* 2006; 25:457-486.
30. Song LZ, Hobaugh MR, Shustak C et al. Structure of staphylococcal alpha-hemolysin, a heptameric transmembrane pore. *Science* 1996; 274:1859-1866.
31. Benson EL, Huynh PD, Finkelstein A et al. Identification of residues lining the anthrax protective antigen channel. *Biochemistry* 1998; 37:3941-3948.
32. Shepard LA, Heuck AP, Hamman BD et al. Identification of a membrane-spanning domain of the thiol-activated pore-forming toxin *Clostridium perfringens* perfringolysin O: an alpha-helical to beta-sheet transition identified by fluorescence spectroscopy. *Biochemistry* 1998; 37:14563-14574.
33. Shatursky O, Heuck AP, Shepard LA et al. The mechanism of membrane insertion for a cholesterol-dependent cytolyisin: a novel paradigm for pore-forming toxins. *Cell* 1999; 99:293-299.
34. Nooren IM, Thornton JM. Diversity of protein-protein interactions. *EMBO J* 2003; 22:3486-3892.
35. Nooren IM, Thornton JM. Structural characterisation and functional significance of transient protein-protein interactions. *J Mol Biol* 2003; 325:991-1018.
36. Anderlüh G, Lakey JH. Disparate proteins use similar architectures to damage membranes. *Trends Biochem Sci* 2008; 33:482-490.
37. Han J-H, Batey S, Nickson AA et al. The folding and evolution of multidomain proteins. *Nat Rev Mol Cell Biol* 2007; 8:319-330.
38. Rossjohn J, Feil SC, McKinstry WJ et al. Aerolysin-A paradigm for membrane insertion of beta-sheet protein toxins? *J Struct Biol* 1998; 121:92-100.

39. Guijarro JI, Sunde M, Jones JA et al. Amyloid fibril formation by an SH3 domain. *Proc Natl Acad Sci USA* 1998; 14:4224-4228.
40. Chiti F, Webster P, Taddei N et al. Designing conditions for in vitro formation of amyloid protofilaments and fibrils. *Proc Natl Acad Sci USA* 1999; 30:3590-3594.
41. Sellman BR, Tweten RK. The propeptide of *Clostridium septicum* alpha toxin functions as an intramolecular chaperone and is a potent inhibitor of alpha toxin-dependent cytolysis. *Mol Microbiol* 1997; 25:429-440.
42. Zhang M, Fishman Y, Sher D et al. Hydralysin, a novel animal group-selective paralytic and cytolytic protein from a noncnidocystic origin in hydra. *Biochemistry* 2003; 42:8939-8944.
43. Sher D, Fishman Y, Zhang M et al. Hydralysins, a new category of beta-pore-forming toxins in cnidaria. *J Biol Chem* 2005; 280:22847-22855.
44. Sher D, Fishman Y, Melamed-Book N et al. Osmotically driven prey disintegration in the gastrovascular cavity of the green hydra by a pore-forming protein. *FASEB J* 2007; 22:207-214.
45. Gilbert RJ. Pore-forming toxins. *Cell Mol Life Sci* 2002; 59:832-844.
46. Owaga M, Takahashi T, Takahashi TC et al. Metamorphic change in EP37 expression: members of the bg-crystallin superfamily in newt. *Development Genes and Evolution* 1997; 206:417-424.
47. Owaga M, Takahashi TC, Takabatake T et al. Isolation and characterization of a gene expressed mainly in the gastric epithelium, a novel member of the ep37 family that belongs to the bg-crystallin superfamily. *Development Growth and Differentiation* 1998; 40:465-473.
48. Perera OP, Shirk PD. cDNA of YP4, a follicular epithelium yolk protein subunit, in the moth, *Plodia interpunctella*. *Arch Insect Biochem Physiol* 1999; 40:157-164.
49. Kobayashi H, Ohta N, Umeda M. Biology of Lysenin, a Protein in the Coelomic Fluid of the Earthworm *Eisenia foetida* *International Review of Cytology*, 2004. pp. 45-99. Academic Press.
50. Cromer BA, Morton CJ, Board PG et al. From glutathione transferase to pore in a CLIC. *Eur Biophys J* 2002; 31:356-364.
51. Gerke V, Moss SE. Annexins: From Structure to Function. *Physiol Rev* 2002; 82:331-371.
52. Kim YE, Isas JM, Haigler HT et al. A helical hairpin region of soluble annexin B12 refolds and forms a continuous transmembrane helix at mildly acidic pH. *J Biol Chem* 2005; 280:32398-32404.
53. Lazebnik Y. Why do regulators of apoptosis look like bacterial toxins? *Curr Biol* 2001. 11:R767-R768.
54. Sharpe JC, Arnoult D, Youle RJ. Control of mitochondrial permeability by Bcl-2 family members. *Biochim Biophys Acta* 2004; 1644:107-113.

CHAPTER 7

Interfacial Interactions of Pore-Forming Colicins

Helen Ridley, Christopher L. Johnson and Jeremy H. Lakey*

Abstract

Colicins are water soluble toxins secreted by *E. coli* cells to kill other *E. coli* and related species. To do this they need to cross the outer membrane, periplasm and inner membrane. Pore forming colicins, as their name suggests form a voltage dependent pore in the inner membrane. This chapter deals with the interfaces, both lipid and protein, that the colicins experience as they make the short but complex journey that brings them to the point of pore formation. The succession of molecular interactions with lipid and protein receptors causes a series of conformational changes which allow these large >40 kDa proteins to outwit the normally tight defensive shield of the target cell. This is done by combining general physico-chemical interfacial interactions, such as the use of amphipathic helical peptides, with precisely targeted protein-protein interactions involving both rigid and natively disordered protein domains.

Introduction

Colicins are toxins encoded on plasmids that infect *Escherichia coli* and related species. The plasmids enable their host cells to kill related bacteria and also provide them with immunity to their own colicin type.¹ The result is therefore a selective advantage for the survival of the bacteria and the plasmid is thus a very simple “selfish gene” system.² They belong to the bacteriocins family which have representatives in other gram negative bacteria (Pyocin = *Pseudomonas*;³ Pesticin = *Yersinia pestis*^{4,5}). Colicin proteins comprise three domains correlating with three activities, the translocation domain, the receptor binding domain and the toxic domain.

The two major groups of colicins are named after the nature of their toxic activity, the nuclease colicins kill by digesting host nucleic acids and the pore-forming toxins create ion channels in the *E. coli* inner membrane.⁶⁻⁹ The three domains work in concert to deliver this toxic moiety to the inner membrane where the pore-forming domain creates a voltage dependent ion channel and the enzymatic domains translocate to digest intracellular nucleic acids.

The first interaction with target cells is the binding to an outer membrane beta barrel membrane receptor such as FepA, BtuB, Tsx, OmpX or OmpF.¹ This is largely a function of the central receptor binding domain but for colicin N both the pore-forming C-terminal¹⁰ and N-terminal translocation domains¹¹ have also been shown to contribute. Some proteins require the presence of two distinct outer membrane proteins and, of these, one seems to act as an independent translocator. The second stage is the binding of an intra periplasmic protein of the Tol or Ton families by the translocation domain. This step is considered critical for the import of the toxic domain. Thus all colicins employ a set of similar components to create the so called translocon which provides the pathway across

*Corresponding Author: Jeremy H. Lakey—Institute for Cell and Molecular Biosciences, University of Newcastle upon Tyne, Framlington Place, Newcastle upon Tyne, NE2 4HH, UK. Email: j.h.lakey@ncl.ac.uk

the outer membrane. The nature of this step is still unclear and how the pore-forming domain is presented to and inserts in the inner membrane is the subject of this review.

Structures

There are currently four high resolution structures known for pore-forming colicins S4, B, N and Ia¹²⁻¹⁵ and two pore-forming domains E1 and A^{16,17} (Fig. 1). The latter was the first to be determined.¹⁷⁻¹⁹ The pore-forming domain consists of ten alpha helices arranged in three layers the middle one being a pair of hydrophobic helices (numbers 8 and 9). Similar structures are found in the Bcl family of apoptosis regulators²⁰ and the diphtheria toxin B subunit.²¹ The colicin pore-forming domains have homologous sequences and structure with the major differences being the shorter hydrophobic helices in colicins K, E1, Ia and Ib (Fig. 2). This motif of a very hydrophobic core surrounded by (and solubilised by) an outer shell of amphipathic helices will be discussed in more detail later.²² The structures of some representative colicins shown in Figure 1 make it clear that, although the pore-forming domain is conserved, its relationship with the other domains is highly variable. Thus as well as exploiting a variety of import pathways it is also clear that the pore-forming domain's relationships with the receptor binding and translocation domains is also highly variable. It is also known from several publications that significant unfolding occurs after receptor binding in order to present the pore-forming domain to the plasma membrane.^{10,23-25} The variation in structures and translocons might suggest that this unfolding is also done in different ways.²⁶

Receptor Binding

The receptor binding step has been studied in detail but the crystal structures for the receptor binding domains of Ia, E2 and E3²⁷⁻²⁹ are all very similar. They reveal a common mode of binding involving the insertion of the end of a coiled coil helical hairpin into the high affinity beta barrel receptor such as BtuB or Cir. In BtuB, high affinity receptor binding is followed by translocation via OmpF whilst Cir appears to be the only protein required. Isothermal titration calorimetry data has been measured¹¹ but no high resolution structure is yet known for the lower affinity colicin N receptor complex.¹⁰ The receptor binding domain is quite different and composed of a beta sheet structure.^{15,30} This resembles the structure of colicin B which has been solved¹³ and is a short compact two domain structure. In a similar way to the relationship between colicin N with OmpF, colicin B appears to use FepA as its one receptor and translocator. Thus it might be thought that a more compact structure may be associated with the use of a single receptor. However, not only does the very long colicin Ia use just Cir but recently the structure of pore-forming colicin S4, which binds OmpW and requires OmpF, was solved and shown to be very compact. Although its pore domain is unexceptional it unusually has a tandemly repeated receptor domain. Experiments show that only one of these two R-domains is required for toxicity and sequence analysis shows this to be a relatively recent duplication event. Thus there currently appears to be no common mechanism following receptor binding. Colicins 5, 10 and E1 do not use OmpF after binding to their receptors (Tsx or BtuB) but instead are translocated via TolC.¹ Although common to many gram negative bacterial species this is an otherwise unusual protein in that it is composed of a trimer which forms a single outer membrane pore and a long helical structure which spans the periplasm.³¹ TolC is a pathway for the export of many molecules from protein toxins to drugs because it associates with a range of inner membrane transporters which feed molecules for export into the bottom of the 140 Å long TolC tunnel. From here they diffuse outwards through the beta-barrel outer membrane pore into the exterior.

Translocation

The translocation domains at the colicins' N-termini bind to periplasmic receptors, either TolA or TolB or Ton B and is generally a disordered structure. How it enters the periplasm is not clear, but it has been proposed to insert via the pore of OmpF in examples where this protein is implicated. It is needed for OmpF binding in colicin N^{11,32} and more recently the translocation

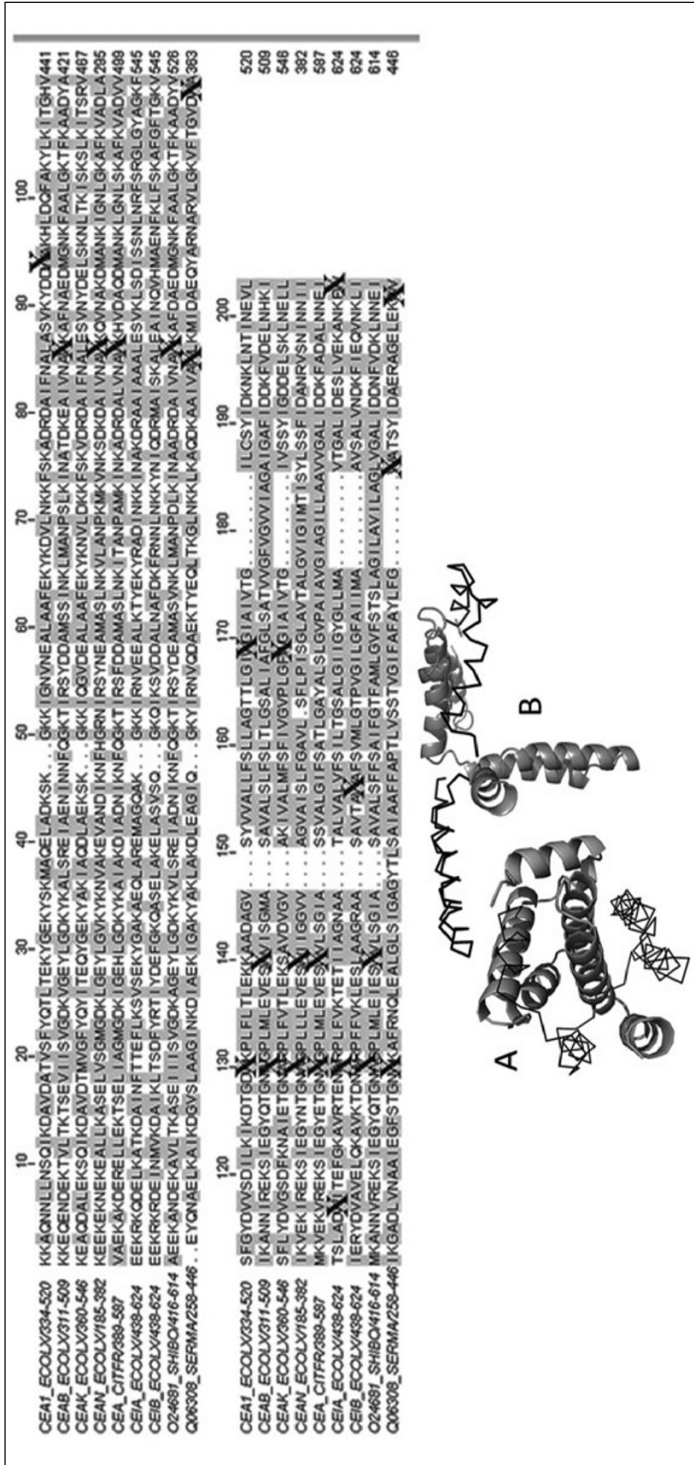


Figure 1. Sequence alignment of some pore-forming colicin toxin C-terminal domains. Tryptophans are highlighted with “X” and hydrophobic residues shaded. The first tryptophan at position 86 of the alignment corresponds to the end of helix 4 and the beginning of the shortest active channel forming segment. CE1: colicin E1, CE2: colicin B, CE3: colicin K, CE4: colicin N, CE5: colicin A, CE6: colicin IA (*Citrobacter*), CE7: colicin IB, 024681: colicin U (*Shigella*), Q06308: Bacteriocin 28b (*Serratia*). Lower panel. Required channel forming helices shown in cartoon form and remainder in ribbon format for colicin A P domain in the soluble¹⁹ (PDB:1col) (A) and one possible proposed inserted state.¹⁸ (B) The latter is based upon minimal unfolding of the X-ray derived structure and the membrane penetrating helix is shown in the extended conformation. Currently no clear evidence exists either way for more unfolded conformations of the helices at the interface.

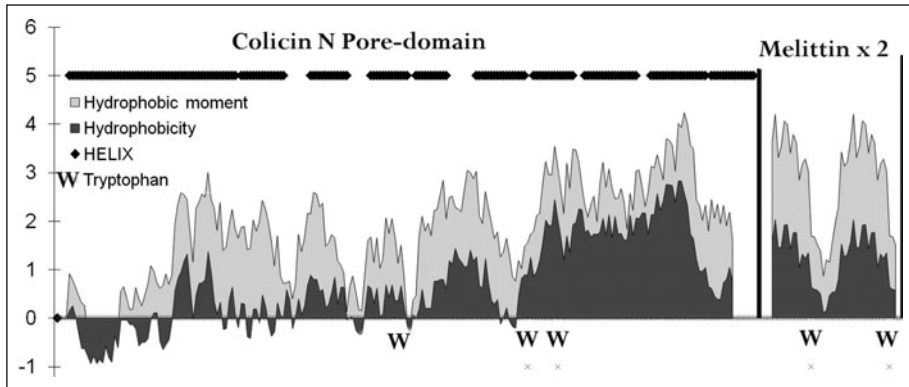


Figure 2. Amphipathic property of colicin N. The plot shows the hydrophobicity and hydrophobic moment (a measure of amphipathic nature)⁶⁶ of the C-terminal region of colicin N. The plot uses a window of 13 residues (which is shorter than normally used to predict transmembrane helices but suitable for the size of helix found in colicins) and plots the result at the central residue. This means that data is not plotted for the six residues at either end. The hydrophobicity scale used was PRIFT⁶⁷ and a repeat of 3.6 residues per turn used for helix.⁶⁶ Note the trend towards greater hydrophobicity and lower ratio of amphipathicity to hydrophobicity from N to C-terminal of this region. Melittin is presented as an example of a lytic peptide but due to its short length a tandem repeat of the sequence was used.

domain of colicin E9 was shown to have OmpF binding regions on either side of the TolB binding site.³³ Isolated T-domains³⁴ as well as full length colicin N³⁵ have been shown to occlude OmpF channels in planar lipid bilayers and biosensors. Thus at least two (T+R) and in the case of colicin N, all three domains play a role in OmpF binding. The TolA binding colicin N T-domain, invisible in the X-ray structure,¹⁵ has been investigated by NMR spectroscopy.^{36,37} This revealed that the 27 amino acid TolA binding region is not only immobilised in the receptor complex but also in uncomplexed colicin N. This suggests a self recognition mechanism where the mobile domain is kept close to the fully folded structure.³⁷ This might be needed to protect the flexible T-domain from protease activity or to simply increase the diffusion rate in solution. This finding is supported by isothermal titration calorimetry data which showed that free T-domain has a higher affinity for TolA than the full length protein. Analysis of the T-domain by the PONDR algorithm³⁸ which detects possible regions of natively unfolded structure, shows the TolA binding region to have the properties of a folded protein and thus is predisposed to undergo an unfolded to folded transition upon binding. Thus, this part of the colicin becomes more ordered during translocation and this combines with ITC evidence that colicin N and OmpF form a more ordered complex with a reduction in entropy.¹¹ It is therefore likely that the disordered regions of colicins play a specific and possibly structural role in the translocon.

Recent data has shown that colicin N (either full length or just the pore-forming domain) displaces bound LPS from OmpF and may bind to the outside of the protein leading to the possibility that it may translocate down the outside of the OmpF beta barrel.^{10,39} Disulphide bonds, introduced into the P-domain by mutagenesis to stabilise the X-ray defined structure, also stop translocation in colicins A and N²³ and prevent in vitro complex formation with OmpF in the case of colicin N.¹⁰ The pore-forming domain is also essential for OmpF binding by colicin N in ITC experiments.^{11,32} Thus a series of binding and refolding events involving the pore-forming domain precede its interaction with the target cytoplasmic membrane. The translocation domains of colicins that use the TolA protein (colicins E2, A, N) do so via the last domain, of about 120 amino acids, called TolAIII. This globular domain is also the binding site of the g3p protein from filamentous phage which also use TolA to attack bacteria. Preceding this domain are domains I, which spans

the inner membrane and II, which is proposed to be highly helical and may resemble the helical region of TolC.⁴⁰ This implies that the helical region is folded so that it crosses the periplasm three times. The parallel with TolC was rendered more believable by experiments with different colicins carried out on mutants which had increasingly large regions of TolAII removed.⁴¹ Colicin E1, which requires TolIII, was nevertheless unaffected by the loss of TolAII whereas colicin A was sensitive to small deletions in TolAII and colicin N sensitive to large deletions. The discovery that the TolC dependent colicin E1 does not need the long periplasmic helices of TolAII strongly suggests that these structures are similar. TolAII has been shown to form complexes with OmpF and related trimeric porins in SDS detergent.⁴² This was later shown to be true for P-domains from colicins A, B and N. It was also shown that the two complexes could not be formed on the same OmpF trimer and thus TolA and P-domains were competing for overlapping sites. Assays with colicin N fragments showed that the first helix of the P domain was capable of binding GST to OmpF and as mentioned above, disulphide bridges which hold the helix in its native structure prevent pore formation. This helix which extends to varying lengths beyond the pore-forming domain is not strongly conserved and in colicin S4 is very short indeed.

Crossing the Periplasm

In order for the pore-forming domain to reach across the periplasm and insert into the inner membrane it has been proposed that the two helices extend and unfold from the rest of the pore domain to provide a long helical linker.³⁰ The need for a linker was suggested in order to span the periplasm (i.e., the distance indicated by the long helices of TolC) and to explain an intriguing result of studies with colicin A. This was revealed by examining the kinetics of killing as revealed by potassium ion release.²⁵ As the colicin pore opens it increases the loss of potassium from cells several fold and this can be recorded by a potassium selective electrode submerged in a few ml of a bacterial suspension. The efflux of potassium begins after a lag phase, thought to reflect the translocation of the colicin to its open state in the inner membrane and when plotted against time rapidly reaches an almost linear slope whose gradient is determined by the ratio of colicins per cell. Above a ratio of 400 toxins per cell the gradient no longer increases and this is considered to be the saturation of the number of binding sites per cell.^{43,44} Since in the case of colicin N there are between 70-100 thousand receptors (OmpF) per cell it is thought that this limiting factor is the number of Tol complexes. Once the rate of potassium release by colicin A is stable it is possible to add a protease, such as trypsin and soon the release of potassium is slowed down or even halted. This was proposed to represent the inhibition of already open channels by the digestion of some part which was still exposed at the surface, e.g., the receptor binding domain and has led to the dogma that colicins span the bacterial envelope during toxicity.²⁵ It is however surprising that the cells thus released from colicin attack do not at least partially reaccumulate the lost potassium and it seems possible that the results can be explained by trypsin preventing new cells from being intoxicated rather than blocking existing channels. In the case of the smaller colicin N the protease experiment revealed a different result. Here addition of protease after 20 seconds incubation with colicin resulted in there being no inhibition of toxicity even though potassium release had not become significant by this stage. Thus it appears that colicin N rapidly gains access to a protected compartments and this was also investigated by Western blot of the remaining colicin and it was found not to be degraded.⁴⁵ Thus it is in some form of protected compartment either at the surface of the cell or in the periplasm. However colicin N is unusual in that it only binds to OmpF whereas the general rule is to bind to a high affinity receptor (e.g., BtuB) and then to OmpF.³³ The T-domain of the BtuB dependent colicin E9 has been shown to bind to OmpF and may show how this complex formation is accomplished.³³ The more usual state for a colicin may therefore be with extracellular domains coexisting with the inner membrane inserted toxic domain. This requires unfolding of the first two helices of the pore-forming domain and this coincides with data that shows colicin A channels to be formed from the seven or five C-terminal helices.^{46,47} One study purified a shortened fragment which was so hydrophobic that it needed to be prepared by phase separation of Triton X-114 detergent.⁴⁷ On addition to

bilayer lipid membranes single channel events could be recorded which closely resembled the wild type pore-forming domain. This displays voltage and pH dependent channels in which the voltage required to open the channel is the correct size and polarisation to account for activation by the resting potential of a respiring bacterium. The only difference observable for the shortened peptide is slower kinetics of opening and closing. A later study used signal peptide fusions with truncated colicin A peptides to show that deletion of the first four helices has no effect on activity *in vitro* and *in vivo*.⁴⁶

The lack of a role for the initial peptides in the channel formation is also supported by their behaviour in the lipid bound P-domain as detected by fluorescence energy transfer distance measurements. Here the tryptophans of the pore-domain were used as fluorescence donors and an acceptor fluorophore (IAEDANS) bound to a site directed cysteine mutations on helices 1, 2, 8 and 9.⁴⁸⁻⁵⁰ These studies were able to measure the distance between the donors and acceptors and showed that the earlier helices unfold easily at lower lipid to protein ratios than the helical hairpin at the core.

Inner Membrane Inserted Forms

Thus the final seven helices are thought to encompass the pore-forming segment. In the closed pore membrane bound state when the majority of protein is at the surface this is accomplished with little change in the helix content according to circular dichroism data.⁵¹ However the near-UV CD signal, which reports the tertiary structure via the signals from aromatic residues shows a complete collapse and hints at a molten globule state for the protein. This is supported by DSC data where the sharp thermal transition of the pore domain in solution is replaced by a broad transition in the membrane bound form. In colicin A this molten globule state is provoked before insertion by low pH at the interface, finding further supported by the discovery that this colicin requires acidic lipids to act *in vivo*. The basis for this instability at low pH is very interesting as colicin A is unusual in that it is stabilised by surface negative charges and when these are lost, by mutagenesis or protonation at low pH, the domain unfolds.⁵² Colicin N is not sensitive to low pH in solution nor acidic lipids *in vivo* so some other effect promotes its membrane insertion *in vivo*. The only treatment *in vitro* to accelerate insertion is pre-incubation with detergents which also promotes a molten globule state.⁵³ Thus a loosely folded group of helices is found at the surface of the lipids but there is no evidence that they form a perfectly circular ring around the transmembrane helical hairpin. This hairpin is not long enough to span the bilayer easily and has no polar groups at its tip to keep it in a transmembrane state so its likely to be as dynamic as the rest of the molecule. Whether the hydrophobic hairpin crosses the bilayer in the closed state is less clear and different results have been found for this step for other colicins.^{48-50,54,55} However it is likely to span the membrane in the voltage dependent open state.⁵⁶ The tryptophans of all the pore-forming domains reside exclusively in the essential pore-forming region of the last seven helices (Fig. 3).⁴⁷ Since these are the amino acid side chains with the greatest interfacial affinity⁵⁷ it hints that they could play a key role in this initial membrane bound state. They certainly insert into the bilayer as it has been shown that brominated or nitroxide labelled lipids are able to quench the tryptophan fluorescence signal of colicin, A⁵⁸⁻⁶⁰ N²⁶, B²⁶ and E1.⁶¹ The level of quenching approaches the maximum efficiency and thus indicates that they are all exposed to the lipid core. For E1 this study has used mutant colicin P-domain peptides containing single tryptophans and depth dependent measurements have established that they are all situated near the interface with one deeply buried.^{61,62} The single tryptophan mutants which lack the native three tryptophans were all active, but detailed information of their relative toxicity is not available. The helices are also characteristic in that they are amphipathic apart from the central helical hairpin (Fig 1). Thus, on average every 3rd or 4th residue is hydrophobic and this provides a face which in solution stabilises the hydrophobic core and in the membrane promotes an interfacial interaction. This resembles the melittin peptide from bee venom which is a representative of amphipathic lytic peptides. Colicin E1 has been studied in most detail for its surface topology in vesicles and the helices generally follow the interface.⁶³

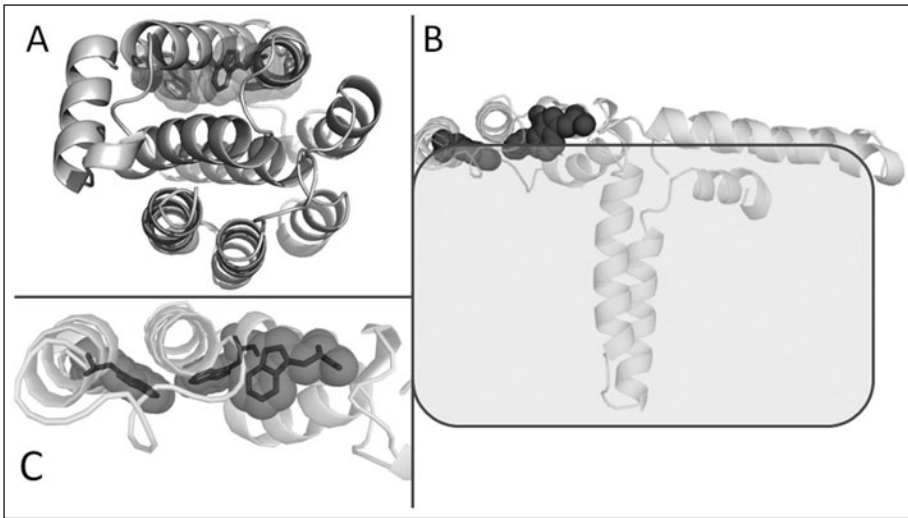


Figure 3. Tryptophan distribution in colicin A. Tryptophans are important interface residues for many membrane interacting molecules⁵⁷ and essential for the activity of melittin. In colicins the tryptophans are found in the minimal channel forming segment but not generally on the hydrophobic hairpin (Fig. 1). They are found on one side of the soluble domain (A)¹⁹ (PDB:1col). They are thus to be found at the membrane-water interface in any model of the closed state (B,C)¹⁸ but more deeply buried in the voltage dependent open channel form.^{6,64}

Some helices are tilted in the closed state and this correlates with an increased hydrophobicity at one end. The tryptophan at position 424 is in a region of interfacial interaction.

The molecule thus delivered by a translocation pathway involving unfolding events and protein-protein interactions is presented to the surface so that it is sufficiently exposed to the transmembrane voltage for the next voltage dependent step to occur, the pore to be formed and the target cell to feel the toxicity of the colicin. This has been estimated to be so efficient that only one colicin may be required to kill the target cell and may justify the complexity of the system in comparison with smaller antibacterial peptides which act in greater numbers. The next pore-forming stage is beyond the scope of this article and has been well described elsewhere.^{6,64} Finally the membrane interactions of this family of proteins should be compared with the Bcl proteins reviewed elsewhere in this volume. The two protein families share a common fold and possibly, in some case a common membrane interaction mechanism. The lipid interactions of colicins and related proteins have been reviewed recently elsewhere.⁶⁵

Conclusion

Colicins have evolved into highly efficient killers of *E. coli* such that it is possible that only one molecule is sufficient to kill a cell. The combination of highly specific protein-protein interactions, protein unfolding and amphipathic helical peptide behaviour succeeds in delivering a large toxin into the cytoplasmic membrane of *E. coli*.

References

1. Cascales E, Buchanan SK, Duche D et al. Colicin biology. *Microbio Mol Biol Rev* 2007; 71:158-229.
2. Dawkins R. *The selfish gene*. Oxford: Oxford University Press; 1976.
3. Kageyama M, Kobayashi M, Sano Y et al. Construction and characterization of pyocin-colicin chimeric proteins. *Bacterio* 1996; 178:103-110.
4. Rakin A, Boolgakowa E, Heesemann J. Structural and functional organization of the *Yersinia pestis* bacteriocin pesticin gene cluster. *Microbiol UK* 1996; 142:3415-3424.

5. Vollmer W, Pils H, Hantke K et al. Pesticin displays muramidase activity. *Bacterio* 1997; 179:1580-1583.
6. Lakey JH, Slatin SL. Pore-forming colicins and their relatives. In: Van Der Goot FG, ed. *Pore-Forming Toxins*. Heidelberg: Springer Verlag; 2001; 257:131-161.
7. James R, Kleanthous C, Moore GR. The biology of E-colicins—paradigms and paradoxes. *Microbio UK* 1996; 142:1569-1580.
8. Zakharov SD, Cramer WA. Colicin crystal structures: pathways and mechanisms for colicin insertion into membranes. *Biochim Biophys Acta-Biomembranes* 2002; 1565:333-346.
9. Riley MA. Molecular mechanisms of bacteriocin evolution. *Ann Rev Gene* 1998; 32:255-278.
10. Baboolal TG, Conroy MJ, Gill K et al. Colicin N binds to the periphery of its receptor and translocator, outer membrane protein F. *Structure* 2008; 16:371-379.
11. Evans LJA, Cooper A, Lakey JH. Direct measurement of the association of a protein with a family of membrane receptors. *J Mol Bio* 1996; 255:559-563.
12. Arnold T, Zeth K, Linke D. Structure and function of colicin S4, a colicin with a duplicated receptor-binding domain. *J Biol Chem* 2009; 284:6403-6413.
13. Hilsenbeck JL, Park H, Chen G et al. Crystal structure of the cytotoxic bacterial protein colicin B at 2.5 and nbsp; and Aring; resolution. *Mol Microbio* 2004; 51:711-720.
14. Wiener M, Freymann D, Ghosh P et al. Crystal structure of colicin Ia. *Nature* 1997; 385:461-464.
15. Vetter IR, Parker MW, Tucker AD et al. Crystal structure of a colicin N fragment suggests a model for toxicity. *Structure* 1998; 6:863-874.
16. Elkins P, Bunker A, Cramer WA et al. A mechanism for toxin insertion into membranes is suggested by the crystal structure of the channel-forming domain of colicin E1. *Structure* 1997; 5:443-458.
17. Parker MW, Postma JP, Pattus F et al. Refined structure of the pore-forming domain of colicin A at 2.4 Å resolution. *J Mol Biol* 1992; 224:639-657.
18. Parker MW, Tucker AD, Tsernoglou D et al. Insights into membrane insertion based on studies of colicins. *Trends Biochem Sci* 1990; 15:126-129.
19. Parker MW, Pattus F, Tucker AD et al. Structure of the membrane-pore-forming fragment of colicin A. *Nature* 1989; 337:93-96.
20. Muchmore SW, Sattler M, Liang H et al. X-ray and nmr structure of human bcl-x(l), an inhibitor of programmed cell-death. *Nature* 1996; 381:335-341.
21. Choe S, Bennett MJ, Fujii G et al. The crystal structure of diphtheria toxin. *Nature* 1992; 357:216-222.
22. Parker MW, Pattus F. Rendering a membrane-protein soluble in water—a common packing motif in bacterial protein toxins. *Trends Biochem Sci* 1993; 18:391-395.
23. Duché D, Parker MW, González-Mañas JM et al. Uncoupled steps of the colicin A pore formation demonstrated by disulfide bond engineering. *J Biol Chem* 1994; 269:6332-6339.
24. Duche D, Baty D, Chartier M et al. Unfolding of colicin A during its translocation through the *Escherichia coli* envelope as demonstrated by disulfide bond engineering. *J Bio Chem* 1994; 269:24820-24825.
25. Benedetti H, Llobes R, Lazdunski C et al. Colicin A unfolds during its translocation in *Escherichia coli* cells and spans the whole cell envelope when its pore has formed. *EMBO J* 1992; 11:441-447.
26. Evans LJA, Goble ML, Hales K et al. Different sensitivities to acid denaturation within a family of proteins; Implications for acid unfolding and membrane translocation. *Biochemistry* 1996; 35:13180-13185.
27. Buchanan SK, Lukacik P, Grizot S et al. Structure of colicin I receptor bound to the R-domain of colicin Ia: implications for protein import. *EMBO* 2007; 26:2594-2604.
28. Sharma O, Yamashita E, Zhalnina MV et al. Structure of the complex of the colicin E2 R-domain and its BtuB receptor—The outer membrane colicin translocon. *J of Biol Chem* 2007; 282:23163-23170.
29. Kurisu G, Zakharov SD, Zhalnina MV et al. The structure of BtuB with bound colicin E3 R-domain implies a translocon. *Nat Struct Biol* 2003; 10:948-954.
30. Vetter IR, Parker MW, Pattus F et al. Insights into membrane insertion based on studies of colicins. In: Parker MW, ed. *Protein Toxin Structure*. Austin TX: R. G. Landes Company; 1996:5-24.
31. Koronakis V, Sharff A, Koronakis E et al. Crystal structure of the bacterial membrane protein TolC central to multidrug efflux and protein export. *Nature* 2000; 405:914-919.
32. Evans LJA, Labeit S, Cooper A et al. The central domain of colicin N possesses the receptor recognition site but not the binding affinity of the whole toxin. *Biochemistry* 1996; 35:15143-15148.
33. Housden NG, Loftus SR, Moore GR et al. Cell entry mechanism of enzymatic bacterial colicins: Porin recruitment and the thermodynamics of receptor binding. *Proc Natn Acad Sci USA* 2005; 102:13849-13854.
34. Zakharov SD, Eroukova VY, Rokitskaya TI et al. Colicin occlusion of OmpF and TolC channels: Outer membrane translocons for colicin import. *Biophy J* 2004; 87:3901-3911.

35. Stora T, Lakey JH, Vogel H. Ion-channel gating in transmembrane receptor proteins: Functional activity in tethered lipid membranes. *Angew Chem Int Ed* 1999; 38:389-392.
36. Anderluh G, Hong Q, Boetzel R et al. Concerted folding and binding of a flexible colicin domain to its periplasmic receptor TolA. *J Biol Chem* 2003; 278:21860-21868.
37. Hecht O, Ridley H, Boetzel R et al. Self-recognition by an intrinsically disordered protein. *FEBS Lett* 2008; 582:2673-2677.
38. Romero P, Obradovic Z, Dunker AK. Natively disordered proteins: functions and predictions. *Appl Bioinformatics* 2004; 3:105-113.
39. Bainbridge G, Armstrong GA, Dover LG et al. Displacement of OmpF loop 3 is not required for the membrane translocation of colicins N and A in vivo. *FEBS Lett* 1998; 432:117-122.
40. Levensgood SK, Beyer WJ, Webster RE. TolA: a membrane protein involved in colicin uptake contains an extended helical region. *Proc Natl Acad Sci USA* 1991; 88:5939-5943.
41. Schendel SL, Click EM, Webster RE et al. The TolA protein interacts with colicin E1 differently than with other group A colicins. *J Bacteriol* 1997; 179:3683-3690.
42. Derouiche R, Gavioli M, Benedetti H et al. TolA central domain interacts with *Escherichia coli* porins. *EMBO J* 1996; 15:6408-6415.
43. Duché D, Letellier L, Geli V et al. Quantification of group-A colicin import sites. *J Bacteriol* 1995; 177:4935-4939.
44. Elkouhen R, Pages JM. Dynamic aspects of colicin N translocation through the *Escherichia coli* outer-membrane. *J Bacteriol* 1996; 178:5316-5319.
45. El-Kouhen R, Pages JM. Dynamic aspects of colicin N translocation through the *Escherichia coli* outer-membrane. *J Bacteriol* 1996; 178:5316-5319.
46. Nardi A, Slatin SL, Baty D et al. The C-terminal half of the colicin A pore-forming domain is active in vivo and in vitro. *J Mol Biol* 2001; 307:1293-1303.
47. Baty D, Lakey J, Pattus F et al. A 136-amino-acid-residue COOH-terminal fragment of colicin A is endowed with ionophoric activity. *Eur J Biochem* 1990; 189:409-413.
48. Lakey J, Baty D, González-Mañas JM et al. Site-directed fluorescence spectroscopy as a tool to study the membrane insertion of colicin A. In: James RP, F and Lazdunski C, ed. *Plasmid encoded toxins*. Heidelberg: Springer Verlag; 1992:127-138.
49. Lakey JH, Baty D, Pattus F. Fluorescence energy transfer distance measurements using site-directed single cysteine mutants. The membrane insertion of colicin A. *J Mol Biol* 1991; 218:639-653.
50. Lakey JH, Duché D, González-Mañas J-M et al. Fluorescence energy transfer distance measurements: the hydrophobic helical hairpin of Colicin A in the membrane bound state. *J Mol Biol* 1993; 230:1055-1067.
51. Lakey JH, Massotte D, Heitz F et al. Membrane insertion of the pore-forming domain of colicin A. A spectroscopic study. *Eur J Biochem* 1991; 196:599-607.
52. Fridd SL, Lakey JH. Surface aspartate residues are essential for the stability of colicin A P-domain: A mechanism for the formation of an acidic molten-globule. *Biochemistry* 2002; 41:1579-1586.
53. Dover LG, Evans LJ, Fridd SL et al. Colicin pore-forming domains bind to *Escherichia coli* trimeric porins. *Biochemistry* 2000; 39:8632-8637.
54. Padmavathi PVL, Steinhoff HJ. Conformation of the closed channel state of colicin A in proteoliposomes: An umbrella model. *J Mol Biol* 2008; 378:204-214.
55. Tory MC, Merrill AR. Adventures in membrane protein topology—A study of the membrane-bound state of colicin E1. *J Biol Chem* 1999; 274:24539-24549.
56. Slatin SL, Qiu XQ, Jakes KS et al. Identification of a translocated protein segment in a voltage-dependent channel. *Nature* 1994;158-161.
57. Yau WM, Wimley WC, Gawrisch K et al. The preference of tryptophan for membrane interfaces. *Biochemistry* 1998; 37:14713-14718.
58. González-Mañas JM, Lakey JH, Pattus F. Brominated phospholipids as a tool for monitoring the membrane insertion of colicin A. *Biochemistry* 1992; 31:7294-7300.
59. González-Mañas JM, Lakey JH, Pattus F. Interaction of the colicin-A pore-forming domain with negatively charged phospholipids. *Eur J Biochem* 1993; 211:625-633.
60. van der Goot FG, González-Mañas JM, Lakey JH et al. A 'molten-globule' membrane-insertion intermediate of the pore-forming domain of colicin A. *Nature* 1991; 354:408-410.
61. Palmer LR, Merrill AR. Mapping the membrane topology of the closed state of the colicin e1 channel. *J Biol Chem* 1994; 269:4187-4193.
62. Tory MC, Merrill AR. Determination of membrane protein topology by red-edge excitation shift analysis: application to the membrane-bound colicin E1 channel peptide. *Biochim Biophys Acta-Biomembranes* 2002; 1564:435-448.
63. Ho D, Merrill AR. Evidence for the amphipathic nature and tilted topology of helices 4 and 5 in the closed state of the colicin E1 channel. *Biochemistry* 2009; 48:1369-1380.

64. Slatin SL, Duche D, Kienker PK et al. Gating movements of colicin A and colicin Ia are different. *J Membr Biol* 2004; 202:73-83.
65. Anderluh G, Lakey JH. Lipid interactions of alpha-helical protein toxins. In: Tamm LK, ed. *Protein-Lipid interactions. From Membrane Domains to Cellular Networks*. Weinheim:Wiley-VCH; 2005:141-162.
66. Visudtiphohle V, Chalton DA, Hong Q et al. Determining OMP topology by computation, surface plasmon resonance and cysteine labelling: The test case of OMPG. *Biochemical And Biophysical Research Communications* 2006; 351:113-117.
67. Cornette JL, Cease KB, Margalit H et al. Hydrophobicity scales and computational techniques for detecting amphipathic structures in proteins. *J Mol Biol* 1987; 195:659-685.

CHAPTER 8

Permeabilization of the Outer Mitochondrial Membrane by Bcl-2 Proteins

Ana J. García-Sáez,* Gustavo Fuertes, Jacob Suckale and Jesús Salgado

Abstract

The proteins of the Bcl-2 family regulate the release of the apoptotic factors from mitochondria during apoptosis, a key event in physiological cell death. Although their molecular mechanisms remain unclear, the Bcl-2 proteins have been proposed to directly control the permeability of the outer mitochondrial membrane by pore formation. Indeed, they share structural features with the pore forming domains of some bacterial toxins and they can give rise to proteolipidic pores in model membranes. The complex level of regulation needed to decide the fate of the cell is achieved by an intricate interaction network between different members of the family. Current models consider multiple parallel equilibria of activation and inhibition that determine whether the permeabilization of the mitochondrial outer membrane is induced or not.

Introduction

Apoptosis is a morphologically defined form of programmed cell death that is highly conserved in eukaryotes.¹ The biochemical pathway of apoptosis ultimately induces the activation of caspases, a family of cysteine proteases that selectively cleave a concrete set of target proteins leading to the dismantling of the cellular components and to cell death. Depending on the nature of the apoptotic stimulus, the signaling pathway proceeds via two different routes. On the one hand, the extrinsic pathway functions downstream of death receptors, like Fas or the tumor necrosis factor receptor family and activates caspase-8 at the death-inducing signaling complex (DISC). On the other hand, the intrinsic pathway is triggered by diverse stress signals, like DNA damage, viral infection or growth factor deprivation. A key event in this latter pathway is the release of the apoptotic factors, like cytochrome c and SMAC/DIABLO, from the mitochondrial inter-membrane space. Once in the cytosol, these factors induce the activation of caspase-9 in the apoptosome complex. Both pathways are interconnected, since during apoptosis Bid is cleaved by caspase-8 to yield the truncated form tBid that induces mitochondrial outer membrane (MOM) permeabilization.

Under normal conditions, the outer mitochondrial membrane is permeable to molecules smaller than 5000 Da due to the presence of numerous porins, which are transmembrane proteins that form relatively big channels (2-3 nm in diameter). However, during apoptosis, the permeability of the MOM is altered to allow the release of cytochrome c and other apoptotic factors.² This MOM permeabilization is thought to be selective, because the mitochondrial integrity is maintained during the first steps of apoptosis in order to provide the energy required for the process. Based on

*Corresponding Author: Ana J. García-Sáez—BIOTEC der TU Dresden, Tatzberg 45-51, 01307 Dresden, Germany. Email: ana.garcia@biotec.tu-dresden.de

extensive work, it is now widely accepted that the proteins of the Bcl-2 family control the MOM permeability during apoptosis.

Bcl-2 (B-cell lymphoma-2), that gives name to this family, was first discovered because of its involvement in follicular lymphoma.³ The finding that Bcl-2 over-expression does not induce cell proliferation, but promotes cell survival was fundamental for our understanding of tumor formation.⁴ Since then, more than 20 proteins have been assigned to the Bcl-2 family and their importance in cancer has become clear.¹ Indeed, the proteins of the Bcl-2 family are important drug targets for anticancer therapies. Moreover, their role in the regulation of programmed cell death during essential biological processes, like development, tissue homeostasis and immunity, has been established during the last years.

The Bcl-2 proteins are conserved in evolution (*C. elegans* contains the homolog CED-9) and show a high level of sequence and structure similarity. Despite this, the members of the family have opposing activities in apoptosis. Depending on their function and on the number of Bcl-2 homology (BH) domains they share, the Bcl-2 proteins are further classified into three subgroups. First, there are pro-survival members, like Bcl-2 itself, Bcl-xL, Bcl-w, A1 or Mcl-1, which contain all four BH domains and inhibit apoptosis. Second, proapoptotic Bax and Bak, which contain BH1-BH3 domains, are thought to participate directly in the permeabilization of the outer mitochondrial membrane. These two proteins exhibit partially redundant activities, but are essential mediators of apoptosis because cells lacking them are resistant to all apoptotic stimuli that activate the intrinsic pathway.⁵ And third, the BH3-only proteins, like Bid, Bim, Bik, PUMA or Noxa, that only share the BH3 domain and have evolved to sense the different apoptotic stimuli and initiate apoptosis.¹ Figure 1 shows a schematic representation of the functions of representative members of the family.

The realization that the release of cytochrome c into the cytosol induces apoptosis was a big step forward in our understanding of the role of mitochondria in the regulation of cell death.⁶ Indeed, MOM permeabilization is considered a “point of no-return” in cell death induction,^{1,7} which shows the importance of the Bcl-2 proteins in governing commitment of the cell to apoptosis. This chapter describes our current understanding of how Bcl-2 proteins control MOM permeabilization. First, it discusses the current structural knowledge of the Bcl-2 proteins in aqueous solution and in lipid membranes. Then, it focuses on their pore-forming activities and on how membrane permeabilization is regulated through a complex interaction network of Bcl-2 family members.

The Structure of the Bcl-2 Proteins

The proteins of the Bcl-2 family, like other pore-forming proteins, can be found in at least two conformations, one in the aqueous environment and the other in the membrane milieu. Thus, refolding in the lipid bilayer is an important step in the activation of these proteins, which can then be classified within the class known as amphitropic.⁸ This holds true even although some members of the family (Bcl-2, Bcl-xL, Bak) can be constitutively bound to intracellular membranes via a C-terminal anchor.⁹ In this case, the latent inactive form retains the core of the protein with a globular structure outside the membrane. Other members, like Bax and Bid, reside in the cytosol and translocate to the MOM in response to apoptotic stimuli.¹⁰⁻¹³ In all cases several membrane-bound conformations with distinct functionality have been proposed.

A number of structural studies have been performed with versions of the proteins in which the C-terminal anchoring domain was removed in order to increase the solubility of the protein for structure determination. So far, the only available high resolution structures of Bcl-2 proteins (Bcl-xL, Bid, Bax, Bcl-2, Bcl-w, Mcl-1 and Bak) correspond to that of water soluble species.¹⁴⁻²²

Structures of Water Soluble Forms

All members of the Bcl-2 family display a similar folding in aqueous environment in spite of their diverse functions (for a review see Petros et al²³) (Fig. 2, top). The protein core consists of an α -helix-hairpin surrounded by a bundle of amphipathic α -helices. The central anti-parallel hairpin is often described as being hydrophobic. However a more careful sequence analysis shows that, although hydrophobic residues predominate in these segments, there are also many ionizable residues placed

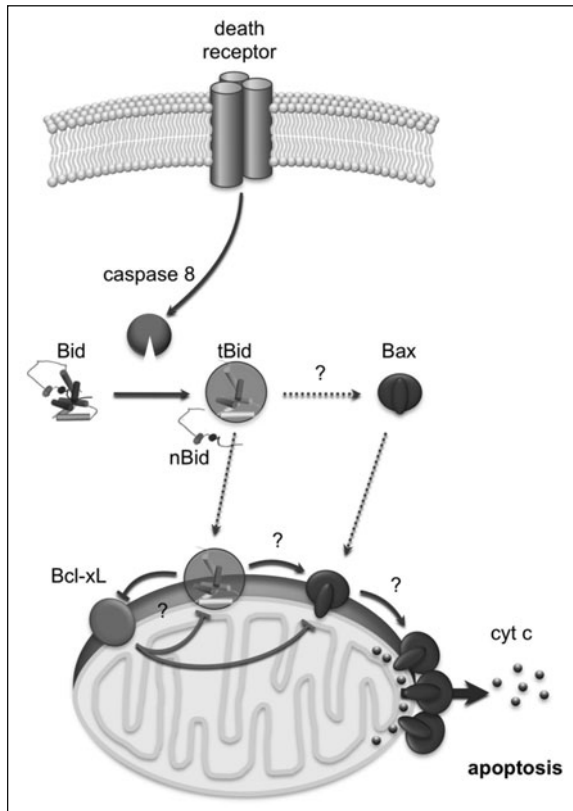


Figure 1. Control of MOM permeabilization by the proteins of the Bcl-2 family. This scheme depicts the functions of representative members of the Bcl-2 family during apoptosis. Bid is inactive in healthy cells. During death receptor induced apoptosis, it is cleaved by caspase-8 to yield the active form tBid. tBid translocates to the MOM, where it activates Bax and induces the release of cytochrome c. Bax is also inactive under normal conditions and during apoptosis it translocates to the MOM, where it oligomerizes and probably participates directly in MOM permeabilization. Bcl-xL is an anti-apoptotic member of the family that inhibits tBid and Bax. The details of the molecular mechanisms of these proteins still remain poorly understood.

in positions that render the two central helices as clearly amphipathic (Fig. 3A). Another important feature of these structures is that the BH1, BH2 and BH3 domains are in close proximity and shape a hydrophobic cleft carved in the protein surface, which has been shown to be the site for docking BH3 domains of other Bcl-2 proteins.²⁴⁻²⁷ Interestingly, the helix 9 of Bax, which resembles the C-terminal hydrophobic domain of Bcl-xL, is buried in the hydrophobic cleft, which has been proposed to have implications for the regulation of membrane binding through BH3-dependent interactions. However, a recent structure of Bax complexed with a BH3 peptide suggests that, apart from that groove, there may be other regions involved in BH3-dependent protein-protein interactions.²⁸ Except for Bid, which has an overall organization similar to multi-domain Bcl-2 proteins, most BH3-only proteins seem to be intrinsically unstructured proteins and fold only when they engage appropriate Bcl-2 partners.²⁹ Overall, the water soluble structures of Bcl-2 family members correspond to the fold class of membrane translocation channel formation domains in the SCOP classification. Specifically, it resembles the pore-forming domain of colicins and diphtheria toxin. The striking similarity between these proteins with very divergent and even opposite functions remains a major mystery.³⁰

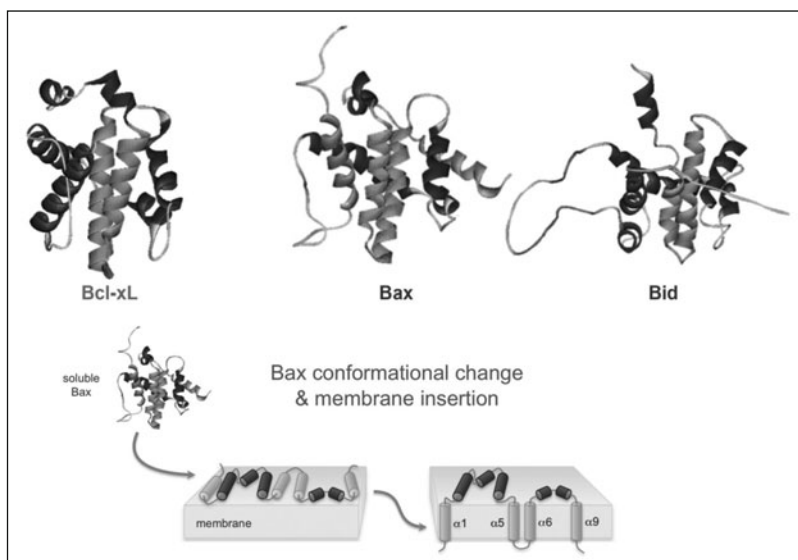


Figure 2. Structure of the Bcl-2 proteins. Top, structures of the soluble form of Bcl-xL, Bax and Bid.^{14,16,17} The putative membrane-interacting fragments are shown in yellow. Bottom, model for Bax structural reorganization associated to membrane insertion and prior to oligomerization and pore formation. When soluble Bax interacts with the surface of the lipid membrane, it unfolds and exposes epitopes in the N-terminal region. Deep extensive insertion is achieved by further conformational changes. The detailed structure of the membrane-inserted conformation is still unclear.

Membrane-Associated Conformations

Since the pore-forming domain is hidden in the interior of the water-soluble structure, it seems obvious that Bcl-2 proteins must unfold in order to make this domain accessible for membrane interactions. However little is known about the membrane-bound structures of the Bcl-2 proteins.

Upon interaction with the MOM, Bax unfolds exposing N-terminal epitopes but without major structural rearrangements and conserving the BH3 domain fold.³¹⁻³⁴ The sequence of events leading to extensive insertion of the protein is unknown, but the membrane-inserted form of Bax probably involves helices 1 and 9 and the hairpin of helices 5 and 6 (Fig. 2, bottom). This proposal is based on *in vitro* glycosylation assays using microsomal membranes.³⁵ Additionally, cysteine accessibility studies have shown that the central hairpin can adopt a membrane inserted conformation in isolated mitochondria.³⁶ Also, helices 1 and 9 have been involved in MOM targeting^{34,37-39} and their corresponding peptides insert deeply into MOM-mimicking model membranes.⁴⁰⁻⁴³ Currently, it is widely accepted that helix 9 will be almost in a transmembrane configuration, while the insertion depth of helices 1, 5 and 6 is more controversial. Since the central hairpin is considered to be the pore-forming domain, it is often imagined (and drawn) as a transmembrane domain within an intact membrane. In fact, the hydrophobic length of these helices is too short to span the bilayer and the only way to avoid exposing charged residues to the lipid acyl chains would be for it to reside at the interface, including at the edge of a pore. In the latter case the tilt angle with respect to the membrane normal is expected to decrease compared to the transmembrane configuration. Oriented circular dichroism experiments suggest that 30% of the helical components of a peptide encompassing helix 5 from Bax were oriented perpendicular to the plane of the bilayer.⁴⁴ Under different conditions, this peptide showed two orientations with tilt angles of 80 and 30 degrees.⁴⁵

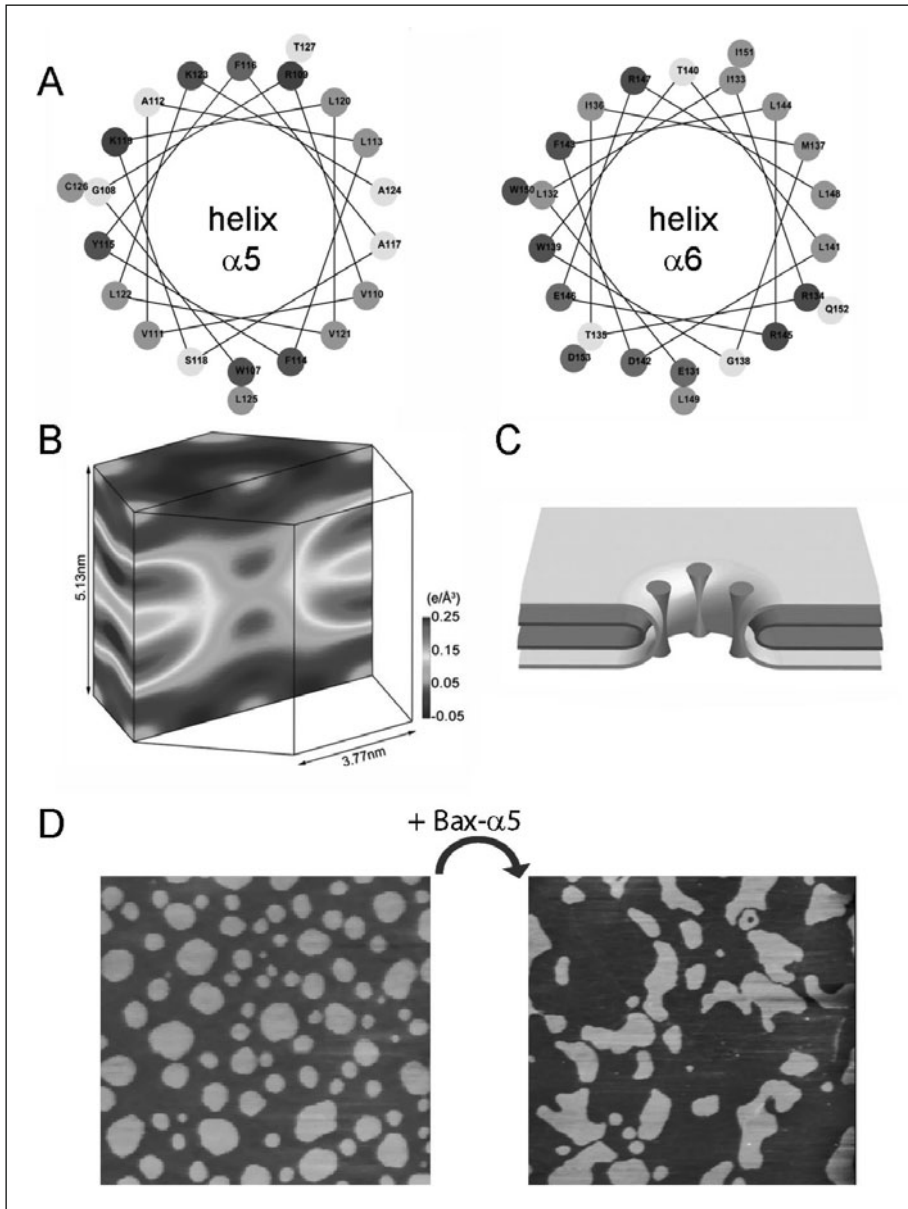


Figure 3. Toroidal pore formed by helix 5 from Bax. A) Edmundson¹⁵⁶ helical wheels show the amphipathic nature of helices 5 and 6 from Bax. B) Normalized electron density distribution of Br atoms in a unit cell of a membrane containing peptides corresponding to helix 5 from Bax (Bax- $\alpha 5$).⁴⁴ C) Model for the toroidal pore formed by Bax- $\alpha 5$.⁴⁴ D) AFM image of a supported lipid bilayer with phase coexistence. The deformation of the lipid domains upon addition of Bax- $\alpha 5$ indicates a decrease in the line tension at the phase boundary.¹⁰³ Panels B and C reproduced from Qian S et al, Proc Natl Acad Sci USA 2008; 105(45):17379-83;⁴⁴ with permission from the National Academy of Sciences, USA.

In vivo, membrane insertion and oligomerization of Bax and Bak are triggered by Bid, Bim and perhaps other BH3-only proteins.⁴⁶⁻⁴⁹ In vitro, Bax activation can be induced by incubating the protein with non-ionic detergents⁵⁰ or by heat.⁵¹ Importantly, once Bax is bound to the membrane it can auto-activate by recruiting other soluble Bax molecules.⁵² A number of experimental techniques, including size-exclusion chromatography, chemical cross-linking and FRET, have shown that Bax, as well as Bak, is able to oligomerize both in mitochondria and in model membrane systems and this is intimately connected to the formation of pores.^{5,36,53-60} However, a recent study cautions since in cells undergoing apoptosis Bax was found to be oligomeric, but in a non-active state.⁶¹

Lipids influence the different steps that eventually lead to Bax adopting the membrane conformation responsible for forming the pore. Cardiolipin appears to be important for the recruitment of Bax and its oligomerization,^{62,63} while phosphatidyl ethanolamine inhibits Bax oligomerization at concentrations larger than 20% mol.⁶⁴ Cholesterol does not affect membrane binding, but inhibits deep insertion and oligomerization of the protein thereby reducing pore-formation.^{64,65} Surprisingly, the effect of cholesterol on cholesterol-dependent cytolysins is exactly the opposite.⁶⁶

The proposed model for antiapoptotic members suggests that these proteins are initially anchored to the MOM through the C-terminal domain while the rest of the protein is folded as in the crystal structure. It is not clear whether the anchored protein is a competent apoptosis inhibitor, but recent pieces of evidence suggest that during apoptosis the protein inserts extensively into the membrane to inhibit apoptosis.^{67,68} In vitro, acidic pH and negatively charged lipids were found to be essential for membrane binding of a Bcl-xL version lacking the C-terminal anchor.^{69,70} For insertion to occur, the protein is believed to unfold so that the central hairpin inserts into the membrane while the other helices remain surface-bound. Pioneering studies in micelles showed that helices 1, 6 and possibly 5 were partially buried in the hydrophobic interior.⁷¹ Glycosylation mapping experiments suggested that helix 5, the hairpin of helices 5 and 6 and the C-terminus of Bcl-xL were able to insert into the membrane while helix 6 alone could not.³⁵ Similarly, cysteine labeling showed that helices 5, 6 and 9 of Bcl-2 inserted deeply in the MOM and that this structural rearrangement is required to inhibit Bax oligomerization.^{67,68}

Bcl-xL dimerizes in water via interactions between the C-terminal domain and the BH3 binding groove⁷² and by three-dimensional domain swapping either at alkaline pH⁷³ or after heat induction.⁷⁴ In non-ionic detergent micelles, Bcl-xL forms two types of dimers distinguishable by the presence or absence of BH3 binding activity.⁷⁵ Similarly, Bcl-2 can homodimerize through two distinct surfaces.⁷⁶ Both, Bcl-2 and Bcl-xL can heterodimerize with Bax partly explaining the ability of Bcl-xL to block Bax pore formation.^{54,67} The fact that antiapoptotic Bcl-2 proteins cannot form higher-order oligomeric species may explain their inability to permeabilize the MOM.

Bid has received considerably less attention in structural terms than the previous proteins. It is made competent for membrane insertion by proteolytic cleavage. The resulting fragment, tBid, translocates to the MOM and cardiolipin seems essential in promoting both tBid binding and activity.^{10,77-81} In general, structural studies agree on a shallow insertion of Bid into the membrane,^{82,83} though glycosylation mapping assays showed that the hairpin of helices 6 and 7 inserts into lipid membranes via hydrophobic interactions.³⁵

Pore-Forming Properties of Bcl-2 Proteins

When the first 3D structure of a Bcl-2 family member became available, its similarity with the pore-forming domains of bacterial toxins, like colicin and diphtheria toxin, was obvious.¹⁶ This prompted researchers to study the ion channel activity of Bcl-2 proteins.⁸⁴

Initially, ion channel recordings of Bax were performed with truncated versions lacking the C-terminus. Bax first formed small anion-selective channels, followed by multiple conductance levels of moderate anion selectivity and, finally, stable ohmic pores.⁸⁵ Further work with full-length Bax showed arbitrary and variable changes in membrane permeability with a marked decrease in membrane stability.⁸⁶ This study suggested for the first time the implication of lipids in Bax-induced pores. The dependence of Bax-induced pores on lipid spontaneous curvature and the increase

in lipid flip-flop were taken as signatures of the formation of proteolipidic toroidal pores.⁸⁷⁻⁹⁰ Besides, cardiolipin has been shown to be necessary for the formation of large pores induced by a mixture tBid and Bax.⁶² Other MOM proteins may also play a role in Bid-assisted Bax pores.⁹¹ However, Bax alone can also form lipidic pores in the absence of Bid as long as it can be targeted to the membrane.^{87,92}

Accumulating evidence indicates that the buried central hairpin is mainly responsible for the pore-forming activity of the Bcl-2 proteins: (i) deletion of the C-terminus domain does not affect Bax functionality,⁹³ (ii) deletion of the central hairpin of Bax abrogates the release of cytochrome c from mitochondria⁹⁴ and (iii) small peptide fragments corresponding to either helix of the hairpin can form pores essentially with the same features as the full-length proteins.^{45,89} Compared to Bcl-xL, Bax-derived sequences show a better “design” for pore formation since positively charged residues are located preferentially in one face of the helix. Moreover, the Bcl-xL central hairpin possesses a greater proportion of negatively charged residues which may reduce membrane binding through electrostatic repulsion. However, pore formation may not be the only function associated with the central hairpin. For example, the mitochondrial localization of Bax, the antiapoptotic effect of Bcl-xL and protein-protein interactions between Bax and other members are thought to be mediated by the pore-forming domain.⁹⁵⁻⁹⁷

Bax pores were first observed at low resolution by AFM.⁹⁸ A more recent X-ray study of a membrane in the presence of a peptide derived from the helix $\alpha 5$ of Bax showed how the two monolayers bend continuously in the rim of the pore, demonstrating that this peptide forms lipidic pores⁴⁴ (Fig. 3B,C). However, the location of the peptide molecules with respect to the pore is unknown. This model of the pore satisfactorily explains both the lipid dependence of leakage caused by Bax and the fast lipid transbilayer diffusion. The toroidal lipid pore has also been proposed to explain the mode of action of structurally similar proteins like colicins.^{99,100} Membrane binding of amphipathic fragments stretches the membrane surface (and simultaneously reduces the membrane thickness) so that when a threshold value of area expansion (or decrease in hydrocarbon thickness) is reached, a pore opens to alleviate the generated tension. Reaching that threshold value is necessary but not sufficient for pore-formation: pore opening is a stochastic process that depends on nucleation of defects in the membrane.¹⁰¹ In this context, the confinement of the amphipathic helical segments of pore-forming proteins, like the Bcl-2 proteins, in a reduced area may provoke the same effect as several individual pore-forming peptides, thus explaining the apparent higher activity of the former with respect to the latter.^{44,102} Protein or peptide induced pores are supposed to be stable and of well defined size, which could be explained in terms of Bax-induced decrease of the line tension^{86,103} (Fig. 3D).

The case of the antiapoptotic proteins is somewhat confusing. As discussed above, their soluble structure is similar to that of proapoptotic members while their function is just the opposite. Furthermore, both Bcl-xL and Bcl-2 can form ion channels in planar lipid bilayers and in liposomes. As with Bax, these channels are pH-sensitive and display different conductance states. But they differ from those of Bax in that they are cation selective, show no decrease in membrane lifetime and have a small opening probability at physiological pH.¹⁰⁴ In the case of Bcl-xL lacking the C-terminus, the pH sensitivity was demonstrated to correlate with protein binding.^{69,105} Poor leakage activity at neutral pH is thus just a consequence of the low membrane affinity in the absence of the C-terminal anchoring domain. So it seems that full-length Bcl-xL is able to form pores at pH 7 although with low efficiency. Similarly, Bcl-2 was found to induce the formation of small pores, which are not cytochrome c permeable, either at physiological pH through tBid-induced conformational changes or acidic pH in the absence of Bid.^{106,107} Interestingly, proteolytic cleavage releasing the N-terminal part of the protein can transform them into pro-apoptotic partners with pore-forming properties essentially identical to that of Bax.¹⁰⁸⁻¹¹¹

The pore-forming capacity of Bid has been studied less than that of other Bcl-2 proteins, since in general it is not able to induce apoptosis on its own.^{5,10,112,113} However, both Bid and tBid are able to destabilize planar lipid bilayers and to induce leakage from and lipid mixing in, liposomes.¹¹⁴⁻¹¹⁷ It has been hypothesized that membrane destabilization by Bid is related to the induction of negative curvature,¹¹⁸ but its lipid transfer activity between membranes could also be involved.^{119,120}

Regulation of MOM Permeabilization by Bcl-2 Proteins

Activation of Bcl-2 Proteins

Under normal conditions, many of the proteins of the Bcl-2 family remain in an apoptosis-inactive form within cells. While the expression levels of some antiapoptotic members of the family can be regulated transcriptionally,¹²¹ Bax and Bak levels are constitutively expressed in cells and their activity is mainly regulated by other Bcl-2 proteins.⁷ Post-translational modifications may also alter Bax binding to the MOM.¹²²⁻¹²⁴ Another way for the cell to control the levels of the different Bcl-2 proteins is by ubiquitination and proteosomal degradation.^{125,126} Increase of the degradation activity have been shown to have a proapoptotic effect on pro-survival members, like Bcl-2 or Mcl-1, while it reduced cell death in the case of proapoptotic proteins, like Bax, Bid, Bak or Bik.¹²⁷

In the presence of apoptotic stimuli, the BH3-only proteins are activated first. They are considered the initial sensors that recognize the diverse apoptotic signals in the cell. The levels of some of them, like NOXA, PUMA or Bim, are increased in response to transcription factor signaling.¹²⁸⁻¹³⁰ Others are activated by posttranslational modifications. For example, Bid is activated via proteolytic cleavage by caspase-8,¹³¹ while Bad and Bim are regulated by phosphorylation.^{132,133} Bim is also activated by release from the dynein motor complex¹³⁴ and Bmf is activated by release from actin-myosin motor complexes.¹³⁵ Once induced or activated, these proteins translocate to the MOM, where they engage with other Bcl-2 proteins to induce apoptosis. Based on their ability to activate Bax and Bak, the BH3-only proteins are classified as “direct activators” or “sensitizer/derepressors”. The latter are unable to directly induce Bax/Bak activation. Instead, they bind to the antiapoptotic proteins with high affinity leading to the release of the “direct activators”, which in turn activate Bax and Bak membrane permeabilizing activity.

Translocation to the MOM is also experienced by other family members when activated for apoptosis induction. Except for a minor fraction weakly associated to mitochondria, Bax exists mostly in a monomeric form in the cytosol of healthy cells.³² During apoptosis, tBid and Bim have been shown to trigger Bax to translocate to the MOM and to potentially induce cytochrome c release.^{12,46,136} Based on experiments with model membranes, it has been suggested that tBid and Bim cooperate with Bax to induce membrane permeabilization.⁶²

Bax translocation to the mitochondria is accompanied by conformational changes³¹ that lead to extensive insertion into the lipid bilayer (see above). In vitro studies have shown that interaction with lipid membranes is enough to initiate Bax conformational rearrangements.¹³⁷ Once in the mitochondria, Bax oligomerizes and induces the release of cytochrome c and the other apoptotic factors, which usually correlates with commitment of the cell to die.^{50,138}

However, the molecular mechanism by which tBid and Bim activate Bax and Bak remains elusive. It seems to be dependent on interactions with the BH3 domains of the direct activators, though difficulties in observing direct binding between them¹³⁹ have led to the proposal of a “kiss-and-run” hypothesis. In an elegant study, Andrews and coworkers have shed light on this process showing that it follows a set of ordered steps that culminate with membrane permeabilization.⁵⁴ Using a reconstituted in vitro system, they found that the presence of membranes was necessary for tBid to interact with Bax. The temporal analysis of their data suggested that tBid/Bax interactions occurred prior to Bax insertion into the lipid bilayer, which was then rapidly followed by Bax/Bax oligomerization. Then, once a threshold concentration of Bax was inserted into the bilayer, membrane permeabilization happened very quickly.

On the other hand, the homolog effector protein Bak is constitutively associated with the MOM under normal conditions. It has been proposed that it is constitutively inhibited through interactions with VDAC-2 and antiapoptotic Mcl-1 and Bcl-xL.¹⁴⁰ During apoptosis, Bak forms small complexes that correlate with cytochrome c release from mitochondria.^{47,49,138} It can also form oligomers with Bax during this process.^{138,141} However, due the difficulty of reconstituting Bak in vitro, much less is known about the molecular mechanism of Bak activation.

Inhibition by Antiapoptotic Bcl-2 Proteins

The antiapoptotic members of the family, which includes Bcl-2, Bcl-xL, Bcl-w, A1 and Mcl-1, inhibit apoptosis by blocking the activation of caspases. The first hypothesis to explain their mechanism of action was the “rheostat model”, in which the relative levels of pro- and antiapoptotic proteins determine the cell’s fate.^{142,143} This was supported by the observation that the over-expression of antiapoptotic Bcl-2 proteins promotes cell survival in tumor cells, while their genetic deletion results in an increase in apoptosis.^{144,145} Also supporting this vision, deletion of the pro-apoptotic members increases resistance to apoptosis.¹⁴⁶ However the “rheostat” model was insufficient to explain the complex regulation of MOM permeabilization by the Bcl-2 proteins. During the last years, alternative models have been proposed to describe this process, but still a lot of controversy remains (see below).

The antiapoptotic Bcl-2 proteins are believed to inhibit the proapoptotic members by direct complex formation. Available structures show that the hydrophobic cleft formed by the BH1, -2 and -3 domains of Bcl-xL can accommodate peptides corresponding to the BH3 regions of Bak, Bad and Bim.²⁴⁻²⁷ This suggests that the hydrophobic pocket is involved in the dimerization with other family members via their BH3 domain. Supporting this idea, BH3 peptides of proapoptotic Bcl-2 proteins have been shown to bind to antiapoptotic members with different affinities.¹⁴⁷ Also, mutations in the BH3 domain of tBid abrogate their interactions with multi-domain Bcl-2 proteins.^{54,106}

Interestingly, Bcl-xL, Bcl-w and Mcl-1 reside partially in the cytosol and translocate to the MOM during apoptosis.¹⁴⁸⁻¹⁵⁰ Once there, tBid has been shown to induce conformational changes in Bcl-2 that are associated with its extensive insertion into the membrane.¹⁰⁶ Although the physiological implications are not completely clear, these observations led to the idea that antiapoptotic Bcl-2 proteins could be “activated” for inhibition of apoptosis at the MOM in a similar way to Bax.¹⁵¹ This hypothesis is also based on the structural similarities between the multi-domain Bcl-2 proteins and on the fact that the both pro- and antiapoptotic members display pore-forming activity. Indeed, Bcl-xL has been shown to compete with soluble Bax for membrane binding induced by tBid.⁵⁴ Once in the membrane, Bcl-xL is able to interact with and inhibit both tBid and Bax. As a consequence, tBid is sequestered, Bax oligomerization is impaired and cytochrome c release is inhibited.

From these experiments, Bcl-xL was proposed to behave as a dominant-negative version of Bax.⁵⁴ This very interesting concept assumes that the antiapoptotic Bcl-2 proteins are incapable of forming high-order oligomers. As a result, they would form small pores after membrane insertion, yet being unable to produce the big membrane pores necessary for MOM permeabilization in apoptosis. In addition, Bcl-xL binding to Bax would result in small oligomerization-defective complexes, unproductive for cytochrome c release.

Bcl-2 Interaction Networks Regulate Apoptosis

As described above, the Bcl-2 proteins interact with other family members to induce or inhibit MOM permeabilization. A major controversy in the field is related to the nature of the interactions that are essential for the regulation of apoptosis. Which protein/protein interactions between family members control the outcome of whether MOM permeabilization is induced or not? For example, do BH3-only proteins induce apoptosis by activating Bax and Bak or by neutralizing the pro-survival members of the family?

In this context, the “indirect” or “neutralization” model considers that Bax and Bak are constitutively inhibited in cells via interactions with the antiapoptotic members.^{139,140,152} When the BH3-only proteins are activated, they bind to and neutralize the pro-survival proteins, leading to the liberation of Bax and Bak, which then induce MOM permeabilization. The main event in this model is the strong interaction between BH3-only proteins and the pro-survival ones. The observation that Bak is forming complexes with several antiapoptotic proteins in healthy cells supports this model.¹⁴⁰ Also, it has been shown that BH3 peptides from different BH3-only proteins exhibit different affinities for the antiapoptotic Bcl-2 proteins.^{147,153}

On the other hand, the “direct” activation model proposes that Bax and Bak need to be activated by direct activator BH3-only proteins to induce MOM permeabilization. Here the essential interaction would be between direct activators and effector proteins.⁶² This model is supported by Bax translocation to the MOM and by the conformational changes described for Bax and Bak during apoptosis.^{31,47,49} Also, only tBid and Bim have been shown to be able to induce membrane permeabilization by Bax in model membrane systems.¹⁵⁴ The sensitizer/derepressor BH3-only proteins would increase mitochondrial sensitivity to the direct activators, while the pro-survival proteins would then inhibit apoptosis by sequestering the direct activators.

The likely scenario is a combination of both situations, with prevalence of one or the other depending on cell type and metabolic state. This implies that commitment to cell death is regulated by a complex interaction network between Bcl-2 proteins that determines MOM permeabilization. Recent work by Chipuk et al reports on “direct activator/antiapoptotic/derepressor” network that controls MOM permeabilization in tumor cells.¹⁵⁵ They found that sensitizer/derepressor molecules cooperated with sequestered direct activators to induce MOM permeabilization. In such system, cancer cells were resistant to apoptosis because they contained high levels of anti-apoptotic proteins that blocked the direct activators. Apoptosis activation could then be achieved by sensitizer/derepressor molecules binding to the antiapoptotic proteins and releasing the direct activators, which in turn activate Bax and Bak.

However, these models pay no or little attention to the role of the lipid membrane in the regulation of MOM permeabilization. The recently proposed “embedded together” model takes this into account and is becoming widely accepted.¹⁵¹ This hypothesis assumes that the final regulation of MOM permeabilization takes place in the lipid membrane and is associated with an extensively inserted conformation of the Bcl-2 proteins. As a consequence, multiple parallel equilibria between the different Bcl-2 proteins happen in solution and within membranes. The relative strength of the interactions in both environments would then shift the equilibrium towards Bax and/or Bak oligomerization and MOM permeabilization, or towards the formation of unproductive complexes associated to maintenance of MOM integrity.⁵⁷

Conclusion

In summary, several questions still need to be addressed in order to fully understand how the Bcl-2 proteins regulate MOM permeabilization. It will be necessary to determine the nature of the pore responsible for the release of the apoptotic factors. Given the increasingly acknowledged importance of the membrane environment, the implication of mitochondrial lipids in the activity of Bcl-2 proteins will need deeper investigation. Also, the detailed structure of the membrane-inserted states of the Bcl-2 proteins is a major question in the field. Finally, it will be crucial to determine the interaction affinities between the Bcl-2 proteins in solution and within the membrane and to identify which of these interactions are key to control MOM permeabilization.

References

1. Danial NN. BCL-2 family proteins: critical checkpoints of apoptotic cell death. *Clin Cancer Res* 2007; 13:7254-7263.
2. Chipuk JE, Bouchier-Hayes L, Green DR. Mitochondrial outer membrane permeabilization during apoptosis: the innocent bystander scenario. *Cell Death Differ* 2006; 13:1396-1402.
3. Tsujimoto Y, Cossman J, Jaffe E et al. Involvement of the bcl-2 gene in human follicular lymphoma. *Science* 1985; 228:1440-1443.
4. Vaux DL, Cory S, Adams JM. Bcl-2 gene promotes haemopoietic cell survival and cooperates with c-myc to immortalize preB-cells. *Nature* 1988; 335:440-442.
5. Wei MC, Zong WX, Cheng EH et al. Proapoptotic BAX and BAK: a requisite gateway to mitochondrial dysfunction and death. *Science* 2001; 292:727-730.
6. Li P, Nijhawan D, Budihardjo I et al. Cytochrome c and dATP-dependent formation of Apaf-1/caspase-9 complex initiates an apoptotic protease cascade. *Cell* 1997; 91:479-489.
7. Youle RJ, Strasser A. The BCL-2 protein family: opposing activities that mediate cell death. *Nat Rev Mol Cell Biol* 2008; 9:47-59.
8. Johnson JE, Cornell RB. Amphitropic proteins: regulation by reversible membrane interactions (review). *Mol Membr Biol* 1999; 16:217-235.

9. Hockenbery D, Nuñez G, Millman C et al. Bcl-2 is an inner mitochondrial membrane protein that blocks programmed cell death. *Nature* 1990; 348:334-336.
10. Gross A, Yin XM, Wang K et al. Caspase cleaved BID targets mitochondria and is required for cytochrome c release, while BCL-XL prevents this release but not tumor necrosis factor-R1/Fas death. *J Biol Chem* 1999; 274:1156-1163.
11. Hsu YT, Wolter KG, Youle RJ. Cytosol-to-membrane redistribution of Bax and Bcl-X(L) during apoptosis. *Proc Natl Acad Sci USA* 1997; 94:3668-3672.
12. Wolter KG, Hsu YT, Smith CL et al. Movement of Bax from the cytosol to mitochondria during apoptosis. *J Cell Biol* 1997; 139:1281-1292.
13. Zha J, Weiler S, Oh KJ et al. Posttranslational N-myristoylation of BID as a molecular switch for targeting mitochondria and apoptosis. *Science* 2000; 290:1761-1765.
14. Chou JJ, Li H, Salvesen GS et al. Solution structure of BID, an intracellular amplifier of apoptotic signaling. *Cell* 1999; 96:615-624.
15. McDonnell JM, Fushman D, Millman CL et al. Solution structure of the proapoptotic molecule BID: a structural basis for apoptotic agonists and antagonists. *Cell* 1999; 96:625-634.
16. Muchmore SW, Sattler M, Liang H et al. X-ray and NMR structure of human Bcl-xL, an inhibitor of programmed cell death. *Nature* 1996; 381:335-341.
17. Suzuki M, Youle RJ, Tjandra N. Structure of Bax: coregulation of dimer formation and intracellular localization. *Cell* 2000; 103:645-654.
18. Day CL, Chen L, Richardson SJ et al. Solution structure of prosurvival Mcl-1 and characterization of its binding by proapoptotic BH3-only ligands. *J Biol Chem* 2005; 280:4738-4744.
19. Denisov AY, Madiraju MSR, Chen G et al. Solution structure of human BCL-w: modulation of ligand binding by the C-terminal helix. *J Biol Chem* 2003; 278:21124-21128.
20. Hinds MG, Lackmann M, Skea GL et al. The structure of Bcl-w reveals a role for the C-terminal residues in modulating biological activity. *EMBO J* 2003; 22:1497-1507.
21. Moldoveanu T, Liu Q, Tocilj A et al. The X-ray structure of a BAK homodimer reveals an inhibitory zinc binding site. *Mol Cell* 2006; 24:677-688.
22. Petros AM, Medek A, Nettlesheim DG et al. Solution structure of the antiapoptotic protein bcl-2. *Proceedings of the National Academy of Sciences of the United States of America* 2001; 98:3012-3017.
23. Petros AM, Olejniczak ET, Fesik SW. Structural biology of the Bcl-2 family of proteins. *Biochim Biophys Acta* 2004; 1644:83-94.
24. Lama D, Sankararamkrishnan R. Anti-apoptotic Bcl-XL protein in complex with BH3 peptides of pro-apoptotic Bak, Bad and Bim proteins: comparative molecular dynamics simulations. *Proteins* 2008; 73:492-514.
25. Petros AM, Nettlesheim DG, Wang Y et al. Rationale for Bcl-xL/Bad peptide complex formation from structure, mutagenesis and biophysical studies. *Protein Sci* 2000; 9:2528-2534.
26. Sattler M, Liang H, Nettlesheim D et al. Structure of Bcl-xL-Bak peptide complex: recognition between regulators of apoptosis. *Science* 1997; 275:983-986.
27. Herman MD, Nyman T, Welin M et al. Completing the family portrait of the anti-apoptotic Bcl-2 proteins: crystal structure of human Bfl-1 in complex with Bim. *FEBS Lett* 2008; 582:3590-3594.
28. Gavathiotis E, Suzuki M, Davis ML et al. BAX activation is initiated at a novel interaction site. *Nature* 2008; 455:1076-1081.
29. Hinds MG, Smits C, Fredericks-Short R et al. Bim, Bad and Bmf: intrinsically unstructured BH3-only proteins that undergo a localized conformational change upon binding to prosurvival Bcl-2 targets. *Cell Death Differ* 2007; 14:128-136.
30. Lazebnik Y. Why do regulators of apoptosis look like bacterial toxins? *Curr Biol* 2001; 11:R767-R768.
31. Desagher S, Osen-Sand A, Nichols A et al. Bid-induced conformational change of Bax is responsible for mitochondrial cytochrome c release during apoptosis. *J Cell Biol* 1999; 144:891-901.
32. Hsu YT, Youle RJ. Bax in murine thymus is a soluble monomeric protein that displays differential detergent-induced conformations. *J Biol Chem* 1998; 273:10777-10783.
33. Peyerl FW, Dai S, Murphy GA et al. Elucidation of some Bax conformational changes through crystallization of an antibody-peptide complex. *Cell Death Differ* 2007; 14:447-452.
34. Nechushtan A, Smith CL, Hsu YT et al. Conformation of the Bax C-terminus regulates subcellular location and cell death. *EMBO J* 1999; 18:2330-2341.
35. Garcia-Saez AJ, Mingarro I, Perez-Paya E et al. Membrane-insertion fragments of Bcl-xL, Bax and Bid. *Biochemistry* 2004; 43:10930-10943.
36. Annis MG, Soucie EL, Dlugosz PJ et al. Bax forms multispansing monomers that oligomerize to permeabilize membranes during apoptosis. *EMBO J* 2005; 24:2096-2103.
37. Cartron PF, Moreau C, Oliver L et al. Involvement of the N-terminus of Bax in its intracellular localization and function. *FEBS Lett* 2002; 512:95-100.

38. Nguyen M, Millar DG, Yong VW et al. Targeting of Bcl-2 to the mitochondrial outer membrane by a COOH-terminal signal anchor sequence. *J Biol Chem* 1993; 268:25265-25268.
39. Priault M, Camougrand N, Chaudhuri B et al. Role of the C-terminal domain of Bax and Bcl-XL in their localization and function in yeast cells. *FEBS Lett* 1999; 443:225-228.
40. Ausili A, Torrecillas A, Martínez-Senac MM et al. The interaction of the Bax C-terminal domain with negatively charged lipids modifies the secondary structure and changes its way of insertion into membranes. *J Struct Biol* 2008; 164:146-152.
41. Mar Martínez-Senac M, Corbalán-García S, Gómez-Fernández JC. Conformation of the C-terminal domain of the pro-apoptotic protein Bax and mutants and its interaction with membranes. *Biochemistry* 2001; 40:9983-9992.
42. Torrecillas A, Martínez-Senac MM, Ausili A et al. Interaction of the C-terminal domain of Bcl-2 family proteins with model membranes. *Biochim Biophys Acta* 2007; 1768:2931-2939.
43. Sani MA, Dufourc EJ, Gröbner G. How does the Bax-alpha1 targeting sequence interact with mitochondrial membranes? The role of cardiolipin. *Biochim Biophys Acta* 2009; 1788:623-631.
44. Qian S, Wang W, Yang L et al. Structure of transmembrane pore induced by Bax-derived peptide: evidence for lipidic pores. *Proc Natl Acad Sci USA* 2008; 105:17379-17383.
45. Garcia-Saez AJ, Coraiola M, Dalla SM et al. Peptides derived from apoptotic Bax and Bid reproduce the poration activity of the parent full-length proteins. *Biophys J* 2005; 88:3976-3990.
46. Eskes R, Desagher S, Antonsson B et al. Bid induces the oligomerization and insertion of Bax into the outer mitochondrial membrane. *Mol Cell Biol* 2000; 20:929-935.
47. Korsmeyer SJ, Wei MC, Saito M et al. Pro-apoptotic cascade activates BID, which oligomerizes BAK or BAX into pores that result in the release of cytochrome c. *Cell Death Differ* 2000; 7:1166-1173.
48. Ruffolo SC, Breckenridge DG, Nguyen M et al. BID-dependent and BID-independent pathways for BAX insertion into mitochondria. *Cell Death Differ* 2000; 7:1101-1108.
49. Wei MC, Lindsten T, Mootha VK et al. tBID, a membrane-targeted death ligand, oligomerizes BAK to release cytochrome c. *Genes Dev* 2000; 14:2060-2071.
50. Antonsson B, Montessuit S, Lauper S et al. Bax oligomerization is required for channel-forming activity in liposomes and to trigger cytochrome c release from mitochondria. *Biochem J* 2000; 345:271-278.
51. Pagliari LJ, Kuwana T, Bonzon C et al. The multidomain proapoptotic molecules Bax and Bak are directly activated by heat. *Proc Natl Acad Sci USA* 2005; 102:17975-17980.
52. Tan C, Dlugosz PJ, Peng J et al. Auto-activation of the apoptosis protein Bax increases mitochondrial membrane permeability and is inhibited by Bcl-2. *J Biol Chem* 2006; 281:14764-14775.
53. Antonsson B, Montessuit S, Sanchez B et al. Bax is present as a high molecular weight oligomer/complex in the mitochondrial membrane of apoptotic cells. *J Biol Chem* 2001; 276:11615-11623.
54. Billen LP, Kokoski CL, Lovell JF et al. Bcl-XL inhibits membrane permeabilization by competing with Bax. *PLoS Biol* 2008; 6(6):e147.
55. Gross A, Jockel J, Wei MC et al. Enforced dimerization of BAX results in its translocation, mitochondrial dysfunction and apoptosis. *EMBO J* 1998; 17:3878-3885.
56. Hardwick JM, Polster BM. Bax, along with lipid conspirators, allows cytochrome c to escape mitochondria. *Mol Cell* 2002; 10:963-965.
57. Lovell JF, Billen LP, Bindner S et al. Membrane binding by tBid initiates an ordered series of events culminating in membrane permeabilization by Bax. *Cell* 2008; 135:1074-1084.
58. Mikhailov V, Mikhailova M, Pulkrabek DJ et al. Bcl-2 prevents Bax oligomerization in the mitochondrial outer membrane. *J Biol Chem* 2001; 276:18361-18374.
59. Roucou X, Montessuit S, Antonsson B et al. Bax oligomerization in mitochondrial membranes requires tBid (caspase-8-cleaved Bid) and a mitochondrial protein. *Biochem J* 2002; 368:915-921.
60. Saito M, Korsmeyer SJ, Schlesinger PH. BAX-dependent transport of cytochrome c reconstituted in pure liposomes. *Nat Cell Biol* 2000; 2:553-555.
61. Valentijn AJ, Upton JP, Gilmore AP. Analysis of endogenous Bax complexes during apoptosis using blue native PAGE: implications for Bax activation and oligomerization. *Biochem J* 2008; 412:347-357.
62. Kuwana T, Mackey MR, Perkins G et al. Bid, Bax and lipids cooperate to form supramolecular openings in the outer mitochondrial membrane. *Cell* 2002; 111:331-342.
63. Lucken-Ardjomande S, Montessuit S, Martinou JC. Contributions to Bax insertion and oligomerization of lipids of the mitochondrial outer membrane. *Cell Death Differ* 2008; 15:929-937.
64. Lucken-Ardjomande S, Montessuit S, Martinou JC. Bax activation and stress-induced apoptosis delayed by the accumulation of cholesterol in mitochondrial membranes. *Cell Death Differ* 2008; 15:484-493.
65. Christenson E, Merlin S, Saito M et al. Cholesterol effects on BAX pore activation. *J Mol Biol* 2008; 381:1168-11683.
66. Giddings KS, Johnson AE, Tweten RK. Redefining cholesterol's role in the mechanism of the cholesterol-dependent cytolysins. *Proc Natl Acad Sci USA* 2003; 100:11315-11320.
67. Dlugosz PJ, Billen LP, Annis MG et al. Bcl-2 changes conformation to inhibit Bax oligomerization. *EMBO J* 2006; 25:2287-2296.

68. Kim PK, Annis MG, Dlugosz PJ et al. During apoptosis bcl-2 changes membrane topology at both the endoplasmic reticulum and mitochondria. *Mol Cell* 2004; 14:523-529.
69. Thuduppathy GR, Hill RB. Acid destabilization of the solution conformation of Bcl-xL does not drive its pH-dependent insertion into membranes. *Protein Sci* 2006; 15:248-257.
70. Thuduppathy GR, Craig JW, Kholodenko V et al. Evidence that membrane insertion of the cytosolic domain of Bcl-xL is governed by an electrostatic mechanism. *J Mol Biol* 2006; 359:1045-1058.
71. Losonczi JA, Olejniczak ET, Betz SF et al. NMR studies of the anti-apoptotic protein Bcl-xL in micelles. *Biochemistry* 2000; 39:11024-11033.
72. Jeong SY, Gaume B, Lee YJ et al. Bcl-x(L) sequesters its C-terminal membrane anchor in soluble, cytosolic homodimers. *EMBO J* 2004; 23:2146-2155.
73. O'Neill JW, Manion MK, Maguire B et al. BCL-XL dimerization by three-dimensional domain swapping. *J Mol Biol* 2006; 356:367-381.
74. Denisov AY, Sprules T, Fraser J et al. Heat-induced dimerization of BCL-xL through alpha-helix swapping. *Biochemistry* 2007; 46:734-740.
75. Feng Y, Lin Z, Shen X et al. Bcl-xL forms two distinct homodimers at non-ionic detergents: implications in the dimerization of Bcl-2 family proteins. *J Biochem* 2008; 143:243-252.
76. Zhang Z, Lapolla SM, Annis MG et al. Bcl-2 homodimerization involves two distinct binding surfaces, a topographic arrangement that provides an effective mechanism for Bcl-2 to capture activated Bax. *J Biol Chem* 2004; 279:43920-43928.
77. Choi SY, Gonzalez F, Jenkins GM et al. Cardiolipin deficiency releases cytochrome c from the inner mitochondrial membrane and accelerates stimuli-elicited apoptosis. *Cell Death Differ* 2007; 14:597-606.
78. Esposti MD, Cristea IM, Gaskell SJ et al. Proapoptotic Bid binds to monolysocardiolipin, a new molecular connection between mitochondrial membranes and cell death. *Cell Death Differ* 2003; 10:1300-1309.
79. Gonzalez F, Pariselli F, Dupaigne P et al. tBid interaction with cardiolipin primarily orchestrates mitochondrial dysfunctions and subsequently activates Bax and Bak. *Cell Death Differ* 2005; 12:614-626.
80. Gonzalez F, Bessoule JJ, Rocchiccioli F et al. Role of cardiolipin on tBid and tBid/Bax synergistic effects on yeast mitochondria. *Cell Death Differ* 2005; 12:659-667.
81. Lutter M, Fang M, Luo X et al. Cardiolipin provides specificity for targeting of tBid to mitochondria. *Nat Cell Biol* 2000; 2:754-761.
82. Gong XM, Choi J, Franzin CM et al. Conformation of membrane-associated proapoptotic tBid. *J Biol Chem* 2004; 279:28954-28960.
83. Oh KJ, Barbuto S, Meyer N et al. Conformational changes in BID, a pro-apoptotic BCL-2 family member, upon membrane binding. A site-directed spin labeling study. *J Biol Chem* 2005; 280:753-767.
84. Schendel SL, Montal M, Reed JC. Bcl-2 family proteins as ion-channels. *Cell Death Differ* 1998; 5:372-380.
85. Schlesinger PH, Gross A, Yin XM et al. Comparison of the ion channel characteristics of proapoptotic BAX and antiapoptotic BCL-2. *Proc Natl Acad Sci USA* 1997; 94:11357-11362.
86. Basanez G, Nechushtan A, Drozhinin O et al. Bax, but not Bcl-x(L), decreases the lifetime of planar phospholipid bilayer membranes at subnanomolar concentrations. *Proc Natl Acad Sci USA* 1999; 96:5492-5497.
87. Basanez G, Sharpe JC, Galanis J et al. Bax-type apoptotic proteins porate pure lipid bilayers through a mechanism sensitive to intrinsic monolayer curvature. *J Biol Chem* 2002; 277:49360-49365.
88. Epan RF, Martinou JC, Montessuit S et al. Transbilayer lipid diffusion promoted by Bax: implications for apoptosis. *Biochemistry* 2003; 42:14576-14582.
89. Garcia-Saez AJ, Coraiola M, Serra MD et al. Peptides corresponding to helices 5 and 6 of Bax can independently form large lipid pores. *Febs Journal* 2006; 273:971-981.
90. Terrones O, Antonsson B, Yamaguchi H et al. Lipidic pore formation by the concerted action of proapoptotic BAX and tBID. *Journal of Biological Chemistry* 2004; 279:30081-30091.
91. Schafer B, Quispe J, Choudhary V et al. Mitochondrial outer membrane proteins assist Bid in Bax-mediated lipidic pore formation. *Molecular Biology of the Cell* 2009; 20:2276-2285.
92. Jürgensmeier JM, Xie Z, Deveraux Q et al. Bax directly induces release of cytochrome c from isolated mitochondria. *Proc Natl Acad Sci USA* 1998; 95:4997-5002.
93. Zha H, Fisk HA, Yaffe MP et al. Structure-function comparisons of the proapoptotic protein Bax in yeast and mammalian cells. *Mol Cell Biol* 1996; 16:6494-6508.
94. Heimlich G, McKinnon AD, Bernardo K et al. Bax-induced cytochrome c release from mitochondria depends on alpha-helices-5 and -6. *Biochem J* 2004; 378:247-255.
95. Asoh S, Ohtsu T, Ohta S. The super anti-apoptotic factor Bcl-xFNK constructed by disturbing intramolecular polar interactions in rat Bcl-xL. *J Biol Chem* 2000; 275:37240-37245.
96. Matsuyama S, Schendel SL, Xie Z et al. Cytoprotection by Bcl-2 requires the pore-forming alpha5 and alpha6 helices. *J Biol Chem* 1998; 273:30995-31001.
97. Nouraini S, Six E, Matsuyama S et al. The putative pore-forming domain of Bax regulates mitochondrial localization and interaction with Bcl-X(L). *Mol Cell Biol* 2000; 20:1604-1615.

98. Epand RF, Martinou JC, Montessuit S et al. Direct evidence for membrane pore formation by the apoptotic protein Bax. *Biochem Biophys Res Commun* 2002; 298:744-749.
99. Sobko AA, Kotova EA, Antonenko YN et al. Effect of lipids with different spontaneous curvature on the channel activity of colicin E1: evidence in favor of a toroidal pore. *FEBS Lett* 2004; 576:205-210.
100. Sobko AA, Kotova EA, Antonenko YN et al. Lipid dependence of the channel properties of a colicin E1-lipid toroidal pore. *J Biol Chem* 2006; 281:14408-1446.
101. Lee MT, Hung WC, Chen FY et al. Mechanism and kinetics of pore formation in membranes by water-soluble amphipathic peptides. *Proc Natl Acad Sci USA* 2008; 105:5087-5092.
102. Huang HW. Free energies of molecular bound States in lipid bilayers: lethal concentrations of antimicrobial peptides. *Biophys J* 2009; 96:3263-3272.
103. Garcia-Saez AJ, Chiantia S, Salgado J et al. Pore formation by a Bax-derived peptide: Effect on the line tension of the membrane probed by AFM. *Biophys J* 2007; 93:103-112.
104. Minn AJ, Velez P, Schendel SL et al. Bcl-x(L) forms an ion channel in synthetic lipid membranes. *Nature* 1997; 385:353-357.
105. Thuduppathy GR, Terrones O, Craig JW et al. The N-terminal domain of Bcl-xL reversibly binds membranes in a pH-dependent manner. *Biochemistry* 2006; 45:14533-14542.
106. Peng J, Tan C, Roberts GJ et al. tBid elicits a conformational alteration in membrane-bound Bcl-2 such that it inhibits Bax pore formation. *J Biol Chem* 2006; 281:35802-35811.
107. Peng J, Lapolla SM, Zhang Z et al. The cytosolic domain of Bcl-2 forms small pores in model mitochondrial outer membrane after acidic pH-induced membrane association. *Sheng Wu Yi Xue Gong Cheng Xue Za Zhi* 2009; 26:130-137.
108. Basanez G, Zhang J, Chau BN et al. Pro-apoptotic cleavage products of Bcl-x(L) form cytochrome c-conducting pores in pure lipid membranes. *J Biol Chem* 2001; 276:31083-31091.
109. Cheng EH, Kirsch DG, Clem RJ et al. Conversion of Bcl-2 to a Bax-like death effector by caspases. *Science* 1997; 278:1966-1968.
110. Jonas EA, Hickman JA, Chachar M et al. Proapoptotic N-truncated BCL-xL protein activates endogenous mitochondrial channels in living synaptic terminals. *Proc Natl Acad Sci USA* 2004; 101:13590-13595.
111. Lin B, Kolluri SK, Lin F et al. Conversion of Bcl-2 from protector to killer by interaction with nuclear orphan receptor Nur77/TR3. *Cell* 2004; 116:527-540.
112. Wei MC, Lindsten T, Mootha VK et al. tBID, a membrane-targeted death ligand, oligomerizes BAK to release cytochrome c. *Genes Dev* 2000; 14:2060-2071.
113. Zong WX, Lindsten T, Ross AJ et al. BH3-only proteins that bind pro-survival Bcl-2 family members fail to induce apoptosis in the absence of Bax and Bak. *Genes Dev* 2001; 15:1481-1486.
114. Epand RF, Martinou JC, Fornallaz-Mulhauser M et al. The apoptotic protein tBid promotes leakage by altering membrane curvature. *J Biol Chem* 2002; 277:32632-32639.
115. Kudla G, Montessuit S, Eskes R et al. The destabilization of lipid membranes induced by the C-terminal fragment of caspase 8-cleaved bid is inhibited by the N-terminal fragment. *J Biol Chem* 2000; 275:22713-22718.
116. Schendel SL, Azimov R, Pawlowski K et al. Ion channel activity of the BH3 only Bcl-2 family member, BID. *J Biol Chem* 1999; 274:21932-21936.
117. Yan L, Miao Q, Sun Y et al. tBid forms a pore in the liposome membrane. *FEBS Lett* 2003; 555:545-550.
118. Epand RF, Martinou JC, Fornallaz-Mulhauser M et al. The apoptotic protein tBid promotes leakage by altering membrane curvature. *J Biol Chem* 2002; 277:32632-32639.
119. Esposti MD, Erler JT, Hickman JA et al. Bid, a widely expressed proapoptotic protein of the Bcl-2 family, displays lipid transfer activity. *Mol Cell Biol* 2001; 21:7268-7276.
120. Esposti MD. The roles of Bid. *Apoptosis* 2002; 7:433-440.
121. Grad JM, Zeng XR, Boise LH. Regulation of Bcl-xL: a little bit of this and a little bit of STAT. *Curr Opin Oncol* 2000; 12:543-549.
122. Gardai SJ, Hildeman DA, Frankel SK et al. Phosphorylation of Bax Ser184 by Akt regulates its activity and apoptosis in neutrophils. *J Biol Chem* 2004; 279:21085-21095.
123. Kim BJ, Ryu SW, Song BJ. JNK- and p38 kinase-mediated phosphorylation of Bax leads to its activation and mitochondrial translocation and to apoptosis of human hepatoma HepG2 cells. *J Biol Chem* 2006; 281:21256-21265.
124. Linseman DA, Butts BD, Precht TA et al. Glycogen synthase kinase-3beta phosphorylates Bax and promotes its mitochondrial localization during neuronal apoptosis. *J Neurosci* 2004; 24:9993-10002.
125. Zhong Q, Gao W, Du F et al. Mule/ARF-BP1, a BH3-only E3 ubiquitin ligase, catalyzes the polyubiquitination of Mcl-1 and regulates apoptosis. *Cell* 2005; 121:1085-1095.
126. Akiyama T, Bouillet P, Miyazaki T et al. Regulation of osteoclast apoptosis by ubiquitylation of proapoptotic BH3-only Bcl-2 family member Bim. *EMBO J* 2003; 22:6653-6664.

127. Tran SE, Meinander A, Eriksson JE. Instant decisions: transcription-independent control of death-receptor-mediated apoptosis. *Trends Biochem Sci* 2004; 29:601-608.
128. Oda E, Ohki R, Murasawa H et al. Noxa, a BH3-only member of the Bcl-2 family and candidate mediator of p53-induced apoptosis. *Science* 2000; 288:1053-1058.
129. Nakano K, Vousden KH. PUMA, a novel proapoptotic gene, is induced by p53. *Mol Cell* 2001; 7:683-694.
130. Dijkers PF, Medema RH, Lammers JW et al. Expression of the pro-apoptotic Bcl-2 family member Bim is regulated by the forkhead transcription factor FKHR-L1. *Curr Biol* 2000; 10:1201-1204.
131. Li H, Zhu H, Xu CJ et al. Cleavage of BID by caspase 8 mediates the mitochondrial damage in the Fas pathway of apoptosis. *Cell* 1998; 94:491-501.
132. Zha J, Harada H, Yang E et al. Serine phosphorylation of death agonist BAD in response to survival factor results in binding to 14-3-3 not BCL-X(L). *Cell* 1996; 87:619-628.
133. Ley R, Ewings KE, Hadfield K et al. Regulatory phosphorylation of Bim: sorting out the ERK from the JNK. *Cell Death Differ* 2005; 12:1008-10014.
134. Puthalakath H, Huang DC, O'Reilly LA et al. The proapoptotic activity of the Bcl-2 family member Bim is regulated by interaction with the dynein motor complex. *Mol Cell* 1999; 3:287-296.
135. Puthalakath H, Villunger A, O'Reilly LA et al. Bmf: a proapoptotic BH3-only protein regulated by interaction with the myosin V actin motor complex, activated by anoikis. *Science* 2001; 293:1829-1832.
136. Goping IS, Gross A, Lavoie JN et al. Regulated targeting of BAX to mitochondria. *J Cell Biol* 1998; 143:207-215.
137. Yethon JA, Epand RF, Leber B et al. Interaction with a membrane surface triggers a reversible conformational change in Bax normally associated with induction of apoptosis. *J Biol Chem* 2003; 278:48935-48941.
138. Mikhailov V, Mikhailova M, Degenhardt K et al. Association of Bax and Bak homo-oligomers in mitochondria. Bax requirement for Bak reorganization and cytochrome c release. *J Biol Chem* 2003; 278:5367-5376.
139. Willis SN, Fletcher JI, Kaufmann T et al. Apoptosis initiated when BH3 ligands engage multiple Bcl-2 homologs, not Bax or Bak. *Science* 2007; 315:856-859.
140. Willis SN, Chen L, Dewson G et al. Proapoptotic Bak is sequestered by Mcl-1 and Bcl-xL, but not Bcl-2, until displaced by BH3-only proteins. *Genes Dev* 2005; 19:1294-1305.
141. Zhou L, Chang DC. Dynamics and structure of the Bax-Bak complex responsible for releasing mitochondrial proteins during apoptosis. *J Cell Sci* 2008; 121:218621-96.
142. Oltvai ZN, Milliman CL, Korsmeyer SJ. Bcl-2 heterodimerizes in vivo with a conserved homolog, Bax, that accelerates programmed cell death. *Cell* 1993; 74:609-619.
143. Korsmeyer SJ, Shutter JR, Veis DJ et al. Bcl-2/Bax: a rheostat that regulates an anti-oxidant pathway and cell death. *Semin Cancer Biol* 1993; 4:327-332.
144. Veis DJ, Sorenson CM, Shutter JR et al. Bcl-2-deficient mice demonstrate fulminant lymphoid apoptosis, polycystic kidneys and hypopigmented hair. *Cell* 1993; 75:229-240.
145. Motoyama N, Wang F, Roth KA et al. Massive cell death of immature hematopoietic cells and neurons in Bcl-x-deficient mice. *Science* 1995; 267:1506-1510.
146. Shindler KS, Latham CB, Roth KA. Bax deficiency prevents the increased cell death of immature neurons in bcl-x-deficient mice. *J Neurosci* 1997; 17:3112-3119.
147. Chen L, Willis SN, Wei A et al. Differential targeting of prosurvival Bcl-2 proteins by their BH3-only ligands allows complementary apoptotic function. *Mol Cell* 2005; 17:393-403.
148. Nijhawan D, Fang M, Traer E et al. Elimination of Mcl-1 is required for the initiation of apoptosis following ultraviolet irradiation. *Genes Dev* 2003; 17:1475-1486.
149. Hausmann G, O'Reilly LA, van Driel R et al. Pro-apoptotic apoptosis protease-activating factor 1 (Apaf-1) has a cytoplasmic localization distinct from Bcl-2 or Bcl-x(L). *J Cell Biol* 2000; 149:623-634.
150. Wilson-Annan J, O'Reilly LA, Crawford SA et al. Proapoptotic BH3-only proteins trigger membrane integration of prosurvival Bcl-w and neutralize its activity. *J Cell Biol* 2003; 162:877-887.
151. Leber B, Lin J, Andrews DW. Embedded together: the life and death consequences of interaction of the Bcl-2 family with membranes. *Apoptosis* 2007; 12:897-911.
152. Leu JI, Dumont P, Hafey M et al. Mitochondrial p53 activates Bak and causes disruption of a Bak-Mcl1 complex. *Nat Cell Biol* 2004; 6:443-450.
153. Kuwana T, Bouchier-Hayes L, Chipuk JE et al. BH3 domains of BH3-only proteins differentially regulate Bax-mediated mitochondrial membrane permeabilization both directly and indirectly. *Mol Cell* 2005; 17:525-535.
154. Terrones O, Etxebarria A, Landajuela A et al. BIM and tBID are not mechanically equivalent when assisting BAX to permeabilize bilayer membranes. *J Biol Chem* 2008; 283:7790-7803.
155. Chipuk JE, Fisher JC, Dillon CP et al. Mechanism of apoptosis induction by inhibition of the anti-apoptotic BCL-2 proteins. *Proc Natl Acad Sci USA* 2008; 105:20327-20332.
156. Jaysinghe S, Hristova K, Wimley W et al. <http://blanco.biomol.uci.edu/mpex>. 2008.

CHAPTER 9

Molecular Mechanism of Sphingomyelin-Specific Membrane Binding and Pore Formation by Actinoporins

Biserka Bakrač and Gregor Anderluh*

Abstract

Actinoporins are potent pore-forming toxins produced by sea anemones. They readily form pores in membranes that contain sphingomyelin. Molecular mechanism of pore formation involves recognition of membrane sphingomyelin, firm binding to the membrane accompanied by the transfer of the N-terminal region to the lipid-water interface and oligomerization of three to four monomers with accompanying pore formation. Actinoporins are an important example of α -helical pore forming toxins, since the final conductive pathway is formed by amphipathic α -helices. Recent structural data indicates that actinoporins are not restricted to sea anemones, but are present also in other organisms. They are becoming an important tool and model system, due to their potency, specificity and similarity to other proteins.

Introduction

Actinoporins are pore-forming toxins from sea anemones. It is believed that these toxins are used by sea anemones for preying and defence, but their biological role is not yet completely understood.¹⁻³ They are soluble in water at high concentration, but are able to undergo a conformational change, which allows tight membrane binding and creation of transmembrane pores. These events are dependent on the presence of the membrane lipid sphingomyelin and are enhanced in the presence of lipid domains.⁴⁻⁶ Their activity is, therefore, tightly regulated and directed mostly to animal cells. Many actinoporin-like proteins have been found in different organisms by sequence^{7,8} or structure comparisons.^{9,10} Of particular interest is a family of fungal lectins, which shares similar structure and ligand-binding site.^{9,11,12} Due to these properties actinoporins have become an important model system and have recently attracted a considerable attention. In this review we will summarise the current knowledge of their molecular mechanism of action and discuss how it relates to other similar proteins. The interested reader may find additional information in other reviews of actinoporins, their properties, biological roles, mechanism of action and their use in biotechnological and biomedical applications.^{1,3,13-16}

*Corresponding Author: Gregor Anderluh—Department of Biology, Biotechnical Faculty, University of Ljubljana, Večna pot 111, 1000 Ljubljana, Slovenia.
Email: gregor.anderluh@bf.uni-lj.si

Structural Properties of Actinoporins

A hallmark of actinoporins (Pfam code PF06369) is that they are an extremely conserved protein family. The most distant members still share more than 60% of identical residues.⁵ Majority of the information about their structure and mechanism of action derives from the studies of equinatoxin II (EqII) and sticholysins I (StI) and II (StII) from the sea anemones *Actinia equina* and *Stichodactyla helianthus*, respectively. They are 20 kDa proteins and possess no cysteines. The functional parts that enable formation of pores are largely conserved in the family and most of the members are highly basic proteins with pI above 9,¹ although one acidic actinoporin was also described.¹⁷

Actinoporins are single-domain proteins composed of a tightly folded 12 strand β -sandwich flanked on two sides by α -helices (Fig. 1).¹⁸⁻²⁰ The C-terminal α -helix is attached at both ends to the β -sandwich, whereas N-terminal α -helix is attached only at its C-terminal end. The helical wheel analysis of the N-terminal region, from residues 10 to 30, encompassing the N-terminal helix, revealed it to be amphipathic and that it showed weak sequence similarity to melittin, a 26-residue peptide from the honey-bee venom.^{21,22} This region is the only part of the molecule that can detach from the core without disrupting the general fold of the protein and the flexibility of the N-terminal region was shown to be crucial for the formation of pores (see below).

Another interesting feature of actinoporin structure is a cluster of exposed aromatic amino acids residues at the bottom of the molecule, which were shown to provide the initial contact of the protein with the membrane.^{5,23-25} Co-crystallisation of StII with phosphocholine (POC), a headgroup of lipids phosphatidylcholine and sphingomyelin, enabled the definition of the POC binding site,²⁰ which was later shown to be crucial for the specific recognition of sphingomyelin.⁵ Residues involved in POC binding (StII numbering; Ser-52, Val-85, Ser-103, Pro-105, Tyr-111, Tyr-131, Tyr-135 and Tyr-136) are strictly conserved in actinoporins and imply that the same mechanism of lipid headgroup recognition is followed by other members of the family.⁵

Actinoporins Specifically Bind Sphingomyelin as the First Step in Pore Formation

Pore forming toxins form transmembrane pores in several discrete steps^{26,27} and actinoporins are no exception to this general rule (Fig. 1). Available functional and structural data imply that this process involves binding to the lipid membrane by specifically recognising sphingomyelin, transfer of the N-terminal region to the lipid-water interface and oligomerization of three to four monomers that finally leads to pore formation (Fig. 1).^{22,24,28}

The membrane lytic activity of actinoporins is highly sphingomyelin dependent (reviewed in Anderluh and Maček¹). It was proposed that sphingomyelin has a major role in the binding,²⁹ which was later supported by a definition of a POC binding site on the surface of StII²⁰ and recent description of sphingomyelin recognition by EqII.⁵ The initial attachment to the membrane is achieved by the aromatic amino acid cluster, which includes five tyrosines and two tryptophans and POC binding site (Figs. 2 and 3). Mutations of the most important residues from the aromatic cluster, Trp-112 and Trp-116 and of the residues that form POC binding site abolished binding and consequently pore formation (Fig. 2).^{23-25,28,30} Combination of POC binding site and exposed tryptophan at position 112 enable specific binding of sphingomyelin, but not other lipids, as shown recently by Bakrač et al.⁵ Dot-blot assays showed that EqII binds to sphingomyelin in a concentration-dependent manner (Fig. 2) and does not bind to any other lipid tested, i.e., cholesterol, phosphatidylcholine, ceramide, monosialoganglioside GM1, etc. Surface plasmon resonance analysis of chip-immobilized EqII additionally showed that it is not able to bind a water soluble phosphatidylcholine analogue, but it bound a comparable sphingomyelin analogue. Actinoporins must specifically recognize regions below the choline headgroup, which itself is common to both phosphatidylcholine and sphingomyelin. Residues Trp-112 and Tyr-113, both located on a broad exposed loop at the bottom of the molecule, are the closest residues to the binding site and are within hydrogen bonding distance of the distinctive hydroxyl and amido groups of the sphingomyelin backbone (Fig. 3). All other amino acids are too distant to directly participate in sphingomyelin

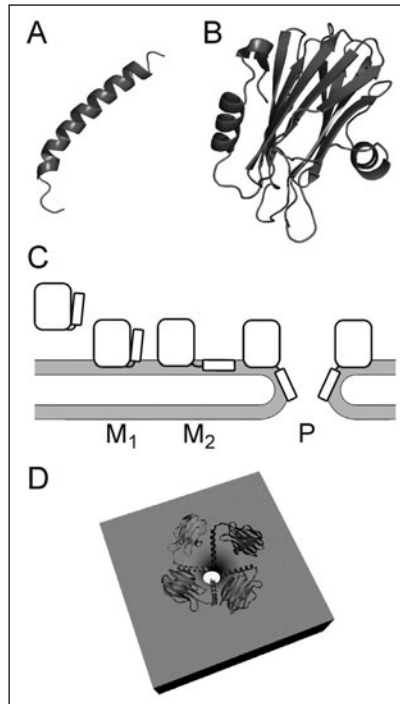


Figure 1. Structural properties of actinoporins and the mechanism of pore formation. A) The NMR structure of the first 32 amino acids of EqII in the presence of the dodecylphosphocholine micelles.³⁷ B) The crystal structure of EqII (PDB code 1IAZ). C) The current model of actinoporin pore formation. It is a multistep process that involves the binding of the soluble monomer to the membrane by a cluster of aromatic amino acids and POC-binding site (M1), translocation of the N-terminal segment to the lipid-water interface (M2) and oligomerization and formation of the final transmembrane pore (P). Adapted from Malovrh et al.²² D) Final transmembrane pore as viewed from the above. It is composed of four monomers, of which each contributes one helix, and membrane lipids.

recognition. Functional analysis of mutants with changes at these two positions confirmed this hypothesis and showed that Trp-112 and Tyr-113 are crucial for the binding and recognition of a single sphingomyelin molecule (Fig. 3).⁵

This mechanism of sphingomyelin recognition puts some previously published data on actinoporins in a clearer structural context. The importance of tyrosyl side chains for the toxin function was shown by Turk et al.,³¹ where chemical modification of three tyrosines in EqII almost completely abolished hemolytic activity. Further, by introducing ¹⁹F label on EqII tryptophans, it was recently shown by NMR that Trp-112 is important for sphingomyelin recognition, as it exhibited changes in NMR chemical shift upon addition of sphingomyelin to phosphatidylcholine micelles.³² Finally, sea anemones are protected against the action of actinoporins by the absence of sphingomyelin in their membranes. Instead, they possess phosphosphingolipids that have an altered phosphorylcholine headgroup.³³

Some recent publications, however, show that addition of cholesterol to phosphatidylcholine liposomes enhance activity of actinoporins, by modulating physical properties of the membrane or by inducing membrane microdomains.^{4,34,35} Recently, giant unilamellar vesicles (GUVs) have been used to investigate the role of sphingomyelin for the binding of EqII and shown that it bound preferentially to the sphingomyelin enriched liquid ordered phase than to the liquid disordered

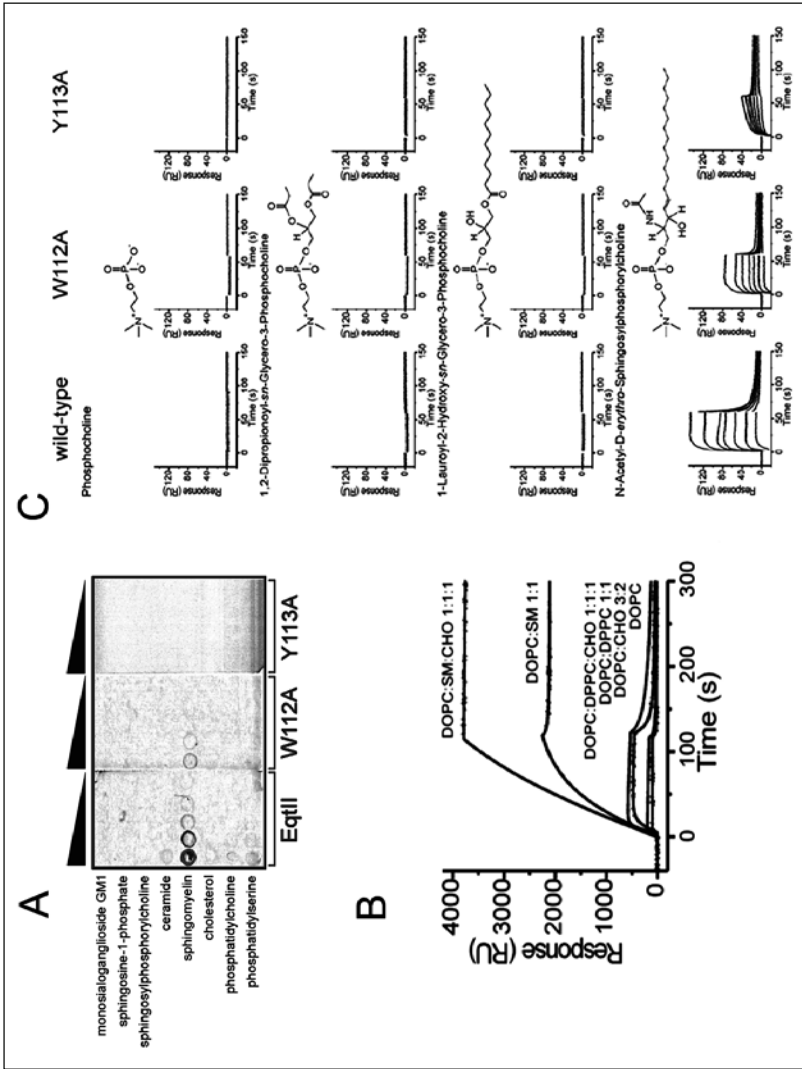


Figure 2. EqtII is a sphingomyelin-binding protein. A) Dot-blot lipid binding assay with a series of most common membrane lipids. The first spot contains 100 pmol of lipid and then two-fold serial dilutions are followed. B) Surface plasmon resonance analysis of EqtII binding to liposomes of different composition as indicated. C) Surface plasmon resonance analysis of lipid analogues binding to the wild-type EqtII or its mutants.⁵

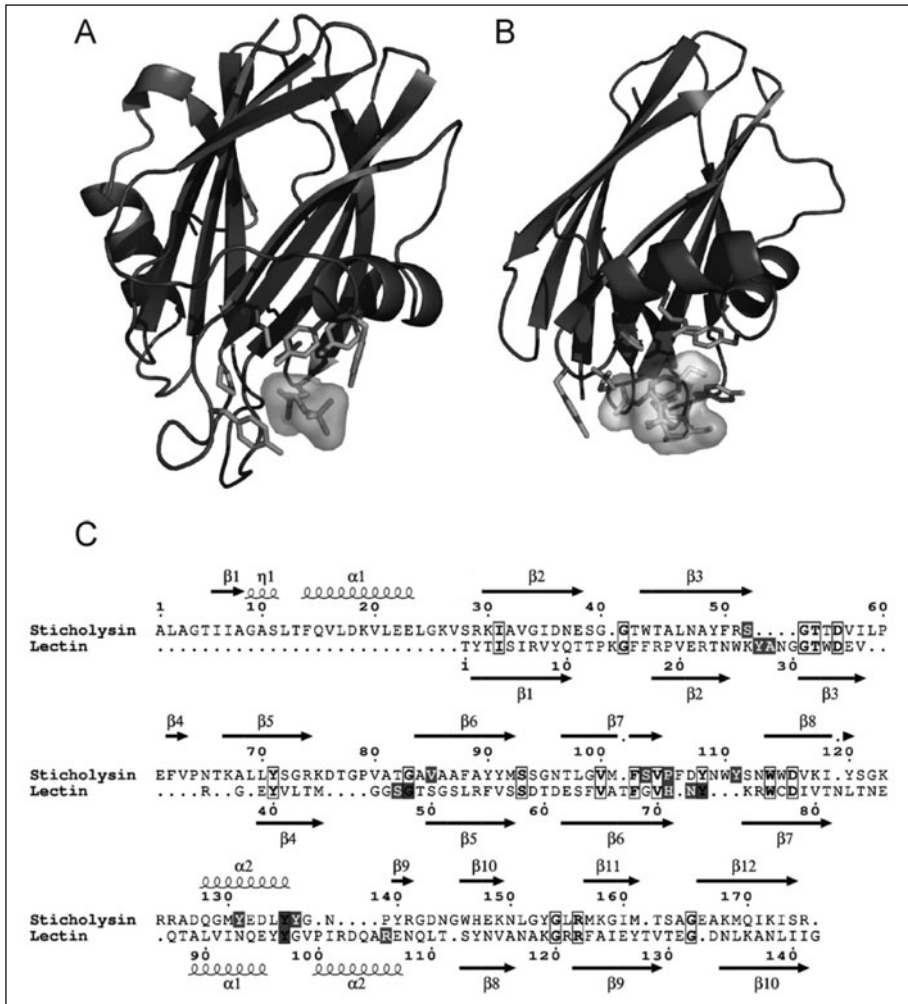


Figure 3. The similarity between actinoporins and fungal lectins. (A) Structure of actinoporin StII (PDB: 1O72).²⁰ (B) A fungal lectin from *Agaricus bisporus* (PDB:1Y2V).¹¹ The amino acids that participate in binding of cognate ligand in both proteins are shown with side chains (actinoporins bind phosphocholine and the fungal lectin binds the disaccharide Gal β 1-3GalNAc). Both ligands are shown with sticks and surface representation. (C) An alignment based on the structural elements. Amino acids that enable binding of ligands are shown shaded. Amino acids that are shared between both proteins are boxed. The secondary structures of StII and lectin are shown above and below the alignment, respectively. α -helices are shown as coils and β -strands are shown as arrows. Adapted from: Anderluh G, Lakey JH, Trends Biochem Sci 2008; 33:482-490,⁵⁶ with permission from Elsevier.

phase.⁶ The presence of sphingomyelin strongly promoted membrane binding, but EqII was able to permeabilize sphingomyelin-containing GUVs only when both phases coexisted. There was no permeabilization when sphingomyelin was only in membranes of only one phase. So, sphingomyelin can also indirectly modulate the activity of actinoporins, by affecting the physical properties of lipid membranes.⁶

Flexibility of the N-Terminal Region Is Required for Pore Formation

In the next step of pore formation the N-terminal segment translocates to the lipid-water interface^{22,24,36} and flexibility of this region is mandatory for the permeabilising activity. The transfer of this segment to the membrane was monitored by double cysteine mutants, where cysteines were introduced at such positions to allow formation of intramolecular disulphide bond and consequently restrict movement of this region.^{24,28} Mutants within the N-terminal region were completely inactive, but were still able to bind to membranes, since the membrane binding site was not affected. The placement of the N-terminal region in a more hydrophobic membrane milieu was further confirmed by cysteine scanning mutagenesis.²² Single cysteine mutagenesis of the N-terminal region from Asp-10 to Asn-28 has shown that the whole region is transferred to the lipid-water interface during pore formation and that it is in an α -helical conformation, which implies that the lipid environment induces additional folding of this segment and prolongs the α -helix, which extends from Ser15 to Leu26 in solution.^{18,19} The NMR structure of the peptide, corresponding to the first 32 residues of EqtII, has shown that it lacks ordered secondary structure in water. However, residues 6-28 form a helix in dodecylphosphocholine micelles, thus clearly showing propensity of this part to spontaneously fold when in membranes.³⁷ Finally, the interaction of the N-terminal helix with the membranes was confirmed by introducing tryptophan residues at various positions along this region.³⁶ This approach allowed measurements of changes in intrinsic tryptophan fluorescence upon membrane interactions and was particularly instructive, since an intermediate in the pore formation was revealed.³⁶ A mutant which possesses tryptophan instead of valine at position 22 had reduced haemolytic and permeabilizing activities, while lipid monolayer insertion was not different to the wild-type protein or other mutants studied. Decreased rates of hemolysis and permeabilization activity arise from the inability to insert the α -helix in the perpendicular orientation that would give rise to the oligomeric pores in membrane bilayers. So this mutant is locked in a membrane-bound topology, where the α -helix lies parallel to the plane of the membrane in a nonlytic state.

Of particular interest for the understanding of actinoporin function is the fact that the peptides that correspond to the actinoporin N-terminal region do not exhibit the same hemolytic or permeabilizing activity as the intact molecule.^{37,38} They showed some residual activity, mostly to negatively charged liposomes, but they lacked the selectivity for sphingomyelin containing membranes.^{37,38} Hence, the actinoporin β -sandwich has an important role in the mechanism of pore formation, by enabling sphingomyelin-specific binding and stability of the final pore, where it probably helps to stabilize slightly tilted helices,²⁰ as discussed below.

Pore Formation Involves Nonlamellar Lipid Structures

In the final step of pore formation toxin monomers bound to the membrane oligomerize and the N-terminal helical part is inserted deeply across the membrane to form the ion-conductive pathway. The secondary structure of the actinoporins does not change much after the binding to the lipid membranes and formation of pores, according to circular dichroism (CD)^{39,40} and Fourier-transform infra red (FTIR) spectroscopy.^{41,42} This was inferred also from the electron microscopy images of 2D crystals of StII.²⁰ The reconstructions enabled to provide the model of pore formed by four molecules of StII, with minimal adjustments of the β -sandwich, which sits on the membrane, while α -helices are slightly tilted with respect to the membrane normal.²⁰ Such arrangement of helices was already proposed by FTIR spectroscopy⁴¹ and later confirmed by cysteine scanning mutagenesis.²² It was recently proposed that the N-terminal part extends to the trans side of the membrane in the final pore, i.e., to the side opposite to the rest of the membrane-bound protein.⁴³ The terminal five amino acids were proposed to act as an anchor, similar to the mechanism recently described for aerolysin, where it was proposed that loops of the β -barrel stabilize it in the membrane in a rivet-like fashion.⁴⁴

Pores formed by actinoporins are 2 nm in diameter⁴⁵⁻⁴⁷ and, hence, cannot be simply formed by four helices. Either other parts of the molecule contribute to the final oligomeric conductive pore, or the pore is composed partially of lipid molecules from the bilayer (Fig. 1). The first possibility

requires considerable unfolding of the β -sandwich and its rearrangements in such a way that remaining space between helices is filled with the polypeptide chain. A disulfide scanning mutagenesis was employed to show that apart from the N-terminal segment there are no other parts, specifically β -sandwich and the C-terminal α -helix, that undergo gross conformational changes.²⁸ These results support a model where the final pore is formed by α -helices and bilayer lipids, as no other part of EqtII inserts sufficiently deeply into the membrane to fill the remaining gaps between the helices.^{48,49} Such, protein-lipid, so called, toroidal pores were also proposed for smaller pore-forming peptides such as melittin⁵⁰ or larger proteins such as apoptotic Bax proteins.^{51,52}

Some experimental evidence is consistent with the toroidal pore model and lipid involvement in pore formation of actinoporins. StI and StII were able to induce lipid flip-flop between internal and external leaflets of liposome membranes and inclusion of small proportions of phosphatidic acid, a strong inducer of negative membrane curvature, markedly increase the release of fluorescent markers from liposomes.⁴⁸ Negatively charged lipids were able to increase the cationic selectivity of the EqtII pore, thus supporting the proposition that lipids are part of the pore lumen.⁴⁹ Finally, an isotropic peak was observed in ³¹P NMR, which was interpreted to occur from lipid disordering.⁴⁹ The reorientation of lipid acyl chains was also observed by FTIR.^{41,42} In conclusion, it is clear that the actinoporin pore formation is unique and distinctively different from other pore forming toxins. They are a good model of how membranes may be damaged by α -helices.

Similarity to Other Proteins

For many years it was believed that actinoporins is isolated family of pore-forming toxins present only in sea anemones. However, first a haemolytic toxin, echotoxin 2, from the salivary gland of the marine gastropod *Monoplex echo* was described and found to be homologous to actinoporins.⁷ Recently, a detailed search of public databases with EqtII sequence as a probe yielded a number of sequences similar to actinoporins.⁸ They were from three animal (chordates, cnidarians and molluscs) and two plant (mosses and ferns) phyla. However, the majority of the sequences were from teleost fishes. The similarity to EqtII is confined to the C-terminal region from residue 83 to residue 179, which is roughly half of the β -sandwich and comprises membrane binding site with a highly conserved P-[WYF]-D pattern, located on the broad loop at the bottom of the molecule. Such conservation of a membrane-binding region suggested that these homologues should be membrane-binding proteins. To test this hypothesis, a homologue from zebrafish was cloned, expressed in *E. coli* and purified. It displayed membrane-binding behaviour, but did not have permeabilising activity or sphingomyelin specificity.⁸

Novel homologues of actinoporins were found in recent years also by structural analysis.⁹⁻¹² A novel family of fungal lectins revealed a remarkable similarity to actinoporins despite having less than 15% sequence identity.^{9,11,12} The structural similarity is confined to the β -sandwich and the most important difference in the structures of both groups is that fungal lectins lack the N-terminal amphipathic region of actinoporins (Fig. 3). The lectins from *Xerocomus chrysenteron* (XCL) and *Agaricus bisporus* (ABL) have antiproliferative properties^{53,54} and they both selectively and with high affinity bind the Thomsen-Friedenreich antigen (TF antigen),¹¹ a disaccharide (Gal β 1-3GalNAc) expressed by about 90% of all human carcinomas.⁵⁵ The binding site for TF-antigen in ABL corresponds to the POC-binding site in actinoporins, the residues used for the binding are located on equivalent sites to the actinoporin residues used for the binding of the phosphocholine headgroup of sphingomyelin (Fig. 3).⁵⁶

Just recently a novel actinoporin-like protein family was described at the structural level.¹⁰ Many bacterial, fungal and oomycete species produce necrosis and ethylene-inducing peptide 1 (Nep1)-like proteins (NLPs) that trigger leaf necrosis and immunity associated responses in various plants. The crystal structure of a Nep1-like protein from phytopathogenic oomycete *Pythium aphanidermatum* was determined and showed to possess a fold that exhibits structural similarities to actinoporins. All of these examples indicate that actinoporins fold is widespread and used by many different protein families primarily for the specific binding to various molecules of the plasma membrane.

Conclusion

The lipid cell membrane is the first obstacle that needs to be overcome and the creation of transmembrane pores is a very efficient way of killing cells, so pore forming toxins are a very important group of natural toxins.^{27,56} In recent years they have been used to study fundamental biological processes such as protein-membrane and protein-protein interactions within the lipid bilayer milieu, as well as conformational changes associated with the change of environment from polar to hydrophobic, as encountered within the core of lipid membranes. While β -PFTs, e.g., *Staphylococcus aureus* α -toxin or cholesterol dependent cytolysins,^{27,57} form structurally stable transmembrane pores, those formed by α -PFTs are not stable. Consequently, there is less structural information available. Final functional pore of EqtII have still not been visualized. It needs to be unambiguously determined what is number of monomers in the final pore and what the interactions between the monomers in the final pore are.

Due to their properties, there may be many opportunities to use actinoporins in biotechnological and biomedical applications. They were used for selective killing of parasites⁵⁸ or cancer cells.⁵⁹ Recently, EqtII was used to selectively permeabilise red blood cells in order to efficiently deliver antibodies for efficient staining of parasites in malaria research.⁶⁰ Due to its sphingomyelin-binding capacity, EqtII could be a useful probe to detect and study the distribution of sphingomyelin within the cells. Most cellular sphingomyelin resides in the outer leaflet of the plasma membrane, but is synthesized de novo by a sphingomyelin synthase I in the Golgi complex.⁶¹ Sphingomyelin has an important role in the lipid membrane, by being a main constituent of so-called lipid-rafts, microdomains enriched with cholesterol and sphingomyelin.⁶² But sphingomyelin also serves as a reservoir for lipid signalling molecules, i.e., ceramide, sphingosine and sphingosine 1-phosphate.⁶³ They are critical regulators of cell proliferation, differentiation and apoptosis. All these facts indicate the importance of sphingomyelin, hence a probe to detect and study its distribution and synthesis at the cellular level is crucially needed.

References

1. Anderluh G, Maček P. Cytolytic peptide and protein toxins from sea anemones (Anthozoa: Actiniaria). *Toxicon* 2002; 40:111-124.
2. Basulto A, Perez VM, Noa Y et al. Immunohistochemical targeting of sea anemone cytolysins on tentacles, mesenteric filaments and isolated nematocysts of *Stichodactyla helianthus*. *J Exp Zool A Comp Exp Biol* 2006; 305:253-258.
3. Alegre-Cebollada J, Oñaderra M, Gavilanes JG et al. Sea anemone actinoporins: the transition from a folded soluble state to a functionally active membrane-bound oligomeric pore. *Curr Protein Pept Sci* 2007; 8:558-572.
4. Barlič A, Gutiérrez-Aguirre I, Caaveiro JM et al. Lipid phase coexistence favors membrane insertion of equinatoxin-II, a pore-forming toxin from *Actinia equina*. *J Biol Chem* 2004; 279:34209-34216.
5. Bakrač B, Gutiérrez-Aguirre I, Podlesek Z et al. Molecular determinants of sphingomyelin specificity of a eukaryotic pore-forming toxin. *J Biol Chem* 2008; 283:18665-18677.
6. Schon P, Garcia-Saez AJ, Malovrh P et al. Equinatoxin II permeabilizing activity depends on the presence of sphingomyelin and lipid phase coexistence. *Biophys J* 2008; 95:691-698.
7. Kawashima Y, Nagai H, Ishida M et al. Primary structure of echotoxin 2, an actinoporin-like hemolytic toxin from the salivary gland of the marine gastropod *Monoplex echo*. *Toxicon* 2003; 42:491-497.
8. Gutiérrez-Aguirre I, Trontelj P, Maček P et al. Membrane binding of zebrafish actinoporin-like protein: AF domains, a novel superfamily of cell membrane binding domains. *Biochem J* 2006; 398:381-392.
9. Bircak C, Damian L, Marty-Detraves C et al. A new lectin family with structure similarity to actinoporins revealed by the crystal structure of *Xerocomus chrysenteron* lectin XCL. *J Mol Biol* 2004; 344:1409-1420.
10. Ottman C, Luberacki B, Kufner I et al. A common toxin fold mediates microbial attack and plant defense. *Proc Natl Acad Sci USA* 2009; 106:10359-10364.
11. Carrizo ME, Capaldi S, Perduca M et al. The antineoplastic lectin of the common edible mushroom (*Agaricus bisporus*) has two binding sites, each specific for a different configuration at a single epimeric hydroxyl. *J Biol Chem* 2005; 280:10614-10623.
12. Leonidas DD, Swamy BM, Hatzopoulos GN et al. Structural basis for the carbohydrate recognition of the *Sclerotium rolfsii* lectin. *J Mol Biol* 2007; 368:1145-1161.
13. Anderluh G, Maček P. Dissecting the actinoporin pore-forming mechanism. *Structure* 2003; 11:1312-1313.

14. Črnigoj Kristan K, Viero G, Dalla Serra M et al. Molecular mechanism of pore formation by actinoporins. *Toxicon* 2009; 54:1125-1134.
15. Alvarez C, Mancheño JM, Martínez D et al. Sticholysins, two pore-forming toxins produced by the Caribbean Sea anemone *Stichodactyla helianthus*: Their interaction with membranes. *Toxicon* 2009; 54:1135-1147.
16. Tejuca M, Anderlüh G, Dalla Serra M. Sea anemone cytolytins as toxic components of immunotoxins. *Toxicon* 2009; 54:1206-1214.
17. Jiang XY, Yang WL, Chen HP et al. Cloning and characterization of an acidic cytolytin cDNA from sea anemone *Sagartia rosea*. *Toxicon* 2002; 40:1563-1569.
18. Athanasiadis A, Anderlüh G, Maček P et al. Crystal structure of the soluble form of equinatoxin II, a pore-forming toxin from the sea anemone *Actinia equina*. *Structure* 2001; 9:341-346.
19. Hinds MG, Zhang W, Anderlüh G et al. Solution structure of the eukaryotic pore-forming cytolytin equinatoxin II: implications for pore formation. *J Mol Biol* 2002; 315:1219-1229.
20. Mancheño JM, Martín-Benito J, Martínez-Ripoll M et al. Crystal and electron microscopy structures of sticholysin II actinoporin reveal insights into the mechanism of membrane pore formation. *Structure* 2003; 11:1319-1328.
21. Belmonte G, Menestrina G, Pederzoli C et al. Primary and secondary structure of a pore-forming toxin from the sea anemone, *Actinia equina* L. and its association with lipid vesicles. *Biochim Biophys Acta* 1994; 1192:197-204.
22. Malovrh P, Viero G, Dalla Serra M et al. A novel mechanism of pore formation: membrane penetration by the N-terminal amphipathic region of equinatoxin. *J Biol Chem* 2003; 278:22678-22685.
23. Malovrh P, Barlič A, Podlesek Z et al. Structure-function studies of tryptophan mutants of equinatoxin II, a sea anemone pore-forming protein. *Biochem J* 2000; 346:223-232.
24. Hong Q, Gutiérrez-Aguirre I, Barlič A et al. Two-step membrane binding by Equinatoxin II, a pore-forming toxin from the sea anemone, involves an exposed aromatic cluster and a flexible helix. *J Biol Chem* 2002; 277:41916-41924.
25. Alegre-Cebollada J, Cunietti M, Herrero-Galan E et al. Calorimetric scrutiny of lipid binding by sticholysin II toxin mutants. *J Mol Biol* 2008; 382:920-930.
26. Gouaux E. Channel-forming toxins: tales of transformation. *Curr Opin Struct Biol* 1997; 7:566-573.
27. Parker MW, Feil SC. Pore-forming protein toxins: from structure to function. *Prog Biophys Mol Biol* 2005; 88:91-142.
28. Kristan K, Podlesek Z, Hojnik V et al. Pore formation by equinatoxin, a eukaryotic pore-forming toxin, requires a flexible N-terminal region and a stable beta-sandwich. *J Biol Chem* 2004; 279:46509-46517.
29. Bernheimer AW, Avigad LS. Properties of a toxin from the sea anemone *Stoichacis helianthus*, including specific binding to sphingomyelin. *Proc Natl Acad Sci USA* 1976; 73:467-471.
30. Alegre-Cebollada J, Lacadena V, Oñaderra M et al. Phenotypic selection and characterization of randomly produced nonhaemolytic mutants of the toxic sea anemone protein sticholysin II. *FEBS Lett* 2004; 575:14-18.
31. Turk T, Maček P, Gubenšek F. Chemical modification of equinatoxin II, a lethal and cytolytic toxin from the sea anemone *Actinia equina* L. *Toxicon* 1989; 27:375-384.
32. Anderlüh G, Razpotnik A, Podlesek Z et al. Interaction of the eukaryotic pore-forming cytolytin equinatoxin II with model membranes: 19F NMR studies. *J Mol Biol* 2005; 347:27-39.
33. Meinardi E, Florin-Christensen M, Paratcha G et al. The molecular basis of the self/nonself selectivity of a coelenterate toxin. *Biochem Biophys Res Commun* 1995; 216:348-354.
34. De Los Rios V, Mancheño JM, Lanío ME et al. Mechanism of the leakage induced on lipid model membranes by the hemolytic protein sticholysin II from the sea anemone *Stichodactyla helianthus*. *Eur J Biochem* 1998; 252:284-289.
35. Caaveiro JM, Echabe I, Gutiérrez-Aguirre I et al. Differential interaction of equinatoxin II with model membranes in response to lipid composition. *Biophys J* 2001; 80:1343-1353.
36. Gutiérrez-Aguirre I, Barlič A, Podlesek Z et al. Membrane insertion of the N-terminal alpha-helix of equinatoxin II, a sea anemone cytolytic toxin. *Biochem J* 2004; 384:421-428.
37. Drechsler A, Potrich C, Sabo JK et al. Structure and activity of the N-terminal region of the eukaryotic cytolytin equinatoxin II. *Biochemistry* 2006; 45:1818-1828.
38. Casallanovo F, de Oliveira FJ, de Souza FC et al. Model peptides mimic the structure and function of the N-terminus of the pore-forming toxin sticholysin II. *Biopolymers* 2006; 84:169-180.
39. Poklar N, Fritz J, Maček P et al. Interaction of the pore-forming protein equinatoxin II with model lipid membranes: A calorimetric and spectroscopic study. *Biochemistry* 1999; 38:14999-15008.
40. Anderlüh G, Barlič A, Potrich C et al. Lysine 77 is a key residue in aggregation of equinatoxin II, a pore-forming toxin from sea anemone *Actinia equina*. *J Membr Biol* 2000; 173:47-55.

41. Menestrina G, Cabiaux V, Tejuca M. Secondary structure of sea anemone cytolytins in soluble and membrane bound form by infrared spectroscopy. *Biochem Biophys Res Commun* 1999; 254:174-180.
42. Alegre-Cebollada J, Martinez Del Pozo A, Gavilanes JG et al. Infrared spectroscopy study on the conformational changes leading to pore formation of the toxin sticholysin II. *Biophys J* 2007; 93:3191-3201.
43. Kristan K, Viero G, Maček P et al. The equinatoxin N-terminus is transferred across planar lipid membranes and helps to stabilize the transmembrane pore. *FEBS J* 2007; 274:539-550.
44. Iacovache I, Paumard P, Scheib H et al. A rivet model for channel formation by aerolysin-like pore-forming toxins. *EMBO J* 2006; 25:457-466.
45. Belmonte G, Pederzolli C, Maček P et al. Pore formation by the sea anemone cytolytin equinatoxin II in red blood cells and model lipid membranes. *J Membr Biol* 1993; 131:11-22.
46. Tejuca M, Dalla Serra M, Ferreras M et al. Mechanism of membrane permeabilization by sticholysin I, a cytolytin isolated from the venom of the sea anemone *Stichodactyla helianthus*. *Biochemistry* 1996; 35:14947-14957.
47. Tejuca M, Dalla Serra M, Potrich C et al. Sizing the radius of the pore formed in erythrocytes and lipid vesicles by the toxin sticholysin I from the sea anemone *Stichodactyla helianthus*. *J Membr Biol* 2001; 183:125-35.
48. Valcarcel CA, Dalla Serra M, Potrich C et al. Effects of lipid composition on membrane permeabilization by sticholysin I and II, two cytolytins of the sea anemone *Stichodactyla helianthus*. *Biophys J* 2001; 80:2761-2774.
49. Anderluh G, Dalla Serra M, Viero G et al. Pore formation by equinatoxin II, a eukaryotic protein toxin, occurs by induction of nonlamellar lipid structures. *J Biol Chem* 2003; 278:45216-45223.
50. Yang L, Harroun TA, Weiss TM et al. Barrel-stave model or toroidal model? A case study on melittin pores. *Biophysical J* 2001; 81:1475-1485.
51. Basañez G, Sharpe JC, Galanis J et al. Bax-type apoptotic proteins porate pure lipid bilayers through a mechanism sensitive to intrinsic monolayer curvature. *J Biol Chem* 2002; 277:49360-49365.
52. Kuwana T, Mackey MR, Perkins G et al. Bid, Bax and lipids cooperate to form supramolecular openings in the outer mitochondrial membrane. *Cell* 2002; 111:331-342.
53. Yu L, Fernig DG, Smith JA et al. Reversible inhibition of proliferation of epithelial cell lines by *Agaricus bisporus* (edible mushroom) lectin. *Cancer Res* 1993; 53:4627-4632.
54. Marty-Detraves C, Francis F, Baricault L et al. Inhibitory action of a new lectin from *Xerochomus chrysenteron* on cell-substrate adhesion. *Mol Cell Biochem* 2004; 258:49-55.
55. Yu LG. The oncofetal Thomsen-Friedenreich carbohydrate antigen in cancer progression. *Glycoconj J* 2007; 24:411-420.
56. Anderluh G, Lakey JH. Disparate proteins use similar architectures to damage membranes. *Trends Biochem Sci* 2008; 33:482-490.
57. Tweten RK. Cholesterol-dependent cytolytins, a family of versatile pore-forming toxins. *Infect Immun* 2005; 73:6199-6209.
58. Tejuca M, Anderluh G, Maček P et al. Antiparasite activity of sea-anemone cytolytins on *Giardia duodenalis* and specific targeting with anti-*Giardia* antibodies. *Int J Parasitol* 1999; 29:489-498.
59. Potrich C, Tomazzolli R, Dalla Serra M et al. Cytotoxic activity of a tumor protease-activated pore-forming toxin. *Bioconjug Chem* 2005; 16:369-376.
60. Jackson KE, Spielmann T, Hanssen E et al. Selective permeabilization of the host cell membrane of *Plasmodium falciparum*-infected red blood cells with streptolysin O and equinatoxin II. *Biochem J* 2007; 403:167-175.
61. Tafesse FG, Ternes P, Holthuis JC. The multigenic sphingomyelin synthase family. *J Biol Chem* 2006; 281:29421-29425.
62. Simons K, Ikonen E. Functional rafts in cell membranes. *Nature* 1997; 387:569-572.
63. Bartke N, Hannun YA. Bioactive sphingolipids: metabolism and function. *J Lipid Res* 2009; 50:S91-S96.

CHAPTER 10

Hemolysin E (HlyE, ClyA, SheA) and Related Toxins

Stuart Hunt, Jeffrey Green and Peter J. Artymiuk*

Abstract

Certain strains of *Escherichia coli*, *Salmonella enterica* and *Shigella flexneri* produce a pore-forming toxin hemolysin E (HlyE), also known as cytolysin A (ClyA) and silent hemolysin, locus A (SheA). HlyE lyses erythrocytes and mammalian cells, forming transmembrane pores with a minimum internal diameter of ~25 Å. We review the current knowledge of HlyE structure and function in its solution and pore forms, models for membrane insertion, its potential use in biotechnology applications and its relationship to a wider superfamily of toxins.

Introduction

Hemolysin E (HlyE; also known as ClyA or SheA) is a novel, pore-forming toxin synthesized by *Escherichia coli* and other enteric bacteria.¹⁻⁶ HlyE lyses mammalian erythrocytes, is cytotoxic toward cultured mammalian cells, induces apoptosis in macrophages and has been reported to induce slow intracellular Ca²⁺ oscillations in epithelial cells.^{7,8} Genes coding for close homologues are present in the genomes of *Salmonella enterica* serovar Typhi or serovar Paratyphi A and *Shigella flexneri*, the causative agents of typhoid fever, paratyphoid and dysentery respectively.⁹ In addition, a more distantly related HlyE occurs in avian *E. coli* strains^{10,11} which lack the more widely studied RTX pore-forming hemolysins.¹² Indeed, evidence to date suggests that the *hlyA* gene, encoding the RTX protein HlyA, that is an established virulence factor in extraintestinal *E. coli* infections is not found in *E. coli* strains that possess *hlyE*.¹³ Recently it has been shown that antibodies to HlyE are present in humans that have been infected with either *S. Typhi* or *S. Paratyphi A* and that *hlyE* is expressed in *S. Typhi* infected human macrophages, where it is thought to constrain bacterial growth and thereby contribute to chronic infection.¹⁴ Furthermore, following the demonstration that all wild-type *S. Typhi* and *S. Paratyphi A* strains tested so far possess functional HlyE proteins it has been suggested that HlyE plays a role in pathogenesis of these bacteria.^{15,16} However, *hlyE* is apparently not associated with sudden infant death syndrome¹⁷ and screening for the presence of functional *hlyE* genes suggests that is likely to act as a virulence factor in a relatively small group of Enterobacteriaceae.¹⁸

Regulation of *hlyE* Expression

Regulation of *hlyE* expression in *E. coli* K-12 is complex and is influenced by several environmental signals. A single site in the *hlyE* promoter enhances expression in response to oxygen starvation when occupied by FNR (regulator of Fumarate Nitrate Reduction)^{2,19} and in response to glucose-starvation when occupied by CRP (cAMP receptor protein).^{19,20} In addition, the

*Corresponding Author: Peter J. Artymiuk—The Krebs Institute, Department of Molecular Biology and Biotechnology, University of Sheffield, Sheffield, S10 2TN, UK.
Email: p.artymiuk@sheffield.ac.uk

nucleoid structuring protein H-NS has a negative effect on FNR-driven *hlyE* expression and a positive effect on CRP-driven *hlyE* expression.^{19,20} Furthermore, H-NS-mediated repression is antagonized by a fourth transcription factor, SlyA, that responds to amino acid starvation.^{3,19,21,22} In *S. Typhi* expression of *hlyE* is activated by the PhoPQ two-component system that is also responsible for the regulation of many genes expressed during host infection, but not by SsrB.¹⁴ The effects of other transcription factors, such as those known to regulate *hlyE* expression in *E. coli*, have not yet been tested in Salmonella.

Structural Studies on HlyE

Crystal Structure of the Water-Soluble Form

The X-ray crystal structure of the water-soluble form of HlyE shows that it is a 34 kDa rod-shaped molecule consisting of a bundle of four long (80-90 Å) helices, which coil around each other with significant elaborations at both poles of the four-helix bundle (Fig. 1).⁹ In the tail domain, which contains the N- and C-terminal regions of the protein, a shorter (30 Å) helix (α G) packs against the four long helices, forming a five-helix bundle for about one third of the length of the molecule. Random and site-directed mutagenesis has revealed that residues in the α G region play important roles in HlyE activity.^{23,24} HlyE possesses only two cysteine residues and the crystal structure revealed that these are positioned very close to each other in the tail domain⁹ (Fig. 1) and can be oxidized to form a disulphide bond.^{23,25} It has been reported that the

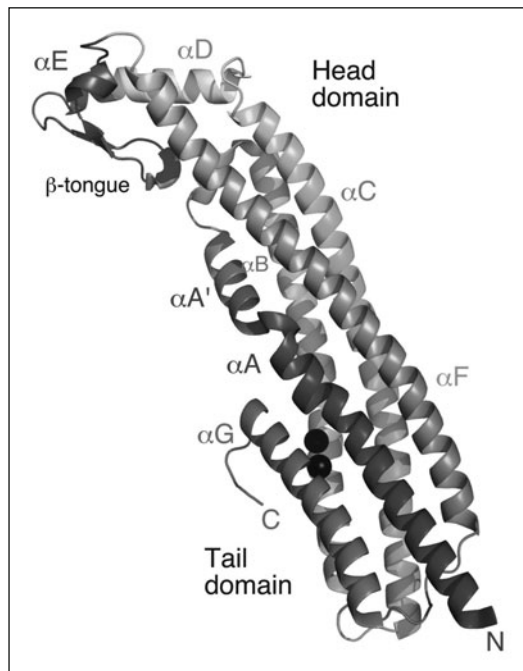


Figure 1. Three-dimensional structure of HlyE. The backbone fold of the HlyE monomer is shown in cartoon representation, rainbow coloured from blue (N-terminal, labelled N) to red (C-terminal, labelled C), except for the hydrophobic region (residues 177-203) which is coloured grey. The head and tail domains are indicated and helices A to G are labelled, together with the beta tongue region. The two cysteine residues are shown as black spheres. Produced using PyMol.⁴⁸ A color version of this image is available at www.landesbioscience.com/curie.

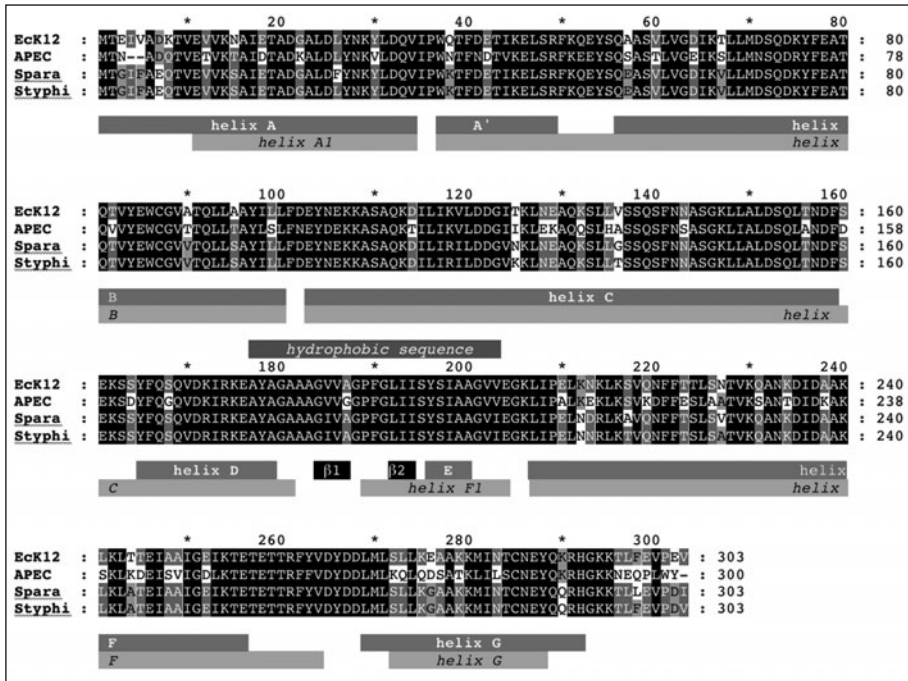


Figure 2. Alignments of HlyE sequences. Sequences from *E. coli* K12 (EcK12), avian *E. coli* (APEC), *Salmonella* Paratyphi (Spara) and *Salmonella* Typhi (Styphi) are shown. Conserved residues are shown in white letters on a black background, residues identical in only three or two sequences as black letters on grey and light grey backgrounds respectively and others as black letters on white background. Red bars below the sequences indicate the positions of alpha helices A to G and black bars show the positions of strands $\beta 1$ and $\beta 2$ in the soluble form. Cyan bars show the positions of the helices in the pore form. The hydrophobic putative transmembrane sequence is indicated by the labelled green bar above the sequences. A color version of this image is available at www.landesbioscience.com/curie

redox state of the protein (dithiol, in the cytoplasm and outer membrane vesicles; or disulphide, in the periplasm) affects the oligomeric state of HlyE,^{23,25} but more recently both reduced and oxidized HlyE have been shown to be active.²⁶ At the other end of the rod there is a subdomain (the head domain) that consists of a short two-stranded hydrophobic antiparallel β -sheet flanked by two short helices, known as the β -tongue⁹ (Fig. 1). These β strands form part of the 20-residue hydrophobic sequence (Fig. 2) that had previously been predicted to be a transmembrane helix in HlyE.²⁴ Site-directed mutagenesis has shown that the hydrophobic nature of the β -tongue has to be maintained to allow HlyE to bind to and lyse target cells.^{9,23} Host cells are disrupted by the formation of pores in target membranes.⁹

Oligomerization in Solution

In the crystal, *E. coli* HlyE molecules form dimers that conceal the hydrophobic β -tongue against a second hydrophobic patch lower down the molecule, which may indicate a possible means of maintaining solubility of the toxin in aqueous media.⁹ Although initial gel filtration experiments suggested that HlyE is a monomer in solution,⁹ more recent investigations have suggested that dimerization—and indeed further oligomerization—occurs in aqueous solution,²³ but that higher order oligomers formed this way are inactive.

Electron Microscopy of HlyE Pores

The first electron micrographs of the toxin⁹ (Fig. 3) revealed that HlyE oligomerizes in the presence of lipid to form circular pores in which the toxin molecules appear to be arranged with their long axes perpendicular to the membrane surrounding a central channel approximately 50 Å in maximum internal diameter. The pore was estimated to contain eight or more HlyE subunits, with a total molecular mass of 250-300 kDa. These initial electron micrographs of the pores were consistent with simple pore models assembled from multiple copies of the soluble HlyE structure, suggesting that HlyE might not undergo large conformational changes during pore formation.⁹ However, two recent electron microscopic three-dimensional reconstructions of HlyE pores have revealed that the pores are significantly longer (ca. 140 Å compared with 100 Å) than the water-soluble form of the protein, indicating that conformational changes must take place in order to form a functional pore.^{26,27} Although both reconstructions were generated from very similar objects, the interpretation of the data has led to the conclusion that the HlyE pore was octameric in one case²⁷ and 13-meric in the other.²⁶ The reason for the discrepancy is unclear.

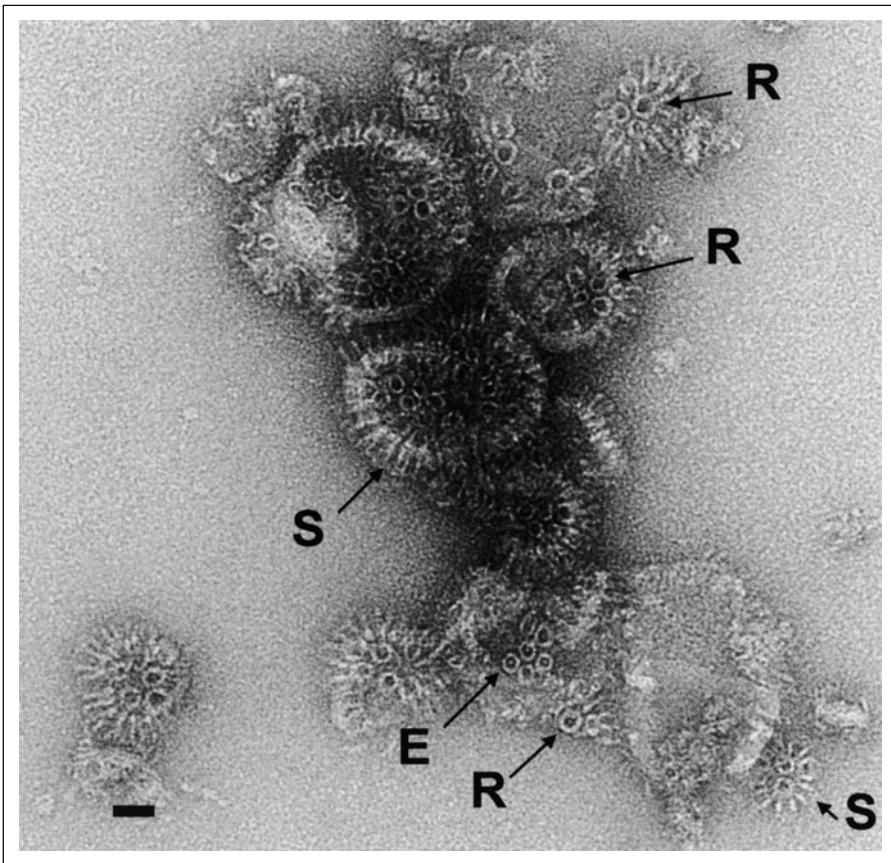


Figure 3. Electron Micrograph of HlyE in lipid vesicles. The micrograph shows negatively stained vesicles containing HlyE with the more heavily stained regions appearing darker. Stain-filled rings (R) are apparent in views parallel to the membrane normal. Some complexes show a central stain-excluding density (E). Side views of the protein complexes are visible at the folded edges of the vesicles as protruding spikes (S). Scale bar (lower left) represents 200 Å. Reproduced from Wallace AJ et al. *Cell* 2000; 100:265-276;⁹ with permission from Elsevier.

Models of the Pore Structure

Both Hunt et al²⁸ and Eifler et al²⁶ proposed a model of pore formation in which membrane bound HlyE monomers undergo a rate-limiting conformational change that precedes formation of a functional pore. The latter authors suggested that the β -tongue region of HlyE may form a 26-standed antiparallel β barrel cap structure as part of the process of insertion into the membrane.²⁶ However it was not suggested that this would comprise the final pore structure and indeed it was unlikely to be so, as there is no β barrel-like peptide sequence at any point in the primary structure of HlyE.⁹ Thus, Parker and Feil (2005) have argued that the transmembrane portion of HlyE is almost certainly helical.²⁹

A possible model which attempted to reconcile the probable α helical structure of the transmembrane sequence with the electron microscopic evidence for an elongated pore was proposed by Hunt et al²⁸ (Fig. 4A). Partial proteolysis of the water-soluble and oligomeric forms of HlyE was employed to identify the inner and outer surfaces of the HlyE pore and the results from this were combined with the structural features from the three-dimensional reconstructions.^{26,27} The orientations of the monomers suggested by the pattern of proteolysis implied that the hydrophobic β -tongue is outward facing and thus has the potential to interact with the lipid tails of a target membrane bilayer. However, both electron microscopy studies indicated a substantially longer pore (~140 Å) than that of the model shown in Figure 4 (~100 Å).

Some of the discrepancy in pore length was accounted for in a more sophisticated model (Fig. 4D) that incorporates a rearrangement in the HlyE head domain.²⁸ In the crystal structure of the soluble form of the toxin, the head domain commences with the amphipathic helix α D, continues

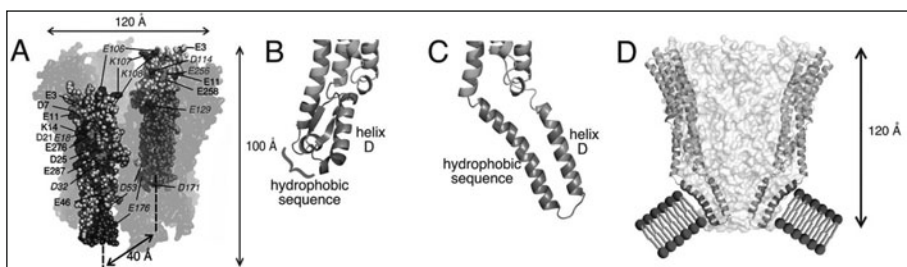


Figure 4. Proposed preliminary models of an octameric HlyE pore. A) A view is shown of a simple space-filling model of an octameric pore assembly illustrating the relative orientations of the HlyE protomers. Six of the protomers are made semi-transparent to give a clear view of the remaining two, chosen to show the positions of the proteolytic cleavage points on the outside (left protomer) and inside (right protomer) of the assembly. The 24-residue hydrophobic sequence that includes the β -tongue, which is required for membrane binding, is coloured dark grey. The C-terminal G helix is coloured light blue. Proteolytic cleavage sites observed in both the water-soluble and oligomeric forms of HlyE are coloured green and labelled in black, cleavage sites protected in the oligomer are coloured and labelled in purple italics and the residue (Asp21) that is sensitive in the oligomer, but not in the water-soluble form of HlyE, is coloured and labelled in dark blue. Approximate dimensions of the proposed assembly are indicated. B) Structure of the head domain of HlyE with the hydrophobic residues in grey and the hydrophilic ones in orange; the hydrophobic putative transmembrane sequence including the β -tongue is on the left, the amphipathic (orange and grey) helix D is on the right; part of the main body of the protomer is in cyan. C) Model in which the hydrophobic sequence becomes a single transmembrane helix (grey, left) which is connected at its N-terminal end to the main body of the protomer via a realigned amphipathic helix D (orange and grey, right). D) The hydrophilic face of helix D (shown entirely in orange for clarity) can then form the inner lining of a pore, while its hydrophobic face packs against the new transmembrane helix (grey) which interacts with lipid (shown schematically). Diagram was produced using PyMOL.⁴⁸ Adapted from Hunt S et al. *Microbiology* 2008; 154:633-642;²⁸ with permission from the Society for General Microbiology. A color version of this image is available at www.landesbioscience.com/curie.

through the long hydrophobic sequence which comprises the C-terminal end of α D, the β -tongue and the short helix α E and ends just before the commencement of helix α F which is part of the main body of the molecule (Figs. 1, 2 and 4B).⁹ It was proposed that by rearrangement of this region of HlyE the amphipathic helix α D could form an octameric α -helical barrel pore,²⁸ similar to that observed in the C-terminus of *E. coli* Wza,³⁰ with the hydrophobic residues facing outwards towards the membrane lipids (Fig. 4C,D). It was argued that the proposed rearrangement would be facilitated if the long hydrophobic sequence (previously predicted to be a transmembrane α helix²⁴) were to undergo a conformational change into an α helix which then returns to the original side of the membrane (Fig. 4C,D). It was suggested that the resulting hydrophobic helix would make favourable interactions with the outward facing side chains of the α helical barrel and with the lipid bilayer (Fig. 4D).²⁸

Crystal Structure of the Pore Form

The speculation regarding the organization of the HlyE pore was resolved very recently when Ban and coworkers³¹ published the 3.3 Å resolution crystal structure of a detergent-stabilised soluble pore-form of HlyE. This revealed that the assembly is a dodecameric pore with a height of 130 Å and a maximum outer diameter of 105 Å (Fig. 5A,B), although given the variability in pore sizes as observed by EM,^{26,27} other oligomeric states and conformations may also be possible.

The pore structure shows that major conformational changes take place between the soluble and pore forms of the HlyE protomers³¹ (Figs. 2 and 5C,D). Although part of the hydrophobic region around the β -tongue and helix E does indeed refold to become a transmembrane α -helix as previously proposed,²⁸ this is accompanied by far more radical changes in the structure of the protomer than had been previously envisaged (Fig. 5C,D), but nevertheless foreshadowed by fluorescence energy transfer, intrinsic fluorescence and site-directed mutagenesis experiments implicating rearrangements of the tail domain during pore formation.^{23,24,26,28} C-terminal to the hydrophobic region the changes are relatively modest: the new helix formed from β 2 and α E (" α F1") forms an N-terminal extension to α F and in addition there is a change in the location of the turn between the two last helices resulting in a 5-residue lengthening of α F at its C-terminal end and a concomitant shortening of α G. N-terminal to the hydrophobic region, however, there are more profound changes: helices α C and α D and strand β 1 become one continuous helix, as do

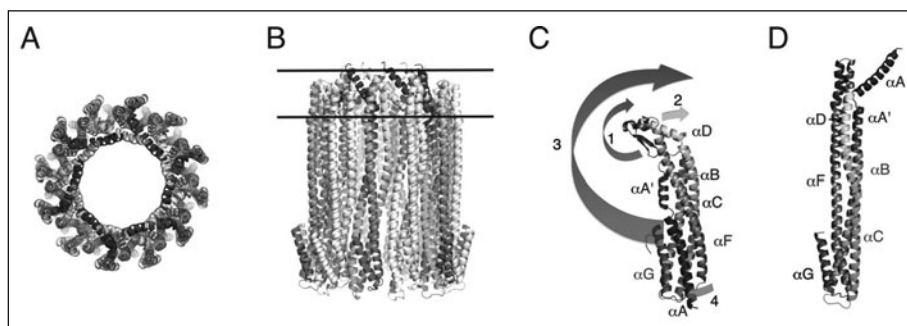


Figure 5. The structure of the pore form of HlyE.³¹ Views of the dodecameric pore complex from (A) above and (B) from the side, with alternate protomers white and coloured; horizontal lines represent the proposed position of a target membrane. C) View of the HlyE protomer in the soluble form⁹ and (D) in the pore. In (C) numbered arrows schematically summarize the proposed sequence of changes: (1) movement of the β -tongue to become a hydrophobic extension of helix α D; (2) α D to β 1 becomes a helical extension to α C and β 2 to α E becomes a helical extension to α F; (3) movement of α A and α A' to the other end of the protomer and (4) movement of α F into the space left by α A. Diagrams are coloured and labelled as Figure 1 and produced using PyMOL.⁴⁸ A color version of this image is available at www.landesbioscience.com/curie.

helices α B and α A' (the final section of α A). As a result of this, α A is rotated by approximately 180° (and the N-terminus moves 140 Å) relative to its position in the soluble form and thus becomes situated at the opposite end of the protomer (Fig. 5C,D). The consequence of all these changes is that the main body of the protomer becomes an elongated three-helix bundle³¹ in contrast to the four-helix bundle observed in the soluble form of the toxin.⁹ New molecular surfaces are formed by these rearrangements and allow the formation of a network of 25 hydrogen bonds and 13 salt bridges between each pair of protomers in the pore.³¹

The dramatically relocated α A helices from the 12 protomers form a cone-shaped α -helical barrel inside the pore and it is this that defines the ~30 Å limiting diameter of the pore (Fig. 5A,B).³¹ The outer part of this α -helical barrel is hydrophobic and it is proposed that this together with the hydrophobic sequence around α F1 insert into and form the interface with the membrane (Fig. 5).

This remarkable new structure of an HlyE pore resolves many of the issues around the mechanism of pore formation by this toxin and allows proposal of a detailed possible mechanism for membrane insertion,³¹ which is discussed further below.

Process of Membrane Insertion

HlyE-mediated cell lysis is the product of a complex series of steps in which HlyE must recognize and bind to the target cell and then assemble to form a functional pore. The data presented by Hunt et al (2008)²⁸ suggest that conversion of HlyE from a water-soluble dimer,^{9,32} in which the hydrophobic surfaces in the head (β -tongue) and tail (residues of helices B, C and G) are shielded from the solvent, to a monomer that can bind to a target membrane is fast. The fluorescence energy transfer experiments suggest that after interaction with a membrane HlyE protomers rapidly begin to oligomerize.²⁸ Thus, it is suggested that neither membrane binding, nor initial interactions between membrane bound HlyE monomers are rate-limiting steps in creating a functional pore. Nevertheless, during these rapid phases HlyE undergoes conformational changes in regions including those (for example the tail region) that are remote from the β -tongue, which is essential for interaction with a membrane.^{9,24} The changes in HlyE conformation were suggested to be required for binding the membrane and facilitating subsequent initial interactions between HlyE protomers to form parallel membrane bound HlyE molecules in a prepore structure. This rapid phase is then followed by a slow component, most apparent as a temperature-dependent lag phase, with relatively high activation energy, before hemolysis occurs. Taken together these observations indicate that whereas HlyE binding to a target and initial oligomerization are rapid, functional pore-formation is a much slower process. Such a mechanism accounts for the relatively poor hemolysis observed at 15°C compared to 37°C and the need for prolonged incubation to observe cell lysis at low HlyE concentrations. Thus, the data presented by Hunt et al²⁸ broadly support the conclusions of Eiffler et al,²⁶ who also suggested that there is a rate-limiting conformational transition in membrane bound HlyE that precedes the formation of a functional pore.

The availability of structures of the soluble HlyE monomer⁹ and the recent description of an HlyE pore³¹ has allowed the proposal of a detailed model for membrane insertion.³¹ In this model the trigger for the structural change (Fig. 5C,D) involves Phe 190 at the tip of the β -tongue which, in the soluble form, interacts with four other aromatic residues (Phe 50, Tyr 54, Phe 159 and Tyr 165).⁹ It is envisioned that in proximity to the membrane Phe 190 and the β -tongue flip out into the lipid bilayer. The removal of Phe 190 destabilizes the cluster of aromatic residues and precipitates the rearrangements of the protomer associated with the transition to the pore form. In these rearrangements helix α D and the first half of the hydrophobic sequence including β 1 become an extension of α C; α A' becomes an extension of α B and the amphipathic α A relocates towards and attaches to the membrane; and finally α F, extended by β 2 and α E at one end and part of α G at the other, takes the place vacated by α A. This refolded protomer is attached to the membrane and then acts as a nucleation site for the recruitment of more protomers. When a complete prepore is assembled on the membrane it is proposed that the target membrane becomes distorted and insertion of α A and α F into the lipid bilayer takes place to form the functional pore.³¹

HlyE Secretion and Exploitation in Vaccine Development and Tumour Targeting

HlyE is a remarkable protein in that it lacks previously recognized protein export signal sequences yet is translocated from the bacterial cytoplasm without modification to the periplasm, where it accumulates.^{3,23,25,33,34} The association between extracellular HlyE and periplasmic proteins has led to speculation that HlyE may be secreted via outer membrane vesicles.³⁴ This theory is further supported by the observation by the Uhlin group that HlyE protein is exposed on the surface of the *E. coli* cell, as demonstrated by immunofluorescence, electron microscopy (EM) and atomic force microscopy (AFM).²⁵ The latter studies revealed small outer-membrane vesicles surrounding the bacterial cells containing HlyE-like assemblies, resembling those described by Wallace et al (2000),⁹ were observed in vesicles from the HlyE-expressing strains.²⁵ These were confirmed as HlyE by immunolocalisation using anti-HlyE antibodies in the immunogold labelling method. However, it is evident that there is still much to learn about the mechanism of HlyE export, but this gap in our knowledge has not inhibited attempts to exploit the properties of HlyE in the design of new vaccines and as a potential therapeutic gene.

Delivery of foreign antigens to induce protective immune responses using live attenuated bacteria is an exciting area of vaccine development. Because surface-exposed or secreted antigens are more immunogenic than cytoplasmic antigens, attention has been drawn to HlyE as an export system for displaying foreign antigens in attenuated *S. Typhi* strains. Taking advantage of the ability of HlyE to facilitate the export of proteins fused at its C-terminus, strains of *S. Typhi* engineered to express several antigens (including: protective *Bacillus anthracis* antigens; and the *Plasmodium falciparum* truncated circumsporozoite surface protein) have been reported to have potential as vaccine candidates.³⁵⁻³⁸ One of the perceived advantages of these strains is that they do not require additional engineering to incorporate a secretion system, which might have a detrimental effect on the strain, because HlyE is readily exported by *S. Typhi*.

The targeting of HlyE to outer membrane vesicles has been used to localize active proteins, again as HlyE fusions, to outer membrane vesicles with the aim of mapping the progress of HlyE-containing vesicles during infection of host cells and for biotechnology applications such as surface display and delivery of therapeutic proteins.³⁹ Also, the cytotoxic properties of HlyE overproduced by attenuated *S. Typhimurium* have been exploited in combination with an engineered hypoxia-regulated promoter to increase necrosis and inhibit growth of tumours in mice.⁴⁰

HlyE-Like Toxins from *Bacillus cereus*

Sequence comparisons suggest that HlyE toxins form a small isolated family of virulence factors restricted to the closely related organisms *E. coli*, *S. flexneri* and *S. Typhi* and *S. Paratyphi*. Moreover, until very recently, the X-ray crystal structure of HlyE appeared to exhibit a unique overall three-dimensional fold, based on searches of the structural databases.⁹ However, even though there is little sequence homology, very recent structural work has revealed a striking three-dimensional fold resemblance between HlyE and a family of pore-forming toxins from the Gram-positive bacterium *B. cereus*.^{41,42}

The Gram-positive bacterium *Bacillus cereus* possesses three putative enterotoxins: hemolysin BL (Hbl), nonhaemolytic enterotoxin (Nhe) and cytotoxin K (CytK). Hbl and Nhe are tripartite toxins and are encoded by three genes cotranscribed as operons in which *hblCDA* encodes Hbl components L₂, L₁ and B and *nheABC* encodes NheA, NheB and NheC (reviewed in Arnesen et al (2008)).⁴³ There is sequence homology between the three components in each complex and between the proteins of Nhe and Hbl.⁴² Recently, the X-ray crystal structure of the B component of hemolysin BL from *B. cereus* was published;⁴¹ despite low sequence homology, it was discovered that *B. cereus* Hbl-B shared significant structural similarities with *E. coli* HlyE^{41,42} (Fig. 6). Both the HlyE and the hemolysin BL structures are based on elongated four-helix bundles with a simple square, left-handed, up-down-up-down arrangement of helices.⁴⁴ This is a fairly commonly encountered folding topology⁴⁵ and so this similarity is not sufficient to allow the inference of an evolutionary

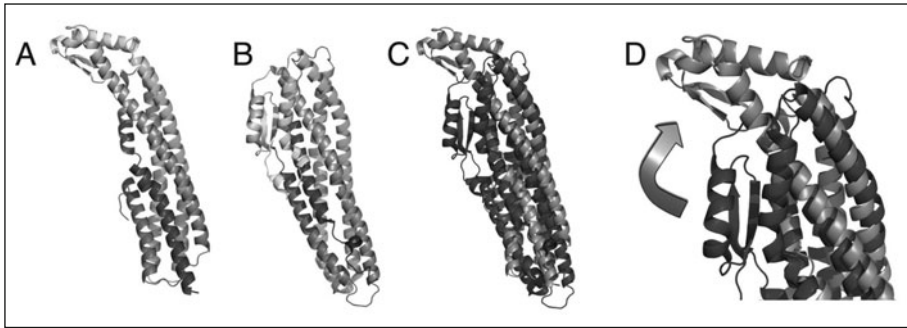


Figure 6. Comparison of *E. coli* HlyE and *B. cereus* Hbl-B structures. A) and B) are cartoons of HlyE and Hbl-B respectively (both rainbow coloured as Fig. 1). C) shows a superposition of HlyE (orange) and Hbl-B (dark blue).^{41,42} D) is a detail of (C) showing the different positions occupied by the head domains in the two protein structures, the arrow indicating the relative displacement between Hbl-B and HlyE. Diagram was produced using PyMOL.⁴⁸ A color version of this image is available at www.landesbioscience.com/curie.

relationship. What is far more significant, however, is that the folds of the tail domains and of the head domains of both proteins are also very similar,^{41,42} even though the folding topologies of the two domains had previously been thought to be unique to HlyE.⁹ Moreover, as with HlyE, the single long hydrophobic sequence in Hbl-B is located in the region of the β hairpin in the head domain. One difference is that the orientation of the head domain with respect to the tail domain differs appreciably between the two proteins (Fig. 6).^{41,42} In the crystal structure of Hbl-B, the head domain is oriented so that it interacts with the main four helix bundle and with the tail domain ($\sim 30^\circ$ interdomain angle), which itself has a longer C-terminal helix.⁴¹ In contrast, in HlyE⁹ the head domain makes relatively few interactions with the rest of the molecule ($\sim 120^\circ$ interdomain angle). Interestingly, the alternate orientations of the head domains in the crystal structures of HlyE and HBL-B (Fig. 6) suggests a degree of flexibility in this region that is consistent with the proposed rearrangements of the head domain and β -tongue in the first steps of model of the HlyE pore formation proposed by Mueller et al.³¹

Hardy, Granum and coworkers have shown Nhe to be cytotoxic to Caco-2 and Vero cells, to form pores in planar lipid bilayers and to be haemolytic against erythrocytes.⁴² Based on the significant sequence similarities to Hbl-B, it was also possible to generate three-dimensional homology models for NheB and NheC:⁴² both contain a predicted hydrophobic segment that correlates with the β -hairpin seen in HlyE and Hbl-B. The structural and functional similarities among Nhe, Hbl and HlyE may indicate that they belong to a superfamily of pore-forming toxins.⁴² As more X-ray crystal structures are determined, it is possible that the number of HlyE homologues identified will increase and so it will become apparent if HlyE, Hbl and Nhe are truly members of a larger superfamily of pore-forming toxins.

Conclusion

Although discovered relatively recently, the importance of HlyE is becoming apparent. The confirmation of involvement in *Salmonella* virulence^{15,46,47} and the presence of homologues in many *E. coli* strains including avian pathogenic *E. coli* (APEC),^{10,11} suggests that HlyE is a versatile virulence factor that contributes to the establishment of a range of infections. Moreover the clear structural resemblances between HlyE and the Hbl and Nhe toxins of *Bacillus cereus* indicate that these proteins are members of a broader superfamily of pore-forming toxins. Furthermore, the availability of structures for both soluble and pore forms of HlyE represents a major step forward in the understanding of α -helical pore forming toxins in general.

References

1. del Castillo FJ, Leal SC, Moreno F et al. The *Escherichia coli* K-12 sheA gene encodes a 34-kDa secreted haemolysin. *Mol Microbiol* 1997; 25:107-115.
2. Green J, Baldwin ML. The molecular basis for the differential regulation of the hlyE-encoded haemolysin of *Escherichia coli* by FNR and HlyX lies in the improved Activating Region 1 contact of HlyX. *Microbiology* 1997; 143:3785-3793.
3. Ludwig A, Bauer S, Benz R et al. Analysis of the SlyA-controlled expression, subcellular localization and pore-forming activity of a 34 kDa haemolysin (ClyA) from *Escherichia coli* K-12. *Mol Microbiol* 1999; 31:557-567.
4. Ludwig A, von Rhein C, Bauer S et al. Molecular analysis of cytolysin a (ClyA) in pathogenic *Escherichia coli* strains. *J Bacteriol* 2004; 186:5311-5320.
5. Oscarsson J, Mizunoe Y, Uhlin BE et al. Induction of haemolytic activity in *Escherichia coli* by the slyA gene product. *Mol Microbiol* 1996; 20:191-199.
6. Oscarsson J, Westermark M, Lofdahl S et al. Characterization of a pore-forming cytotoxin expressed by *Salmonella enterica* serovars Typhi and Paratyphi A. *Infect Immun* 2002; 70:5759-5769.
7. Lai XH, Arencibia I, Johansson A et al. Cytocidal and apoptotic effects of the ClyA protein from *Escherichia coli* on primary and cultured monocytes and macrophages. *Infect Immun* 2000; 68:4363-4367.
8. Soderblom T, Oxhamre C, Wai SN et al. Effects of the *Escherichia coli* toxin cytolysin A on mucosal immunostimulation via epithelial Ca²⁺ signalling and Toll-like receptor 4. *Cell Microbiol* 2005; 7:779-788.
9. Wallace AJ, Stillman TJ, Atkins A et al. *E. coli* hemolysin E (HlyE, ClyA, SheA): X-ray crystal structure of the toxin and observation of membrane pores by electron microscopy. *Cell* 2000; 100:265-276.
10. Reingold J, Starr N, Maurer J et al. Identification of a new *Escherichia coli* She haemolysin homolog in avian *E. coli*. *Vet Microbiol* 1999; 66:125-134.
11. Nagai S, Yagihashi T, Ishihama A. An avian pathogenic *Escherichia coli* strain produces a hemolysin, the expression of which is dependent on cyclic AMP receptor protein gene function. *Vet Microbiol* 1998; 60:227-238.
12. Coote JG. Structural and functional relationships among the RTX toxin determinants of Gram negative bacteria. *FEMS Microbiol Rev* 1992; 88:137-162.
13. Kerenyi M, Allison HE, Batai I et al. Occurrence of hlyA and sheA genes in extraintestinal *Escherichia coli* strains. *J Clin Microbiol* 2005; 43(6):2965-2968.
14. Faucher SP, Forest C, Beland M et al. A novel PhoP-regulated locus encoding the cytolysin ClyA and the secreted invasin TaiA of *Salmonella enterica* serovar Typhi is involved in virulence. *Microbiology* 2009; 155:477-488.
15. von Rhein C, Hunfeld KP, Ludwig A. Serologic evidence for effective production of cytolysin A in *Salmonella enterica* serovars Typhi and Paratyphi A during human infection. *Infect Immun* 2006; 74:6505-6508.
16. von Rhein C, Bauer S, Sanjurjo EJM et al. ClyA cytolysin from *Salmonella*: Distribution within the genus, regulation of expression by SlyA and pore-forming characteristics. *Int J Med Microbiol* 2009; 299:21-35.
17. Hight AR, Berry AM, Bettelheim KA et al. The frequency of molecular detection of virulence genes encoding cytolysin A, high-pathogenicity island and cytolethal distending toxin of *Escherichia coli* in cases of sudden infant death syndrome does not differ from that in other infant deaths and healthy infants. *J Med Microbiol* 2009; 58:285-289.
18. von Rhein C, Bauer S, Simon V et al. Occurrence and characteristics of the cytolysin A gene in *Shigella* strains and other members of the family Enterobacteriaceae. *FEMS Microbiol Lett* 2008; 287:143-148.
19. Wyborn NR, Stapleton MR, Norte VA et al. Regulation of *Escherichia coli* hemolysin E expression by H-NS and *Salmonella* SlyA. *J Bacteriol* 2004; 186:1620-1628.
20. Westermark M, Oscarsson J, Mizunoe Y et al. Silencing and activation of ClyA cytotoxin expression in *Escherichia coli*. *J Bacteriol* 2000; 182:6347-6357.
21. Lithgow JK, Haider F, Roberts IS et al. Alternate SlyA and H-NS nucleoprotein complexes control hlyE expression in *Escherichia coli* K-12. *Mol Microbiol* 2007; 66:685-698.
22. Zhao G, Weatherspoon N, Kong W et al. A dual-signal regulatory circuit activates transcription of a set of divergent operons in *Salmonella typhimurium*. *Proc Natl Acad Sci USA* 2008; 105:20924-20929.
23. Atkins A, Wyborn NR, Wallace AJ et al. Structure-function relationships of a novel bacterial toxin, hemolysin E—The role of alpha(G). *J Biol Chem* 2000; 275:41150-41155.
24. Oscarsson J, Mizunoe Y, Li L et al. Molecular analysis of the cytolytic protein ClyA (SheA) from *Escherichia coli*. *Mol Microbiol* 1999; 32:1226-1238.
25. Wai SN, Lindmark B, Soederblom T et al. Vesicle-mediated export and assembly of pore-forming oligomers of the enterobacterial ClyA cytotoxin. *Cell* 2003; 115:25-35.

26. Eifler N, Vetsch M, Gregorini M et al. Cytotoxin ClyA from *Escherichia coli* assembles to a 13-meric pore independent of its redox-state. *EMBO J* 2006; 25:2652-2661.
27. Tzokov SB, Wyborn NR, Stillman TJ et al. Structure of the hemolysin E (HlyE, ClyA and SheA) channel in its membrane-bound form. *J Biol Chem* 2006; 281:23042-23049.
28. Hunt S, Moir AJG, Tzokov S et al. The formation and structure of *Escherichia coli* K-12 haemolysin E pores. *Microbiology* 2008; 154:633-642.
29. Parker MW, Feil SC. Pore-forming protein toxins: from structure to function. *Prog Biophys Mol Biol* 2005; 88:91-142.
30. Dong CJ, Beis K, Nesper J et al. Wza the translocon for *E. coli* capsular polysaccharides defines a new class of membrane protein. *Nature* 2006; 444:226-229.
31. Mueller M, Grauschkopf U, Maier T et al. The structure of a cytolytic alpha-helical toxin pore reveals its assembly mechanism. *Nature* 2009; 459:726-730.
32. Wyborn NR, Clark A, Roberts RE et al. Properties of haemolysin E (HlyE) from a pathogenic *Escherichia coli* avian isolate and studies of HlyE export. *Microbiology* 2004; 150:1495-1505.
33. Ludwig A, Tengeli C, Bauer S et al. SlyA, a regulatory protein from *Salmonella typhimurium*, induces a haemolytic and pore-forming protein in *Escherichia coli*. *Mol Gen Genet* 1995; 249:474-486.
34. del Castillo FJ, Moreno F, del Castillo I. Secretion of the *Escherichia coli* K-12 sheA hemolysin is independent of its cytolytic activity. *FEMS Microbiol Lett* 2001; 204:281-285.
35. Galen JE, Zhao LC, Chinchilla M et al. Adaptation of the endogenous *Salmonella enterica* serovar typhi clyA-encoded hemolysin for antigen export enhances the immunogenicity of anthrax protective antigen domain 4 expressed by the attenuated live-vector vaccine strain CVD 908-htrA. *Infect Immun* 2004; 72:7096-7106.
36. Stokes MGM, Titball RW, Neeson BN et al. Oral administration of a *Salmonella enterica*-based vaccine expressing *Bacillus anthracis* protective antigen confers protection against aerosolized B-anthraxis. *Infect Immun* 2007; 75:1827-1834.
37. Baillie LWJ, Rodriguez AL, Moore S et al. Towards a human oral vaccine for anthrax: The utility of a *Salmonella Typhi* Ty21a-based prime-boost immunization strategy. *Vaccine* 2008; 26:6083-6091.
38. Chinchilla M, Pasetti MF, Medina-Moreno S et al. Enhanced immunity to *Plasmodium falciparum* circumsporozoite protein (PfCSP) by using *Salmonella enterica* serovar Typhi expressing PfCSP and a PfCSP-encoding DNA vaccine in a heterologous prime-boost strategy. *Infect Immun* 2007; 75:3769-3779.
39. Kim JY, Doody AM, Chen DJ et al. Engineered bacterial outer membrane vesicles with enhanced functionality. *J Mol Biol* 2008; 380:51-66.
40. Ryan RM, Green J, Hunt S et al. Bacterial delivery of a novel cytolysin to hypoxic areas of solid tumors. *Gene Ther* 2009; 16:329-339.
41. Madegowda M, Eswaramoorthy S, Burley SK et al. X-ray crystal structure of the B component of Hemolysin BL from *Bacillus cereus*. *Proteins Struct Funct Bioinform* 2008; 71:534-540.
42. Fagerlund A, Lindback T, Storset AK et al. *Bacillus cereus* Nhe is a pore-forming toxin with structural and functional properties similar to the ClyA (HlyE, SheA) family of haemolysins, able to induce osmotic lysis in epithelia. *Microbiology* 2008; 154:693-704.
43. Arnesen LPS, Fagerlund A, Granum PE. From soil to gut: *Bacillus cereus* and its food poisoning toxins. *FEMS Microbiology Reviews* 2008; 32:579-606.
44. Presnell SR, Cohen FE. Topological distribution of 4 alpha helix bundles. *Proc Natl Acad Sci USA* 1989; 86:6592-6596.
45. Harris NL, Presnell SR, Cohen FE. 4 helix bundle diversity in globular proteins. *J Mol Biol* 1994; 236:1356-1368.
46. Ansong C, Yoon H, Norbeck AD et al. Proteomics analysis of the causative agent of typhoid fever. *J Proteome Res* 2008; 7:546-557.
47. Fuentes JA, Villagra N, Castillo-Ruiz M et al. The *Salmonella typhi* hlyE gene plays a role in invasion of cultured epithelial cells and its functional transfer to *S. typhimurium* promotes deep organ infection in mice. *Res Microbiol* 2008; 159:279-287.
48. DeLano WL, Lam JW. PyMOL: A communications tool for computational models. *Abstracts of Papers of the American Chemical Society* 2005; 230:254-COMP.

CHAPTER 11

Pore Formation by Cry Toxins

Mario Soberón, Liliana Pardo, Carlos Muñoz-Garay, Jorge Sánchez, Isabel Gómez, Helena Porta and Alejandra Bravo*

Abstract

B*acillus thuringiensis* (Bt) bacteria produce insecticidal Cry and Cyt proteins used in the biological control of different insect pests. In this review, we will focus on the 3d-Cry toxins that represent the biggest group of Cry proteins and also on Cyt toxins. The 3d-Cry toxins are pore-forming toxins that induce cell death by forming ionic pores into the membrane of the midgut epithelial cells in their target insect. The initial steps in the mode of action include ingestion of the protoxin, activation by midgut proteases to produce the toxin fragment and the interaction with the primary cadherin receptor. The interaction of the monomeric Cry1A toxin with the cadherin receptor promotes an extra proteolytic cleavage, where helix α -1 of domain I is eliminated and the toxin oligomerization is induced, forming a structure of 250 kDa. The oligomeric structure binds to a secondary receptor, aminopeptidase N or alkaline phosphatase. The secondary receptor drives the toxin into detergent resistant membrane microdomains forming pores that cause osmotic shock, burst of the midgut cells and insect death. Regarding to Cyt toxins, these proteins have a synergistic effect on the toxicity of some Cry toxins. Cyt proteins are also proteolytic activated in the midgut lumen of their target, they bind to some phospholipids present in the mosquito midgut cells. The proposed mechanism of synergism between Cry and Cyt toxins is that Cyt1Aa function as a receptor for Cry toxins. The Cyt1A inserts into midgut epithelium membrane and exposes protein regions that are recognized by Cry11Aa. It was demonstrated that this interaction facilitates the oligomerization of Cry11Aa and also its pore formation activity.

Introduction

Bacillus thuringiensis (Bt) bacteria produce insecticidal δ -endotoxins proteins (also named Cry and Cyt toxins) during the sporulation phase.¹ These proteins are the mayor determinants involved in Bt insect-toxicity. They are highly specific to their target, innocuous to other organisms including all vertebrates and plants and completely biodegradable. These entomopathogenic proteins are considered the perfect insecticide representing a viable alternative for the control of insect pests in agriculture and disease vectors as mosquitoes, that are important in public health.¹ During the last years, different Cry toxins have been expressed in transgenic plants mainly corn, cotton and soybean. These Bt-crops, are being grown worldwide and have proven to effectively control insect pests, reducing the use of chemical insecticides.^{1,2}

Cry and Cyt proteins are produced as parasporal inclusions during the sporulation phase of the bacteria. They have been classified based on their primary sequence identity.^{1,3} The different Cry toxins are organized in three main groups that are not related phylogenetically: the three domain (3d-Cry) toxins, the mosquitocidal-like (Mtx-like) toxins and the binary-like (Bin-like) toxins and it was proposed that each of these groups have different mechanism of action³ (Table 1).

*Corresponding Author: Alejandra Bravo—Instituto de Biotecnología UNAM. Departamento de Microbiología Molecular, Instituto de Biotecnología, Universidad Nacional Autónoma de México. Email: bravo@ibt.unam.mx

Table 1. Classification of Cry, Cyt and Vip proteins produced by *Bacillus thuringiensis*

Name of the General Group	Members of the Group	Specificity
Cry-Three domain toxins (3d-Cry)	Cry1A-Cry1K	Lep and also some to Col
	Cry2	Dip and also some to Lep
	Cry3A-Cry3C	Col
	Cry4A-Cry4C	Dip
	Cry5A-Cry5B	Nem
	Cry7A-Cry7C	Col
	Cry8A-Cry8J	Col
	Cry9A-Cry9E	Lep and some to Dip
	Cry10	Dip
	Cry11A-Cry11B	Dip
	Cry12	Nem
	Cry13	Nem
	Cry14	Col
	Cry16	Dip
	Cry17	Dip
	Cry18A-Cry18C	Col
	Cry19A-Cry19B	Dip
	Cry20	Dip
	Cry21A-Cry21B	Nem
	Cry24A-Cry24C	Dip
	Cry25	Dip
	Cry26	Unknown
	Cry27	Dip
	Cry28	Unknown
	Cry29	Dip
	Cry30A-Cry30G	Dip
	Cry31	Human leukemic cell
	Cry32A-Cry32C	Dip
	Cry39	Dip
	Cry40A-Cry40D	Dip
	Cry41	Human cancer cells
	Cry42	Unknown
	Cry43	Col
	Cry44	Dip

continued on next page

Table 1. Continued

Name of the General Group	Members of the Group	Specificity
Cry-Three domain toxins (3d-Cry)	Cry47	Dip
	Cry48	Dip
	Cry50	Dip
	Cry52A-Cry52B	Dip
	Cry53	Unknown
	Cry54	Dip
	Cry15	Lep
Cry-Mtx like	Cry33	Human leukemic cell
	Cry23	Col
	Cry38	Unknown
	Cry51	Lep
Cry-Bin like	Cry35A -Cry35B	Col
	Cry36A	Col
Other Cry related to Cry6	Cry6A-Cry6B	Nem
	Cry22A-Cry22B	Col and some to Him
	Cry37	Col
Other Cry non-related to other toxins	Cry34A-Cry34B	Col
	Cry45	Human cancer cells
	Cry46	Human cancer cells
	Cry49	Dip
Cyt	Cyt1A-Cyt1C	Dip
	Cyt2A-Cry2C	Dip
Vip	Vip1A-Vip1D	Col
	Vip2A-Vip2B	Col
	Vip3A-Vip3B	Lep

Lep, Lepidoptera; Col, Coleoptera; Dip, Diptera; Nem, nematodes; Him, Himenopteran. Information from http://www.lifesci.sussex.ac.uk/home/Neil_Crickmore/Bt/index.html

The Mtx-like and the Bin-like toxins have similarity with the Mtx or Bin toxins produced by *B. sphaericus*, although in the case of *B. sphaericus* these toxins are toxic against mosquitoes whereas in Bt they are toxic against coleopteran larvae.³

In this review we will mainly focus on the 3d-Cry toxins, that represent the biggest group of Cry proteins.^{1,3} Some members of this group are toxic to Lepidopteran, Coleopteran, Dipteran, or Himenopteran insects or to nematodes (Table 1). The alignment of their protein sequences revealed the presence of five conserved blocks, suggesting that they share a similar fold and thus a

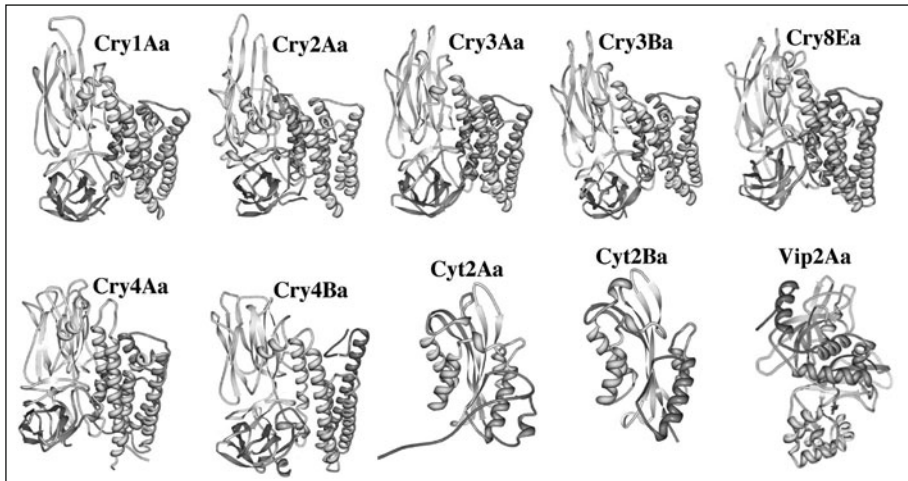


Figure 1. Structure of Cry and Cyt toxins produced by *Bacillus thuringiensis*. Structures of proteins were produced with the protein workshop program using the following PDB files: 1CIY Cry1Aa, 1I5P Cry2Aa, 1DLC Cry3Aa, 1JI6 Cry3Bb, 2C9K Cry4Aa, 1W99 Cry4Ba, 3eb7 Cry8Ea, 1CBY Cyt2Aa, 2rci Cyt2Ba, 1qs1 VIP2.

similar mechanism of action.¹ The activated form of the 3d-Cry toxins has an approximately size of 60 kDa, although their corresponding protoxins may have a size of 70 kDa or 130 kDa. The C-terminal extension found in the long protoxins is cleaved out by the midgut proteases during toxin activation, it is proposed that this C-terminal region may play a role in the formation of the crystal inclusion body within the bacterium.^{1,3}

The three dimensional structure of some activated toxins (Cry1Aa, Cry3Aa, Cry3B, Cry4Aa, Cry4Ba and Cry8Ea) and one short-protoxin (Cry2Aa) revealed that all of them are globular proteins with similar topology composed of three domains⁴⁻⁹ (Fig. 1). The Domain I is located at the N-terminal end, it is composed of seven α -helices and is implicated in the formation of membrane pores. The Cry2Aa protoxin has an extra 49-amino acid region forming two extra α -helices in the N-terminal end that are cleaved out after proteolytic activation of the toxin.⁶ Domain I shares structural similarities with other pore forming toxins such as colicin Ia and N (PDB codes: 1cii, 1a87) and diphtheria toxin (1ddt), supporting the role of this domain in pore-formation.³ Domain II consists of a beta-prism of three anti-parallel β -sheets packed around a hydrophobic core and Domain III is a β -sandwich of two antiparallel β -sheets. Domains II and III are involved in receptor binding and specificity,^{1,3} they share some structural similarities with carbohydrate-binding proteins³ (domain II with vitelline (1vmo), lectin jacalin (1jac) and lectin Mpa (1jot) and domain III with the cellulose binding domain of 1,4- β -glucanase C (1ulo), galactose oxidase (1gof), sialidase (1eut), β -glucuronidase (1bgh), the carbohydrate-binding domain of xylanase U (1gmm) and β -galactosidase (1bgl)). All these data suggest that toxin interaction with carbohydrate moieties could have an important role in Cry toxicity. Although most of the reported studies have demonstrated that interaction of Cry toxins with receptors involve protein-protein interactions¹ for some Cry toxins as Cry1Ac, Cry5Ba and Cry14Aa, interactions with some carbohydrate moieties present in receptors as N-acetylgalactosamine (GalNAc) or present in specific-glycolipids that are conserved between insects and nematodes but not in vertebrates, have been reported.^{10,11}

The Cyt toxins comprise two highly related groups¹ (Table 1). They have a single α - β domain constituted by two outer layers of α -helix hairpins wrapped around a β -sheet^{12,13} (Fig. 1). Cyt proteins are almost exclusively found in Bt strains active against Dipteran insects although a few exceptions have been found.¹⁴ The Cyt toxins synergize the toxic effect of some Cry proteins active against mosquitoes and also the Bin toxin produced by *B. sphaericus*.^{15,16} Based on the length of the

secondary structures present in Cyt toxin, it was proposed that the inner core of β -sheets (β -5, β -6, β -7) could span the cell membrane and this proposition was confirmed by analyzing some Cyt2Aa mutant proteins labeled with a polarity-sensitive fluorescent dye.¹⁷ Cyt toxins share structural similarity with volvatxin A2, a cardiotoxin produced by *Volvariella volvacea*.¹⁸

Mechanism of Action of Cry Toxins

The 3d-Cry toxins have been described as pore-forming toxins that induce cell death by forming ionic pores into the membrane of midgut epithelial cells in their target insect^{1,5,19,20} (Fig. 2). However, recently an alternative model proposed that insect death is triggered by the activation of a cascade signal pathway through toxin interaction with a specific receptor named cadherin (CAD)²¹ (Fig. 2). The initial steps in the mode of action in both models are similar, from ingestion of the protoxin and activation by midgut proteases to the interaction with the primary CAD receptor (Fig. 2). In the pore formation model the Cry toxin interacts sequentially with several receptors including CAD and glycosylphosphatidyl-inositol (GPI) anchored receptors such as aminopeptidase N (APN) or alkaline phosphatase (ALP) resulting in toxin oligomerization and insertion into membrane microdomains forming pores that cause osmotic shock, burst of the midgut cells and insect death^{1,3,20} (Fig. 2).

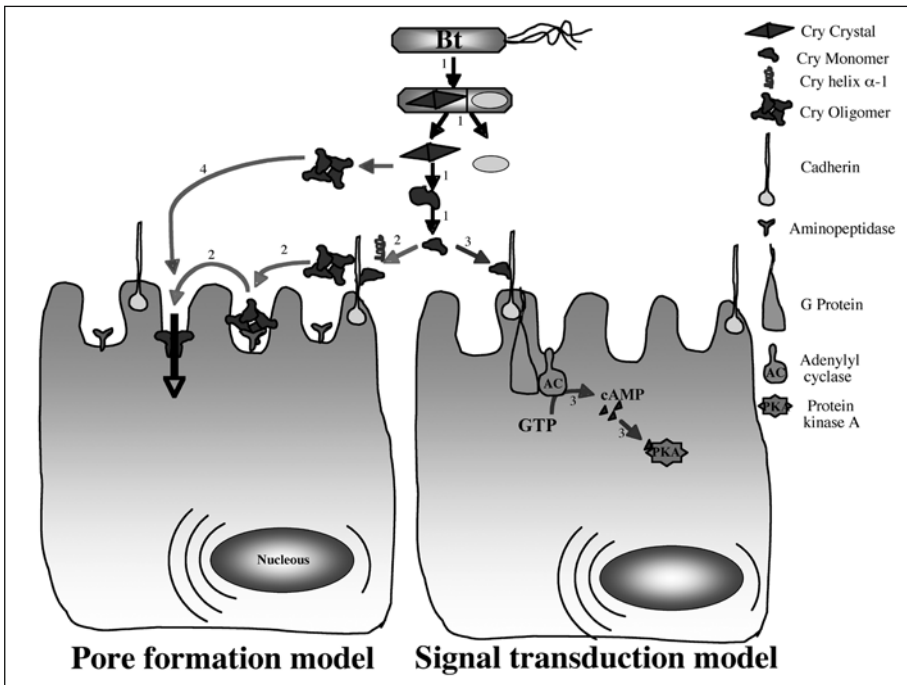


Figure 2. Models of the mode of action of Cry toxins from *Bacillus thuringiensis*. Pore formation model and signal transduction model. Arrow number 1 show general steps: crystal production during sporulation of Bt, solubilization and activation by midgut proteases. Arrows number 2 show the different steps in the pore formation model: Binding to cadherin receptor, cleavage of helix α -1, oligomerization of the toxin, binding to aminopeptidase and membrane insertion to form a pore in lipid rafts that ends with cell death. Arrows number 3 show the steps involved in signal transduction model: binding to cadherin, activation of a protein G that increase activity of adenylyl cyclase resulting in increased levels of cAMP that triggers activity of protein kinase A that induce cell death. Finally, arrows number 4 show the mechanism of the CryMod toxins that were deleted of helix α -1 and skip cadherin interaction, forming pores after binding to aminopeptidase receptor and killing the cells by pore formation.

The signal transduction model does not involve interaction with other receptors besides CAD and neither involves oligomerization or membrane insertion. In this model it is proposed that the toxicity is triggered by activation of a Mg^{+2} dependent signal cascade pathway through the interaction of the monomeric 3d-Cry toxin with CAD receptor. This interaction activates a G protein, which in turn activates an adenylyl cyclase promoting the production of intracellular cAMP. The increased cAMP levels activate protein kinase A that starts an intracellular pathway resulting in cell death.²¹ This model was based in studies performed in insect cell line transfected with the *Manduca sexta* cadherin gene exclusively²¹ (Fig. 2).

Solubilization and Proteolytic Activation of Cry Toxins

As mentioned above, most of the 3d-Cry proteins are produced as crystalline inclusions of 130 kDa-prototoxins and some other are of 70 kDa prototoxins. The larvae ingest the crystalline inclusions, which are solubilized in the gut lumen. In the case of Lepidoptera and Diptera insects their midgut lumen has highly alkaline and reducing conditions.²² In contrast, Coleopteran guts have a neutral to slightly acidic pH.²² In few cases prototoxin solubilization has been shown to be a determinant of insect specificity. Cry1Ba is toxic to the Coleopteran *Leptinotarsa decemlineata* only if the prototoxin is previously solubilized in vitro at alkaline pH, suggesting insolubility of the toxin at the neutral pH of Coleopteran insects.²³

After solubilization, the Cry prototoxins are cleaved by midgut proteases in both the N- and C-terminal ends²⁴ to yield activated monomeric 60-kDa-toxins with the three domain structure described above (Fig. 1). Serine proteases are the main digestive proteases found in Lepidoptera and Diptera, whereas cysteine and aspartic proteases are abundant in Coleopteran guts.²⁵

Activation of Cry toxins involves the proteolytic removal of 25-60 residues from N-terminal end of both 130 or 70 kDa prototoxins and approximately 600 residues from the C-terminus in the case of the 130-kDa prototoxins.^{1,3,25} The only prototoxin whose structure was solved is the Cry2Aa of 70 kDa.⁶ This structure showed the 49 residues at N-terminus that are cleaved out during activation. This region forms two α -helices that occlude a region of the toxin involved in the interaction with the receptor⁶ (Fig. 1). Thus it was speculated that processing of the N-terminal end of Cry prototoxins might unmask a hydrophobic patch of the toxin involved in toxin-receptor or toxin-membrane interaction.^{6,26}

Proteolytic activation of Cry toxins is a limiting step in the toxicity of Cry toxins. The lack of a major gut proteinase in *Plodia interpunctella* is responsible for their resistance to Cry toxins produced by the *Bt* HD198 strain.²⁷ On the other hand, it has been reported that the rapid degradation of Cry1Ca or Cry1Ab toxins is associated with the low sensitivity in *Spodoptera littoralis* and *S. frugiperda* larvae^{28,29} and that serine protease inhibitors may enhance the insecticidal activity of some Cry toxins up to 20 fold.³⁰

Binding Interaction with Receptors

The activated toxin binds to specific receptors located on the microvilli membrane of the midgut epithelium columnar cells.^{1,3} Cry toxins are highly selective and kill only a limited number of insect species. This selectivity is mainly due to the interaction with specific receptors. A number of putative receptor molecules for the lepidopteran-specific Cry1 toxins have been identified. Among them CAD proteins, APN and ALP are the best characterized. However, other proteins³¹ and glycolipids¹¹ have also been reported as binding sites for Cry toxins (Table 2).

The CAD proteins bind Cry1As toxins and have been identified in several lepidopteran insects³²⁻³⁷ and more recently in the dipteran *A. gambiae*³⁸ (Table 2). CAD are transmembrane glycoproteins composed of three domains, the ectodomain formed by 11 to 12 cadherin repeats (CR), the transmembrane domain and the intracellular domain.³³ In *M. sexta* and *A. gambiae* larvae they are located in the microvilli of midgut epithelium cells, the site of action of Cry toxins.^{38,39}

Cry1As toxins also bind GPI-anchored 120 kDa glycosylated APN, which have been identified in several Lepidopteran species³⁹⁻⁴⁵ and in the Dipteran *A. quadramaculatus*.⁴⁶ Several APN isoforms have been characterized in Lepidopteran insects and classified in five groups⁴⁷ (Table 2).

Table 2. Receptors of Cry-3D toxins described in different insects

Cry-Receptor	Cry Toxin Recognized	Insect
APN 1	Cry1Aa, Cry1Ab Cry1C Cry1Aa, Cry1Ab, Cry1Ac, Cry1Fc Cry1Aa, Cry1Ab, Cry1Ac n.d.	<i>Plutella xylostella</i> , <i>Bombyx mori</i> <i>Spodoptera exigua</i> <i>Heliothis virescens</i> <i>Manduca sexta</i> , <i>Helicoverpa armigera</i> <i>Lymantria dispar</i> , <i>Trichoplusia ni</i> , <i>Helicoverpa punctigera</i>
APN 2	Cry1Aa, Cry1Ab Cry1Ab n.d.	<i>P. xylostella</i> , <i>B. mori</i> <i>M. sexta</i> <i>S. exigua</i> , <i>H. armigera</i> , <i>T. ni</i> , <i>L. dispar</i>
APN 3	Cry1C Cry1Aa, Cry1Ab Cry1Ac Cry1Ac, Cry1F Cry1Ac, Cry1B n.d.	<i>Spodoptera litura</i> , <i>S. exigua</i> <i>P. xylostella</i> , <i>B. mori</i> <i>H. armigera</i> , <i>L. dispar</i> <i>H. virescens</i> <i>Epiphyas postvittana</i> <i>M. sexta</i> , <i>T. ni</i> , <i>Plodia interpunctella</i> , <i>H. punctigera</i>
APN 4	Cry1Aa, Cry1Ab Cry1C Cry1Ac, Cry1Fa n.d.	<i>B. mori</i> <i>S. litura</i> <i>H. virescens</i> <i>M. sexta</i> , <i>S. exigua</i> , <i>H. armigera</i> , <i>H. punctigera</i> , <i>T. ni</i>
APN5	Cry1Aa, Cry1Ab n.d.	<i>P. xylostella</i> <i>H. armigera</i>
APN-106	Cry1C	<i>M. sexta</i>
APN-96	Cry1Ac	<i>B. mori</i>
APN	Cry11Aa, Cry11Ba, Cry4Ba	<i>Anopheles quadrimaculatus</i>
Cadherin	Cry1Aa, Cry1Ab, Cry1Ac Cry1Aa Cry1Ac n.d.	<i>M. sexta</i> , <i>H. virescens</i> <i>B. mori</i> <i>Pectinophora gossypiella</i> , <i>H. armigera</i> <i>Ostrinia nubilalis</i> , <i>L. dispar</i> , <i>P. xylostella</i> , <i>Chilo suppressalis</i> , <i>Helicoverpa zea</i> , <i>Agrotis ipsilon</i> , <i>S. frugiperda</i>
ALP	Cry1Ac Cry11Aa	<i>M. sexta</i> , <i>H. virescens</i> <i>Aedes aegypti</i>
Glycolipids	Cry5Ba Cry/Aa, Cry1Ab, Cry1Ac	<i>Caenorhabditis elegans</i> <i>M. sexta</i>
Glycoconjugated	Cry1Aa, Cry1Ab, Cry1Ba	<i>L. dispar</i>

APN, aminopeptidase; ALP, alkaline phosphatase; nd, not determined; Information obtained from reference 47.

The ALP are 70 kDa proteins also GPI anchored to the membrane that were identified as Cry1Ac receptors in *H. virescens* and *M. sexta*.^{48,49} In the Dipteran *Aedes aegypti* an ALP that binds Cry11Aa toxin was identified⁵⁰ (Table 2).

The interaction of Cry1A toxins with the CAD receptor is rather complex involving at least three binding epitopes. Using a library of single chain antibodies displayed in M13 phage, a Cry1A toxin-binding region was mapped in CAD receptor of *M. sexta*.^{51,52} This region corresponds to the CR7 (869-HITDTNKK-876).⁵² It was further demonstrated that loop 2 of Cry1Ab toxin was the cognate binding epitope of this CR7 region.⁵² The second region in CAD is the CR11 (1331-IPLPASILTVTV-1342) that interacts with loop α 8 and loop 2 of Cry1Ab toxin.⁵³ Finally, the third region of CAD receptor involved in Cry1A interaction was mapped by using truncated derivatives of CAD in toxin overlay assays.⁵⁴ In the case of *M. sexta* this region corresponds to CR12 (residues 1363-1464).⁵⁵ For the *H. virescens* CAD, site-directed mutagenesis narrowed this binding region to residues 1423-GVLTLNFQ-1430 and shown to bind Cry1Ac toxin by interacting with loop 3 of domain II.⁵⁶ Similarly Cry1Aa domain II loop 3 binds the corresponding CR12 region in the *B. mori* CAD-receptor.⁵⁷

Some data support the role of CAD as an important receptor for Cry1A toxins in lepidopterans. Expression of the *M. sexta* and *B. mori* CAD proteins, on the surface of different cell lines render them sensitive to Cry1A toxins.^{36,54,58-60} Also, the Cry1Aa toxin was shown to lyse isolated midgut epithelial cells from *B. mori* and this toxic effect was inhibited if the cells were preincubated with an anti-cadherin antibody.⁶¹ Similarly, a single-chain antibody (scFv73) inhibits binding of Cry1A toxins to CAD receptor, but not to APN and reduced the toxicity of Cry1Ab to *M. sexta* larvae.⁵¹ Moreover, several cadherin deletion and insertion mutations were linked to high levels of resistance to Cry1Ac toxin in *H. virescens*,³⁷ *Pectinophora gossypiella*³³ and *Helicoverpa armigera*.³² Finally the silencing of CAD expression using RNAi in *M. sexta* resulted in lower susceptibility to Cry1A toxins.⁶² Overall, these results suggest that binding to CAD receptor is an important step in the mode of action Cry1A toxins.

The interaction with APN is also complex, involving several binding epitopes of Cry1A located in domains II and III. In the case of the Cry1Ac toxin, domain III recognized a GalNAc moiety located in APN receptor.⁶³ In addition the loops 2 and 3 of domain II of Cry1A toxins are important in their interaction with APN⁶⁴ and a sequential binding mechanism was proposed in the interaction of Cry1Ac with APN. Cry1Ac domain III first interacts with APN GalNAc sugar moiety facilitating the subsequent interaction of domain II loop regions with another region in this receptor.⁶⁴ More recent data demonstrated that Cry1Aa and Cry1Ab toxins bind APN through β 16 and β 22 of domain III.^{65,66}

The role of APN as a Cry toxin receptor is supported by inhibition of APN expression on *S. litura* larvae by dsRNA interference resulting in insects that produce low APN levels and became tolerant to Cry1C toxin.⁶⁷ Also, heterologous expression of *M. sexta* APN in midgut and mesodermal tissue of transgenic *Drosophila melanogaster* caused sensitivity to Cry1Ac toxin.⁶⁸ Anti-domain III antibodies that inhibit Cry1Ab binding with *M. sexta* APN but not with CAD lower the toxicity of Cry1Ab to *M. sexta* larvae.⁶⁵ Additionally, previous reports demonstrated that incorporation of *M. sexta* APN into black lipid bilayers lower the concentration of Cry1Aa toxin needed to induce pore formation activity.⁶⁹ Finally, the APN receptor is anchored to the membrane by a GPI anchor.⁴⁰⁻⁴⁵ The phosphatidylinositol specific phospholipase C (PIPLC) treatment of *Trichoplusia ni* midgut membrane resulted in cleavage of GPI-anchored proteins from the membrane and in a significant reduction of pore-formation activity of Cry1Ac.⁷⁰ Overall, these reports suggest that APN binding is also an important step in the mode of action of Cry1 toxins.

Finally, the binding epitopes in the interaction of Cry1A toxins with ALP have not been described yet. Only in the mosquitocidal specific Cry11Aa toxin, the loop α -8 of domain II was identified as the binding epitope with ALP in *A. aegypti*.⁵⁰ The role of ALP as Cry toxin receptor was demonstrated in a study of the *H. virescens* resistant line YHD2 to Cry1Ac, where part of the Cry1Ac resistant phenotype is due to mutations that affect expression of ALP receptor⁴⁸ and in

the case of *A. aegypti* a peptide-phage that bound ALP and inhibit Cry11Aa binding with ALP lowered the toxicity of Cry11Aa in bioassays.⁵⁰

Role of Cry Toxin-Receptor Interaction in Toxicity

Surface plasmon resonance experiments showed that the binding affinity of monomeric Cry1A toxins to the *M. sexta* CAD receptor is on the range of 1 nM³⁵ while that of APN is on the range of 100 nM.⁶⁴ Also it was reported that affinity of Cry1Ab to APN is increased 200 fold upon toxin oligomerization.²⁰ These binding affinities differences may suggest that binding of monomeric Cry1A toxin to CAD might be the first event on the interaction with microvilli membranes and, therefore, the primary determinant of insect specificity. Immunoprecipitation experiments demonstrated that initial Cry1Ab toxin binding to CAD is followed by the binding to APN²⁰ and it was proposed that Cry1A toxins interact sequentially with both receptors depending on the toxin oligomeric structure. The interaction of the monomeric Cry1A toxin with the CAD promotes an extra proteolytic processing where helix α -1 of domain I is cleaved out and the toxin oligomerization is induced, forming a structure of 250 kDa.⁷¹ The oligomeric structure binds APN with 0.75 nM affinity.²⁰ The APN drives the toxin into the detergent resistant membrane microdomains causing pore formation.²⁰

Recently, Cry1A toxins were genetically modified by deletion of N-terminal end including helix α -1 (named CryMod toxins). The Cry1AMod toxins are able to form oligomeric structures of 250 kDa when treated with trypsin in the absence of the CAD receptor.⁶² In addition, the Cry1AMod toxins are able to kill insects that are resistant to native Bt toxins due to mutations in the CAD receptor such as *P. gossypiella* AZP-R strain that have deletion mutations in the cadherin gene^{33,62} or to kill *M. sexta* insects that have reduced susceptibility to wild type toxin due to silencing of the CAD protein expression by RNAi⁶² (Fig. 2). These data indicate that interaction of the toxin with CAD receptor is not absolutely necessary to kill the larvae and contradicts the signal transduction model that proposed that the interaction of Cry1Ab with CAD activates a G protein that starts the signal cascade ending with death of the cell.

As mentioned previously, APN and ALP receptors are anchored to the membrane by GPI. These proteins are preferably localized in membrane microdomains (lipid rafts).⁷² Lipid rafts are detergent-resistant microdomains enriched in cholesterol, sphingolipids and GPI-anchored proteins and have been implicated in membrane and protein sorting and in signal transduction.⁷³ Also, they have been described as portals for different virus, bacteria and toxins. The interaction of different mammalian-specific bacterial toxins with their receptors located in lipid rafts is a crucial step in the oligomerization and insertion of these bacterial toxins into the membrane.⁷⁴ Like their mammalian counterparts, *H. virescens* and *M. sexta* lipid rafts are enriched in sphingolipids and GPI-anchored proteins.⁷² After toxin exposure, Cry1A toxins were associated with lipid rafts and the integrity of these microdomains was essential for in vitro Cry1Ab pore forming activity.⁷² Therefore the possible role of APN could be to drive Cry1A prepore to the lipid rafts microdomains where the toxin inserts and forms pores. The participation of lipid rafts in the mode of action of Cry toxins could suggest a possible role of signal transduction events and/or the internalization of Cry toxins, since lipid rafts have an active role in these cellular processes. In the case of the Cry1Ac toxin it was shown that interaction with APN facilitated membrane insertion of this toxin.⁷⁵ In addition, the presence of APN in synthetic membranes diminished more than 100 fold the concentration of Cry1Aa toxin required to induce pore-activity.⁶⁹

Oligomerization of Cry Toxins

The interaction of Cry toxin with its CAD receptor is a necessary step for proteolysis of helix α -1 and induction of toxin oligomerization. When Cry1A protoxin was incubated with a single chain antibody scFv73, that mimics a cadherin-epitope,^{51,71} or a cadherin fragment CR12 that contain the toxin binding region^{62,76} in the presence of *M. sexta* midgut proteases, resulted in the formation of a 250 kDa oligomer that form stable ionic channels with high open probability.⁷⁷ The CAD fragment CR12 potentiates the activity of Cry1A toxins in different Lepidopteran insects⁷⁸

and it has been shown that the enhancement of toxicity of Cry1A toxins by the CAD fragment CR12 correlates with enhanced oligomer formation.⁷⁶

Other Cry toxins form oligomeric structures when activated in the presence of their natural receptors, like Cry1Aa, Cry1Ab, Cry1Ca, Cry1Da, Cry1Ea and Cry1Fa that form oligomers when activated in the presence of midgut membranes of target insect as *M. sexta*,^{71,79-82} *S. exigua*⁸² or *Bombyx mori*.⁸³ The Cry3 toxins, that are toxic to Coleopteran insects, also formed oligomeric structures after activation in the presence of membranes from a susceptible *Leptinotarsa decemlineata*.⁸⁴ In all cases studied, the presence of oligomeric structures correlated with higher K⁺ permeability than samples containing monomeric toxins.^{71,79,84} In the case of dipteran-specific toxins, it was reported that Cry11Aa was able to form oligomeric structures of 250 kDa after activation in the presence of BBMV of the mosquito *A. aegypti*.⁸⁵ The Cry4Ba also formed oligomeric structures after activation.⁸⁶ In fact the membrane-associated structure of the Cry4Ba toxin was further analyzed by Atomic Force Microscopy (AFM)⁸⁷ and by electron crystallography.⁸⁸ The AFM studies indicated that the toxin preferentially inserts into the membrane in a self-assembled structure, showing a pore-like structure with four-fold symmetry, suggesting that tetramers are the preferred oligomerization state of this toxin.⁸⁷ However the calculated projection structures from 2D crystal patches analyzed by electron crystallography at 17 Å resolution showed a trimeric organization.⁸⁸ The AFM was also used to analyze the structure of Cry1Aa toxin inserted into monolayer membranes, these studies suggested that the pores are composed of four subunits surrounding a 1.5 nm diameter central depression.⁸⁹

Recently it was reported that helix α -3 of domain I of Cry1Ab toxin is involved in toxin oligomerization since synthetic peptides corresponding to this helix inhibited oligomer formation. In contrast with other helices, that did not affect oligomer formation.⁹⁰ Some Cry1Aa and Cry1Ab helix α -3 mutants were affected in the rate of pore-formation and toxicity to *M. sexta* larvae.^{90,91} The phenotype in these mutants could be explained if they were affected in oligomer formation. In fact, it was demonstrated that Y107E and R99E mutants completely lost toxicity and were unable to form oligomeric structures.⁹⁰ Their binding characteristics to CAD receptor were similar to the wild type toxin⁹⁰ suggesting that oligomerization is key step in toxicity and that binding to CAD was not enough to kill the larvae.

In addition, it was also suggested that helix α -5, located in the central position of domain I, could be involved in Cry1Ac toxin oligomerization, since several point mutations in this helix disrupted oligomerization and were severely affected in toxicity against *M. sexta*.⁸⁰

Finally, there are examples of mutants outside the domain I that affect oligomerization. The Cry1Ca mutants Q374A and T440A located in loops 2 and 3 of domain II, respectively, showed a major decrease in toxicity against *S. exigua* larvae, were also severely affected in oligomer formation when activated in the presence of *S. exigua* membranes.⁸² Apparently the affinity of these mutants to the insect membrane was two-fold lower when compared with the wild type suggesting that changes in domain II may affect the interaction with membrane receptors that is necessary for oligomer formation of Cry1Ca in *S. exigua*.⁸²

Pore Formation

Following binding to receptor, Cry toxins insert into membrane of midgut epithelial cells to form lytic pores. Insertion of Cry toxins into membranes requires a conformational change in the toxin to expose hydrophobic surface that could interact with the membrane bilayer. Domain I has been recognized as the pore-forming domain based on mutagenesis studies⁹⁰⁻⁹³ and on the structure similarities with other pore-forming domains of bacterial toxins as colicin Ia and diphtheria.³ The α -helices of domain I are long enough to span the membrane and have an amphipatic character.^{4,5} Cross-linking experiments done in Cry1Ac mutants that were genetically engineered to create disulphide bridges between some α -helices of domain I, showed that domain I swings away from the rest of the toxin during interaction with the membrane, resulting in the insertion of the hairpin formed by helices α -4 and α -5 into the membrane.⁹⁴ Analysis of the insertion capabilities of synthetic peptides corresponding to the α -helices of domain I from

Cry3A showed that helix α -1 is the only helix that does not interact with the membrane⁹⁵ and a hairpin composed of helices α -4 and α -5 adopted a transmembrane orientation.⁹⁵ These data agree with the proposed "umbrella model" of toxin insertion in which helices α -4 and α -5 insert into the membrane leaving the rest of the α -helices in the interface of the membrane.⁹⁴ The location of domains II-III in the membrane-inserted state is unknown. However, with exception of helix α -1, membrane-inserted Cry1Ac resist proteinase K treatment, suggesting that domains II-III might be also, somehow protected from proteolysis after insertion into the membrane.^{80,96} It may be proposed that during the conformational changes of the toxin during membrane insertion, some epitopes of the proteolytical cleavage sites may be buried, resulting a toxin conformation more resistant to proteolytical cleavage, than the soluble toxin. On the other side, studies of fluorescent quenching with iodide of the Trp545 located in domain III of Cry1Ac indicated that this residue is exposed to the solvent when the toxin is inserted into the membrane,⁷⁵ suggesting that at least domain III may be exposed to the solvent.

A different model of toxin insertion based on calorimetric determinations, proposed that the structure of the membrane-inserted pore does not change dramatically compared to the soluble monomer.⁹⁹ In this model, pore lumen is provided by residues of domains II and III while hydrophobic surface of domain I (without helices α -1 to α -3) faces the lipid bilayer in an oligomeric structure.⁹⁷ In this regard it is interesting to note that mutagenesis of conserved arginine residues in Cry1Aa domain III affected the voltage dependence of the pore.⁹⁸ However, extensive mutagenesis studies in domain I of Cry1A toxins,⁹⁰⁻⁹⁴ contradict this hypothesis and supports the umbrella model⁹⁴ since it was demonstrated that the polar face of the helix α -4 is facing the lumen pore⁹² and mutagenesis in this helix severely affect pore formation.⁹² Future work directed to solve the structure of Cry toxins in the membrane-inserted state will be important to determine the possible roles of other domains in pore-formation.

The pore activity of Cry toxins has been studied by a variety of electrophysiological techniques⁹⁹ such as black lipid bilayers composed by synthetic membranes with or without incorporated APN receptor or in isolated midgut brush border membrane containing natural receptors.¹⁰⁰⁻¹⁰² In all cases the presence of toxin receptors improves pore formation by Cry toxins. Cry toxins induced pores with high conductance that are poorly selective to cationic ions.¹⁰⁰⁻¹⁰² In contrast to other pore forming toxins, pore-formation activity of Cry proteins is not regulated by low pH,¹⁰³ suggesting that Cry toxins are not internalized into acidic vesicles. It was reported that alkaline pH induce a molten globule structure of the Cry1Ab toxin and that flexibility of the toxin was enhanced upon oligomerization.¹⁰⁴ These data are interesting since they correlated with the high pH conditions inside the midgut lumen of susceptible insects.²²

Finally, it has been shown the Cry1Ab oligomeric structure, in contrast with the monomer, efficiently inserts into synthetic membranes and that alkaline pH induces a looser conformation of this structure enhancing membrane insertion and pore formation.¹⁰⁴

Synergism between Cry and Cyt Toxins

Bt subsp. *israelensis* (Bti) that is highly toxic to mosquitoes, produces a crystal inclusion composed of Cry4A, Cry4B, Cry11A and Cyt1A.¹³

The toxicity of the crystal inclusion is, by far, greater than the toxicity of the isolated Cry and Cyt components. Toxicity of different combinations of Cry toxins with Cyt1A was higher than the addition of expected toxicities of the isolated components¹⁵ suggesting that Cyt1A have a synergistic effect on the toxicity of the Cry toxins. In addition, it was reported that Cyt1A toxin overcome or suppress resistance of mosquitoes to the Cry toxins.¹⁰⁵ *C. quinquefasciatus* populations resistant to Cry4A, Cry4B or Cry11A recovered sensitivity when assayed in the presence of Cyt1A toxin.¹⁰⁵ Even more, it has not been possible to select resistant mosquitoes against Cry toxins when selection is performed in the presence of Cyt1A toxin.¹⁰⁵ The Cyt toxins are also produced as protoxins that are soluble under the alkaline and reducing conditions of the midgut. These proteins are proteolytic activated in the midgut lumen, the Cyt toxin binds to the epithelium surface of midgut cells inducing pore-formation leading to cell lysis.¹² An important difference between Cyt and Cry toxins is

the lack of a protein receptor for the Cyt toxin. Cyt binds phospholipids and are capable of forming pores in cell lines of different origin.¹² The proposed mechanism of synergism between Cry and Cyt toxins is that Cyt1Aa function as a receptor for Cry toxins. The Cyt1A inserts into midgut epithelium membrane and exposes protein regions that are recognized by Cry11Aa. It was demonstrated that this interaction facilitates the oligomerization of Cry11Aa and its pore formation activity.^{85,106} Cry11Aa binds Cyt1Aa using the loop α -8 that is also involved in interaction with its ALP receptor.⁵⁰ Mutations in the binding regions of Cry11Aa or Cyt1Aa reduced binding between both toxins and correlated with a severe reduction in their synergism.¹⁰⁶ The reduction in synergism of Cyt and Cry mutants correlated with a reduced oligomer formation of Cry11Aa.⁸⁵

Conclusion

Cry toxins, as several other pore forming toxins, convert from a water-soluble protein into a stable membrane inserted structure. In doing so a similar mechanism was selected, the production of a prepore oligomeric-structure that is a membrane-insertion intermediate, killing the cells by forming pores in the midgut cells of susceptible insects.

Cry toxins are highly selective against their target insect, they present a complex mechanism that involves interaction with several receptors. However, insects may become resistant to these proteins and alternatives to counteract this potential problem must be generated soon. The CryMod toxins represent an efficient strategy to control resistant insects affected in CAD receptors. Also, it is clear that the future engineering of Cyt toxins with the objective of induce synergism with other Cry toxins, as those specific for Coleopteran or Lepidopteran larvae could have a potential impact in preventing the development of Cry-resistant insect populations in nature and brooding the scope of targets of Cry toxins.

References

1. Schnepf E, Crickmore N, Van Rie J et al. *Bacillus thuringiensis* and its pesticidal crystal proteins. *Microbiol Mol Biol Rev* 1998; 62:705-806.
2. James C. Global status of commercialized biotech/GM crops, 2006. *ISAAA Briefs* 2006; 35:1-9
3. de Maagd RA, Bravo A, Berry et al. Structure, diversity and evolution of protein toxins from spore-forming entomopathogenic bacteria. *Ann Rev Genet* 2003; 37:409-433.
4. Li J, Carroll J, Ellar DJ. Crystal structure of insecticidal δ -endotoxin from *Bacillus thuringiensis* at 25Å resolution. *Nature* 1991; 353:815-821.
5. Grochulski P, Masson L, Borisova S et al. *Bacillus thuringiensis* Cry1A(a) insecticidal toxin crystal structure and channel formation. *J Mol Biol* 1995; 254:447-464.
6. Morse RJ, Yamamoto T, Stroud RM. Structure of Cry2Aa suggests an unexpected receptor binding epitope. *Structure* 2001; 9:409-417.
7. Galitsky N, Cody V, Wojtczak A et al. Structure of insecticidal bacterial δ -endotoxin Cry3Bb1 of *Bacillus thuringiensis*. *Acta Cryst* 2001; D57:1101-1109.
8. Boonserm P, Davis P, Ellar DJ et al. Crystal structure of the mosquito-larvicidal toxin Cry4Ba and its biological implications. *J Mol Biol* 2005; 348:363-382.
9. Boonserm P, Mo M, Angsuthanasombat Ch et al. Structure of the functional form of the mosquito larvicidal Cry4Aa toxin from *Bacillus thuringiensis* at a 28 Angstrom resolution. *J Bacteriol* 2006; 188:3391-3401.
10. Cooper MA, Carroll J, Travis E et al. *Bacillus thuringiensis* Cry1Ac toxin interaction with *Manduca sexta* aminopeptidase N in a model membrane environment. *Biochem J* 1998; 333:677-683.
11. Griffiths JS, Haslam SM, Yang T et al. Glycolipids as receptors for *Bacillus thuringiensis* crystal toxin. *Science* 2005; 307:922-925.
12. Li J, Pandelakis AK, Ellar DJ. Structure of the mosquitocidal δ -endotoxin CytB from *Bacillus thuringiensis* sp *kyushuensis* and implications for membrane pore formation. *J Mol Biol* 1996; 257:129-152.
13. Cohen S, Dym O, Albeck S et al. High resolution crystal structure of activated Cyt2Ba Monomer from *Bacillus thuringiensis* subsp. *israelensis*. *J Mol Biol* 2008; 380:820-927.
14. Guerchicoff A, Delécluse A, Rubinstein CP. The *Bacillus thuringiensis* cyt genes for hemolytic endotoxin constitute a gene family. *Appl Environ Microbiol* 2001; 67:1090-1096.
15. Wu D, Johnson JJ, Federeci BA. Synergism of mosquitocidal toxicity between CytA and CryIVD proteins using inclusions produced from cloned genes of *Bacillus thuringiensis*. *Mol Microbiol* 1994; 13:965-972.

16. Wirth MC, Delécue A, Walton WE. CytAb1 and Cyt2Ba1 from *Bacillus thuringiensis* subsp medellin and *Bacillus thuringiensis* subsp israelensis synergize *Bacillus sphaericus* against *Aedes aegypti* and resistant *Culex quinquefasciatus* (Diptera Culicidae). *Appl Environ Microbiol* 2001; 67:3280-3284.
17. Promdonkoy B, Ellar DJ. Membrane pore architecture of a cytolytic toxin from *Bacillus thuringiensis*. *Biochem J* 2000; 350:275-282.
18. Lin SC, Lo YC, Lin JY et al. Crystal structure and electron micrographs of fungal volvatoxin A2. *J Mol Biol* 2004; 343:477-491.
19. Knowles BH, Ellar DJ. Colloid-osmotic lysis is a general feature of the mechanism of action of *Bacillus thuringiensis* δ -endotoxins with different insect specificity. *Biochim Biophys Acta* 1987; 924:507-518.
20. Bravo A, Gómez I, Conde J et al. Oligomerization triggers binding of a *Bacillus thuringiensis* Cry1Ab pore-forming toxin to aminopeptidase N receptor leading to insertion into membrane microdomains. *Biochim Biophys Acta* 2004; 1667:38-46.
21. Zhang X, Candas M, Griko NB et al. A mechanism of cell death involving an adenylyl cyclase/PKA signaling pathway is induced by the Cry1Ab toxin of *Bacillus thuringiensis*. *Proc Natl Acad Sci USA* 2006; 103:9897-9902.
22. Dow JAT. Insect midgut function. *Adv Insect Physiol* 1986; 19:187-238.
23. Bradley D, Harkey MA, Kim MK et al. The insecticidal Cry1B crystal protein of *Bacillus* spp *thuringiensis* has dual specificity to Coleopteran and Lepidopteran larvae. *J Invertebr Pathol* 1995; 65:162-173.
24. Choma CT, Surewicz WK, Carey PR et al. Unusual proteolysis of the protoxin and toxin from *Bacillus thuringiensis* and structural implications. *Eur J Biochem* 1990; 189:523-527.
25. Terra W, Ferreira C. Insect digestive enzymes: properties compartmentalization and function. *Comp Biochem Physiol* 1994; 109B:1-62.
26. Bravo A, Sánchez J, Kouskoura T et al. N-terminal activation is an essential early step in the mechanism of action of the *Bacillus thuringiensis* Cry1Ac insecticidal toxin. *J Biol Chem* 2002; 277:23985-23987.
27. Oppert B, Kramer KJ, Beeman RW et al. Proteinase-mediated insect resistance to *Bacillus thuringiensis* toxins. *J Biol Chem* 1997; 272:23473-23476.
28. Keller M, Sneh B, Strizhov N et al. Digestion of δ -endotoxin by gut proteases may explain reduced sensitivity of advanced instar larvae of *Spodoptera littoralis* to Cry1C. *Insect Biochem Mol Biol* 1996; 26:365-373.
29. Miranda R, Zamudio F, Bravo A. Processing of Cry1Ab δ -endotoxin from *Bacillus thuringiensis* by midgut proteases: role in toxin activation and inactivation. *Insect Biochem Mol Biol* 2001; 31:1155-1163.
30. MacIntosh SC, Kishore GM, Perlak FJ et al. Potentiation of *Bacillus thuringiensis* insecticidal activity by serine protease inhibitor. *J Agric Food Chem* 1990; 38:1145-1152.
31. Valaitis AP, Jenkins JL, Lee MK et al. Isolation, partial characterization of Gypsy moth BTR-270 an anionic brush border membrane glycoconjugate that binds *Bacillus thuringiensis* Cry1A toxins with high affinity *Arch Ins Biochem Physiol* 2001; 46:186-200.
32. Xu X, Yu L, Wu Y. Disruption of a cadherin gene associated with resistance to Cry1Ac delta-endotoxin of *Bacillus thuringiensis* in *Helicoverpa armigera*. *Appl Environ Microbiol* 2005; 71:948-954.
33. Morin S, Biggs RW, Shriver L et al. Three cadherin alleles associated with resistance to *Bacillus thuringiensis* in pink bollworm. *Proc Natl Acad Sci USA* 2003; 100:5004-5009.
34. Flannagan RD, Yu CG, Mathis JP et al. Identification cloning and expression of a Cry1Ab cadherin receptor from European corn borer *Ostrinia nubilalis* (Hübner) (Lepidoptera Crambidae). *Insect Biochem Mol Biol* 2005; 35:33-40.
35. Vadlamudi RK, Weber E, Ji I et al. Cloning and expression of a receptor for an insecticidal toxin of *Bacillus thuringiensis*. *J Biol Chem* 1995; 270:5490-5494.
36. Nagamatsu Y, Koike T, Sasaki K et al. The cadherin-like protein is essential to specificity determination and cytotoxic action of the *Bacillus thuringiensis* insecticidal. *FEBS Lett* 1999; 460:385-390.
37. Gahan LJ, Gould F, Heckel DG. Identification of a gene associated with Bt resistance in *Heliothis virescens*. *Science* 2001; 293:857-860.
38. Hua G, Zhang R, Abdullah MA et al. *Anopheles gambiae* cadherin AgCad1 binds the Cry4Ba toxin of *Bacillus thuringiensis israelensis* and a fragment of AgCad1 synergizes toxicity. *Biochemistry* 2008; 47:5101-5110.
39. Chen J, Brown MR, Hua G et al. Comparison of the localization of *Bacillus thuringiensis* Cry1A delta endotoxins and their binding proteins in larval midgut of tobacco hornworm *Manduca sexta*. *Cell Tissue Res* 2005; 321:123-129.
40. Knight P, Crickmore N, Ellar DJ. The receptor for *Bacillus thuringiensis* Cry1A(c) delta-endotoxin in the brush border membrane of the lepidopteran *Manduca sexta* is aminopeptidase N. *Mol Microbiol* 1994; 11:429-436.

41. Garczynski SF, Adang MJ. Bacillus thuringiensis CryIA(c) δ -endotoxin binding aminopeptidase in the Manduca sexta midgut has a glycosyl-phosphatidylinositol anchor. *Insect Biochem Molec Biol* 1995; 25:409-415.
42. Yaoi K, Kadotani T, Kuwana H et al. Aminopeptidase N from Bombyx mori as a candidate for the receptor of Bacillus thuringiensis CryIAa toxin. *Eur J Biochem* 1997; 246:652-657.
43. Lee MK, You TH, Young BA et al. Aminopeptidase N purified from gypsy moth brush border membrane vesicles is a specific receptor for Bacillus thuringiensis CryIAc toxin. *Appl Environ Microbiol* 1996; 62:2845-2849.
44. Luo K, Tabashnik BE, Adang MJ. Binding of Bacillus thuringiensis CryIAc toxin to aminopeptidase in susceptible and resistant Diamondback Moths (Plutella xylostella). *Appl Environ Microbiol* 1997; 63:1024-1027.
45. Agrawal N, Malhotra P, Bhatnagar RK. Interaction of gene-cloned, insect cell-expressed aminopeptidase N of Spodoptera litura with insecticidal crystal protein CryIc. *Appl Environ Microbiol* 2002; 68:4583-4592.
46. Abdullah MA, Valaitis AP, Dean DH. Identification of a Bacillus thuringiensis Cry11Ba toxin-binding aminopeptidase from the mosquito Anopheles quadramaculatus. *BMC Biochem* 2006; 7:16.
47. Pigott CR, Ellar DJ. Role of receptors in Bacillus thuringiensis crystal toxin activity. *Microbiol Mol Biol Rev* 2007; 71:265-281.
48. Jurat-Fuentes JL, Adang MJ. Characterization of a CryIAc-receptor alkaline phosphatase in susceptible and resistant Heliothis virescens larvae. *Eur J Biochem* 2004; 271:3127-3135.
49. McNail RJ, Adang MJ. Identification of novel Bacillus thuringiensis CryIAc binding proteins in Manduca sexta midgut through proteomic analysis. *Insect Biochem Mol Biol* 2003; 33:999-1010.
50. Fernandez LE, Aimanova KG, Gill SS et al. A GPI-anchored alkaline phosphatase is a functional midgut receptor of Cry11Aa toxin in Aedes aegypti larvae. *Biochem J* 2006; 394:77-84.
51. Gómez I, Oltean DI, Sanchez J et al. Mapping the epitope in Cadherin-like receptors involved in Bacillus thuringiensis CryIA toxin interaction using phage display. *J Biol Chem* 2001; 276:28906-28912.
52. Gómez I, Miranda-Rios J, Rudiño-Piñera E et al. Hydrophobic complementarity determines interaction of epitope ⁸⁶⁹HITDTNKK⁸⁷⁶ in Manduca sexta Bt-R₁ receptor with loop 2 of domain II of Bacillus thuringiensis CryIA toxins. *J Biol Chem* 2002; 277:30137-30143.
53. Gómez I, Dean DH, Bravo A et al. Molecular basis for Bacillus thuringiensis Cry1Ab toxin specificity, two structural determinants in the Manduca sexta Bt-R₁ receptor interact with loops α -8 and 2 in domain II of Cry1Ab toxin. *Biochemistry* 2003; 42:10482-10489.
54. Dorsch JA, Candas M, Griko NB et al. CryIA toxins of Bacillus thuringiensis bind specifically to a region adjacent to the membrane-proximal extracellular domain of Bt-R₁ in Manduca sexta: involvement of a cadherin in the entomopathogenicity of Bacillus thuringiensis. *Insect Biochem Mol Biol* 2002; 32:1025-1036.
55. Hua G, Jurat-Fuentes JL, Adang MJ. Bt-R1a extracellular cadherin repeat 12 mediates Bacillus thuringiensis Cry1Ab binding and cytotoxicity. *J Biol Chem* 2004; 279:28051-28056.
56. Xie R, Zhuang M, Ross LS et al. Single amino acid mutations in the cadherin receptor from Heliothis virescens affect its toxin binding ability to CryIA toxins. *J Biol Chem* 2005; 280:8416-8425.
57. Atsumi S, Inoue Y, Ishizaka T et al. Location of the Bombyx mori 175 kDa cadherin like protein-binding site on Bacillus thuringiensis CryIAa toxin. *FEBS J* 2008; 276:4913-4926.
58. Tsuda Y, Nakatani F, Hashimoto K et al. Cytotoxic activity of Bacillus thuringiensis Cry proteins on mammalian cells transfected with cadherin-like Cry receptor gene of Bombyx mori (silkworm). *Biochem J* 2003; 369:697-703.
59. Hua G, Jurat-Fuentes JL, Adang MJ. Fluorescent-based assays establish Manduca sexta Bt-R(1a) cadherin as a receptor for multiple Bacillus thuringiensis CryIA toxins in Drosophila S2 cells. *Insect Biochem Mol Biol* 2004; 34:193-202.
60. Zhang X, Candas M, Griko NB et al. Cytotoxicity of Bacillus thuringiensis Cry1Ab toxin depends on specific binding of the toxin to the cadherin receptor BT-R1 expressed in insect cells. *Cell Death Differ* 2005; 12:1407-416.
61. Hara H, Atsumi S, Yaoi K et al. A cadherin-like protein functions as a receptor for Bacillus thuringiensis CryIAa and CryIAc toxins on midgut epithelial cells of Bombyx mori larvae. *FEBS Lett* 2003; 538:29-34.
62. Soberón M, Pardo-López L, López I et al. Engineering Modified Bt Toxins to Counter Insect Resistance. *Science* 2007; 318:1640-1642.
63. Masson L, Lu YJ, Mazza A et al. The CryIA(c) receptor purified from Manduca sexta displays multiple specificities. *J Biol Chem* 1995; 270:20309-20315.
64. Jenkins JL, Lee MK, Valaitis AP et al. Bivalent sequential binding model of a Bacillus thuringiensis toxin to gypsy moth aminopeptidase N receptor. *J Biol Chem* 2000; 275:14423-14431.

65. Gómez I, Arenas I, Benitez I et al. Specific epitopes of Domains II and III of *Bacillus thuringiensis* Cry1Ab toxin involved in the sequential interaction with cadherin and aminopeptidase-N receptors in *Manduca sexta*. *J Biol Chem* 2006; 281:34032-34039.
66. Atsumi S, Mizuno E, Hara H et al. Localization of the *Bombyx mori* aminopeptidase N type 1 binding site on *Bacillus thuringiensis* Cry1Aa toxin. *Appl Environ Microbiol* 2005; 71:3966-3977.
67. Rajagopal R, Sivakumar S, Agrawal N et al. Silencing of midgut aminopeptidase N of *Spodoptera litura* by double-stranded RNA establishes its role as *Bacillus thuringiensis* toxin receptor. *J Biol Chem* 2002; 277:46849-46851.
68. Gill M, Ellar D. Transgenic *Drosophila* reveals a functional in vivo receptor for the *Bacillus thuringiensis* toxin Cry1Ac. *Ins Mol Biol* 2002; 11:619-625.
69. Schwartz JL, Lu YJ, Sohnlein P et al. Ion channels formed in planar lipid bilayers by *Bacillus thuringiensis* toxins in the presence of *Manduca sexta* midgut receptors. *FEBS Lett* 1997; 412:270-276.
70. Lorence A, Darszon A, Bravo A. The pore formation activity of *Bacillus thuringiensis* Cry1Ac toxin on *Trichoplusia ni* membranes depends on the presence of aminopeptidase N. *FEBS Lett* 1997; 414:303-307.
71. Gómez I, Sánchez J, Miranda R et al. Cadherin-like receptor binding facilitates proteolytic cleavage of helix α -1 in domain I and oligomer prepore formation of *Bacillus thuringiensis* Cry1Ab toxin. *FEBS Lett* 2002; 513:242-246.
72. Zhuang M, Oltean DI, Gómez I et al. *Heliothis virescens* and *Manduca sexta* lipid rafts are involved in Cry1A toxin binding to the midgut epithelium and subsequent pore formation. *J Biol Chem* 2002; 277:13863-13872.
73. Simons K, Toomre D. Lipid rafts and signal transduction. *Nature Rev Mol Cell Biol* 2000; 1:31-39.
74. Cabiaux V, Wolff Ch, Ruysschaert JM. Interaction with a lipid membrane: a key step in bacterial toxins virulence. *Int J Biol Macromol* 1997; 21:285-298.
75. Pardo-López L, Gómez I, Rausell C et al. Structural changes of the Cry1Ac oligomeric prepore from *Bacillus thuringiensis* induced by N-acetylgalactosamine facilitates toxin membrane insertion. *Biochemistry* 2006; 45:10329-10336.
76. Pacheco S, Gómez I, Gill SS et al. Enhancement of insecticidal activity of *Bacillus thuringiensis* Cry1A toxins by fragments of a toxin-binding cadherin correlates with oligomer formation. *Peptides* 2008; 30:583-588.
77. Rausell C, Muñoz-Garay C, Miranda-CassoLuengo et al. Tryptophan spectroscopy studies and black lipid bilayer analysis indicate that the oligomeric structure of Cry1Ab toxin from *Bacillus thuringiensis* is the membrane-insertion intermediate. *Biochemistry* 2004; 43:166-174.
78. Chen J, Hua G, Jurat-Fuentes JL et al. Synergism of *Bacillus thuringiensis* toxins by a fragment of a toxin-binding cadherin. *Proc Natl Acad Sci USA* 2007; 104:13901-13906.
79. Muñoz-Garay C, Sánchez J, Darszon A et al. Permeability changes of *Manduca sexta* midgut brush border membranes induced by oligomeric structures of different Cry toxins. *J Membr Biol* 2006; 212:61-68.
80. Aronson AI, Chaoxianm G, Wu L. Aggregation of *Bacillus thuringiensis* Cry1A toxin upon binding to target insect larval midgut vesicles. *Appl Environ Microbiol* 1999; 65:2503-2507.
81. Tigue NJ, Jacoby J, Ellar DJ. The alpha-helix 4 residue Asn135, is involved in the oligomerization of Cry1Ac1 and Cry1Ab5 *Bacillus thuringiensis* toxins. *Appl Environ Microbiol* 2001; 67:5715-5720.
82. Herrero S, González-Cabrera J, Ferré J et al. Mutations in the *Bacillus thuringiensis* Cry1Ca toxin demonstrate the role of domains II and III in specificity towards *Spodoptera exigua* larvae. *Biochem J* 2004; 384:507-513.
83. Ihara H, Himeno M. Study of irreversible binding of *Bacillus thuringiensis* Cry1Aa to brush border membrane vesicles from *Bombyx mori* midgut. *J Invertebr Pathol* 2008; 98:177-183.
84. Rausell C, García-Robles I, Sánchez J et al. Role of toxin activation on binding and pore formation activity of the *Bacillus thuringiensis* Cry3 toxins in membranes of *Leptinotarsa decemlineata* [Say]. *Biochem Biophys Acta* 2004; 1660:99-105.
85. Pérez C, Muñoz-Garay C, Portugal LC et al. *Bacillus thuringiensis* subsp *israelensis* Cyt1Aa enhances activity of Cry11Aa toxin by facilitating the formation of a prepore oligomeric structure. *Cellular Microbiol* 2007; 9:2931-2937.
86. Likitvivanavong S, Katzenmeier G, Angsuthanasombat Ch. Asn183 in helix α 5 is essential for oligomerization and toxicity of the *Bacillus thuringiensis* Cry4Ba toxin. *Arch Biochem Biophys* 2006; 445:46-55.
87. Puntheeranurak T, Stroth C, Zhu R et al. Structure and distribution of the *Bacillus thuringiensis* Cry4Ba toxin in lipid membranes. *Ultramicroscopy* 2005; 105:115-124.
88. Ounjai P, Unger VM, Sigworth FJ et al. Two conformational states of the membrane-associated *Bacillus thuringiensis* Cry4Ba delta-endotoxin complex revealed by electron crystallography: implications for toxin-pore formation. *Biochem Biophys Res Commun* 2007; 36:890-895.

89. Vié V, Van Mau N, Pomarède P et al. Lipid-induced pore formation of the *Bacillus thuringiensis* Cry1Aa insecticidal toxin. *J Membr Biol* 2001; 180:195-203.
90. Jiménez-Juárez N, Muñoz-Garay C, Gómez I et al. *Bacillus thuringiensis* Cry1Ab mutants affecting oligomer formation are non toxic to *Manduca sexta* larvae. *J Biol Chem* 2007; 282:21222-21229.
91. Vachon V, Préfontaine G, Coux F et al. Role of helix 3 in pore formation by the *Bacillus thuringiensis* insecticidal toxin Cry1Aa. *Biochemistry* 2002; 41:6176-6184.
92. Girard F, Vachon V, Préfontaine G et al. Cysteine scanning mutagenesis of α -4 a putative pore lining helix of the *Bacillus thuringiensis* insecticidal toxin Cry1Aa. *Appl Environ Microbiol* 2008; 74:2565-2572.
93. Wu D, Aronson AI. Localized mutagenesis defines regions of the *Bacillus thuringiensis* δ -endotoxin involved in toxicity and specificity. *J Biol Chem* 1992; 267:2311-2317.
94. Schwartz JL, Juteau M, Grochulski P et al. Restriction of intramolecular movements within the Cry1Aa toxin molecule of *Bacillus thuringiensis* through disulfide bond engineering. *FEBS Lett* 1997; 410:397-402.
95. Gazit E, La Rocca P, Sansom MSP et al. The structure and organization within the membrane of the helices composing the pore-forming domain of *Bacillus thuringiensis* α -endotoxin are consistent with an umbrella-like structure of the pore. *Proc Natl Acad Sci USA* 1998; 95:12289-12294.
96. Nair MS, Dean DH. All domains of Cry1A toxins insert into insect brush border membranes. *J Biol Chem* 2008; 283:26324-26331.
97. Loseva OI, Toktopulo EI, Vasilev VD et al. Structure of Cry3A α -endotoxin within phospholipid membranes. *Biochem* 2001; 40:14143-14151.
98. Schwartz JL, Potvin L, Chen XJ et al. Single-site mutations in the conserved alternating-arginine region affect ionic channels formed by Cry1Aa, a *Bacillus thuringiensis* toxin. *Appl Environ Microbiol* 1997; 63:3978-3984.
99. Schwartz JL, Laprade R. Membrane permeabilization by *Bacillus thuringiensis* toxins: protein insertion and pore formation In: *Entomopathogenic bacteria: from laboratory to field application*. (ed J F Charles A Delécluse, C Nielsen-LeRoux) Kluwer Academic Publishers, 2000:199.
100. Lorence A, Darszon A, Díaz C et al. Delta-endotoxins induce cation channels in *Spodoptera frugiperda* brush border membrane in suspension and in planar lipid bilayers. *FEBS Letters* 1995; 360:353-356.
101. Peyronnet O, Vachon V, Schwartz JL et al. Ion channels induced in planar lipid bilayers by the *Bacillus thuringiensis* toxin Cry1Aa in the presence of gypsy moth (*Lymantria dispar*) brush border membranes. *J Membr Biol* 2001; 184:45-54.
102. Peyronnet O, Nieman B, Génèreux F et al. Estimation of the radius of the pores formed by the *Bacillus thuringiensis* Cry1C δ -endotoxin in planar lipid bilayers. *Biochim Biophys Acta* 2002; 1567:113-122.
103. Parker MW, Feil SC. Pore-forming protein toxins: from structure to function. *Progr Biophys Mol Biol* 2005; 88:91-142.
104. Rausell C, Pardo-López L, Sánchez J et al. Unfolding events in the water-soluble monomeric Cry1Ab toxin during transition to oligomeric prepore and membrane inserted pore channel. *J Biol Chem* 2004; 279:55168-55175.
105. Wirth MC, Georghiou GP, Federeci BA. CytA enables CryIV endotoxins of *Bacillus thuringiensis* to overcome high levels of CryIV resistance in the mosquito, *Culex quinquefasciatus*. *Proc Natl Acad Sci USA* 1997; 94:10536-10540.
106. Pérez C, Fernandez LE, Sun J et al. Bti Cry11Aa and Cyt1Aa toxins interactions support the synergism-model that Cyt1Aa functions as membrane-bound receptor. *Proc Natl Acad Sci USA* 2005; 102:18303-18308.

CHAPTER 12

Role of Heparan Sulfates and Glycosphingolipids in the Pore Formation of Basic Polypeptides of Cobra Cardiotoxin

Wen-guey Wu,* Siu-Cin Tjong, Po-long Wu, Je-hung Kuo and Karen Wu

Abstract

Cobra venom contains cardiotoxins (CTXs) that induce tissue necrosis and systolic heart arrest in bitten victims. CTX-induced membrane pore formation is one of the major mechanisms responsible for the venom's designated cytotoxicity. This chapter examines how glycoconjugates such as heparan sulfates (HS) and glycosphingolipids, located respectively in the extracellular matrix and lipid bilayers of the cell membranes, facilitate CTX pore formation. Evidences for HS-facilitated cell surface retention and glycosphingolipid-facilitated membrane bilayer insertion of CTX are reviewed. We suggest that similar physical steps could play a role in the mediation of other pore forming toxins (PFT). The membrane pores formed by PFT are expected to have limited lifetime on biological cell surface as a result of membrane dynamics during endocytosis and/or rearrangement of lipid rafts.

Introduction

Biological membrane consists of many glycoconjugates that promote protein-protein interaction. HS are a class of negatively charged glycosaminoglycans (GAGs) that are composed of heterogeneous disaccharide repeating units. The binding of HS with biologically active ligands, such as basic polypeptides of chemokines or cytokines,¹⁻⁴ plays a significant role in many disease and cell development.¹⁵ Glycosphingolipids usually exist in the outer leaflet of membrane bilayer as a dynamic lipid domain, termed as lipid raft and are crucial for cell signaling and membrane translocation.⁶⁻⁹ They are also targets for toxin bindings, as demonstrated by the interactions between the cholera toxin and GM1 glycosphingolipids, where they induce an oligomerization process that leads to pore formation. Although the significance of protein conformational changes during pore formation has been widely acknowledged,¹⁰⁻¹² the exact mechanisms that allow proteins to anchor and insert the cell membrane remain unclear. In this review, we will explain the significant role of other molecules distributed on cell surface, such as HS and glycosphingolipids, in membrane pore formation. Specific focus is placed on the PFT of three-fingered CTX, a basic polypeptide whose core structure is tightened by four disulfide linkages that minimize conformational change.

*Corresponding Author: Wen-guey Wu—National Synchrotron Radiation Research Center and Department of Life Science, National Tsing Hua University, 101 Kuang Fu Road 2nd Sec., Hsinchu 30043, Taiwan. Email: wgwu@life.nthu.edu.tw

Amphiphilic Properties of Three-Fingered CTXs

Cobra CTXs are β -sheet polypeptides with hydrophobic residues located mainly on the tips of the three-fingered loops (Fig. 1A,B). Similar to other basic proteins like defensin, anti-microbial and cell penetrating peptides,^{13,14} they contain positively charged clusters that interact with negatively charged molecules on the cell membranes. In the case of CTXs, most of their positively charged residues are flanking on the two sides of the continuous hydrophobic stretch formed by the

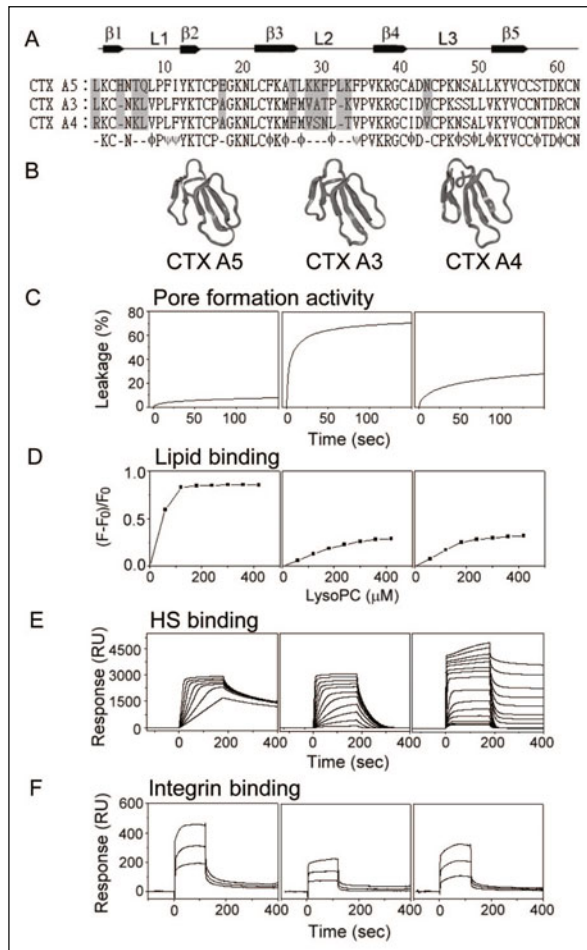


Figure 1. Structure and activity correlation of CTX homologues (A) Sequence alignment of CTX homologues indicates that amino acid residues located near the tips of loop 1 (L1) and loop 2 (L2) play an important role in target selection. The consensus sequence of CTX is also shown with symbols ϕ and ψ to indicate semi-conserved residues with similar physical property. (B) Three-fingered CTXs with similar β sheet structures among all CTX homologues (CTX A5 PDB ID: 1kxi; CTX A3 PDB ID: 1i02; CTX A4 PDB ID: 1kbs) (C) Representative traces of CTXs-induced leakage of fluorescence probe in sulfatide containing vesicles. (D) Representative binding isotherm as measured by the change of Tyr intrinsic fluorescence intensity after CTXs binding to Lyso-PC micelles. (E) Surface plasma resonance studies on the binding of CTXs to immobilized heparin. (F) Surface plasma resonance studies on the binding of CTXs to immobilized α v β 3 integrin. For the details, please see references 22,23,28.

three-fingered loops. While the CTXs share structural similarity, the amino acid groups on the loop ends differ exhibiting different lipid binding preferences.^{15,16} Most CTXs, although water-soluble, can bind to membrane lipid bilayers and induce leakage of membrane vesicles through pore formation activities. Interestingly, the lipid binding ability is not directly related to the toxin's pore forming property, suggesting that toxin insertion and oligomerization could be more significant in the pore formation processes. This is illustrated in Figure 1C,D, in which noncytotoxic CTX A5 with the highest membrane binding has the least pore forming activity.

Diverse Targets of CTX Homologues

In the crude venom, there are seven to ten CTX homologues with distinct biological activities.¹⁷⁻²¹ CTXs exhibit binding specificity toward not only HS and lipid, but also membrane proteins such as integrin (Fig. 1E,F). Recent X-ray structural determination of a CTX A3-heparin hexasaccharide complex revealed a structural basis responsible for the differences in the binding strengths among CTX homologues toward HS.²² The structure also suggests a molecular mechanism for toxin retention near the membrane surface, in which heparin-induced conformational changes of CTX A3 lead to citrate-mediated dimerization. Citrate is a major component of snake, bee, scorpion and ant venom and serves as a counter ion for the basic polypeptides of many types of venoms.

Despite of the overall structural similarity, not all CTX homologues are PFT (Fig.2A). A similar scenario should be considered for other basic polypeptides with pore forming activity. For instance, diverse activities of defensin homologues have been reported. While some defensins bring about membrane pore formation in bacteria, others could function as chemokines in order to promote cell-signaling process. Similarly the CTX A3 homologue A5 can bind with $\alpha_v\beta_3$ integrin to perturb the wound-healing processes of the bitten victim.²³ The synergistic action between the toxin-induced pore forming activity and toxin-induced cell signaling process is expected to be crucial for the overall cell cytotoxicity.

CTX A3 Pores in Sulfatide Containing Membranes

Although CTX A3 has been shown to induce membrane leakage in model membranes,¹⁵ the formation of specific membrane pores in biological membrane has only recently been demonstrated. First, whole cell recording of H9C2 cardiomyocytes by electrophysiological methods has demonstrated that CTX A3 could induce extra conductance formation in a voltage- and dose-dependent manner.²⁴ This is due to the single channel-like events as observed by the outside-out patch clamp experiments. However, CTX A3-induced conductance is sensitive to pretreatment of the cells with sulfatase, anti-sulfatide IgG or anti-sulfatide IgM, which indicates that sulfatide, a sulfated-galactose glycosphingolipid, is involved with the process. The dose-response curve of the sulfatide dependent CTX A3-induced conducting pathway corresponded roughly to the square of the CTX A3 concentration.²⁴ These results indicate that a bimolecular interaction, such as sulfatide-induced dimerization of CTX A3 molecules might be the rate-limiting step for the observed effect.

Pore Formations also Trigger Endocytosis

After CTX A3 form pore in H9C2 or rat cardiomyocytes, it becomes internalized. The internalization is due to endocytosis of the cell membrane as part of the membrane repair mechanism,²⁹ which also regulates the lifetime of the CTX A3 pore. This process involves the 3'-sulfated galactose headgroup of sulfatide, because either the removal of the preexisting sulfate moiety by sulfatase or blocking of the negatively charged sulfate through the pre-incubation of anti-sulfatide antibody can block the internalization of CTX A3. The extragenously added sulfatide-enhanced CTX A3 internalization further confirmed sulfatide as a membrane target of CTX A3 on the membrane surface. In fact, cocrystallization of sulfatide with CTX A3 in the presence of C₁₀E₆ detergent (an artificial membrane environment) shows that the sulfatide lipid headgroup is buried within the pocket formed by the CTX A3 dimer (PDB ID: 2bhi).

HS Facilitate Cell Surface Retention of CTXs

HS have been suggested to be responsible for inducing gradient of biologically active ligands, such as growth factors, near the cell membranes and mediate cell development. CTX contains positively charged cluster domains that are attracted to the anionic pockets of HS.²⁵ This electrostatic attraction leads to a local CTX enrichment because the multiple binding sites allows for cross-linking with HS in the extracellular matrix. By immobilizing Chinese hamster ovary cells in micro-capillary tubes and heparin on sensor chips, we showed that HS-mediated cell retention of CTX A3 near membrane surface is citrate dependent.²² This observation- together with crystal structure of CTX A3/HS complex (PDB ID: 1xt3), provides a structural basis of cell retention through the interaction of the molecules (Fig 2B). Not all CTX homologues behave similarly in the HS-induced cell surface retention; different CTX homologues target different cell type depending on their HS binding specificity.²⁶

HS Stabilizes Membrane Bound Form of CTX

Understanding HS-induced conformational change of GAG binding protein is essential for the study of its function. The X-ray structure of the FGF, FGF receptor and heparin ternary complex provides a basis for investigating the role of HS in FGF signaling.²⁷ Under the same token, proton NMR study on the binding of heparin-derived hexasaccharide to CTX A3 at the β -sheet region induces a *local* conformational change of CTX A3 near its membrane binding loops and promotes the binding activity of CTX toward phospholipid micelles.²⁸ The detected change is due to the structural coupling between the connecting loop and its β -strains without involving a *global* conformational change. This explains how the association of hydrophilic carbohydrate molecule of HS with amphiphilic proteins of CTX could initiate protein-lipid interaction without involving extensive structural alteration. A similar mechanism that favors the lipid-protein interaction through the HS binding may be operative at the membrane surface.

From HS to Membrane Sulfatides

Many toxins hijack GAGs in the extracellular matrix for specific targeting. The negatively charged HS may, therefore, serve as a high capacity region for concentrating basic toxins that can be specifically transferred to a glycosphingolipid domain in the outer leaflet of the membrane bilayer. Although CTX A3 fails to bind to gangliosides at the lipid rafts, it shows specificity in binding with sulfatide as a dimer.²⁴ Similar to cell signaling molecules, the location of sulfatide, with respect to proteoglycans that contain specific HS sequences, affect CTX pore forming activity significantly. Taken together, we suggest that animal toxins use a complex strategy to find their targets by using sequential events of binding to molecules that contain a similar motif within a protein molecule (Fig. 2).

Peripheral Binding Modes

The peripheral binding structural model of CTX A3/sulfatide complex in sulfatide containing phosphatidylcholine micelles has been determined by NMR and molecular docking methods.²³ The intermolecular NMR nuclear Overhauser effect has been observed in order to allow the computer docking of sulfatide headgroup against the available CTX A3 structure. The three-fingered hydrophobic loops of CTX A3 can be seen to penetrate into the fatty acyl region of the lipid bilayers (Fig. 3). Such a binding mode may allow a deep CTX A3 penetration into lipid bilayers without major conformational change of the structure. This is in sharp contrast to the sulfatide-CTX A3 complex structure determined by X ray method, which shows that the three-fingered hydrophobic loops are in opposite direction to the fatty acyl chain of sulfatide molecule.

Lipid Headgroup Conformational Change to Facilitate CTX Insertion

The relative orientation of sulfatide against CTX A3 in lipid bilayers is likely to change during the pore forming process- if the hydrophobic interaction between CTX A3 and sulfatide is to be maximized. In fact, in order to form a stable CTX A3 dimer with sulfatide chelated in between,

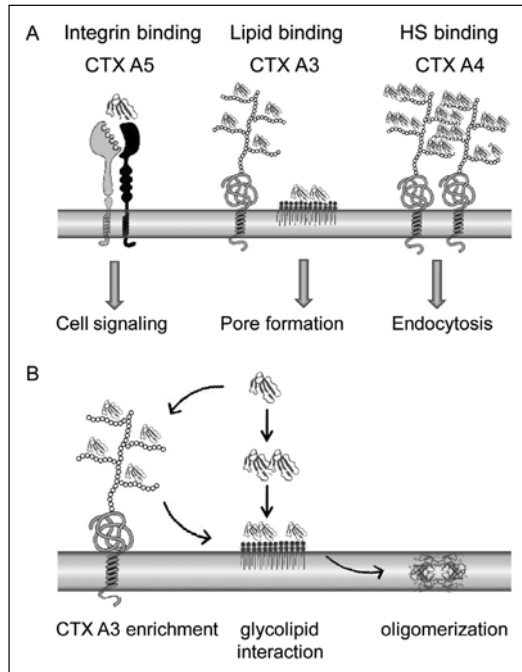


Figure 2. Schematic diagrams show how CTX homologues can interact with diverse targets on the cell membrane to trigger different cell response (A) and how HS in proteoglycan could facilitate cell surface retention of CTXs and its pore formation (B).

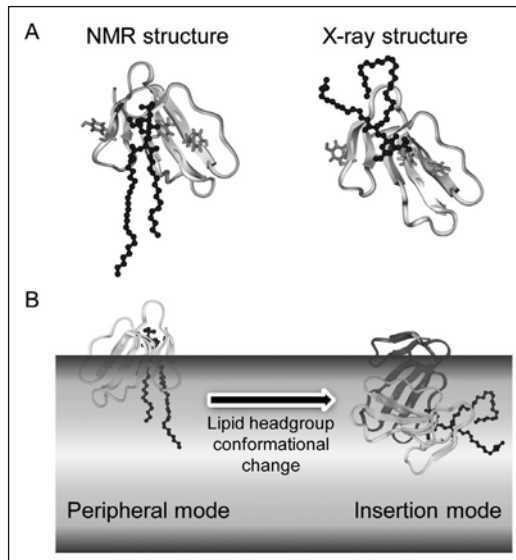


Figure 3. Available NMR and X-ray structures of sulfatide-CTX A3 complex (A) suggest that lipid headgroup conformational change play a role in the insertion and dimerization of CTX A3 (B) to account for the pore forming activity.

both the Gal-3S headgroup and the fatty acyl chain will have to experience *global* reorientation relative to the CTX A3 molecule. The sulfatide headgroup conformation will undergo sequential change from CTX free form of *-sc/ap/sc/ap* to the peripheral mode of *sc/ap/sc/ap* and then to the insertion mode of *sc/ap/ap/ap*.²⁹ Such a conformational change is likely to be soft and dynamic. Our results suggest a scenario for CTX A3 pore that is closer to the recent theoretical simulation for the distorted toroidal model,^{30,31} with lipid as an essential element³² to participate as an agent to stabilize the CTX dimer and a facilitator to promote CTX insertion and oligomerization during the pore formation process.

Pore Dynamics

The lifetime of CTX A3 pore formation in sulfatide containing vesicles has been studied by the quenching process of lipid vesicles using entrapped fluorescence probe. Assuming that the pore size of the vesicle fall in the range of 35 to 40 Å, the open lifetime of the pore can be determined to be longer than 1-3 msec.²⁹ The estimated lifetime of the CTX pore formed in vesicles is thus comparable to that of the lifetime of the sulfatide dependent single conductance in the biological membrane, as determined by the patch-clamp experiment. It should be noted that pore formation dynamics in the biological membrane also depend on the endocytosis process triggered by calcium influx.³³ The apparent consistency of the pore lifetime in the model and biological membranes should therefore be considered with caution. Nevertheless, we can investigate whether dynamics of nano-size lipid raft would affect the stability of the pore because glycosphingolipid functions as part of the pore.

Conclusion

The acidic glycoconjugates on membrane surface are shown to be able to interact with basic polypeptides of cobra CTX and induce pore formation. HS retain CTX at the membrane surface and induce the formation of membrane bound form; while the sulfatide lipid domain facilitates CTX dimerization and promote membrane insertion through lipid headgroup conformational change. Since many PFT are also basic polypeptides, the physical process established for cobra CTX might be applicable to the pore formation mechanism of PFT. It remains to be seen how the dynamics of lipid raft, the rate of calcium dependent endocytosis and the flip-flop process within lipid bilayer in the cell membrane, could mediate the dynamics of PFT pore formation.

Acknowledgements

This work was supported by grants from National Science Council, Taiwan.

References

1. Lindahl U. Heparan sulfate-protein interactions—a concept for drug design? *Thromb Haemost* 2007; 98:109-115.
2. Murphy JW, Cho Y, Sachpatzidis A et al. Structural and functional basis of CXCL12 (stromal cell-derived factor-1 alpha) binding to heparin. *J Biol Chem* 2007; 282:10018-10027.
3. Schenauer MR, Yu Y, Sweeney MD et al. CCR2 chemokines bind selectively to acetylated heparan sulfate octasaccharides. *J Biol Chem* 2007; 282:25182-25188.
4. Laguri C, Arenzana-Seisdedos F, Lortat-Jacob H. Relationships between glycosaminoglycan and receptor binding sites in chemokines—the CXCL12 example. *Carbohydr Res* 2008; 343:2018-2023.
5. Taylor KR, Gallo RL. Glycosaminoglycans and their proteoglycans: host-associated molecular patterns for initiation and modulation of inflammation. *FASEB J* 2006; 20:9-22.
6. Lajoie P, Goetz JG, Dennis JW et al. Lattices, rafts and scaffolds: domain regulation of receptor signaling at the plasma membrane. *J Cell Biochem* 2009; 185:381-385.
7. Holthuis JC, Levine TP. Lipid traffic: floppy drives and a superhighway. *Nat Rev Mol Cell Biol* 2005; 6:209-220.
8. Sillence DJ. New insights into glycosphingolipid functions—storage, lipid rafts and translocators. *Int Rev Cytol* 2007; 262:151-189.
9. Eggeling C, Ringemann C, Medda R et al. Direct observation of the nanoscale dynamics of membrane lipids in a living cell. *Nature* 2009; 457:1159-1163.
10. Gilbert RJC, Jimenez JL, Chen S et al. Two structural transitions in membrane pore formation by pneumolysin, the pore-forming toxin of *Streptococcus pneumoniae*. *Cell* 1999; 97:647-655.

11. Walz T. How cholesterol-dependent cytolysins bite holes into membranes. *Mol Cell* 2005; 18:393-394.
12. Tilley SJ, Orlova EV, Gilbert RJC et al. Structural basis of pore formation by the bacterial toxin pneumolysin. *Cell* 2005; 121:247-256.
13. Taylor K, Barran PE, Dorin JR. Structure-activity relationships in beta-defensin peptides. *Biopolymers* 2008; 90:1-7.
14. Aerts AM, François IE, Cammue BP et al. The mode of antifungal action of plant, insect and human defensins. *Cell Mol Life Sci* 2008; 65:2069-2079.
15. Chien KY, Chiang CM, Hseu YC et al. Two distinct types of cardiotoxin as revealed by the structure and activity relationship of their interaction with zwitterionic phospholipid dispersions. *J Biol Chem* 1994; 269:14473-14483.
16. Efremov RG, Volynsky PE, Nolde DE et al. Interaction of cardiotoxins with membranes: a molecular modeling study. *Biophys J* 2002; 83:144-53.
17. Lai MK, Wen CY, Lee CY. Local lesions caused by cardiotoxin isolated from Formosan cobra venom. *J Formosan Med Assoc* 1972; 71:328-332.
18. Hider RC, Khader F. Biochemical and pharmacological properties of cardiotoxins isolated from cobra venom. *Toxicon* 1982; 20:175-179.
19. Sun JJ, Walker MJ. Actions of cardiotoxins from the southern Chinese cobra (*Naja naja atra*) on rat cardiac tissue. *Toxicon* 1986; 24:233-245.
20. Dufton MJ, Hider RC. Structure and pharmacology of elapid cytotoxins. *Pharmacol Ther.* 1988; 36:1-40.
21. Fletcher JE, Jiang MH. Possible mechanisms of action of cobra snake venom cardiotoxins and bee venom melittin. *Toxicon* 1993; 31:669-695.
22. Lee SC, Guan HH, Wang CH. Structural basis of citrate-dependent and heparin sulfate-mediated cell surface retention of cobra cardiotoxin A3. *J Biol Chem* 2005; 280:9567-9577.
23. Wu PL, Lee SC, Chuang CC et al. Non-cytotoxic cobra cardiotoxin A5 binds to $\alpha_5\beta_1$ integrin and inhibit bone resorption. Identification of cardiotoxins as nonRGD integrin-binding proteins of the Ly-6 family. *J Biol Chem* 2006; 281:7937-7945.
24. Wang CH, Liu JH, Lee SC et al. Glycosphingolipid-facilitated membrane insertion and internalization of cobra cardiotoxin. *J Biol Chem* 2006; 281:656-667.
25. Tjong SC, Chen TS, Huang WN et al. Structures of heparin-derived tetrasaccharide bound to cobra cardiotoxins: Heparin binding at a single protein site with diverse side chain interactions. *Biochemistry* 2007; 46:9941-9952.
26. Vyas KA, Patel HM, Vyas AA et al. Glycosaminoglycans bind to homologous cardiotoxins with different specificity. *Biochemistry* 1998; 37:4527-4534.
27. Schlessinger J, Plotnikov AN, Ibrahimi OA et al. Crystal structure of a ternary FGF-FGFR-heparin complex reveals a dual role for heparin in FGFR binding and dimerization. *Mol Cell* 2000; 6:43-50.
28. Sue SC, Chien KY, Huang WN et al. Heparin binding stabilizes the membrane-bound form of cobra cardiotoxin. *J Biol Chem* 2002; 277:2666-2673.
29. Tjong SC, Wu PL, Wang CM et al. Role of glycosphingolipid conformational change in membrane pore forming activity of cobra cardiotoxin. *Biochemistry* 2007; 46:12111-12123.
30. Leontiadou H, Mark AE, Marrink SJ. Antimicrobial peptides in action. *J Am Chem Soc* 2006; 128:12156-12161.
31. Melo MN, Ferre R, Castanho MA. Antimicrobial peptides: linking partition, activity and high membrane-bound concentrations. *Nat Rev Microbiol* 2009; 7:245-250.
32. Dowhan W, Bogdanov M. Lipid-dependent membrane protein topogenesis. *Annu Rev Biochem* 2009; 78:5.1-5.26.
33. Idone V, Tam C, Goss JW et al. Repair of injured plasma membrane by rapid Ca²⁺-dependent endocytosis. *J Cell Biol* 2008; 180:905-914.

CHAPTER 13

Amyloid Peptide Pores and the Beta Sheet Conformation

Bruce L. Kagan* and Jyothi Thundimadathil

Abstract

Over 20 clinical syndromes have been described as amyloid diseases. Pathologically, these illnesses are characterized by the deposition in various tissues of amorphous, Congo red staining deposits, referred to as amyloid. Under polarizing light microscopy, these deposits exhibit characteristic green birefringence. X-ray diffraction reveals cross-beta structure of extended amyloid fibrils. Although there is always a major protein in amyloid deposits, the predominant protein differs in each of the clinical syndromes. All the proteins exhibit the characteristic nonnative beta-sheet state. These proteins aggregate spontaneously into extended fibrils and precipitate out of solution. At least a dozen of these peptides have been demonstrated to be capable of channel formation in lipid bilayers and it has been proposed that this represents a pathogenic mechanism. Remarkably, the channels formed by these various peptides exhibit a number of common properties including irreversible, spontaneous insertion into membranes, production of large, heterogeneous single-channel conductances, relatively poor ion selectivity, inhibition of channel formation by Congo red and related dyes and blockade of inserted channels by zinc. In vivo amyloid peptides have been shown to disrupt intracellular calcium regulation, plasma membrane potential, mitochondrial membrane potential and function and long-term potentiation in neurons. Amyloid peptides also cause cytotoxicity. Formation of the beta sheet conformation from native protein structures can be induced by high protein concentrations, metal binding, acidic pH, amino acid mutation and interaction with lipid membranes. Most amyloid peptides interact strongly with membranes and this interaction is enhanced by conditions which favor beta-sheet formation. Formation of pores in these illnesses appears to be a spontaneous process and available evidence suggests several steps are critical. First, destabilization of the native structure and formation of the beta-sheet conformation must occur. This may occur in solution or may be facilitated by contact with lipid membranes. Oligomerization of the amyloid protein is then mediated by the beta strands. Amyloid monomers and extended fibrils appear to have little potential for toxicity whereas there is much evidence implicating amyloid oligomers of intermediate size in the pathogenesis of amyloid disease. Insertion of the oligomer appears to take place spontaneously although there may be a contribution of acidic pH and/or membrane potential. Very little is known about the structure of amyloid pores, but given that the amyloid peptides must acquire beta-sheet conformation to aggregate and polymerize, it has been hypothesized that amyloid pores may in fact be beta-sheet barrels similar to the pores formed by alpha-latrotoxin, Staphylococcal alpha-hemolysin, anthrax toxin and clostridial perfringolysin.

*Corresponding Author: Bruce L. Kagan—Department of Psychiatry and Biobehavioral Sciences, Semel Institute for Neuroscience and Human Behavior, David Geffen School of Medicine at UCLA, Los Angeles, California, USA. Email: bkagan@mednet.ucla.edu

Introduction

The 19th century term “amyloid” was coined by Rudolf Virchow upon his viewing amorphous starch-like deposits that stained with iodine, thinking that they were largely composed of carbohydrates. However, these deposits were later found to be largely proteinaceous, although there was a carbohydrate component consisting of glycosaminoglycans. The deposits show a characteristic staining pattern with dyes such as Congo red and exhibit green birefringence under polarized light. Electron microscopy studies showed fibrils with a width of 1800 angstroms and often indeterminate length (for a review see ref. 1). A large number of distinct clinical syndromes have now been reported to exhibit the same pathological features (see Table 1). In each case, a unique protein which forms amyloid fibrils has been demonstrated to be the chief component of these deposits. The various proteins which form amyloid do not exhibit any primary sequence homology, common biophysical characteristics, or similar biochemical functions. However, they all share the ability to convert under the appropriate conditions into the beta-sheet conformation. The most intensively investigated amyloidosis is Alzheimer’s disease (AD). Recent investigations strongly implicated the Alzheimer amyloid peptide A-beta in the pathogenesis of this illness. While the detailed molecular mechanism by which A-beta causes cellular and tissue dysfunction has remained controversial, pore formation in plasma or mitochondrial membranes has become a leading theory of pathogenesis. A-beta pore blockers discovered *in vitro* have shown the ability to protect cells in culture from A-beta cytotoxicity. Over a dozen pore forming amyloid peptides

Table 1. Diseases of protein misfolding: amyloidoses

Disease	Protein	Abbreviation
Alzheimer’s disease, Down’s syndrome (Trisomy 21), Heredity cerebral angiopathy (Dutch)	Amyloid precursor protein (Abeta 1-42)	APP (Abeta 1-42)
Kuru, Gerstmann-Straussler-Scheinker Syndrome (GSS), Creutzfeld-Jacob disease, Scrapie (sheep) Bovine spongiform encephalopathy (“mad cow”)	Prion protein	PrP ^c /PrP ^{Sc}
Type II diabetes mellitus (adult onset)	Islet amyloid polypeptide (amylin)	IAPP
Dialysis-associated amyloidosis	Beta-2-microglobulin	B2M
Senile cardiac amyloidosis	Atrial natriuretic factor	ANF
Familial amyloid polyneuropathy	Transthyretin	TTR
Reactive amyloidosis familial mediterranean fever	Serum amyloid A	SAA
Familial amyloid polyneuropathy (Finnish)	Gelsolin	Agel
Macroglobulinemia	Gamma-1 heavy chain	AH
Primary systemic amyloidoses	Ig-lambda, Ig-kappa	AL
Familial polyneuropathy—Iowa (Irish)	Apolipoprotein A1	ApoA1
Hereditary cerebral myopathy—Iceland	Cystatin C	Acys
Nonneuropathic hereditary amyloid with renal disease	Fibrinogen alpha	AFibA
Nonneuropathic hereditary amyloid with renal disease	Lysozyme	ALys
Familial British dementia	FBDP	A Bri
Familial Danish dementia	FDDP	A Dan

have been reported (see Table 4) including amylin (or islet amyloid polypeptide, IAPP), prion proteins (PrP), beta-2 microglobulin, serum amyloid, atrial natriuretic factor, polyglutamine, transthyretin, alpha synuclein (AS), calcitonin, lysozyme, human stefin B, Ure2p, HypF-N and proteins associated with Danish and British familial dementia.²⁻¹⁶

Aggregation and Fibril Formation: Hallmark of Amyloid Peptides

Amyloid peptides are defined in part by their ability to adopt beta sheet conformation and to form extended fibrillar aggregates, which precipitate out of solution. In the early 1990s, the discovery of familial forms of amyloidoses linked to specific mutations in amyloid proteins lent credence to the idea that amyloid proteins themselves played a direct role in the pathogenesis of disease.¹⁷⁻¹⁹ The amyloid theory of AD was strengthened by research that showed that the A-beta 1-42 peptide could be toxic to cells in vitro and specifically to neurons, which were the cell types lost in the disease itself. Furthermore, PrP106-126 was shown to be neurotoxic and amylin was shown to be toxic to pancreatic beta cells, which are the cells that die in type II diabetes mellitus.^{20,21} These studies also showed that while amyloid fibrils or monomers lack toxicity, some kind of amyloid peptide aggregation was essential for cell toxicity. Indeed, early experiments in this regard were plagued by a lack of reproducibility of cytotoxicity. This was eventually clarified by the studies of Pike et al²² which showed the differences in the aggregation state of A-beta under different experimental conditions could lead to differing cytotoxic potencies. Harper and Lansbury showed that the aggregation of amyloid peptides was a highly complex and variable process.²³ The initial phases of monomer aggregation tended to occur quite slowly. However, once a critical mass or seed was achieved, addition to this aggregate tended to proceed quite rapidly. Aggregate growth could be accelerated by the addition of seeds to a solution of monomers. Thus, the variability of the aggregation process was likely responsible for the many differing results found in the early 1990s regarding cytotoxicity of amyloid peptides. Eventually it became clear that amyloid peptide aggregation was a necessary condition for cytotoxicity. However, too much aggregation could actually lead to a decline in toxicity when the aggregates became too large.²⁴ Transgenic mouse models of AD show learning and memory deficits before the development of significant amyloid deposits, but correlate better with the presence of oligomeric forms of A-beta.²⁵ It has also been demonstrated that oligomeric forms of A-beta can inhibit long-term potentiation as well as synaptic growth.²⁶ Nonfibrillar aggregates were also shown by atomic force microscopy to be critical for A-beta mediated cytotoxicity in fibroblasts.²⁷ These smaller oligomeric aggregates appeared to form quite rapidly on addition of peptide to aqueous solution. Oligomeric aggregates were also implicated in cytotoxicity mediated by AS and amylin.²⁸⁻²⁹

Kayed et al (2003) developed an antibody to soluble oligomers which recognized this conformation in several different amyloid peptides.³⁰ The antibody was able to block cytotoxicity of a variety of amyloid peptides of varying sequences, suggesting that this conformation was common to these various peptides and that they shared a common toxicity mechanism. This group went on to propose that these amyloid oligomers mediated toxicity through a nonchannel permeabilization of membranes. This was postulated to occur by a thinning of the membrane without direct penetration of the peptide into the lipid bilayer. This work was quite controversial as it contrasted with the numerous reports from various laboratories of pore formation by many different amyloid peptides. (for review see ref. 31). Recent results by Capone et al³² indicate that the nonchannel permeabilities seen by this group are most likely the result of contamination from the solvent HFIP. The solvent is used to prepare the soluble oligomers from these various peptides and can be difficult to remove completely. Capone et al also showed that HFIP could not only permeabilize membranes in a graded nonchannel fashion, but was also cytotoxic to the various cell types that were killed by these amyloid peptides. They went on to demonstrate that discrete pores were easily observed once the HFIP was removed.

It remains a mystery as to why such a rich variety of primary sequences of proteins and peptides can form such similar amyloid aggregates and fibrils. Indeed several non-amyloid disease proteins (Table 2) and nondisease associated proteins (Table 3) have been shown to form amyloid. Biological

Table 2. Diseases of protein misfolding: non-amyloidoses

Disease	Protein	Abbreviation
Diffuse Lewy body disease, Parkinson's disease	Alpha-synuclein	AS
Fronto-temporal dementia	tau	tau
Amyotrophic lateral sclerosis	Superoxide dismutase-1	SoD-1
Triplet-repeat diseases: (Huntington's, Spinocerebellar ataxias, etc.)	Polyglutamine tracts in the following proteins: <i>Huntingtin</i>	PG
Spinal and bulbar muscular atrophy	Androgen receptor	
Spinocerebellar ataxias	Ataxins	
Spinocerebellar ataxia 17	TATA box-binding protein	

function and three dimensional structures of proteins have long been assumed to be a direct result of the primary amino acid sequence. However, amyloid proteins appear to adopt a similar conformation despite highly divergent primary sequences. It is also now well established that the native amyloid proteins may be destabilized or unfold to a certain degree to catalyze the formation of beta-sheet conformation and then aggregation. The unfolding and changed beta-sheet conformation may open up new hydrogen bonding possibilities and thermodynamically drive aggregation. The hydrophobic effect requiring hydrophobic amino acids to be shielded from the aqueous environment may also thermodynamically contribute to the drive for these proteins to aggregate. Beta sheets as well tend to self-aggregate, catalyzed by their propensity to form intermolecular bonds. It is of note that proteins with hydrogen bonding defects have a strong propensity to interact with lipid membranes.³³ Thus, emerging evidence suggests that the beta-sheet conformation plays a critical role in enhancing both the aggregation of amyloid peptides and their interaction with phospholipid membranes.

Protein misfolding can be catalyzed by mutations, low pH, oxidation, proteolysis, increased concentration, high temperature, or interactions with metal ions. All of these have been shown to play a role in the destabilization and formation of various amyloid proteins.³⁴ Lipid membranes may also play an important role in catalyzing the destabilization of native conformation in the aggregation of amyloid proteins. For example, McLaurin et al³⁵ have shown that lipid membranes

Table 3. Nondisease related amyloid forming proteins/peptides

SH3 domain p 85 phosphatidylinositol—3-kinase	Fibronectin type III phosphoglycanase acylphosphatase
HypF N-terminal domain (<i>E.coli</i>)	Amphoterin (human)
Apomyoglobin (equine)	Apocytochrome c
Endostatin (human)	Met aminopeptidase
Stefin B (human)	ADA2H
Fibroblast growth factor (<i>N. viridescens</i>)	Apolipoprotein CII
VI domain (murine)	B1 domain of IgG binding protein
Curlin CgsA subunit	Monellin

can enhance the tendency of amyloid peptides to enter the beta-sheet conformation and their tendency to aggregate. Thus, a variety of lines of evidence now seem to converge on the idea that there is a tight linkage between beta-sheet conformation, amyloid peptide aggregation and binding and insertion of these proteins into lipid membranes.

Interaction of Amyloid Peptides and Membranes during Ion Channel Formation

Amyloid-Beta Peptide

The interaction of A-beta has been studied in great detail in model lipid bilayers as well as cellular membranes. Unfortunately, there is a fair degree of conflicting evidence from a large number of studies. At least some of this conflict has arisen from the propensity of the A-beta molecule to self-aggregate, initially into oligomeric forms and later into protofibrils and fibrils. This propensity to aggregate and form fibrils is the basis for amyloid formation. However, because of the nonlinear nature of this process the measurement of A-beta interactions with membranes has been subject to some error, depending on whether the predominant species is monomeric, oligomeric, protofibrillar or fibrillar. Nevertheless, some fairly clear generalizations have emerged.

There has been a long and intensive search for membrane receptors for A-beta. Although many have been proposed, including tachykinin receptors, serpin enzyme complex receptors, integrins, P75 neurotrophin receptors and the receptor for advanced glycosylation end-products (RAGE), the evidence for these proteins being true receptors of A-beta remains limited. Furthermore, there is now an overwhelming body of evidence that indicates that A-beta peptides can interact directly with phospholipid bilayer membranes lacking any proteins whatsoever. These interactions include not only binding but membrane insertion and ion channel formation, as well as cytotoxic properties. This indicates that there is no need to invoke a proteinaceous receptor for A-beta and for its toxic effects. In studies with both planar lipid membranes and liposomes, several conclusions have emerged. First, anionic phospholipids appear to be essential for A-beta binding and insertion.³⁵⁻⁴¹ Although A-beta appears to bind to neutral phospholipids, these lipids do not appear to be capable of allowing membrane insertion. This interaction is sensitive to ionic strength as would be expected for a charge-charge interaction.⁴¹ When A-beta is incorporated into the membrane, it adopts a toxic beta sheet structure, which disrupts the membrane more severely. When unstructured, A-beta is associated with the membrane surface. Data from IR spectra and high sensitivity circular dichroism indicates it is the interaction of A-beta with phospholipids which catalyzes the insertion of the molecule into the membrane.⁴² The insertion of this beta sheet structure is consistent with one of the theoretical models proposed by Durell et al of the A-beta ion channel structure.⁴³ It is also consistent with more recent mathematical models proposed by Jang et al.⁴⁴ In solution, A-beta maintains an equilibrium amongst beta sheet, alpha helix and random coil conformations. Contact with uncharged lipids does not appear to affect the conformation of A-beta in solution and indeed there seems to be little binding of A-beta to membranes formed from neutral phospholipids.³⁶ Lee et al (2002) showed that an apolipoprotein E2 which bound phosphatidylserine could competitively inhibit the toxicity of A-beta peptide.⁴⁵ A-beta has also been suggested to bind other components of the plasma membrane, including GM1^{46,47} Yanagisawa et al⁴⁸ identified a unique A-beta peptide species in Alzheimer's disease brain which was characterized by strong binding to GM1. They proposed that A-beta's conformation was altered by GM1 binding, creating a seed for amyloid aggregation.

Cholesterol has also been demonstrated to play a key role in the interaction of A-beta with membranes. Increasing amounts of cholesterol in planar lipid bilayer membranes, liposomal membranes and cellular membranes inhibit A-beta channel insertion but without affecting A-beta binding.^{35,37} Furthermore, depleting membranes of cholesterol, thus increasing membrane fluidity, facilitates peptide insertion and pore formation.⁴⁹ More recent data using synchrotron radiation circular dichroism of A-beta incorporated into lipid bilayers suggests that incorporated A-beta has more beta sheet structure compared to when A-beta is just bound to membranes. This is consistent with other data suggesting that membrane insertion alters the conformation of A-beta peptides.

Table 4. Pore properties of amyloid peptides

Peptide	Ring Diameter (Inner/Outer, in Angstroms Microscopy)	Single Channel Conductance	Ion Selectivity (Permeability Ratio)	Blockade by Zinc	Inhibition by Congo Red	Reference
A β 25-35		10-400 pS	Cation ($P_K/P_{Cl} = 1.6$)	+	+	85,86
A β 1-40		10-2000 pS	Cation ($P_K/P_{Cl} = 1.8$)	+		37
A β 1-40		50-4000 pS	Cation ($P_K/P_{Cl} = 11.1$)	+		87,88
A β 1-40 ARC (E22G)	15-20/70-100					89
A β 1-42		10-2000 pS	Cation ($P_K/P_{Cl} = 1.8$)	+	+	37
CT105 (C-terminal fragment of Amyloid precursor protein (APP))		120 pS	Cation	+	+	90
Islet amyloid polypeptide (Amylin)		7.5 pS	Cation ($P_K/P_{Cl} = 1.9$)	+	+	51
PrP106-126		10-400 pS	Cation ($P_K/P_{Cl} = 2.5$)	+	+	60
PrP106-126		140, 900, 1444 pS	Cation ($P_K/P_{Cl} > 10$)			91
PrP 82-146			Cation (variable)			12,63
Serum amyloid A		10-1000 pS	Cation ($P_K/P_{Cl} = 2.9$)	+	+	9
SAA 2.2 (murine hexamer)	25/80					92
C-type natriuretic peptide		21, 63 pS	Cation ($P_K/P_{Cl} > 10$)	+	+	93,94
Atrial natriuretic factor		68, 160, 273 pS	Variable			5
Beta2-microglobulin		0.5-120 pS	Non-selective	+	+	3
Transthyretin		Variable	Cation (Variable)	+	+	7
Polyglutamine (AVG MW = 6000)		19-220 pS	Non-selective	-	-	6
Polyglutamine 40		17 pS	Cation			95

Continued on next page

Table 4. Continued

Peptide	Ring Diameter (Inner/Outer, in Angstroms Microscopy)	Single Channel Conductance	Ion Selectivity (Permeability Ratio)	Blockade by Zinc	Inhibition by Congo Red	Reference
NAC (alpha-synuclein 65-95)		10-300 pS	Variable	+	+	8,31
Alpha synuclein A30P or A53T	20-25/80-120					29
Calcitonin						10
Human		2 pS	Non-selective			
Salmon		580 ps				
Lysozyme 87-114	Permeable to β -Galactosidase MW 116 kD		Non-selective			95,96
Cu/Zn superoxide dismutase	50/190					97
ABri ADan		Variable	N.D.	+	+	13

A critical issue is the aggregation state of A-beta upon binding and insertion into membranes. Data from Hirakura et al.³⁷ indicated that monomeric A-beta could not form pores, although it was unclear whether this inhibition represented an inhibition of binding to membranes or an inhibition of the insertion step. The heterogeneity of A-beta pores observed in planar lipid bilayer membranes has suggested that different sized oligomers of A-beta might be forming these pores with different conductances. In fact, conductances of A-beta pores range over several orders of magnitude, thus indicating that the variation in oligomer size may be quite dramatic. Several observations suggest that oligomer formation occurs prior to membrane binding and insertion. First, evidence cited above that monomerization of A-beta preparations inhibits channel activity, as well as toxicity despite the fact that monomers are known to be able to insert into liposomal membranes, strongly suggests that the oligomers required for pore formation form prior to membrane insertion. Second, aging of A-beta peptides or treatment at low pH prior to membrane exposure causes a dramatic increase in both channel activity and single channel conductance. Both these treatments are known to increase A-beta aggregation and oligomer formation. This data suggests that the oligomers can form in solution prior to interaction with the membranes. Third, the addition of Congo red, an agent which binds strongly to A-beta and inhibits aggregation and fibril formation, also inhibits channel formation. If A-beta monomers were able to insert in the membrane and then combine there, Congo red would not be able to inhibit them. Fresh and globular A-beta, which has not had time to extensively aggregate, has been shown to rapidly bind to and permeabilize fibroblast membranes to calcium.²⁷ Finally reduced membrane fluidity decreases membrane insertion and permeabilization but not binding, which is dependent on negatively charged lipids.³⁶

Amylin (or Islet Amyloid Polypeptide, IAPP)

Type 2 Diabetes mellitus (DM) is a common disease in the United States and the world with nearly 20 million sufferers in the United States alone. In addition to the direct effect on blood vessels throughout the body associated with hyperglycemia, individuals with DM suffer from elevated rates of strokes, hypertension, coronary artery disease, kidney disease and infections. Although insulin resistance is a major issue in DM, a second major pathology is mediated by amylin. This 37-residue peptide is a hormone cosecreted with insulin in the same vesicles located in the beta cells of the pancreas in the islets of Langerhans. The physiological role of amylin is not well understood. It is known that the normal ratio of amylin to insulin of 1:50 increases as DM progresses. Amyloid deposits consisting largely of amylin are strongly correlated with the clinical severity of DM, and are inversely proportional to beta cell mass in the pancreas.⁵⁰ In vitro, amylin has been shown to be toxic to beta cells²¹ and there is now strong evidence that the mechanism of this toxicity is channel formation by amylin. Rat amylin which differs from human at only 5 amino acid residues, is non-amyloidogenic and nontoxic.^{28,51} Rats and mice do not suffer from diabetes. Transgenic mice carrying the human form of amylin develop a diabetes-like illness characterized by fibrillar deposits of amylin as well as hyperglycemia. The S20 gene mutation of amylin has been linked to a familial form of early-onset DM. S20 amylin peptide is more cytotoxic than wild-type amylin and has a tendency to aggregate much more quickly⁵² (see also ref. 53 for review).

Several groups have shown that the presence of lipid membranes catalyzes the aggregation of amylin.⁵⁴⁻⁵⁸ Anionic lipids are particularly strong enhancers of aggregation. This is believed to be due to an electrostatic interaction between positive charges on the amylin peptide and the negative charges on the lipids. Additional evidence comes from the demonstration that membrane-mediated aggregation is strongly inhibited by ionic strength. In solution amylin is primarily a random coil structure, with only relatively small amounts of beta-sheet or alpha-helical conformation.^{56,58} When amylin aggregates, it becomes fibrillar, adopting beta sheet conformation in the process. Spectroscopic studies have indicated that the membrane-mediated aggregation of amylin occurs through a transient alpha-helical conformation. Approximately half of the peptide is incorporated into alpha helical structure upon interaction with membranes containing negatively charged lipids. The remainder of the peptide appears to remain in an unfolded state. The amyloidogenic region residues 20 to 29, would then be allowed to come into intermolecular contact in the process of aggregation.⁵⁶

Studies by Mirzabekov et al⁵¹ are consistent with this view. Using planar lipid bilayers, they showed that human amylin readily formed ion pores at physiologic pH and concentration whereas rat amylin did not. Furthermore, they demonstrated a strong dependence on lipid composition with amylin channel activity inversely proportional to the amount of negative surface charge in the membrane. They further demonstrated that increasing ionic strength dramatically inhibited amylin pore activity. These investigators also reported that amylin pores were irreversibly associated with the membrane. Preincubation with Congo red inhibited amylin channel activity and zinc was capable of blocking channels in a reversible manner. Intriguingly, unlike virtually every other amyloid peptide, amylin displayed a unique and homogeneous single channel conductance suggesting that unlike other amyloid peptides, the channel was formed by aggregates of a unique molecular species with defined size, ion selectivity and voltage dependent behavior. Other studies have confirmed the membrane permeabilizing and pore forming activity of amylin and demonstrated that it is the basis for the observed cytotoxicity of beta cells.²⁸

A tantalizing clue to the insertion process is the fact that addition of even small amounts of cholesterol to the membranes strongly inhibits amylin channel formation. This membrane stiffening effect of cholesterol would make it harder for the amylin peptide to insert, in contrast with pore-forming cytolysins which are dependent on the presence of cholesterol in the membrane to form pores. This inhibition by cholesterol, which has been observed for A-beta as well, seems to mark a strong distinction between the pore-forming cytolysins and the amyloid peptide pores.

Prion Peptides

Prion protein, PrP, can convert between 2 tertiary conformations known as PrP-C for the normal cellular prion protein and PrP-Sc for the scrapie version. PrP-Sc is responsible for transmissible neurodegenerative diseases, such as scrapie in sheep and mad cow disease. Human forms of prion disease include kuru, Creutzfeldt-Jakob, Gerstmann-Straussler-Scheinker syndrome and fatal familial insomnia. The nature of these illnesses can be hereditary, infectious, or sporadic. Mutations in the prion protein are responsible for hereditary forms of these illnesses.⁵⁹ Susceptibility to transmissible prion diseases requires that the cellular form of prion protein be present in the susceptible cell. There is evidence to suggest that PrP-Sc is able to induce a conformational transition in PrP-C which is propagated throughout the host resulting in disease. The cellular mechanism and pathogenesis of prion diseases remains elusive, but pore formation by the prion protein has been proposed as a toxic mechanism.⁶⁰ Regions of the prion protein which are predicted from their primary sequence to be alpha-helical peptide have been noted to form beta sheet peptides when synthesized. These beta sheet peptides are capable of self-aggregation into amyloid fibrils, very similar to those found in prion-related encephalopathy. Furthermore, it is also well established that the major difference in conformation between PrP-C and PrP-Sc is that alpha-helical regions of PrP-C have been converted to beta sheet conformation in PrP-Sc.⁶¹ One of these regions, PrP 106-126 is capable of self-aggregation and known to bind to membranes.⁶² This peptide has also been demonstrated to be neurotoxic to cultured cells.²⁰ Lin et al⁶⁰ demonstrated that this peptide was capable of pore formation in planar lipid bilayers at neurotoxic concentrations. This pore formed rapidly, spontaneously and irreversibly. Treatments which caused PrP 106-126 to self-aggregate at an increased rate, such as aging in solution or exposure to acidic pH, caused a dramatic increase in the channel-forming activity of this peptide. Furthermore, the single channel conductances were shifted to larger conductances suggesting that the larger oligomers formed after peptide aging or acid exposure formed structurally larger pores. This aggregation took place independently of the presence of membranes. A much larger segment of the prion protein was later shown to form pores, PrP 82 to 145, which is the peptide found in the amyloid in the brains of patients with Gerstmann-Straussler-Scheinker syndrome, but the 106-126 sequence was essential to pore formation.⁶³

The PrP 106-126 pores can be inhibited by preincubation with Congo red indicating that they must be in beta sheet structure to aggregate and form pores. Zinc ion is capable of reversibly blocking these pores after they have formed. At least one other segment of the prion protein, PrP

170-175, which bears the mutation that results in schizoaffective disorder, N171, has been found to form pores in planar lipid bilayers.¹⁵ The pores induced by this peptide have a conductance of 8 to 26 pS, in 0.5 M potassium chloride. The native PrP 170-175 does not form pores. Thus, a mutation resulting in a pore-forming peptide appears to induce disease in humans. These observations suggest that conformational transitions and oligomer formation are critical to prion disease pathogenesis.

Alpha-Synuclein

Alpha-synuclein (AS) is a synaptic protein of length 140 amino acids, which is the primary component of the amyloid deposits found in Lewy bodies of patients with Parkinson's disease (PD). The peptide NAC, (an acronym for the misnomer "non-amyloid component") which consists of residue 66-95 of AS is the actual fragment of the protein found in these amyloid deposits. Mutations in AS have been associated with familial cases of Parkinson's disease. Both full length AS and NAC, have been demonstrated to be capable of permeabilizing lipid vesicles and planar lipid bilayers in a pore-like fashion.^{8,64,65} Using electron microscopy, AS was shown to form annular pore-like oligomeric structures.⁶⁶ Mutations in AS which lead to familial PD accelerated the formation of these structures. Similar structures had been described by this group with the A-beta peptide of AD when it contained the "arctic" mutation.

While beta sheet structures are the hallmark of amyloid proteins, AS may adopt different conformations in its pathogenic role. Zakharov et al⁶⁵ showed that the protein which is natively disordered in an aqueous environment becomes highly alpha-helical upon interaction with phospholipid membranes. Intriguingly, these investigators used monomeric wild-type AS. The monomeric form required phosphatidylethanolamine and 25-50% anionic lipid and a transnegative membrane potential for pore formation. Two familial PD causing mutants, E46K and A53T, also formed pores but another disease causing mutation, A30P, which has a lower membrane affinity, did not appear to form pores. These pores were inhibited by calcium that was preadded to the membrane and calcium decreased channel conductance as well. Oligomeric AS was also capable of creating a permeability increase in the membrane but did not appear to form discrete channels. Oligomeric AS also did not have a requirement for phosphatidylethanolamine or membrane potential, thus, indicating perhaps different mechanisms of membrane interaction and disruption. Channel activity and alpha-helical content of AS were correlated as determined by fluorescence correlation spectroscopy. The mechanism of the membrane disruption by oligomeric AS remains somewhat undefined.

NAC channels exhibited properties very similar to that of other amyloid peptides, i.e., NAC channels could be inhibited by Congo red, an inhibitor of amyloid fibrillization and blocked by zinc ions.⁸ The NAC channels also showed a heterogeneous dispersion of single channel conductances perhaps indicating various oligomeric states of the NAC peptide. The channels were long-lived, reversibly associated with the membrane and poorly selective amongst physiological ions.

Similarities between Pore-Forming Toxins and Amyloid Pores

Structural and functional similarities between bacterial pore-forming toxins (porins) and amyloid pore-forming proteins have been noted previously. Atomic force microscopy (AFM) imaging studies of A-beta peptides revealed the formation of doughnut shaped structures protruding out of the membrane surface with a centralized pore-like depression presumably representing individual pores.²⁷ Theoretical models of A-beta peptides suggest a transmembrane annular polymeric structure.⁶⁷ On the basis of the effects of pH, Congo red binding and solvents on amyloid beta 1-42 pores Kagan and coworkers hypothesized the formation of β barrel structures similar to the pore structures described for porins.³⁷ Porins are pore forming proteins found in the outer membrane of gram negative bacteria, mitochondria and chloroplast.⁶⁸⁻⁷² These proteins form one of the two distinct structural classes of integral membrane proteins called β barrel membrane proteins (transmembrane β barrels, TMBs) as they have membrane spanning segments formed by antiparallel β strands creating a channel in the form of a β barrel. In addition to these native proteins, the β barrel motif is also used by a large

diverse set of secreted membrane permeabilizing protein toxins (pore forming toxins or PFTs) that assemble into β barrels on exogenous membranes.⁷³ The main difference between TMBs and PFTs is that, in the former a β barrel is formed by the folding of a single polypeptide chain, while in the latter through the association of several individual β strand monomers. Like PFTs, the amyloid proteins require aggregation and membrane surface activation to initiate pore formation. PFTs are usually water-soluble monomers that are converted through this process into a membrane inserted pore. There is often a conformational change involved as there is with amyloid proteins which undergo a conformational change from a native structure into a beta-sheet structure. The bacterial toxins, latrotoxin, alpha-hemolysin, aerolysin and anthrax toxin have all been demonstrated to form oligomeric membrane-spanning beta-barrel pores. The beta-barrels comprise approximately 8 to 22 beta strands of about 10 to 13 residues each. Average pore diameter is in the range of 1.5 to 3.5 nm for the PFTs, comparable to the pore diameters reported for amyloid proteins. It should be noted, however, that certain kinds of PFTs such as streptolysin O and perfringolysin O can form much larger pores from 15 to 45 nm.^{74,75} There are no reports of pore sizes this large for amyloid proteins, however, the large heterogeneity of single-channel conductance sizes seen with amyloid proteins suggest that it is not impossible that larger pores exist. Some PFTs have also shown heterogeneity in pore size and oligomeric state.^{76,77} In both classes of proteins, pore formation is dependent upon membrane binding and oligomerization which in turn are sensitive to membrane composition. However, a key difference emerges here in that cholesterol tends to inhibit membrane penetration and insertion by amyloid peptides whereas cholesterol appears to play a necessary role in certain kinds of PFT insertion.⁷⁸ Although it may seem odd to compare toxins produced by bacteria in order to kill other cells with amyloid proteins, the amyloid proteins themselves actually become a kind of autotoxin when they have adopted a beta-sheet confirmation. These toxic effects include dysregulation of calcium homeostasis, increased production of reactive oxygen species, apoptosis, dysfunction of the proteasomal system, impairments of long-term potentiation and synaptic growth as well as ultimately cell death. Thus, amyloid peptides may possess a similar toxic function to bacterial pore-forming toxins although it seems clear that this function was not intended by nature.

B-Sheet Peptide Pores

Thundimadathil et al showed that short beta sheet peptides are able to form porin-like, high conductance voltage-gated channels in lipid bilayer membranes (Fig. 1).⁷⁹ In general the formation of high conductance, voltage gated (two state gating of individual channels with closing at both positive and negative applied potentials) channels exhibiting several sub-conductance states and a complex kinetic behavior is a characteristic feature of β barrel porins.⁸⁰⁻⁸² Experimental evidence of a close similarity between the ion channel characteristics of beta sheet peptides and that of β barrel porins revealed for the first time the possibility of self-association of several β -sheet peptide units in presence of membranes into a β -barrel-like structure as in the case of β -barrel pore forming toxins (PFTs).

The ion channel properties of (xSxG)₆ peptide resemble that of β -barrel porin channels in several respects. It forms highly conductive channels (mean single channel conductance = 1.37 nS) and exhibits two state gating at potentials $>\pm 40$ mV. Fast and slow kinetic events and sub-conductance states were observed. The permeation of a wide variety of ions of different sizes suggests the formation of nonselective channels with a pore diameter > 10.5 Å (corresponding to calculated diameter of the largest permeating cation, NEt_3Bz^+). Low cation selectivity in the presence of KCl concentration gradient indicates only a minor interaction of ions with the pore interior in spite of the presence of six serine hydroxyls which would be possibly arrayed in the same direction in a β sheet structure. Also it seems that the presence of two positively charged arginine residues does not influence the ion selectivity. This could be related to the larger size of the pore. The pore diameter calculated from single channel conductance is only approximate due to the assumption of a cylindrical pore and free moving ions without any interaction with pore interior. Nevertheless, the calculated pore diameter (~ 11 Å) is close to that reported for several porins. It has been proposed that short-lived substates found in the ion channel traces of porins represent the flickering of monomer channels

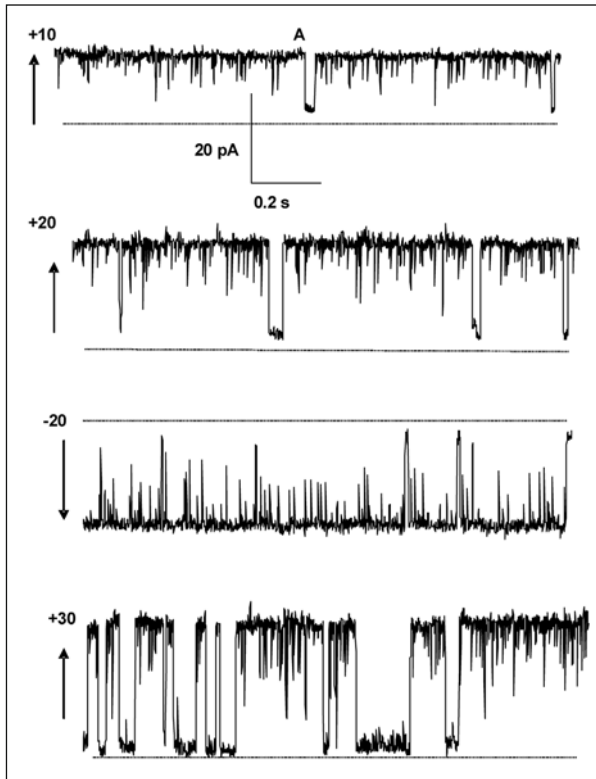


Figure 1. The peptide incorporation into the lipid bilayer took place immediately after the addition of about 3 μL methanolic solution of $(\text{xSxG})_6$ peptide (0.05 mg/mL) to cis side of the membrane containing 1000 μL of 100-1000 mM electrolyte (final concentration of peptide $\sim 10^{-8}$ M), as evidenced by an increase in membrane conductance and induction of square current events indicating the formation of ion channels. High conductance channels formed under symmetrical conditions (1M CsCl, unbuffered) at low applied potentials (10-30 mV) are shown in Figure 1. At the low applied potentials, the ion channels were in the high conductance open state most of the time and complete closures were rarely seen. An important characteristic of the channel was the presence of fast flickering type events along with several short-lived sub-conductance states. In many cases, the fast flickering events were the only manifestation of the presence of ion channels due to the complete opening of the channel to a high conductance state for several minutes. In most patches a mean single channel conductance of 1.37 nS was observed. In channel traces, an increase in number of well defined sub-conductance states could be seen with increase in applied potential. This reflects the tendency of the channel to close or return to a low conductance state at higher membrane potentials as in porins.

between open and closed states whereas large conductance openings represent multimer channels. For $(\text{xSxG})_6$ peptide the kinetic analysis of open channels showed that the large conductance opening events could not be modeled by a single time constant, suggesting that the high conductance opening events represent a complex channel. Usually, such channels could result from the cooperation of several individual pore forming protein units or an individual pore-forming unit could adopt distinct conformations resulting in multiple conductance states. If direct transitions between two or more conductance levels occur, (interconverting conductances), such levels could be considered as

sub-conductance states of the same channel. In some experiments interconversion among different conductance levels could be clearly resolved.

The evidence that peptide aggregation is needed for pore formation was obtained from Congo red binding studies. The inhibition of channel formation by Congo red must be due to the loss of active aggregates as it inserts into β pleated sheet structure thereby preventing aggregation. This strongly suggests that only peptide aggregates but not monomers form pores. A general mechanism of β barrel pore formation by PFTs involves the formation of a membrane bound prepore oligomer from a membrane bound monomer and insertion of the oligomer into the membrane followed by pore formation via cooperative events.⁸³ Due to the hydrophobic nature and poor solubility of $(xSxG)_6$ in water unlike β -PFTs, it is believed that the addition of a methanolic solution of the peptide to a high ionic strength salt solution during bilayer experiments would lead to the spontaneous aggregation of the peptide into an oligomeric structure before it is finally inserted into the membrane and possibly folded into a β barrel-like structure. Moreover, in this study the channel conductance was found to be similar over a wide range of peptide concentrations suggesting that same type of peptide aggregates are formed irrespective of the amount of peptide added to the bilayer chamber and insert in to the membrane.

Oligomerization of the peptide into fibrillar structures in an aqueous environment is revealed by electron microscopy. Furthermore, the observation of oligomeric structures in association with lipid vesicles suggests insertion of the peptide as polymeric species into lipid bilayers. Liposomes decorated with peptide oligomeric species were seen during peptide-liposome binding studies as well as in the case of sonicated peptide-lipid vesicles. In an aqueous environment the formation of short fibrillar structures occurs only under harsh conditions (incubation at 60°C for 2-3 hours), whereas in the presence of lipid bilayers it seems that the aggregation into fibrillar structures is facilitated even under milder conditions (immediately after the addition of methanolic solution of peptide to preformed liposomes at room temperature).

CD studies have shown that $(xSxG)_6$ is only partially folded in methanol as indicated by large fraction of unordered and β turn components from secondary structure analysis. Upon binding to lipid bilayers the peptide adopts a conformation rich in β sheet secondary structure compared to that in solution. These observations are consistent with the finding of a lipid induced β sheet aggregation in A-beta peptides. The formation of low conductance channels in some experiments prior to the appearance of large conductance channels may be due to the presence of smaller peptide aggregates which can further self assemble to form larger pores. Hence it is presumed that the size of the pore and channel conductance depend on the extent of peptide aggregation and number of peptide subunits. In this type of structure, each peptide subunit (smaller aggregates) also could behave as an ion channel. In this way such channels would resemble complex porin channels which are themselves multimers of more than one β barrel pore.

The electrophoresis of $(xSxG)_6$ incorporated liposomes revealed the existence of at least three stable multimeric structures along with dimeric species. This indicates that ion channel may be composed of different number of subunits. It is proposed that short-lived sub-conductance states associated with high conductance single channels represent transitions between open and closed states of individual peptide subunits. A large peptide pore formed by the association of several individual β sheets or smaller β sheet aggregates is thus expected to have a complex behavior in membranes. Also, a dynamic assembly-disassembly process is possible inside the membrane where a peptide oligomeric pore is in equilibrium with individual peptide units of different sizes.

Mechanism of Ion Channel Formation by Beta Sheet Peptides

As discussed in the previous section, on the basis of porin-like ion channel properties, CD and IR studies indicating a β -sheet conformation in membranes stabilized by anti-parallel hydrogen bonding and β -turns, channel inhibition by Congo red, electron microscopic observation of oligomeric structures in association with lipid bilayers and gel electrophoresis of peptide-incorporated-liposomes indicating multimeric species, Thundimadathil et al suggested a mechanistic pathway (Fig. 2) for the ion channel formation by $(xSxG)_6$ peptide.⁸⁴ In this model

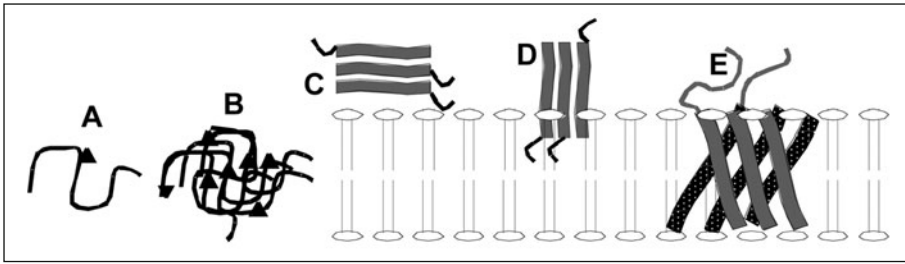


Figure 2. A schematic representation of the possible pathway of channel formation by $(xSxG)_6$ peptide. A,B) The addition of a dilute methanolic solution ($3 \mu\text{L}$ of $100\text{--}0.1 \mu\text{g/mL}$) of the peptide (partially folded and possibly monomeric) to the bilayer chamber containing high ionic strength salt solution (1 M) would lead to the spontaneous aggregation into a more disordered state. C) The peptide aggregate interacts with the membrane surface resulting in a conformational change to a β sheet-rich structure followed by aggregation into well ordered oligomeric species. D,E) The oligomer inserts into the bilayer and fold into a β barrel-like structure inside the hydrophobic membrane.

the insertion of the peptide as oligomers into the lipid bilayer is followed by the formation of a complex β -barrel-like pore structure comprising several β -sheets or β -sheet aggregate units.

A detailed study of the conformation properties of beta sheet peptide was subsequently undertaken by Thundimadathil et al to understand the structural changes of the peptide during membrane association and channel formation.⁸⁵ The lipid-induced β -sheet formation was confirmed by the formation of a characteristic β -sheet structure upon adding partially folded peptide solution to preformed liposomes. They noticed that the CD spectra of both the liposome-bound and liposome-incorporated peptide samples are reminiscent of a β -sheet structure. However, a significant variation in the peak positions of two β -sheet structures was noticed. The effect is pronounced for the positive band showing a red shift ($\sim 10 \text{ nm}$) in the band position of peptide-bound sample (192 nm) after peptide incorporation (202 nm). The characteristic β -sheet minimum was found at 215 and 220 nm for peptide-bound and peptide-incorporated samples respectively. The peak positions of β -sheet proteins are known to vary due to changes in geometries of different β -strand structures such as barrels, sheets, β helices etc. The observed red shift could be a result of the twisting of β -strands in membranes and the presence of β -turns. So, the authors concluded that the overall β -sheet geometries of peptide-bound and peptide-incorporated liposomes are different. The IR spectra of both the samples were similar with respect to band shapes and peak positions. This means that in both cases the structure is stabilized by antiparallel hydrogen bonding (IR is sensitive to hydrogen bonding whereas CD spectrum is sensitive to backbone structure). Peptide aggregation via β -sheet formation is possible in solutions also at high peptide concentrations and upon prolonged aging.

In summary, the conformational studies of a pore forming $(xSxG)_6$ peptide in different micro-environments showed that β -sheet formation is enhanced in the presence of membrane-mimicking liposomes and SDS micelles compared to that in solutions where the peptide exists in a partially folded state. Collectively, these findings suggest that the formation of β -sheet aggregates proceeds via partially folded or unfolded states of the peptide as seen in the case of amyloid proteins. Moreover, it can be argued that the β -sheet aggregate bound to the membrane undergoes a rearrangement upon insertion into the membrane. This is reasonable as the membrane interior is highly hydrophobic compared to surface layer. Different factors such as the intrinsic hydrophobicity and amphipathicity of the peptide, increased hydrogen bonding, hydrophilic nature of membrane surface, reduction in dimensionality, membrane-peptide interaction forces and the presence of flexible glycine residues could be contributing towards β -sheet formation in membrane mimicking environments. As several amyloid β -peptides have an appreciable fraction of glycine residues (in some cases in a repeating pattern) the role of

glycine residues in peptide-membrane interactions warrant further study using model and mutant peptides.

Conclusion

Amyloid peptides possess an inherent tendency to adopt the beta sheet conformation. As we have seen, beta sheet peptides are adept at binding to and inserting into membranes. Several known pore forming toxins also appear to possess a beta sheet structure in the membrane. While the tendency to form beta sheets accounts for the ability of amyloid peptides to form extended insoluble fibrils in disease, it also seems to lead directly to the formation of pores in lipid membranes. The similarities between PFTs and amyloid pores suggests a critical role for beta sheets in pore formation by toxic peptides.

Acknowledgements

BLK was supported in part by IIRG-05-14089 from the Alzheimer's Association.

References

1. Sipe JD, Cohen AS. Review: history of the amyloid fibril. *J Struct Biol* 2000; 130:88-98.
2. Anguiano M, Nowak RJ, Lansbury PT. Protofibrillar islet amyloid polypeptide permeabilizes synthetic vesicles by a pore-like mechanism that may be relevant to type II diabetes. *Biochemistry* 2002; 41:11338-11343.
3. Hirakura Y, Kagan BL. Pore formation by beta-2-microglobulin: a mechanism for the pathogenesis of dialysis associated amyloidosis. *Amyloid* 2001; 8:94-100.
4. Sipe JD. Serum amyloid A: from fibril to function. Current status. *Amyloid* 2000; 7:10-12.
5. Kourie JI, Hanna EA, Henry CL. Properties and modulation of alpha human atrial natriuretic peptide (alpha-hANP)-formed ion channels. *Can J Physiol Pharmacol* 2001; 79:654-64.
6. Hirakura Y, Azimov R, Azimova R et al. Polyglutamine-induced ion channels: a possible mechanism for the neurotoxicity of huntington and other CAG repeat diseases. *J Neurosci Res*, 2000; 60:490-494.
7. Hirakura Y, Azimov R, Azimova R et al. Ion channels with different selectivity formed by transthyretin. *Biophys J* 2001; 80:120a.
8. Azimova RK, Kagan BL. Ion channels formed by a fragment of alpha-synuclein (NAC) in lipid membranes. *Biophys J* 2003; 84:53a.
9. Hirakura Y, Carreras I, Sipe JD et al. Channel formation by serum amyloid A: a potential mechanism for amyloid pathogenesis and host defense. *Amyloid* 2002; 9:13-23.
10. Stipani V, Galluci E, Micelli S et al. Channel formation by salmon and human calcitonin in black lipid membranes. *Biophys J* 2001; 81:3332-3338.
11. Malisaukas M, Zamotin V, Jass J et al. Amyloid protofilaments from the calcium-binding protein equine lysozyme: formation of ring and linear structures depends on pH and metal ion concentration. *J Mol Biol* 2003; 330:879-890.
12. Bahadi R, Farrelly PV, Kenna BL et al. Channels formed with a mutant prion protein PrP(82-146) homologous to a 7-kDa fragment in diseased brain of GSS patients. *Am J Physiol Cell Physiol* 2003; 285:C862-872.
13. Quist A, Doudevski J, Lin H et al. Amyloid ion channels: a common structural link for protein-misfolding disease. *Proc Natl Acad Sci USA* 2005; 102:10427-10432.
14. Pieri L, Bucciantini M, Guasti P et al. Synthetic lipid vesicles recruit native-like aggregates and affect the aggregation process of the prion Ure2p: Insights on vesicle permeabilization and charge selectivity. *Biophys J* 2009; 96:3319-3330.
15. Canale C, Torrassa S, Rispoli P et al. A. Natively folded HypF-N and its early amyloid aggregates interact with phospholipid monolayers and destabilize supported phospholipid bilayers. *Biophys J* 2006; 91:4575-4588.
16. Ceru S, Kokalj SJ, Rabzelj S et al. Size and morphology of toxic oligomers of amyloidogenic proteins: a case study of human stefin B. *Amyloid* 2008; 15:147-159.
17. Hawkins PN, Richardson S, MacSweeney JE et al. Scintigraphic quantification and serial monitoring of human visceral amyloid deposits provide evidence for turnover and regression. *Q J Med* 1993; 86:365-374.
18. Hardy J, Alsup D. Amyloid deposition as the central event in the etiology of Alzheimer's disease. *Trends Pharmacol* 1991; 12:383-388.
19. Samaia HB, Mari JJ, Vallada HP et al. A prion-linked psychiatric disorder. *Nature* 1997; 20; 390:241.
20. Forloni G, Angeretti N, Chiesa R et al. Neurotoxicity of a prion fragment. *Nature* 1993; 362:543-546.

21. Lorenzo A, Razzaboni B, Weir GC et al. Pancreatic islet cell toxicity of amylin associated with type-2 diabetes mellitus. *Nature* 1994; 368:756-760.
22. Pike CJ, Burdick D, Walencewicz AJ et al. Neurodegeneration induced by beta-amyloid peptides in vitro: the role of peptide assembly state. *J Neurosci* 1993; 13:1676-1687.
23. Harper JD, Lansbury PT. Models of amyloid seeding in Alzheimer's disease and scrapie: mechanistic truths and physiological consequences of the time-dependent solubility of amyloid proteins. *Ann Rev of Biochem* 1997; 66:385-407.
24. Hirakura Y, Satoh Y, Hirashima N et al. Membrane perturbation by the neurotoxic Alzheimer amyloid fragment beta 25-35 requires aggregation and beta-sheet formation. *Biochem Mol Biol Int* 1998; 46:787-794.
25. Lesne S, Koh MT, Kotilinek L et al. A specific amyloid-beta protein assembly in the brain impairs memory. *Nature* 2006; 440:352-357.
26. Walsh DM, Klyubin I, Fadeeva JV et al. Naturally secreted oligomers of amyloid beta protein potently inhibit hippocampal long-term potentiation in vivo. *Nature* 2002; 416:535-539.
27. Lin H, Bhatia R et al. Amyloid beta protein forms ion channels: implications for Alzheimer's disease pathophysiology. *Faseb J* 2001; 15:2433-2444.
28. Janson J, Ashley RH, Harrison D et al. The mechanism of islet amyloid polypeptide toxicity is membrane disruption by intermediate-sized toxic amyloid particles. *Diabetes* 1999; 48:491-498.
29. Lashuel HA, Petre BM, Wall J et al. Alpha-synuclein, especially the Parkinson's disease-associated mutants, forms pore-like annular and tubular protofibrils. *J Mol Biol* 2002; 322:1089-1102.
30. Kaye R, Head E, Thompson JL et al. Common structure of soluble amyloid oligomers implies common mechanism of pathogenesis. *Science* 2003; 300:486-489.
31. Kagan BL, Azimov R, Azimova R. Amyloid peptide channels. *J Membr Biol* 2004; 202:1-10.
32. Capone R, Garcia-Quinn F, Prangkio R et al. Amyloid beta ion channels in artificial lipid bilayer and neuronal cells. *Neurotoxicity Res* 2009 (in press).
33. Fernandez A, Berry RS. Proteins with H-bond packing defects are highly interactive with lipid bilayers: Implications for amyloidogenesis. *Proc Natl Acad Sci USA* 2003; 100:2391-2396.
34. Stefani M, Dobson CM. Protein aggregation and aggregate toxicity: new insights into protein folding, misfolding diseases and biological evolution. *J Mol Med* 2003; 81:678-699.
35. McLaurin J, Chakrabarty A. Characterization of the interactions of Alzheimer beta-amyloid peptides with phospholipid membranes. *Eur J Biochem* 1997; 245:355-363.
36. Wong PT, Schauerte JA, Wisser KC et al. Amyloid-beta membrane binding and permeabilization are distinct processes influenced separately by membrane charge and fluidity. *J Mol Biol* 2009; 386:81-96.
37. Hirakura Y, Lin MC, Kagan BL. Alzheimer amyloid abeta1-42 channels: effects of solvent, pH and Congo Red. *J Neurosci Res* 1999; 57:458-466.
38. Terzi E, Holzmann G, Seelig J. Interaction of Alzheimer beta-amyloid peptide (1-40) with lipid membranes. *J Mol Biochem* 1997; 36:14845-14852.
39. Boqvist M, Lindstrom F, Watts A et al. Two types of Alzheimer's beta-amyloid (1-40) peptide membrane interaction aggregation preventing transmembrane anchoring versus accelerated fibril formation. *J Mol Biol* 2004; 335:1039-1049.
40. Alarcon JM, Brito JA, Hermosilla T et al. Ion channel formation by Alzheimer's disease amyloid beta-peptide (Abeta40) in unilamellar liposomes is determined by anionic phospholipids. *Peptides* 2006; 27:365-363.
41. Hertel C, Terzi E et al. Inhibition of the electrostatic interaction between beta-amyloid peptide and membranes prevents beta-amyloid-induced toxicity. *Proc Natl Acad Sci USA* 1997; 94:9412-9416.
42. Lau TL, Ambroggio EE et al. Amyloid-beta peptide disruption of lipid membranes and the effect of metal ions. *J Mol Biol* 2006; 356:759-770.
43. Durell SR, Guy HR, Arispe N et al. Theoretical models of the ion channel structure of amyloid beta-protein. *Biophys J* 1994; 67:2137-2145.
44. Jang H, Ma B, Lal R et al. Models of toxic beta-sheet channels of proteoglycan-1 suggest a common subunit organization motif shared with toxic Alzheimer beta-amyloid ion channels. *Biophys J* 2008; 95:4631-4642.
45. Lee G, Pollard HB, Arispe N. Annexin 5 and apolipoprotein against Alzheimer's amyloid beta-peptide cytotoxicity by competitive inhibition of a common phosphatidylserine receptor site. *Peptides* 2002; 23:1249-1263.
46. Kakio A, Nishimoto S, Yanagisawa K et al. Interactions of amyloid beta-protein with various gangliosides in raft-like membranes: importance of GM1 ganglioside-bound form as an endogenous seed for Alzheimer amyloid. *Biochemistry* 2002; 41:7385-7390.
47. Yanagisawa K. Role of gangliosides in Alzheimer's disease. *Biochim Biophys Acta* 2007; 1768:1943-1951.

48. Yanagisawa K, Odaka A, Suzuki N et al. GM1 ganglioside-bound amyloid beta-protein (A-beta): a possible form of preamyloid in Alzheimer's disease. *Nat Med* 1995; 1:1062-1066.
49. Arispe N, Doh M. Plasma membrane cholesterol controls the cytotoxicity of Alzheimer's disease Aβ₂₅₋₃₅ (1-40) and (1-42) peptides. *FASEB J* 2002; 16:1526-1536.
50. Westermark P, Wilander E. The influence of amyloid deposits on the islet volume in maturity onset diabetes mellitus. *Diabetologia* 1978; 15:417-421.
51. Mirzabekov TA, Lin MC, Kagan BL. Pore formation by the cytotoxic islet amyloid peptide amylin. *J Biol Chem* 1996; 271:1988-1992.
52. Sakagashira S, Hiddinga HJ, Tateishi K et al. S20G mutant amylin exhibits increased in vitro amyloidogenicity and increased intracellular cytotoxicity compared to wild-type-amylin. *Am J Pathol* 2000; 157:2101-2109.
53. Jayasinghe SA, Langen R. Membrane interaction of islet amyloid polypeptide. *Biochim Biophys Acta* 2007; 1768:2002-2009.
54. Knight JD, Miranker AD. Phospholipid catalysis of diabetic amyloid assembly. *J Mol Biol* 2004; 341:1175-1187.
55. Knight JD, Hebda JA, Miranker AD. Conserved and cooperative assembly of membrane-bound alpha-helical states of islet amyloid polypeptide. *Biochem* 2006; 45:9496-9508.
56. Jayasinghe SA, Langen R. Lipid membranes modulate the structure of islet amyloid polypeptide. *Biochemistry* 2005; 45:12113-12119.
57. Sparr F, Engel MF, Sakharov DV et al. Islet amyloid polypeptide-induced membrane leakage involves uptake of lipids by forming amyloid fibers. *FEBS Lett* 2004; 577:117-120.
58. Kaye J, Bernhagen N, Greenfield K et al. Conformational transmissions of islet amyloid polypeptide. (IAPP) in amyloid formation in vitro. *J Mol Biol* 1999; 287:781-796.
59. DeArmond SJ, Prusiner SB. Perspectives on prion biology, prion disease pathogenesis and pharmacologic approaches to treatment. *Clin Lab Med* 2003; 23:1-41.
60. Lin MC, Mirzabekov T, Kagan BL. Channel formation by a neurotoxic prion protein fragment. *J Biol Chem* 1997; 272:44-47.
61. Pan KM, Baldwin M, Nguyen J et al. Conversion of alpha-helices into beta-sheets features in the formation of the scrapie prion proteins. *Proc Natl Acad Sci USA* 1993; 90:10962-10966.
62. Kazlauskaitė J, Sanghera N, Sylvester I et al. Structural changes of the prion protein in lipid membranes leading to aggregation and fibrillization. *Biochemistry* 2003; 42:3295-3304.
63. Bahadi R, Farrelly PV, Kenna BL et al. Channels formed with a mutant prion protein PrP(82-146) homologous to a 7-kDa fragment in diseased brain of GSS patients. *Am J Physiol Cell Physiol* 2003b; 285:C862-872.
64. Volles MJ, Lansbury PT. Vesicle permeabilization by protofibrillar AS is sensitive to Parkinson's disease-linked mutations and occurs by a pore-like mechanism. *Biochemistry* 2002; 41:4595-4602.
65. Zakharov SD, Hulleman JD, Dutseva EA et al. Helical alpha-synuclein forms highly conductive ion channels. *Biochemistry* 2007; 46:14369-14379.
66. Arispe N. Architecture of the Alzheimers Aβ₂₅₋₃₅ ion channel pore. *J Membrane Biol* 2004; 197:33-48.
67. Schutz GE. The structure of bacteria: outer membrane proteins. *Biochim Biophys Acta* 2002; 1565:308-317.
68. Benz R, Schmid A, Hancock RW. Ion selectivity of gram-negative bacterial porins. *J Bacteriol* 1983; 153:241-252.
69. Hill K, Model K, Ryan MT et al. Tom40 forms the hydrophilic channel of the mitochondrial import pore for preproteins. *Nature* 1998; 395:516-521.
70. Schleiff E, Soll J, Kuchler M et al. Characterization of the translocon of the outer envelope of chloroplasts. *J Cell Biol* 2003; 160:541-551.
71. Wimley WC. The versatile β-barrel membrane protein. *Curr Opin Struct Biol* 2003; 13:404-411.
72. Song L, Hobaugh MR, Shustak C et al. Structure of staphylococcal alpha-hemolysin, a heptameric transmembrane pore. *Science* 1996; 274:1859-1866.
73. Sekiya K, Satoh R, Danbara H et al. A ring-shaped structure with a crown formed by streptolysin O on the erythrocyte membrane. *J Bacteriol* 1993; 175:5953-5961.
74. Olofsson A, Hebert, Thiestam M. The projection structure of perfringolysin O (Clostridium perfringens theta-toxin). *FEBS Lett* 1993; 319:125-127.
75. Sharpe JC, London E. Diphtheria toxin forms pores of different sizes depending on its concentration in membranes: probable relationship to oligomerization. *J Membr Biol* 1999; 171:209-221.
76. Tadjibaeva G, Sabirov R, Tomita T. Flammutoxin, a cytolytic toxin from the edible mushroom *Flammulina velutipes*, forms two different types of voltage-gated channels in lipid bilayer membranes. *Biochem Biophys Acta* 2000; 1467:431-443.
77. CabiauxV, Wolff C, Ruyschaert JM. Interaction with a lipid membrane: a key step in bacterial toxins virulence. *Int J Biol Macromol* 1997; 21:285-298.

78. Thundimadathil J, Roeske RW, Guo L. A synthetic peptide forms voltage-gated porin-like ion channels in lipid bilayer membranes. *Biochem Biophys Res Commun* 2005; 330:585-590.
79. Conlan S, Zhang Y et al. Biochemical and biophysical characterization of OmpG: A monomeric porin. *Biochemistry* 2000; 39:11845-11854.
80. Bainbridge G, Gokce I, Lakey JH. Voltage gating is a fundamental feature of porin and toxin β -barrel membrane channels. *FEBS Lett* 1998; 431:305-308.
81. Berrier C, Coulombe A et al. Fast and slow kinetics of porin channels from *Escherichia coli* reconstituted into giant liposomes and studied by patch-clamp. *FEBS Lett* 1992; 306:251-256.
82. Valeva A, Weisser A, Walker B et al. Molecular architecture of a toxin pore: a 15-residue sequence lines the transmembrane channel of staphylococcal alpha-toxin. *EMBO J* 1996; 15:1857-1864.
83. Thundimadathil J, Roeske RW et al. Aggregation and porin-like channel activity of a β -sheet peptide. *Biochemistry* 2005; 44:10259-10270.
84. Thundimadathil J, Roeske RW et al. Effect of membrane mimicking environment on the conformation of a pore forming (xSxG)₆ peptide, *Biopolymers*. *Peptide Science* 2006; 84:317-328.
85. Mirzabekov T, Lin MC, Yuan WL et al. Channel formation in planar lipid bilayers by a neurotoxic fragment of the beta-amyloid peptide. *Biochem Biophys Res Commun* 1994; 202:1142-1148.
86. Lin MC, Kagan, BL. Electrophysiological properties of channels induced by Abeta 25-26 in planar lipid bilayers. *Peptides* 2002; 23:1215-1228.
87. Arispe N, Rojas E, Pollard HB. Alzheimer disease amyloid beta protein forms calcium channels in bilayer membranes: blockade by tromethamine and aluminum. *Proc Natl Acad Sci USA* 1993; 90:567-571.
88. Arispe N, Pollard HB, Rojas E. Giant multilevel cation channels formed by Alzheimer disease amyloid beta-protein (Abeta P(1-40)) in bilayer membranes. *Proc Natl Acad Sci USA* 1993; 90:10573-10577.
89. Lashuel HA, Hartley DM, Petre BM et al. Mixtures of wild-type and a pathogenic (E22G) form of Abeta40 in vitro accumulate protofibrils, including amyloid pores. *J Mol Biol* 2003; 332:795-808.
90. Kim HJ, Suh YH, Lee MH et al. Cation selective channels formed by a C-terminal fragment of beta-amyloid precursor protein. *Neuroreport* 1999; 10:1427-1431.
91. Kourie JI, Culverson A. Prion peptide fragment PrP(106-126) forms distinct cation channel types. *Neurosci Res* 2000; 62:120-133.
92. Wang L, Lashuel HA, Walz T et al. Murine apolipoprotein serum amyloid A in solution forms a hexamer containing a central channel. *Proc Natl Acad Sci USA* 2002; 99:15947-15952.
93. Kourie JI. Characterization of a C-type natriuretic peptide (CNP-39)—formed cation-selective channel from platypus (*Ornithorhynchus anatinus*) venom. *J Physiol* 1999; 518:359-369.
94. Kourie JI. Synthetic mammalian C-type natriuretic peptide forms large cation channels. *FEBS Lett* 1999; 445:57-62.
95. Monoi H, Futaki S, Kugimiya S et al. Poly-L-glutamine forms cation channels: relevance to the pathogenesis of the polyglutamine diseases. *Biophys J* 2000; 78:2892-2894.
96. Ibrahim HR, Thomas U, Pellegrini A. A helix-loop-helix peptide at the upper lip of the active site cleft of lysozyme confers potent antimicrobial activity with membrane permeabilization action. *J Biol Chem* 2002; 276:43767-43774.
97. Chung J, Yang H, de Beus MD et al. Cu/Zn superoxide dismutase can form pore-like structures. *Biochem Biophys Res Commun* 2003; 312:873-876.

INDEX

A

Acidic phospholipid 26, 41
Actinoporin 32, 36-38, 106-108, 110-113
Aerolysin 2, 7-9, 38, 67-69, 71-78, 111, 160
Alamethicin 3, 8, 19, 21, 24-26, 41, 42, 47
Alkaline phosphatase 127, 131, 133
 α -Hemolysin 9, 10, 19, 20, 36, 38, 72, 75, 150, 160
 α -Pore forming protein (α -PFP) 1-4, 6-9, 32, 36-38, 41
Aminopeptidase 7, 127, 131, 133, 153
Amphipathicity 20, 22, 32, 35, 37, 84, 163
Amyloid 76, 150-155, 157-160, 163, 164
Anthrax toxin 7, 150, 160
Antimicrobial peptide 17-22, 26, 27, 34, 36, 45
Apoptosis 6, 27, 36, 58, 78, 82, 91-93, 96, 97-100, 113, 116, 160
Area expansion 42, 44, 97
Aromatic amino acid 16, 107, 108
Atomic-force microscopy (AFM) 44, 95, 97, 123, 136, 159

B

Bacillus cereus 123, 124
Bacillus thuringiensis (*Bt*) 4, 6, 127, 128, 130, 131
Barrel stave pore 20, 21
Bax 36, 38, 41-44, 47, 61, 92-100, 112
Bcl 2, 6, 27, 34-36, 38, 41, 43, 45, 78, 82, 87, 91-94, 96-100
Bcl-2 2, 6, 27, 34-36, 38, 41, 43, 45, 78, 91-94, 96-100
Bcl-xL 6, 27, 38, 92-94, 96-99
 β -sheet 2, 5-10, 18, 20, 36, 37, 56, 57, 61, 67-76, 111, 118, 130, 131, 144, 146, 160, 162, 163
Bid 91-94, 96-98
Bilayer disruption 39
Bilayer interface 16-18, 32, 35
Bilayer perturbation 31
Blockade 150, 155, 156

C

Cadherin 127, 131-135
Cancer 28, 56, 92, 100, 113, 128, 129
Cardiolipin (CL) 31, 32, 36, 47, 96, 97
Cardiotoxin (CTX) 131, 143-148
Carpet model 21, 42
Cecropin 21, 26, 34
Cell surface retention 143, 146, 147
Ceramide 40, 41, 107, 113
Channel 1, 2, 6, 7, 9, 10, 14, 20-22, 24-27, 32, 35, 37, 40, 41, 47, 71, 78, 81, 83-87, 91, 93, 96, 97, 119, 135, 145, 150, 154-163
Charge 14, 15, 17, 18, 27, 33, 34, 41, 47, 61, 86, 144, 154, 157, 158
Chloride intracellular channel (CLIC) 6, 7, 9
Cholesterol (Cho) 2, 6, 7, 19, 31, 32, 34, 36, 38, 39, 41, 56-60, 62, 72, 96, 107, 108, 113, 135, 154, 158, 160
Cholesterol dependent cytolysin (CDC) 2, 4, 6-9, 19, 32, 36-38, 41, 56-62, 72, 96, 113
Cobra venom 143
Coleoptera (Col) 128, 129
Colicin 1, 3-10, 19, 21, 27, 35, 37, 43, 44, 47, 81-87, 93, 96, 97, 130, 136
Complement 2, 6, 32, 56-58, 62
Conformation 8, 9, 24-27, 37, 58, 61, 83, 92, 94, 96, 100, 111, 121, 122, 137, 148, 150-154, 157-159, 161-164
Conformational change 1, 6, 8, 10, 37, 38, 57, 60, 67, 69, 71, 75, 81, 94, 97, 99, 100, 106, 112, 113, 119-122, 136, 137, 143, 145-148, 160, 163
Congo red 150, 151, 155-159, 162
Cooperativity 34, 44, 45, 61
CryMod toxin 131, 135, 138
Cryo electron microscopy 57, 62
Crystallography 24, 136
Crystal structure 4-9, 57, 61, 67-69, 71, 72, 75, 76, 82, 96, 108, 112, 117, 120, 121, 123, 124, 146

Cry toxin 127, 129-138
 Cysteine 7, 9, 58, 86, 91, 94, 96, 107, 111, 117
 Cytochrome *c* 36, 91-93, 97-99
 Cytolysin A (ClyA) 116
 Cyt toxin 127, 130, 131, 137, 138

D

Detergent 21, 27, 33, 42, 44, 85, 86, 96, 121, 127, 135, 145
 Dimerization 99, 118, 145, 147, 148
 Diphtheria toxin (DT) 4, 7, 10, 19, 27, 37, 44, 82, 93, 130
 Diptera (Dip) 128, 129, 132
 Disordered 9, 36, 43, 81, 82, 84, 108, 159, 163
 Disulfide 7, 9, 68, 69, 75, 112, 143
 Domain 3-9, 27, 35-37, 39, 41, 44, 57, 58, 60-62, 67-76, 78, 81-87, 91-99, 106, 107, 117, 118, 120, 121, 124, 127-130, 132, 134-137, 143, 146, 148, 153
 Dynamics 24, 27, 31, 32, 35, 37, 38, 40, 41, 60, 62, 75, 86, 143, 148, 162

E

Electron microscopy (EM) 8, 57, 58, 61, 62, 111, 119, 120, 121, 123, 151, 159, 162
 Electrostatic 8, 15, 17-21, 26, 31, 32, 34, 36, 97, 146, 157
 Electrostatic interaction 8, 15, 17, 18, 20, 21, 26, 34, 36, 157
 Embedded together 38, 100
 Endotoxin A 2, 5
 Energy barrier 39, 44
 Equilibrium 14, 18, 20, 39, 40, 42, 43, 69, 72, 73, 100, 154, 162
 Equinatoxin 3, 5, 7, 8, 10, 61, 107
Escherichia coli 3, 5, 73, 81, 87, 112, 116-118, 121, 123, 124
 Extracellular matrix 143, 146

F

Fluidity 36, 60, 154, 157
 Foldase activity 35, 37
 Free energy 15-18, 37, 39, 44
 Fusion 32, 34, 41, 46, 60-62, 86, 123

G

Giant 42, 108
 Globule 35, 37, 86, 137
 Glycosphingolipid domain 146
 Gouy-Chapman theory 34
 Gramicidin 19
 Grazing angle X-ray diffraction 42

H

Helix polar angle 33
 Hemagglutination 70
 Hemolysin E (HlyE) 116-124
 Hemolytic lectin 67-69
 Heparan sulfate 143
 Hydrocarbon core 14-16, 18, 20, 21, 33, 35
 Hydrophobic 4-6, 8-10, 14-21, 25-27, 32, 33-35, 37-39, 47, 68, 69, 71, 73, 74, 76, 78, 82-87, 92-94, 96, 99, 111, 113, 117, 118, 120-122, 124, 130, 132, 136, 137, 144, 146, 153, 162, 163

I

Insecticidal δ -endotoxin (Cry) 2, 4, 6, 7, 9, 127-138
 Insertion 1, 3-5, 7-10, 15, 18, 24-27, 32, 34, 36, 37, 43, 60, 61, 69, 82, 86, 94, 96, 98, 99, 111, 116, 120, 122, 131, 132, 134-138, 143, 145-148, 150, 154, 157, 158, 160, 162, 163
 Integrin 8, 61, 122, 136, 144-146, 150, 154
 Interaction network 91, 92, 99, 100
 Interfacial activity 20, 21, 32
 Ionic channel 41, 135

K

Kinetic 32, 34, 42-44, 58, 60, 85, 86, 160, 161

L

Lectin 7, 67-71, 73, 106, 110, 112, 130
 Lepidoptera 129, 132
 Line tension 36, 44, 47, 95
 Lipid 6-9, 14-22, 24-27, 31-47, 59, 61, 62, 75, 81, 84, 86, 87, 92, 94-98, 100, 106-113, 119-122, 124, 131, 134, 135, 137, 143, 145-148, 150, 152-154, 157-164

Lipid composition 25, 27, 31, 47, 59, 158
Lipid flip-flop 31, 39-41, 97, 112
Lipidic pore 32, 40, 41, 44, 47, 97
Lipid raft 36, 38, 131, 135, 143, 146, 148
Lipid spontaneous curvature 47, 96
Liquid 31, 33, 36, 108
Liquid-ordered 36, 108
Listeriolysin 56
LukF 5
Lysis 1, 20, 27, 116, 122, 134, 137

M

Magainin 21, 22, 26, 33, 34, 37, 38, 40, 41
Melittin 18, 19, 24, 26, 37, 38, 42, 43, 46,
47, 84, 86, 87, 107
Membrane 1-10, 14-22, 24-27, 31-47,
56-62, 67-71, 73-76, 78, 81-87, 91-100,
106-113, 116, 118-123, 127, 130-132,
134-138, 143-148, 150-154, 157-164
Membrane attack complex/perforin
(MACPF) 2, 4, 6, 56, 57, 62
Membrane binding 7, 15, 18, 32, 36, 37, 38,
58, 93, 96, 97, 99, 106, 110-112, 120,
122, 145, 146, 157, 160
Membrane fusion 60, 62
Membrane insertion 1, 3-5, 7-10, 24-27, 34,
36, 43, 60, 61, 86, 94, 96, 99, 116, 122,
131, 132, 135, 137, 148, 154, 157
Membrane interface 16, 21, 26, 32-34, 37,
38
Membrane protein 1, 8, 14, 16, 20, 24, 25,
27, 32, 36, 60, 62, 81, 145, 159
Membrane thinning 26, 41, 44-47
Microdomain 36, 38, 59, 108, 113, 127,
131, 135
Mitochondria 6, 36, 91, 92, 94, 96, 98, 159
Mitochondrial permeability 36
Model membrane 21, 26, 91, 94, 96, 98,
100, 145
Molecular dynamic 24, 32, 37, 38
Molten 35, 37, 86, 137

N

NMR 5, 24-26, 62, 84, 108, 111, 112, 146,
147
Nonlamellar lipid 41, 111
Nucleation 41-44, 46, 97, 122

O

Oligomeric pore 38, 76, 111, 162
Oligomerization 1, 7, 8, 10, 25, 35-38, 57,
58, 61, 62, 68, 72, 75, 76, 78, 94, 96,
98-100, 106-108, 118, 120, 122, 127,
131, 135-138, 143, 145, 148, 150, 152,
157-160, 162, 163
OmpF 81, 82, 84, 85
OmpX 81
Oriented circular dichroism (OCD) 41, 43,
94
Outer membrane vesicle 118, 123

P

Partial proteolyses 120
Partition coefficient 16
Partitioning 15-19, 21, 22, 25-27, 34, 35, 37
Partitioning-folding coupling 35, 37
Partitioning-refolding 35, 37
Passive ion permeation 39
Peptide bond 18
Peptide-lipid interactions 24, 27
Perforin 6, 56-58, 62
Perfringolysin 6, 56-62, 72, 150, 160
Pertussis toxin 7
Phase coexistence 36, 95
Phase diagram 27, 38
Phase transition 26, 27, 41
Phosphatidic acid (PA) 36, 47, 112
Phosphatidylcholine 16, 107, 108, 146
Phosphatidylethanolamine (PE) 5, 10, 46,
47, 159
Phosphatidylglycerol (PG) 34, 47, 153
Phosphatidylinositol (PI) 34, 36, 47, 134,
153
Phosphatidylserine (PS) 34, 36, 47, 154
Phospholipid bilayer 22, 33, 154
Planar lipid bilayer 6, 24, 25, 84, 97, 124,
154, 157-159
Pneumolysin 8, 56, 59-62
Pore 1-10, 14-16, 18-22, 24-27, 31, 32,
34-48, 56-62, 67-78, 81-87, 91-97, 99,
100, 106-108, 111-113, 116, 118-124,
127, 130, 131, 134-138, 143, 145-148,
150-152, 154, 155, 157-164
Pore dynamic 148

Pore-formation 1-6, 7, 8, 9, 10, 4-16,
18-22, 24, 26, 27, 31, 32, 34-48, 56-62,
67-74, 76-78, 81-87, 91-94, 96, 97, 99,
106-108, 111-113, 116, 119-124, 127,
130, 131, 134-138, 143, 145-148, 151,
152, 154, 157-164
Pore-forming 151, 158-161, 163, 164
Pore-forming polypeptide (PFPP) 16, 19-21,
32, 34, 36-39, 41, 44-46
Pore-forming toxin (PFT) 1-3, 5-10, 36,
56, 67, 68, 69, 70, 73, 81, 106, 107, 112,
113, 116, 123, 124, 127, 130, 131, 137,
138, 143, 145, 148, 159, 160, 162, 164
Prepore 6, 7, 8, 38, 44, 57-59, 60, 61, 122,
135, 138, 162
Protein domain 8, 67, 68, 81
Protein folding 37, 71
Proteolipid pore 60, 61

R

Receptor 1, 3, 6-8, 10, 19, 25, 26, 32, 34, 36,
38, 58, 59, 69, 78, 81, 82, 84, 85, 91, 93,
116, 127, 130-138, 146, 153, 154
Resistance 25, 99, 132, 134, 137, 157

S

Salmonella enterica 116-118, 124
Secondary structure 8, 20, 34, 35, 37, 71,
110, 111, 131, 162
SheA 116
Shigella 83, 116
Signalling 7, 91, 98, 113, 143, 145, 146
Single vesicle 43, 47
Sinking raft 42
Solid-state NMR 25, 26, 62
Sphingolipid (SL) 31, 32, 36, 135
Sphingomyelin 7, 32, 106-113
Spontaneous 8, 31, 32, 39, 41, 46, 47, 96,
150, 162, 163
Sticholysin 5, 7, 35, 36, 47, 107
Stochastic 39, 41, 43, 97
Streptolysin 56, 160
Structural rearrangement 73, 94, 96
Sulfatide 144-148

Surface plasma resonance 144
Surface tension 44
Syringomycin E 41

T

tBid 36, 38, 91, 93, 96-100
Threshold peptide-to-lipid mole fraction 38
Tol 81, 82, 84, 85
Topology 24, 25, 27, 73, 86, 111, 124, 130
Toroidal 20, 21, 32, 41-47, 59-61, 95, 97,
112, 148
Toroidal pore 20, 21, 32, 42-47, 95, 97, 112
Toxin activation 130
Toxin oligomerization 7, 127, 131, 135, 136
Transient pore 21, 43
Translocation 3-8, 68, 81, 82, 84, 85, 87, 93,
98, 100, 108, 143
Translocon 81, 82, 84
Transmembrane 3-6, 9, 21, 24-27, 31, 32,
35, 38, 40, 41, 59, 61, 67, 71, 72, 74, 78,
84, 86, 87, 91, 94, 106-108, 113, 116,
118, 120, 121, 132, 137, 159
Transmembrane helix 118, 120
Transmembrane β -barrel 5, 9, 67, 159
Two state model 15, 38, 43

V

Vaccine 56, 123

W

Wall 32, 41, 42, 59, 60, 75
Water pore 31, 40
Wimley-White hydrophobicity scale 15,
16, 84

X

X-ray 24, 33, 41, 42, 61, 83, 84, 97, 117,
123, 124, 145-147, 150

Z

Zinc 60, 150, 155, 156, 158, 159